

REPORT NO. SM-43105

EVALUATION OF MARAGING STEEL FOR APPLICATION
TO SPACE LAUNCH VEHICLES
CONTRACT NAS 7-214 WOO-PR-63-172

Final Report

Prepared by
Z. P. Saperstein, Project Director
W. V. Mixon

METALS-CERAMICS BRANCH



Approved by

A handwritten signature in black ink, appearing to read "G. V. Bennett", is written over a horizontal line.

G. V. Bennett, Branch Chief
Metals-Ceramics
Materials Research & Production Methods

ABSTRACT

An investigation was undertaken to evaluate mechanical and metallurgical properties of 3/4-in thick airmelted 18Ni-7Co-5Mo alloy plate and of welds deposited in the alloy. Plates from three heats were included in the study. Welds were made under a wide range of conditions and with a variety of filler wire compositions.

The evaluations included determinations of the effects of aging heat treatment on the mechanical properties of welds and plate. Uniaxial tensile, plane strain fracture toughness (employing partial thickness crack specimens), hardness, and sustained load properties were studied. The development of a sub-size plane strain fracture toughness specimen was also undertaken.

Metallurgical investigations included the use of novel electron fractographic methods. Such methods supplemented with electron diffraction and x-ray microprobe analysis techniques were employed for phase identification.

The principal results of this investigation may be summarized as follows:

1. Significant differences in the tensile and fracture toughness properties of the three airmelted 18Ni-7Co-5Mo plate heats were observed despite similar chemical compositions.
2. A small partial thickness crack specimen was developed which produced fracture toughness results agreeing closely with results obtained from more conventional larger specimens.
3. Tensile efficiency of weld joints generally exceeded 90 per cent after most aging treatments and approached 100 per cent after some.

ABSTRACT (Cont'd.)

4. Welds exhibited inferior fracture toughness properties compared to plate. Fracture toughness was found to be relatively independent of welding procedure, gross chemical composition, and post weld heat treatment.
5. Titanium nitride was identified as a prevalent constituent on the fracture surfaces of weldmetal. The phase was found to be present in the form of semi-continuous networks. This phase appears to be the cause of degraded weldmetal toughness and the occasional occurrence of poor heat-affected zone toughness. Titanium nitride was also found to be prevalent in plate, however, not in the form of semi-continuous networks.
6. Practical welding problems were encountered in applying laboratory welding procedures to production prototype conditions.
7. Radiographic inspection of welds does not appear to be capable of detecting damaging crack-like defects.
8. Plate and welds both exhibited some slow crack growth susceptibility when subjected to sustained loads in various liquid environments, However, welds appear to be far more susceptible.

The results of this investigation demonstrate that several problem areas must be subjected to further study.

TABLE OF CONTENTS

	Page
ABSTRACT	i
LIST OF FIGURES	vii
LIST OF TABLES	xiv
Section 1 INTRODUCTION	i
Section 2 EVALUATION OF PLATE PROPERTIES	4
2.1 Plate Properties	4
2.2 Plate Inspection Procedures	5
2.3 Plate Layout	5
2.4 Test Specimen Types and Testing	7
2.5 Heat Treatment Procedures	18
2.6 Preparation of Partial Thickness Crack Specimens	18
2.7 Results and Discussion	19
2.7.1 Dimensional, Soundness and Hardness Inspection	19
2.7.2 Metallographic Examination	25
2.7.3 Tensile Property Check	32
2.7.4 Effect of Rolling Direction and Aging Treatment on Tensile Properties	35
2.7.5 Effects of Aging Treatment on Hardness	37
2.8 Fracture Toughness of Plate	48
2.8.1 Heat I	49
2.8.2 Heat A	49
2.8.3 Heat B	50
2.8.4 Plane Strain Fracture Toughness Parameter, K_{IC}	50
2.8.5 Effect of Aging Duration and Temperature on K_{IC}	
2.8.6 Comparison of Experimental and Theoretical Dependence of Fracture Stress on Crack Size	51
2.9 Evaluation of Small PTC Specimen	57
2.9.1 Background	59
2.9.2 Effect of Specimen Size and Orientation on Net Fracture Stress	60
2.9.3 Effect of Specimen Size on K_{IC}	67
2.9.4 Fracture Surface Appearance	69
Section 3 PROPERTIES OF WELDED PLATE	75
3.1 Introduction	75
3.2 Flat Plate Welding-Specimen Preparation	76

TABLE OF CONTENTS (Cont'd.)

	Page
3.3 Inspection of Weldments	82
3.4 Post-Weld Heat Treatment	89
3.5 Mechanical Testing	89
3.6 Weldment Soundness	92
3.7 Effects of Welding and Heat Treatment Variables on Aging Response	93
3.7.1 Effects of Aging Heat Treatment on the Aging Response of Type W9 Weldmetal	93
3.7.2 Effects of Aging Heat Treatment on the Aging Response of Types W7 and W8 Weldmetal	100
3.7.3 Effects of Welding Procedure and Aging Heat Treatment on the Aging Response of Heat-Affected Regions	102
3.8 Effect of PTC Specimen Type and Orientation on the Net Fracture Stress of Weldmetal	118
3.9 Effects of Weld Deposit Chemical Composition, Welding Procedure, and Post-Weld Aging Treatment on Weldmetal Fracture Toughness	119
3.9.1 Welds in Heat I Plate	122
3.9.2 Welds in Heat B Plate	123
3.9.3 Effect of Re-Solution Heat Treatments on Weldmetal Toughness	130
3.10 Fracture Toughness of Plate Heat-Affected Regions	138
Section 4 CONTOURED PLATE WELDING	143
4.1 Preparation of Test Plates	143
4.2 Tensile Properties of Contoured Plate Welds	150
4.3 Fracture Toughness of Contoured Plate Welds	151
Section 5 EFFECT OF ENVIRONMENT ON THE SUSTAINED LOAD BEHAVIOR OF PLATE AND WELDS	158
5.1 Sustained Load Testing Procedure	158
5.2 Sustained Load Behavior of Plate	160
5.3 Sustained Load Behavior of Welds	163
Section 6 METALLOGRAPHIC OBSERVATIONS MADE BY OPTICAL AND ELECTRON MICROSCOPY AND ELECTRON FRACTOGRAPHY	166
6.1 Parent Plate and Heat-Affected Zone Microstructure	166
6.2 Weldmetal Microstructure	171

TABLE OF CONTENTS (Cont'd.)

	Page
Section 7 IDENTIFICATION OF THE ANGULAR PHASE BY MEANS OF SELECTED AREA ELECTRON DIFFRACTION	179
7.1 Carbon Extraction Replication Technique and Electron Diffraction	179
7.2 Identification of the Angular Phase	179
Section 8 ELECTRON MICROPROBE X-RAY ANALYSIS	185
8.1 Scanning Weldmetal Fracture Surfaces	185
8.2 Scanning Polished Weldmetal Surfaces	187
8.3 Dilution Effects	190
Section 9 THE INFLUENCE OF TIN AND RELATED FACTORS ON MARAGING STEEL WELD PROPERTIES	191
9.1 Properties of TiN and TiC	191
9.2 TiN in Weldmetal	193
9.3 Possible Effects of Austenite in Weldmetal	195
9.4 Toughness Degredation and TiN	196
Section 10 SUMMARY, CONCLUSIONS, AND RECOMMENDATIONS	199
Section 11 ACKNOWLEDGEMENTS	204
Section 12 REFERENCES	205
APPENDIX I PLATE SPECIFICATION	207
APPENDIX II WELDWIRE SPECIFICATION	212
APPENDIX III PROCEDURE FOR CRACKING PTC COUPONS	219
APPENDIX IV PLATE UNIAXIAL TENSILE DATA	232
APPENDIX V PLATE FRACTURE TOUGHNESS DATA, 48-IN AND 24-IN. PTC COUPONS	238
APPENDIX VI PLATE FRACTURE TOUGHNESS DATA, 8-IN. PTC COUPONS	242
APPENDIX VII WELDMENT TENSILE DATA, W9 WELDS	244
APPENDIX VIII WELDMENT TENSILE DATA, W7 AND W8 WELDS	246

TABLE OF CONTENTS (Cont'd.)

	Page
APPENDIX IX WELDMETAL FRACTURE TOUGHNESS DATA	249
APPENDIX X HEAT-AFFECTED ZONE FRACTURE TOUGHNESS DATA	255

LIST OF FIGURES

<u>FIGURE</u>		<u>PAGE</u>
1	Layout, Heat 1, Plate 1	8
2	Layout, Heat 1, Plate 2	9
3	Heat A Plate Layout	10
4	Layout, Heat B, Plate 1	11
5	Layout, Heat B, Plate 2	12
6	Uniaxial Tensile Test Specimen, 0.505-in Diameter Round Bar	13
7	Partial Thickness Crack Fracture Toughness Specimen - 48" x 4" x 3/4"	14
8	Partial Thickness Crack Fracture Toughness Specimen - 24" x 3" x 3/4"	15
9	8" x 11/16" x 5/16" Partial Thickness Crack Fracture Toughness Specimen	16
10	Uniaxial Tensile Test Specimen 0.250-in. Diameter Round Bar	17
11	Diagram Showing Visual Defects, Pits and Scars, Heat B, Plate 1 - Side 1	26
12	Diagram Showing Visual Defects, Pits and Scars, Heat B, Plate 1 - Side 2	27
13	Diagram Showing Visual Defects, Pits and Scars, Heat B, Plate 2 - Side 1	28
14	Diagram Showing Visual Defects, Pits and Scars, Heat B, Plate 2 - Side 2	29
15	As-Received Heat A Plate-Transverse Sections Illustrating Characteristic Banded Appearance and Inclusions	30
16	As-Received Heat B Plate - Transverse Sections Illustrating Microstructure and Inclusions	31
17	Effect of Aging Time at 875°F on The Uniaxial Tensile Properties of Heat A 18Ni-7Co-5Mo Airmelted Plate	38

LIST OF FIGURES (Cont'd.)

<u>FIGURE</u>		<u>PAGE</u>
18	Effect of Aging Time at 900°F on the Uniaxial Tensile Properties of Heat A 18Ni-7Co-5Mo Airmelted Plate	39
19	Effect of Aging Time at 950°F on the Uniaxial Tensile Properties of Heat A 18Ni-7Co-5Mo Airmelted Plate	40
20	Effect of Aging Time at 875°F on the Uniaxial Tensile Properties of Heat B 18Ni-7Co-5Mo Airmelted Plate	41
21	Effect of Aging Time at 900°F on the Uniaxial Tensile Properties of Heat B 18Ni-7Co-5Mo Airmelted Plate	42
22	Effect of Aging Time at 950°F on the Uniaxial Tensile Properties of Heat B 18Ni-7Co-5Mo Airmelted Plate	43
23	Effect of Aging Time at Temperatures From 875. to 1000°F on the Uniaxial Tensile Properties of Heat I 18Ni-7Co-5Mo Airmelted Plate	44
24	Effect of Aging Time and Temperatures on Ultimate Tensile Strength of Heats I, A, and B Plate	45
25	Effect of Aging Time on Percent Reduction in Area and Percent Elongation for Heats A and B Plate	46
26	Effect of Aging Temperature and Time on Hardness for Heats I, A, and B Plate	47
27	Relationship Between Measured Crack Area and Calculated Crack Area	52
28	Effect of Crack Depth on the Net Fracture Stress of 3/4-in. Thick Airmelted 18Ni-7Co-5Mo Plate, Heats I and A Plate	53
29	Effect of Crack Depth on the Net Fracture Stress of Heat B 18Ni-7Co-5Mo Plate, 875°F Aging	54
30	Effect of Crack Depth on the Net Fracture Stress of Heat B 18Ni-7Co-5Mo Plate 900°F Aging	55

LIST OF FIGURES (Cont'd.)

<u>FIGURE</u>		<u>PAGE</u>
31	Effect of Aging Treatment on K_{IC} of the Three Plate Heats	56
32	Comparison of Experimental and Theoretical Dependence of Fracture Stress on Crack Size	58
33	Partial Thickness Crack Fracture Toughness Test Specimen (8" x 1/2" x 1/8")	62
34	Fracture Strength vs. Crack Depth Type W2 Welds in 3/4" 18Ni-7Co-5Mo Airmelted Plate	63
35	Orientations of the 8" x 11/16" x 5/16" Partial Thickness Crack Specimens	64
36	Effect of Crack Depth on Net Fracture Stress for Two Specimen Configurations, Several Orientations and Aging Treatments - Heat B Plate	65
37	Relationship Between Crack Length and Depth in Partial Thickness Crack Specimens	66
38	Effect of K_{IC} Method of Calculation on the Dependence of K_{IC} on Crack Size for 8-in. and 24-in. PTC Specimens	70
39	Effect of Relative Crack Area, Specimen Orientation, and Aging Treatment on K_{IC} - Heat B Plate	71
40	Fracture Surfaces of 8" x 11/16" x 5/16" and 24" x 3" x 3/4" PTC Specimens Illustrating Representative Appearance	72
41	Typical 24" x 3" x 3/4" PTC Fracture Surfaces Heats A and B Plate	74
42	Setup for Welding Flat Plate	80
43	Joint Configuration and Welding Conditions for Types W1 and W2 Welds	83
44	Joint Configuration and Welding Conditions for Type W3 Welds	84
45	Joint Configuration and Welding Conditions for Type W4 Welds	85
46	Joint Configuration and Welding Conditions for Type W5 Welds	86

LIST OF FIGURES (Cont'd.)

<u>FIGURE</u>		<u>PAGE</u>
47	Joint Configuration and Welding Conditions for Type W6 Welds	87
48	Joint Design and Welding Conditions for Types W7, W8, and W9 Welds	88
49	10" x 3/4" x 3/4" Tensile Specimen	90
50	Transverse Cross Section Illustrating the Location of the 0.250-inch Diameter All-Weldmetal Tensile Specimen	91
51	Effect of Aging Time at 875°F of Type W9 All Weldmetal Uniaxial Tensile Properties	97
52	Effect of Aging Time at 900°F on Type W9 All Weldmetal Uniaxial Tensile Properties	98
53	Effect of Aging Time at 950°F on Type W9 All Weldmetal Uniaxial Tensile Properties	99
54	Typical Columnar Features on Type W9 All Weldmetal Tensile Specimen Fracture Surface	101
55	Effect of Aging Time at 875°F on All Weldmetal Uniaxial Tensile Properties of Deposits in Heat B Plate - W7 and W8 Welds	103
56	Effect of Aging Time at 900°F on All Weldmetal Uniaxial Tensile Properties of Deposits in Heat B Plate - W7 and W8 Welds	104
57	Effect of Aging Time at 950°F on All Weldmetal Uniaxial Tensile Properties of Deposits in Heat B Plate - W7 and W8 Welds	105
58	Effect of Aging Time and Temperature on Weld-metal Hardness	106
59	Hardening Response Impairment in Plate Heat-Affected Zone Type W2 Welds in Heat I Plate	110
60	Effect of Welding Energy Input on Minimum Heat-Affected Zone Tensile Strength After 900°F, 12 Hours Aging	111
61	Across-the-Joint Tensile Specimen Illustrating Typical Location of Tensile Fracture in Vicinity of Heat-Affected Zone Eyebrow	112

LIST OF FIGURES (Cont'd.)

<u>FIGURES</u>		<u>PAGE</u>
62	Effect of Aging Time at 875, 900, and 950°F on the Across-the Joint Tensile Properties of Type W2 Welds Deposited in Heat I Plate	113
63	Effect of Aging Time at 875°F on the Across-the-Joint Tensile Properties of Types W8 and W9 Welds deposited in Heat B Plate	114
64	Effect of Aging Time at 900°F on the Across-the Joint Tensile Properties of Types W7, W8, and W9 Welds Deposited in Heat B Plate	115
65	Effect of Aging Time at 950°F on the Across-the Joint Tensile Properties of Types W7, W8, and W9 Welds Deposited in Heat B Plate	116
66	PTC Specimens and Crack Locations Used for Weldmetal Fracture Toughness Evaluations	120
67	Effect of PTC Specimen Type and Orientation on the Net Fracture Stress of Weldmetal Deposited in Heat B Plate	121
68	Macrosection of Type W6 Weld	124
69	Macrosection of Type W4 Weld	125
70	Macrosection of Type W7 Weld	126
71	Macrosection of Type W9 Weld	127
72	Effect of Weldmetal Composition and Deposition Technique on the Net Fracture Strength of Weld Deposits in Heat I Plate	128
73	Dependence of Net Fracture Stress on Crack Depth for Weldmetal Aged at 875°F for Times Ranging from 1 1/2 to 12 Hours - W7 and W8 Welds	131
74	Dependence of Net Fracture Stress on Crack Depth for Weldmetal Aged at 900°F for Times Ranging from 1 1/2 to 12 Hours - W7 and W8 Welds	132
75	Dependence of Net Fracture Stress on Crack Depth for Weldmetal Aged at 950°F for Times Ranging from 1 1/2 to 12 Hours - W7 and W8 Welds	133

LIST OF FIGURES (Cont'd.)

<u>FIGURES</u>		<u>PAGE</u>
76	Effect of 875°F Aging Time on K_{IC} of Weldmetal Deposited in Heat B Plate - W7 and W8 Welds	134
77	Effect of 900°F Aging Time on K_{IC} of Weldmetal Deposited in Heat B Plate - W7 and W8 Welds	135
78	Effect of 950°F Aging Time on K_{IC} Weldmetal Deposited in Heat B Plate - W7 and W8 Welds	136
79	Effect of Crack Depth on the Net Fracture Strength of Weldmetal as Influenced by Re-solution Heat Treatment	137
80	Effect of Crack Depth on Net Fracture Stress in Heat-Affected-Zone Regions of Weldments in Heat B Plate - Longitudinal PTC Specimens	140
81	Effect of Crack Depth on Net Fracture Stress in Heat-Affected-Zone Regions of Weldments in Heat B Plate-Transverse PTC Specimens	141
82	Effect of Crack Depth on Net Fracture Stress in Heat-Affected-Zone Regions of Weldments in Heat B Plate-Transverse and Longitudinal PTC Specimens	142
83	Setup for Forming Ten Foot Radius Contoured Segments Using Bending Press	145
84	Joint Configuration and Welding Conditions for Contoured Plate Welds	146
85	Contoured Plate Welding Fixture for Inside Weld	147
86	Contoured Plate Fixture for Outside Weld	148
87	Typical Spatter Accumulation on the Underside of the Trailing Shield and Torch Nozzle After the Completion of One Contoured Plate Weld	149
88	Typical Lack-of Fusion Defect in Contoured Plate Tensile Specimens	153
89	Typical Porosity Defect in Contoured Plate Tensile Specimens	154

LIST OF FIGURES (Cont'd.)

<u>FIGURES</u>		<u>PAGE</u>
90	Dependence of Net Fracture Stress on Crack Depth for Contoured Plate Weldmetal Aged at 900°F for 3 Hours	157
91	Effect of Environment of Net Fracture Stress of Plate and Type W7 Weldments Under Sustained Load	164
92	Histogram Illustrating Frequency of Failures in Various Time Ranges for Specimens Subjected to Sustained Loads	165
93	Angular Inclusions Observed on the Fracture Surfaces of 3/4-in. Thick 18Ni-7Co-5Mo Plate	168
94	Typical Dimpled Structure on the Fracture Surface of 3/4-in Thick 18Ni-7Co-5Mo Plate	169
95	Unusually High Concentration of Angular Inclusions on the Rapid Propagation Fracture Surface Through a Heat-Affected Zone	170
96	Typical Aged Weldmetal Microstructure	172
97	Aged Weld Deposit Fracture Surface Illustrating a High Concentration of Angular Inclusions	174
98	Aged Weld Deposit Fracture Surface Illustrating The Angular Phase and Its Associated Microstructure	175
99	Aged Weld Deposit Fracture Surface Illustrating The Angular Phase and Its Associate Microstructure	176
100	Selected Area Diffraction of Angular Inclusion Segregates	182
101	Typical Extraction Fractograph from Weldmetal	183
102	Back Scattered Electron Scanning Image	188
103	Phase Diagram of TiC and TiN Based on Available Data	192

LIST OF TABLES

<u>TABLE</u>		<u>PAGE</u>
I	Chemical Compositions of Heats I, A, and B Airmelted 18Ni-7Co-5Mo 3/4-in Thick Plate	6
II	Ultrasonic Thickness Traverse for Heat I, Plate 1	20
III	Ultrasonic Thickness Traverse for Heat I - Plate 2	21
IV	Ultrasonic Thickness Traverse for Heat A Plate	22
V	Ultrasonic Thickness Traverse for Heat B, Plate 1	23
VI	Ultrasonic Thickness Traverse for Heat B, Plate 2	24
VII	Inclusion Content Determined in Accordance with ASTM Designation E-45 Method A, Heats I, A, and B Plate	33
VIII	Tensile Data on Heats A and B Plate to Check Specification Conformance	34
IX	Chemical Compositions of Weldwires	77
X	Tabulation of Mechanical Test Specimens Machined from Heat B Welded Test Plates	78
XI	Welding Procedures and Weldmetal Chemical Compositions	81
XII	Longitudinal All Weldmetal Tensile Data, Summary - Type W9 Welds in Heat B Plate	95
XIII	Code Definitions for Various Types of Observed Failures	96
XIV	Tensile Property Data on Types W7 and W8 Welds- 10" x 3/4" x 3/4" Specimens	117
XV	Tensile Property Data for Contoured Plate Welds	152
XVI	Fracture Toughness Property Data for Contoured Plate Welds	156
XVII	Effect of Various Environments on Net Fracture Strength of Plate and W7 Type Weldments Under Sustained Load	161
XVIII	Comparison of Interplanar Spacings Calculated from Selected Area Electron Diffraction Patterns	184

LIST OF TABLES (Cont'd.)

TABLE

PAGE

XIX

Some Physical and Thermodynamic Properties of
Titanium Carbide and Titanium Nitride

193

1.

INTRODUCTION

This program was conducted under the sponsorship of NASA, Space Vehicle Research and Technology. The purpose was to evaluate the properties of airmelted 18Ni-7Co-5Mo maraging steel plate and welds, and to investigate the associated processing techniques for potential application to space launch vehicle construction. Welding was performed both by Douglas Aircraft Co., and Newport News Shipbuilding and Dry Dock Co., (acting as a subcontractor) to determine the reproducibility of welding procedures.

During the last two years, Douglas Aircraft Co. has been active in company sponsored research and development programs to evaluate 3/4-inch thick airmelted 18Ni-7Co-5Mo plate. The programs were undertaken to determine the properties and fabricability of the alloy, and to define potential problems areas.

Under the current NASA contract, 3/4-inch thick plate from two new heats of airmelted 18Ni-7Co-5Mo steel was evaluated and the results related to those previously obtained.

Included in the present program were evaluations of the effects of aging treatment on uniaxial tensile properties and fracture toughness of both plate and welds. Welds were deposited in plate from one of the two new heats using the inert-gas shielded metal arc technique, using filler wire selected during the earlier company-sponsored program. Sustained-load behavior of plate and weldments exposed to various environments was also investigated.

Fracture toughness results generated using subsize partial thickness

1.

INTRODUCTION (Cont'd.)

crack (PTC) specimens were compared to those obtained with large PTC specimens. The results demonstrated the suitability of the subsize specimen.

Metallurgical evaluations were undertaken employing novel electron fractographic techniques. These studies resulted in the tentative identification of titanium nitride as the cause of inferior weld-metal fracture toughness.

The first progress report (Ref. 23) presented data on Heat I and preliminary data on Heat A. Included in the report was information on chemistry, metallographic inspection, dimensional and soundness examination, uniaxial tensile properties, fracture toughness and plane-strain toughness characteristics.

Progress Report No. 2 (Reference 24) presented the remainder of the data on Heat A, preliminary data on Heat B, and initial inspection results on the weld wire. Information on Heat A included examination of fracture surfaces of the 24" x 3" x 3/4" partial thickness crack (PTC) coupons by use of the electron microscope. Heat B results included data on uniaxial tensile properties, fracture toughness, chemical analysis and metallographic examination.

This final report includes the data presented previously in Progress Reports 1 and 2 and presents all new data, a substantial portion of which pertains to weld evaluations.

The results of this study indicate that several problem areas

I. INTRODUCTION (Cont'd.)

require further study. Among the more important are those related to: a) banding and the prevalence of titanium nitride inclusions in plate, b) the effects of titanium nitride inclusions in weldmetal, c) control and reproducibility of the aging response of plate with respect to strength and fracture toughness and, d) environmental influence on fracture, especially with respect to welds.

2. EVALUATION OF PLATE PROPERTIES

Data are presented in this section describing the mechanical properties of plate from three different heats of 18Ni-7Co-5Mo alloy steel. Tensile, fracture toughness, hardness, and plate quality properties are described. Effects of aging treatment and specimen orientation (with respect to rolling direction) are comprehensively treated.

2.1 Plate Properties

Plate from three different heats of air melted 18Ni-7Co-5Mo steel was evaluated. The three heats were produced by U.S. Steel Corporation by electric furnace, air melting techniques. They are referred to throughout this report as Heats I, A, and B.

Heat I plate was part of a twenty-two ton melt donated by U.S. Steel Corporation for a previous company sponsored program (References 5 and 6). Two plates, approximately 240-in. x 110-in. x 3/4-in. were used in this evaluation.

Heat A material was received as one air melted plate approximately 84-in. x 60-in. x 3/4-in.

Heat B material was procured in accordance with Douglas' tentative specification DMS 1835 (Appendix I). The material was received in the form of two air melted plates, hereafter designated plates 1 and 2. One plate was 348-in. x 120-in. x 3/4-in. and the other was 300-in. x 120-in. x 3/4-in.

2.1 Plate Properties (Cont'd.)

Table I presents the chemical compositions of the three heats. Heat I chemistry was determined by the supplier and the chemistries of Heats A and B were determined by the supplier, Douglas and Newport News. The analyses conform quite closely to the requirements in Appendix I. The titanium contents were purposely selected for Heats A and B to bracket the nominal range for the 18Ni-7Co-5Mo alloy. Heat I contains the nominal amount (0.46), Heat A is near the lower limit (0.40) and Heat B is near the upper limit (0.55). Also in Heat B the cobalt and molybdenum are at the upper limits and aluminum is slightly higher than DMS 1583 specifies.

2.2 Plate Inspection Procedures

The plates were received from the mill at Newport News Shipbuilding and Dry Dock Co. wrapped in rust inhibiting paper. All plates were visually inspected and any defects such as pits and inclusions were recorded. The plates were then ultrasonically inspected for thickness uniformity and soundness. Pulse-echo techniques were employed for test of soundness using full saturation back reflection and a rejection criteria of 10 percent loss of back reflection. Inspection points were located on a six inch grid intersect.

2.3 Plate Layout

Figure 1 through 5 schematically illustrate the plate layouts and specimen coding used in this program. Plasma arc cutting and abrasive sawing were used to rough cut the specimen blanks prior to finish machining. Liberal allowances were provided to permit

TABLE I

CHEMICAL COMPOSITIONS OF HEATS I, A, AND B AIRMELTED 18Ni-7Co-5Mo 3/4"-THICK PLATE

CHEMICAL COMPOSITION, WEIGHT PERCENT

HEAT CODE	U.S.S. HEAT NO.	C	Mn	P	S	Si	Cu	Ni	Cr	Mo	Al	Ti	Co	B	Zr	N ₂	SOURCE
PLATE																	
I	X13371	0.02	0.04	0.004	0.009	0.08	0.05	17.83	0.01	4.70	0.11	0.46	7.41	NA	NA	NA 0.005	U.S.S. Douglas U.S.S.
A	X14359	0.02	0.03	0.005	0.005	0.09	0.11	17.73	0.01	4.80	0.07	0.39	7.40	0.004	0.01	NA	
A	X14359	0.01	0.06	0.002	0.006	0.07	NA	17.35	NA	4.79	NA	0.41	7.81	NA	0.01	0.006	Douglas
A	14359	0.02	0.06	0.009	0.004	0.08	0.05	17.83	NA	4.68	0.15	0.39	6.98	0.0004	0.0022	NA	Newport News
B	52911	0.02	0.02	0.008	0.009	0.03	0.14	18.11	NA	4.90	0.09	0.58	NA	0.003	0.01	LADLE CHEMISTRY	U.S.S.
B	52911	0.02	0.02	0.004	0.009	0.03	0.15	18.09	NA	4.90	0.08	0.49	8.07	NA	NA	CHECK CHEMISTRY	U.S.S.
B	52911	0.01	0.007	0.005	0.013	NIL	NA	17.90*	NA	5.0*	0.18	0.58 0.54*	8.38*	NA	NA	0.009	Douglas
B	52911	0.02	0.035	0.006	0.010	0.06	0.07	17.67	NA	4.85	0.16	0.56	7.36	0.01	NIL	NA	Newport News

* Spectrographic Analysis

NA No Analysis

2.3 Plate Layout (Cont'd.)

the removal of all material affected by the heat of plasma arc cutting.

2.4 Test Specimen Types and Testing

Uniaxial tensile data for parent plate were obtained for the three heats using standard ASTM 0.505-in. diameter specimens illustrated in Figure 6. Fracture toughness evaluations on Heat 1, parent plate and weldments, were conducted using 48-in. x 4-in. x 3/4-in. partial thickness crack (PTC) specimens shown in Figure 7. Heat A parent plate fracture toughness properties were investigated by using the 24-in. x 3-in x 3/4-in. PTC specimens, Figure 8. Heat B parent plate and weldment fracture toughness evaluation also employed the use of the 24-in PTC as well as a slab-type 8-in, PTC coupon Figure 9. Uniaxial tensile data on weldments were obtained with 0.505-in. diameter specimens for across-the-joint tests Subsize 0.250-in. diameter specimens, (Figure 10) were used for all-weld-metal tensile evaluation described in later sections. Sustained load evaluations employed the 24-in and the 8-in PTC coupons.

Load rates were maintained at approximately 100,000 PSI per minute for both tensile and fracture toughness testing. All tests that were conducted in the ambient atmosphere were accomplished at temperatures ranging from 70 to 80°F, and with relative humidity from about 25 to 65%.

LAYOUT, HEAT-1, PLATE NO. 1

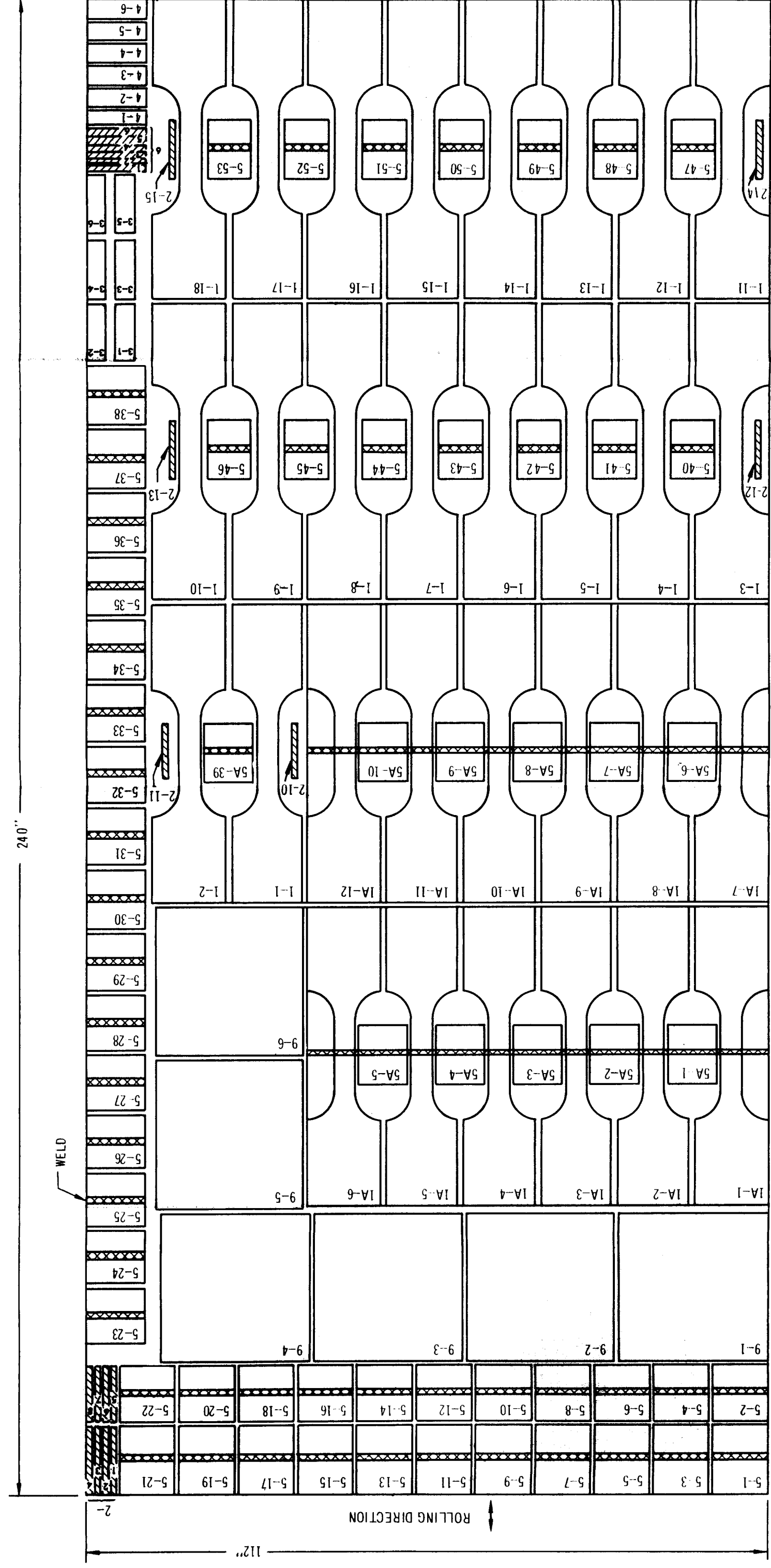
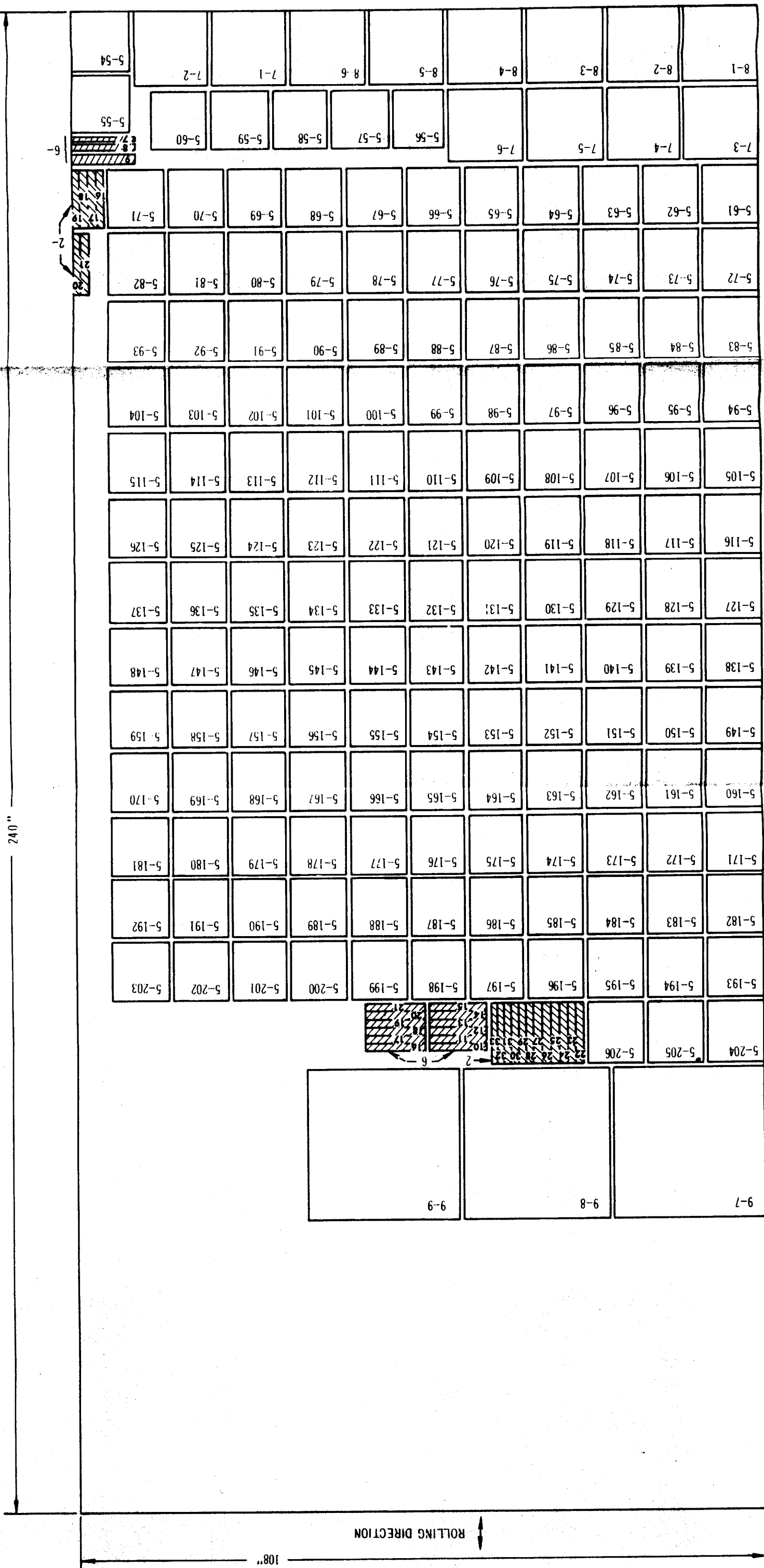


FIGURE 1

9



HEAT "A" PLATE LAYOUT

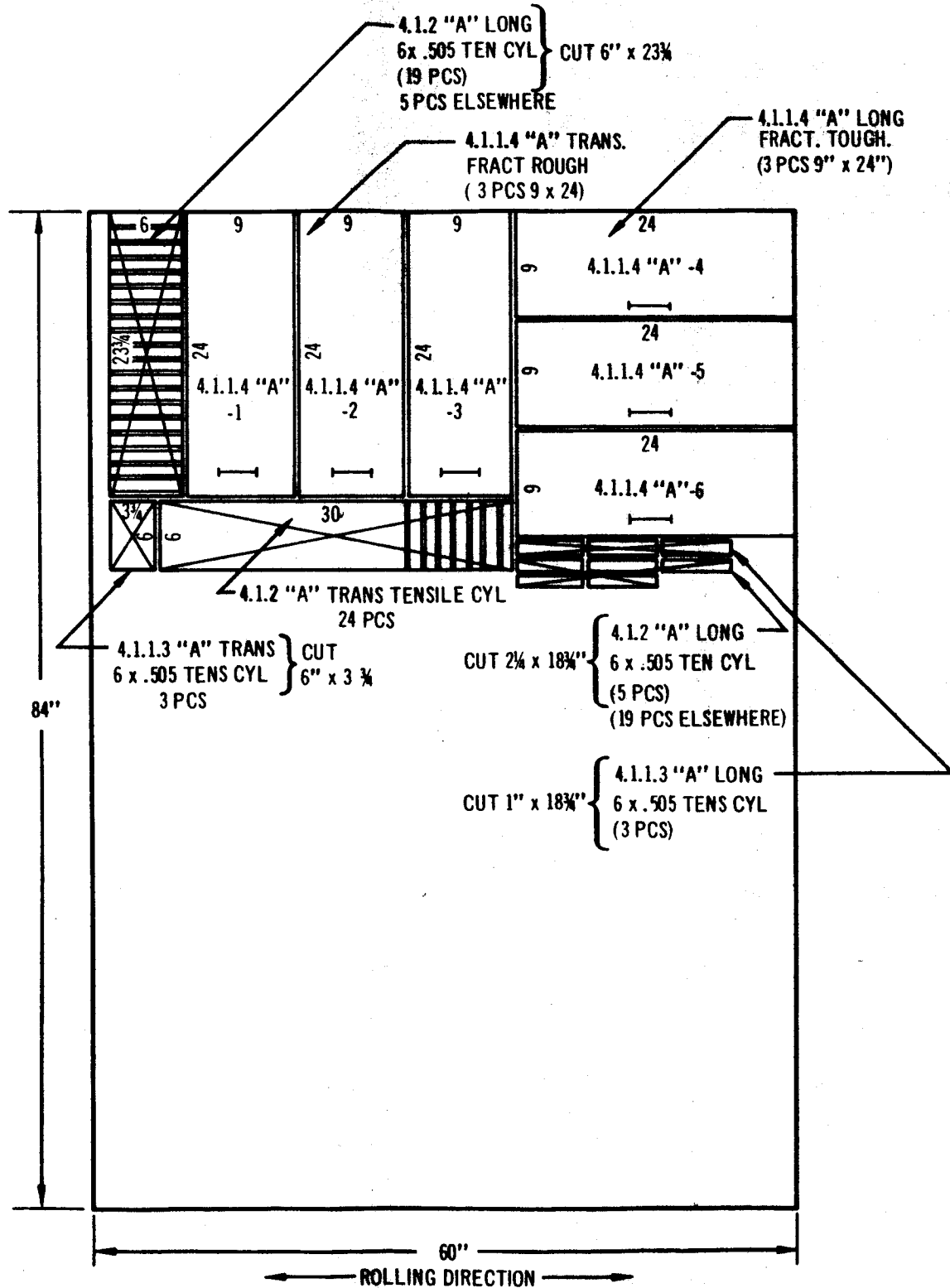


FIGURE 3

ROLLING DIE



LAYOUT, HEAT-B, PLATE NO. 2

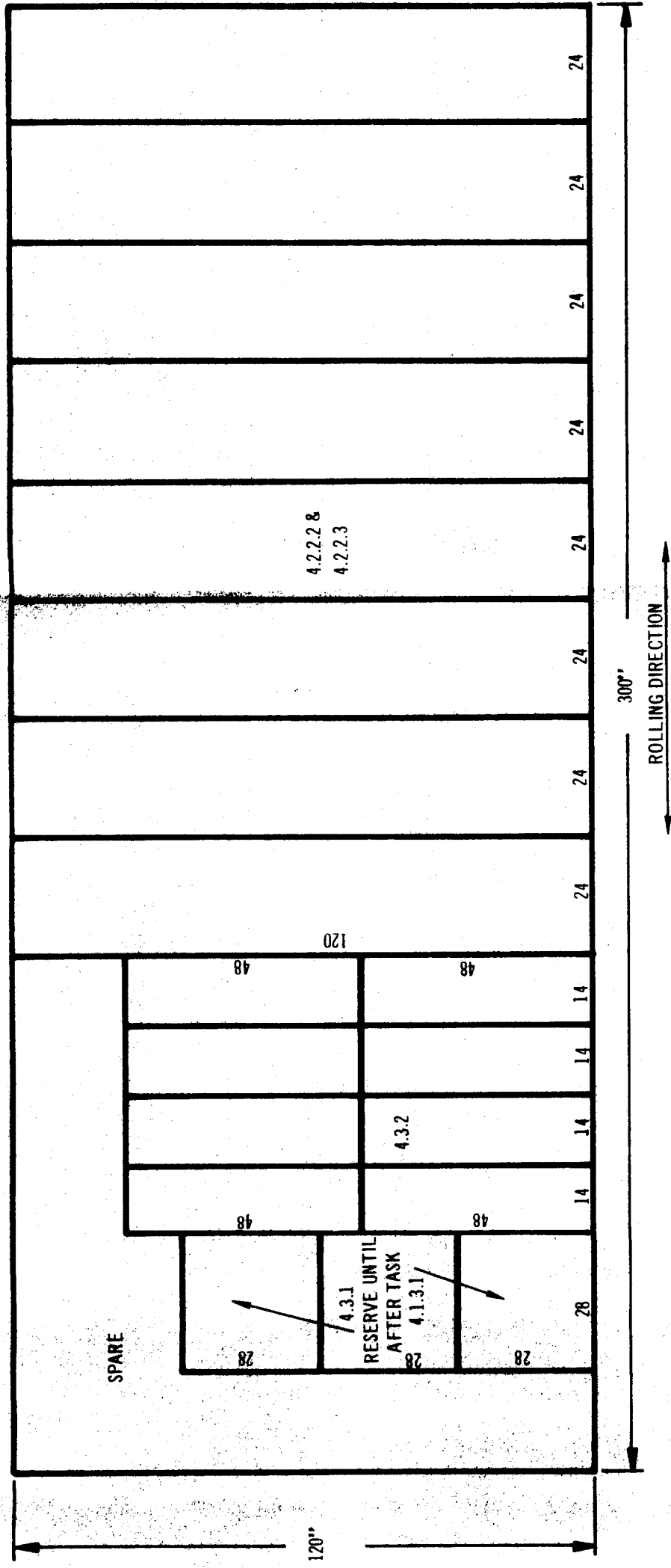


FIGURE 5

UNIAXIAL TENSILE TEST SPECIMEN
0.505-IN. DIAMETER ROUND BAR

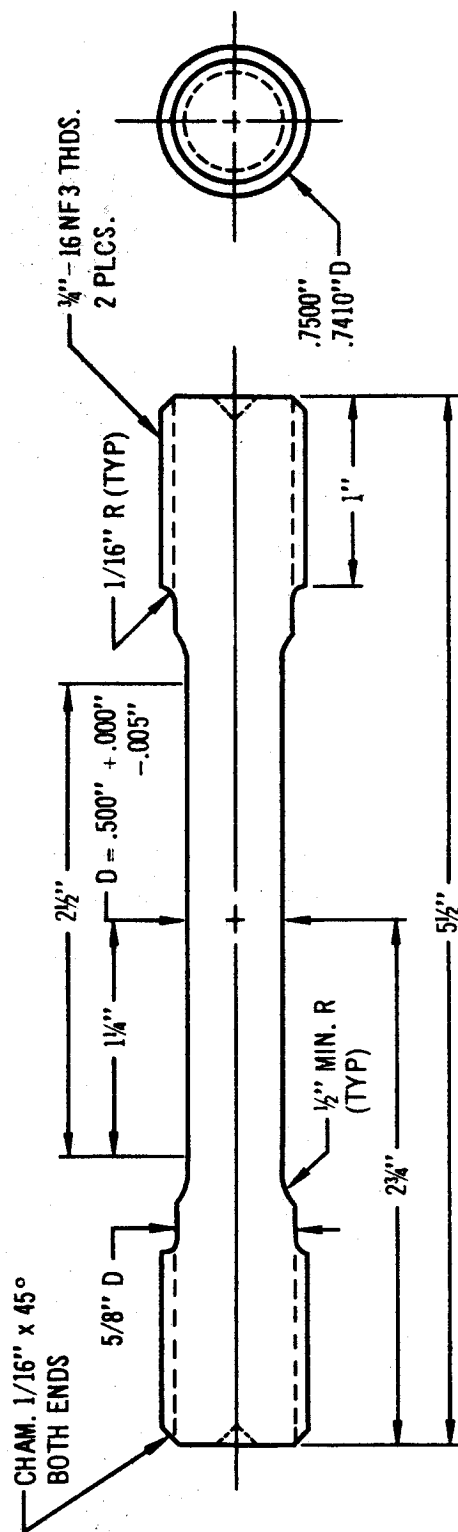


FIGURE 6

Technical drawing of a mechanical part, likely a bracket or support, showing dimensions and features. The drawing includes the following specifications:

- Overall Dimensions:**
 - Top horizontal dimension: 21"
 - Bottom horizontal dimension: 20"
 - Left vertical dimension: 48"
 - Right vertical dimension: 48"
- Internal Features and Dimensions:**
 - Top circular hole: 750" D.I.A.
 - Bottom circular hole: 4.005" D.I.A.
 - Top horizontal slot: 10.000" wide, 5.000" deep.
 - Bottom horizontal slot: 12" wide, 6" deep.
 - Top horizontal distance from centerline to hole center: 12"
 - Bottom horizontal distance from centerline to hole center: 8"
 - Top horizontal distance from centerline to slot center: 6"
 - Bottom horizontal distance from centerline to slot center: 6"
 - Top horizontal distance from centerline to slot edge: 5.000"
 - Bottom horizontal distance from centerline to slot edge: 4.000" ± .005"
 - Top horizontal distance from centerline to slot edge: 4.000" ± .005"
 - Bottom horizontal distance from centerline to slot edge: 2.000"
 - Top horizontal distance from centerline to slot edge: 4.000" ± .005"
 - Bottom horizontal distance from centerline to slot edge: 4.000" ± .005"
- Labels and Notes:**
 - "LOCATION OF PART THRU CRACK" with arrows pointing to the top and bottom horizontal slots.
 - "4" R." indicating a 4-inch radius for the bottom horizontal slot.

FIGURE 7

Technical drawing of a mechanical part with the following dimensions and features:

- Overall width: 24"
- Overall height: 12"
- Top edge: 3/4" D (fillet)
- Bottom edge: 3/4" D (fillet)
- Left side: 1" thick, 4 1/2" wide, 3" from bottom edge.
- Right side: 1" thick, 4" wide, 2" from bottom edge.
- Internal features: Two circular holes, each 3" R (radius), 3.005" ± .000" diameter, 3.000" from the bottom edge.
- Crack location: Indicated by a line and the text "CRACK LOCATION".

15

8" X 11/16" X 5/16" PARTIAL THICKNESS CRACK FRACTURE TOUGHNESS SPECIMEN

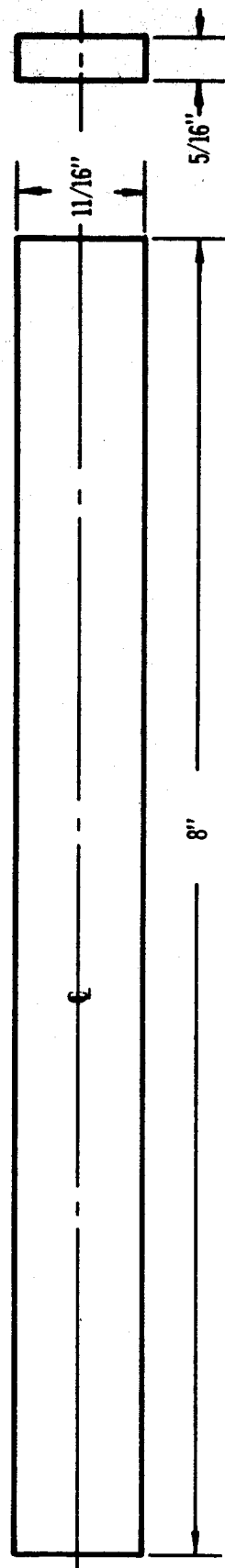


FIGURE 9

UNIAXIAL TENSILE TEST SPECIMEN
0.250-IN. DIAMETER ROUND BAR

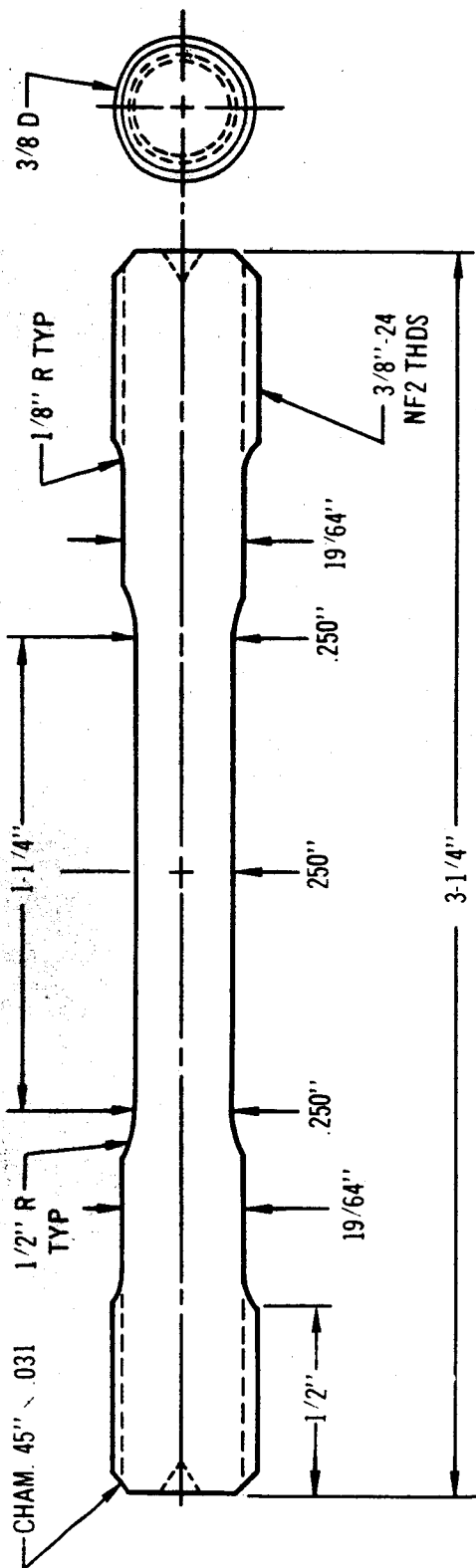


FIGURE 10

2.5

Heat Treatment Procedures

All aging heat treatments were performed on as-machined specimens taken from the as-received, mill-annealed, plate. The mill anneal was performed at 1500°F for 1 hour followed by air cooling. All specimens were subsequently aged at temperatures ranging from 875 to 1000°F in convective air furnaces. Specimens were batch loaded, when possible, into a hot furnace which had been previously heated to the desired aging temperature. The specimens were then allowed to come to thermal equilibrium with the furnace before the nominal aging period was started. Temperature was monitored by means of independent thermocouples located at different positions within the furnace, and by thermocouples located on the test parts.

The attainment of thermal equilibrium took from 30 to 45 minutes for 0.250 and 0.505-inch diameter round bar and 8-inch PTC specimens. Approximately 1 1/2 hours was required for the 3/4" thick fracture toughness specimens. Once thermal equilibrium was achieved, temperature control was maintained to within $\pm 7^{\circ}\text{F}$. The aging times reported are those recorded subsequent to the attainment of thermal equilibrium. All specimens were cooled to room temperature in ambient still air following the aging heat treatment.

2.6

Preparation of Partial-Thickness Crack Specimens

Partial thickness cracks were induced in the fracture toughness specimens by means of a flexural fatigue procedure similar to that described in Douglas Laboratory Procedure, DLP 13.822 presented in Appendix III. The DLP presents the procedure used for sheet material,

2.6 Preparation of Partial-Thickness Specimens

rather than plate. However, the general procedures are identical for plate, except that the fixtures are more massive.

Approximately 5,000 to 10,000 cycles were required to initiate a visible crack, and up to 50,000 cycles were needed to achieve the desired crack size. Flexure was performed at maximum fiber stresses ranging from 120,000 to 160,000 psi (flexed in aged condition).

2.7 Results and Discussion

2.7.1 Dimensional, Soundness and Hardness Inspection

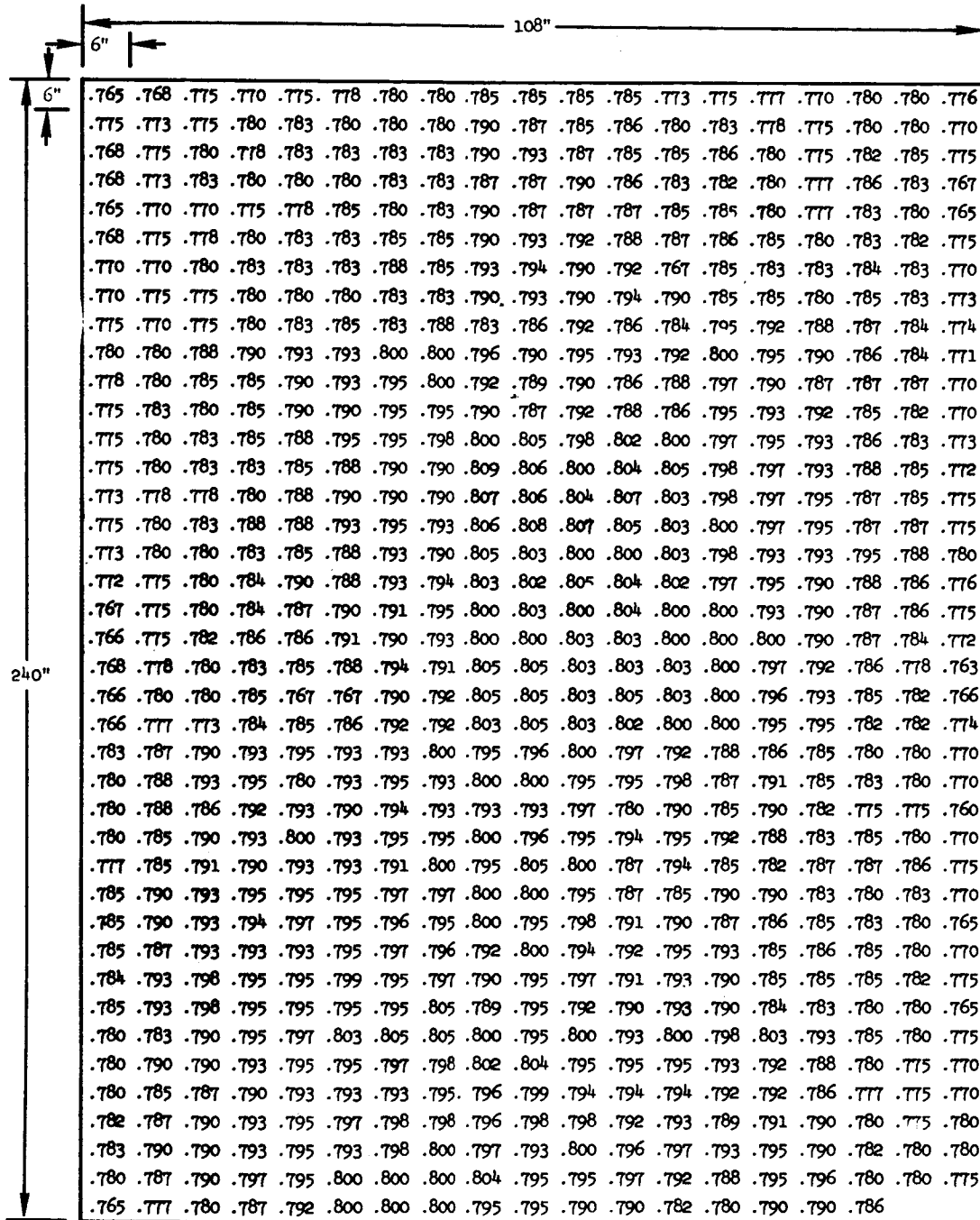
Ultrasonic inspection failed to indicate any defects which could be rejected based upon DMS 1835, in either Heat 1, A or B Plate.

Thickness transverse data are tabulated in Tables II thru VI. The tolerances for Heat 1 plates exceed the maximum specified in AMS 2252 (plus 0.044, minus 0.010-in.) ranging between 0.750-in. plus 0.059, minus zero for plate 1 and plus 0.088, minus zero for plate 2.

Heat A plate thickness ranges between 0.750-in. plus 0.044, minus zero. The latter bordered on the upper limits of AMS 2252 requirements. Heat B plate thickness ranged between 0.750-in. plus 0.150, minus zero. However, the excessive thickness was located in one region only, and the rest of the points were nominally 0.750-in plus 0.050-in, minus zero. Because of the experimental nature of this program the material was accepted. However, under other conditions the heat might have been rejected because the plate thickness tolerances exceeded the limits of AMS 2252.

TABLE 11

ULTRASONIC THICKNESS TRAVERSE FOR HEAT-1, PLATE 1



.765	.768	.775	.770	.775	.778	.780	.780	.785	.785	.785	.785	.773	.775	.777	.770	.780	.780	.776
.775	.773	.775	.780	.783	.780	.780	.780	.790	.787	.785	.786	.780	.783	.778	.775	.780	.780	.770
.768	.775	.780	.778	.783	.783	.783	.783	.790	.793	.787	.785	.785	.786	.780	.775	.782	.785	.775
.768	.773	.783	.780	.780	.780	.783	.783	.787	.787	.790	.786	.783	.782	.780	.777	.786	.783	.767
.765	.770	.770	.775	.778	.785	.780	.783	.790	.787	.787	.787	.785	.785	.780	.777	.783	.780	.765
.768	.775	.778	.780	.783	.783	.785	.785	.790	.793	.792	.788	.787	.786	.785	.780	.783	.782	.775
.770	.770	.780	.783	.783	.783	.788	.785	.793	.794	.790	.792	.767	.785	.783	.783	.784	.783	.770
.770	.775	.775	.780	.780	.780	.783	.783	.790	.793	.790	.794	.790	.785	.785	.780	.785	.783	.773
.775	.770	.775	.780	.783	.785	.783	.788	.783	.786	.792	.786	.784	.795	.792	.788	.787	.784	.774
.780	.780	.788	.790	.793	.793	.800	.800	.796	.790	.795	.793	.792	.800	.795	.790	.786	.784	.771
.778	.780	.785	.785	.790	.793	.795	.800	.792	.789	.790	.786	.788	.797	.790	.787	.787	.787	.770
.775	.783	.780	.785	.790	.790	.795	.795	.790	.787	.792	.788	.786	.795	.793	.792	.785	.782	.770
.775	.780	.783	.785	.788	.795	.795	.798	.800	.805	.798	.802	.800	.797	.795	.793	.786	.783	.773
.775	.780	.783	.783	.785	.788	.790	.790	.809	.806	.800	.804	.805	.798	.797	.793	.788	.785	.772
.773	.778	.778	.780	.788	.790	.790	.790	.807	.806	.804	.807	.803	.798	.797	.795	.787	.785	.775
.775	.780	.783	.788	.788	.793	.795	.793	.806	.808	.807	.805	.803	.800	.797	.795	.787	.787	.775
.773	.780	.780	.783	.785	.788	.793	.790	.805	.803	.800	.800	.803	.798	.793	.793	.795	.788	.780
.772	.775	.780	.784	.790	.788	.793	.794	.803	.802	.805	.804	.802	.797	.795	.790	.788	.786	.776
.767	.775	.780	.784	.787	.790	.791	.795	.800	.803	.800	.804	.800	.800	.793	.790	.787	.786	.775
.766	.775	.782	.786	.786	.791	.790	.793	.800	.800	.803	.803	.800	.800	.800	.790	.787	.784	.772
.768	.778	.780	.783	.785	.788	.794	.791	.805	.805	.803	.803	.803	.800	.797	.792	.786	.778	.763
.766	.780	.780	.785	.767	.767	.790	.792	.805	.805	.803	.805	.803	.800	.796	.793	.785	.782	.766
.766	.777	.773	.784	.785	.786	.792	.792	.803	.805	.803	.802	.800	.800	.795	.795	.782	.782	.774
.783	.787	.790	.793	.795	.793	.793	.800	.795	.796	.800	.797	.792	.788	.786	.785	.780	.780	.770
.780	.788	.793	.795	.780	.793	.795	.793	.800	.800	.795	.795	.798	.787	.791	.785	.783	.780	.770
.780	.788	.786	.792	.793	.790	.794	.793	.793	.793	.797	.780	.790	.785	.790	.782	.775	.775	.760
.780	.785	.790	.793	.800	.793	.795	.795	.800	.796	.795	.794	.795	.792	.788	.783	.785	.780	.770
.777	.785	.791	.790	.793	.793	.791	.800	.795	.805	.800	.787	.794	.785	.782	.787	.787	.786	.775
.785	.790	.793	.795	.795	.795	.797	.797	.800	.800	.795	.787	.785	.790	.790	.783	.780	.783	.770
.785	.790	.793	.794	.797	.795	.796	.795	.800	.795	.798	.791	.790	.787	.786	.785	.783	.780	.765
.785	.787	.793	.793	.793	.795	.797	.796	.792	.800	.794	.792	.795	.793	.785	.786	.785	.780	.770
.784	.793	.798	.795	.795	.799	.795	.797	.790	.795	.797	.791	.793	.790	.785	.785	.785	.782	.775
.785	.793	.798	.795	.795	.795	.795	.805	.789	.795	.792	.790	.793	.790	.784	.783	.780	.780	.765
.780	.783	.790	.795	.797	.803	.805	.805	.800	.795	.800	.793	.800	.798	.803	.793	.785	.780	.775
.780	.790	.790	.793	.795	.795	.797	.798	.802	.804	.795	.795	.795	.793	.792	.788	.780	.775	.770
.780	.785	.787	.790	.793	.793	.793	.795	.796	.799	.794	.794	.794	.792	.792	.786	.777	.775	.770
.782	.787	.790	.793	.795	.797	.798	.798	.796	.798	.798	.792	.793	.789	.791	.790	.780	.775	.780
.783	.790	.790	.793	.795	.793	.798	.800	.797	.793	.800	.796	.797	.793	.795	.790	.782	.780	.780
.780	.787	.790	.797	.795	.800	.800	.800	.804	.795	.795	.797	.792	.788	.795	.796	.780	.780	.775
.765	.777	.780	.787	.792	.800	.800	.800	.795	.795	.790	.790	.782	.780	.790	.790	.786		

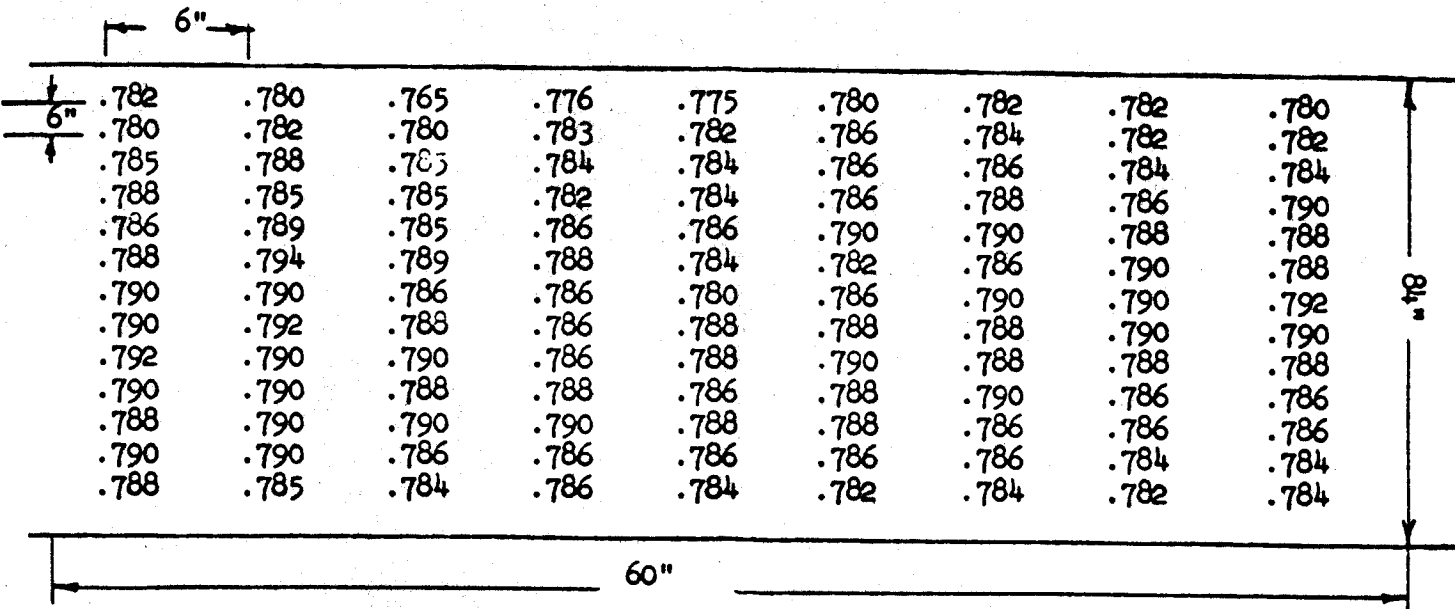
TABLE III

ULTRASONIC THICKNESS TRAVERSE FOR HEAT 1 - PLATE 2

																				112"																			
																				6"																			
																				6"																			
																				240"																			
.795	.800	.803	.805	.805	.805	.805	.805	.805	.805	.805	.805	.805	.803	.803	.800	.798	.790	.803	.795	.780																			
.795	.800	.805	.805	.808	.810	.810	.810	.810	.810	.810	.810	.805	.805	.803	.800	.793	.805	.795	.785																				
.795	.803	.810	.810	.813	.815	.815	.815	.805	.805	.805	.803	.798	.795	.800	.800	.808	.800	.788																					
.803	.808	.810	.813	.813	.815	.815	.185	.808	.818	.818	.815	.815	.810	.810	.808	.813	.805	.790																					
.803	.810	.808	.818	.818	.818	.818	.818	.825	.825	.825	.818	.815	.813	.810	.803	.815	.803	.793																					
.803	.805	.810	.815	.818	.818	.820	.820	.825	.825	.825	.823	.818	.815	.815	.810	.815	.805	.795																					
.805	.808	.810	.818	.818	.818	.820	.820	.825	.825	.825	.825	.820	.815	.818	.808	.815	.805	.800																					
.800	.803	.805	.813	.818	.820	.825	.820	.825	.825	.825	.823	.818	.815	.818	.810	.815	.810	.795																					
.803	.788	.813	.818	.818	.818	.820	.820	.830	.830	.825	.825	.820	.815	.813	.805	.818	.805	.793																					
.803	.805	.810	.813	.818	.818	.818	.818	.825	.825	.825	.823	.820	.820	.813	.808	.818	.805	.795																					
.803	.813	.815	.813	.825	.823	.823	.820	.830	.825	.823	.820	.825	.820	.815	.813	.818	.808	.795																					
.803	.808	.810	.820	.820	.823	.825	.823	.830	.830	.830	.825	.823	.820	.813	.813	.818	.810	.800																					
.808	.810	.815	.818	.820	.823	.823	.823	.835	.833	.830	.833	.823	.820	.815	.810	.818	.810	.795																					
.805	.808	.813	.820	.818	.820	.823	.823	.828	.825	.825	.828	.823	.818	.815	.810	.815	.805	.795																					
.805	.810	.813	.818	.820	.828	.825	.828	.833	.835	.830	.830	.825	.820	.815	.815	.820	.810	.803																					
.805	.813	.815	.825	.825	.828	.830	.833	.838	.838	.838	.833	.828	.828	.823	.815	.823	.813	.803																					
.805	.810	.818	.820	.823	.823	.825	.825	.833	.835	.835	.833	.828	.825	.815	.813	.820	.810	.803																					
.803	.808	.810	.820	.818	.825	.825	.825	.830	.830	.830	.825	.828	.825	.825	.820	.810	.820	.810	.800																				
.808	.810	.815	.825	.823	.828	.815	.830	.835	.838	.833	.833	.828	.823	.823	.815	.825	.810	.800																					
.808	.813	.820	.823	.825	.825	.835	.828	.835	.838	.835	.835	.830	.823	.820	.818	.823	.818	.803																					
.810	.815	.815	.820	.825	.828	.828	.828	.833	.835	.833	.830	.825	.828	.820	.815	.820	.815	.805																					
.805	.805	.810	.815	.818	.820	.820	.823	.830	.828	.825	.825	.820	.818	.818	.810	.820	.810	.795																					
.798	.803	.805	.806	.808	.813	.813	.813	.818	.818	.818	.815	.810	.810	.805	.805	.813	.800	.788																					
.795	.800	.800	.808	.808	.810	.810	.810	.818	.818	.818	.815	.813	.808	.805	.803	.810	.800	.785																					
.793	.798	.803	.805	.805	.810	.805	.808	.810	.815	.813	.810	.808	.805	.803	.800	.803	.795	.780																					
.790	.793	.798	.800	.803	.803	.803	.803	.805	.808	.810	.810	.808	.803	.800	.795	.803	.793	.780																					
.788	.790	.790	.798	.798	.803	.800	.800	.805	.805	.808	.808	.805	.803	.800	.798	.800	.790	.775																					
.785	.790	.793	.795	.795	.798	.800	.800	.800	.803	.805	.795	.800	.795	.795	.790	.798	.788	.778																					
.785	.790	.790	.793	.795	.795	.795	.795	.798	.810	.800	.800	.800	.795	.793	.790	.790	.795	.788	.775																				
.783	.788	.790	.793	.795	.795	.795	.795	.795	.795	.795	.793	.795	.793	.790	.788	.785	.793	.785	.775																				
.783	.788	.790	.793	.795	.793	.793	.793	.793	.793	.795	.790	.790	.788	.788	.783	.785	.790	.785	.770																				
.783	.788	.790	.790	.790	.793	.790	.793	.790	.790	.788	.788	.775	.783	.783	.780	.790	.783	.773	.765																				
.778	.780	.780	.783	.785	.785	.785	.785	.785	.783	.785	.783	.780	.778	.778	.775	.773	.785	.773	.765																				
.775	.780	.780	.780	.780	.780	.780	.780	.780	.778	.778	.780	.770	.773	.770	.770	.770	.780	.773	.768																				
.780	.780	.783	.785	.785	.785	.785	.785	.785	.783	.785	.785	.783	.780	.778	.778	.775	.785	.778	.768																				
.788	.790	.793	.795	.795	.795	.795	.795	.795	.808	.795	.795	.790	.790	.788	.785	.785	.795	.790	.775																				
.798	.800	.808	.808	.808	.813	.810	.808	.805	.810	.805	.803	.795	.793	.800	.790	.805	.795	.783																					

TABLE IV

ULTRASONIC THICKNESS TRAVERSE FOR HEAT-A PLATE



.782	.780	.765	.776	.775	.780	.782	.782	.780
.780	.782	.780	.783	.782	.786	.784	.782	.782
.785	.788	.785	.784	.784	.786	.786	.784	.784
.788	.785	.785	.782	.784	.786	.788	.786	.790
.786	.789	.785	.786	.786	.790	.790	.788	.788
.788	.794	.789	.788	.784	.782	.786	.790	.788
.790	.790	.786	.786	.780	.786	.790	.790	.792
.790	.792	.788	.786	.788	.788	.788	.790	.790
.792	.790	.790	.786	.788	.790	.788	.788	.788
.790	.790	.788	.788	.786	.788	.790	.786	.786
.788	.790	.790	.790	.788	.788	.786	.786	.786
.790	.790	.786	.786	.786	.786	.786	.784	.784
.788	.785	.784	.786	.784	.782	.784	.782	.784

.780	.785	.788	.783	.775	.790	.770	.785	.790	.790	.795	.793	.792	.788	.788	.792	.790	.790	.790
.780	.787	.790	.780	.775	.793	.795	.785	.783	.795	.794	.795	.793	.790	.788	.790	.770	.788	.783
.783	.783	.790	.788	.785	.793	.793	.793	.794	.796	.797	.795	.795	.793	.790	.790	.772	.787	.783
.783	.787	.786	.793	.793	.794	.792	.793	.793	.794	.794	.798	.794	.790	.790	.788	.780	.793	.790
.782	.777	.783	.790	.795	.793	.792	.792	.794	.795	.796	.797	.794	.792	.793	.777	.776	.789	.785
.780	.785	.782	.788	.787	.790	.787	.791	.793	.794	.795	.795	.793	.790	.790	.788	.790	.775	.793
.780	.780	.782	.775	.777	.784	.790	.788	.793	.795	.793	.785	.790	.790	.790	.789	.790	.793	.790
.780	.784	.787	.780	.773	.780	.785	.775	.793	.794	.794	.793	.790	.790	.794	.791	.793	.773	.790
.770	.785	.788	.790	.778	.780	.790	.787	.795	.795	.794	.794	.792	.793	.792	.790	.790	.772	.786
.773	.787	.790	.793	.775	.777	.782	.780	.797	.798	.795	.794	.794	.795	.793	.790	.793	.790	.790
.745	.787	.790	.793	.786	.785	.783	.797	.798	.798	.795	.794	.794	.794	.792	.790	.790	.790	.791
.770	.790	.790	.794	.786	.782	.785	.800	.798	.805	.795	.795	.795	.795	.793	.790	.777	.790	.790
.757	.787	.786	.794	.787	.777	.800	.795	.795	.798	.796	.795	.794	.794	.793	.787	.780	.790	.792
.764	.788	.790	.794	.795	.781	.795	.800	.795	.798	.795	.794	.793	.792	.791	.782	.792	.790	.791
.782	.787	.791	.793	.796	.786	.797	.795	.798	.798	.795	.795	.794	.795	.794	.790	.790	.794	.791
.780	.790	.792	.795	.780	.797	.797	.795	.795	.797	.797	.797	.797	.794	.793	.795	.795	.795	.790
.773	.787	.790	.793	.775	.793	.796	.795	.796	.796	.794	.795	.794	.793	.793	.795	.794	.792	.793
.770	.787	.790	.793	.793	.797	.795	.797	.797	.796	.795	.795	.795	.795	.794	.793	.792	.793	.792
.774	.786	.790	.794	.795	.796	.795	.797	.795	.796	.800	.800	.797	.795	.794	.793	.793	.792	.793
.760	.787	.793	.795	.796	.796	.800	.797	.795	.795	.795	.795	.795	.794	.794	.778	.793	.792	.790
.785	.787	.793	.795	.796	.798	.797	.798	.798	.798	.797	.796	.796	.796	.795	.784	.793	.793	.792
.783	.785	.790	.799	.799	.797	.798	.800	.797	.800	.795	.796	.787	.785	.792	.780	.793	.793	.791
.785	.790	.793	.795	.795	.797	.797	.798	.798	.793	.795	.793	.787	.785	.791	.791	.782	.783	.783
.788	.793	.796	.795	.795	.797	.796	.797	.797	.791	.797	.792	.786	.791	.793	.793	.786	.779	.790
.784	.788	.791	.795	.796	.797	.797	.798	.799	.791	.801	.788	.798	.796	.795	.795	.793	.794	.793
.785	.790	.791	.795	.796	.797	.798	.798	.799	.796	.798	.797	.797	.796	.796	.796	.796	.801	.792
.788	.790	.791	.794	.795	.797	.797	.798	.796	.791	.798	.791	.795	.798	.794	.795	.795	.795	.793
.786	.789	.793	.795	.796	.798	.797	.799	.799	.800	.801	.792	.796	.796	.800	.796	.790	.795	.793
.786	.790	.794	.796	.800	.799	.800	.800	.799	.801	.799	.801	.798	.801	.797	.799	.791	.796	.794
.784	.787	.792	.798	.798	.799	.800	.799	.801	.801	.799	.801	.802	.799	.797	.797	.798	.795	.793
.785	.790	.793	.794	.797	.803	.797	.798	.799	.799	.799	.797	.797	.800	.797	.797	.798	.796	.794
.791	.791	.793	.784	.797	.797	.798	.798	.801	.794	.800	.797	.798	.800	.800	.800	.793	.789	.800
.791	.791	.795	.790	.797	.797	.797	.797	.800	.793	.795	.800	.800	.800	.800	.800	.775	.783	.795
.791	.791	.792	.797	.797	.797	.796	.796	.796	.797	.802	.801	.801	.799	.800	.799	.789	.796	.794
.790	.792	.795	.795	.795	.796	.797	.796	.798	.797	.802	.800	.798	.800	.802	.800	.779	.800	.794
.788	.772	.790	.796	.797	.800	.800	.800	.798	.892	.800	.800	.799	.799	.799	.797	.791	.795	.793
.787	.778	.797	.797	.799	.799	.797	.798	.801	.800	.797	.796	.797	.797	.799	.787	.773	.795	.793
.788	.791	.787	.796	.796	.799	.798	.779	.801	.800	.801	.801	.798	.800	.800	.797	.786	.796	.794
.789	.792	.795	.796	.797	.799	.798	.788	.801	.802	.791	.799	.798	.799	.799	.779	.787	.799	.799
.788	.791	.794	.796	.796	.801	.798	.799	.801	.801	.790	.798	.799	.799	.797	.783	.782	.795	.794
.786	.791	.794	.796	.796	.798	.798	.797	.801	.801	.797	.795	.798	.797	.796	.783	.784	.794	.794
.785	.790	.792	.795	.797	.798	.798	.785	.801	.800	.798	.783	.800	.795	.800	.787	.787	.796	.794
.786	.790	.793	.796	.796	.798	.790	.788	.800	.799	.800	.790	.795	.795	.798	.786	.786	.795	.795
.785	.790	.792	.794	.795	.797	.800	.786	.799	.796	.796	.786	.796	.797	.796	.786	.786	.794	.793
.786	.788	.795	.795	.796	.796	.792	.782	.796	.796	.800	.790	.796	.796	.796	.790	.775	.792	.790
.785	.787	.793	.794	.795	.797	.795	.783	.797	.797	.795	.783	.796	.795	.795	.777	.779	.792	.791
.784	.790	.790	.795	.794	.793	.794	.795	.795	.780	.798	.780	.795	.795	.738	.794	.783	.792	.790
.780	.788	.790	.793	.795	.793	.794	.793	.795	.787	.795	.780	.794	.794	.794	.775	.777	.793	.790
.785	.790	.785	.793	.794	.777	.795	.796	.797	.795	.795	.785	.795	.794	.794	.790	.788	.789	.788
.787	.794	.788	.793	.792	.778	.794	.795	.793	.792	.780	.793	.795	.789	.788	.777	.774	.788	.787
.784	.785	.793	.792	.795	.777	.796	.795	.787	.795	.786	.796	.793	.794	.794	.793	.786	.794	.790
.782	.786	.791	.793	.794	.785	.794	.794	.787	.794	.794	.794	.794	.792	.765	.752	.775	.790	.790
.784	.788	.790	.793	.794	.794	.795	.795	.798	.797	.796	.782	.794	.793	.792	.780	.773	.794	.794
.787	.789	.795	.795	.797	.795	.795	.794	.798	.800	.796	.775	.795	.793	.792	.775	.747	.793	.790
.787	.787	.788	.793	.795	.794	.792	.793	.795	.797	.794	.794	.790	.783	.791	.784	.782	.793	.789
.787	.788	.789	.775	.793	.793	.793	.793	.792	.790	.793	.794	.787	.793	.786	.787	.783	.787	.787
.787	.790	.775	.780	.793	.793	.798	.794	.795	.783	.793	.794	.783	.791	.784	.796	.790	.794	.789

TABLE V - HEAT B PLATE, PLATE NO. 1
ULTRASONIC THICKNESS TRAVERSE DATA

24

6"

120"

6"

300"

.783	.784	.785	.786	.790	.791	.795	.797	.797	.796	.800	.800	.793	.794	.792	.793	.793	.793	.789
.785	.786	.786	.790	.790	.793	.795	.797	.799	.797	.797	.800	.796	.796	.793	.794	.793	.792	.793
.784	.788	.788	.791	.792	.795	.796	.797	.795	.796	.797	.800	.800	.797	.797	.797	.797	.796	.787
.786	.786	.789	.790	.791	.795	.790	.795	.797	.799	.800	.800	.795	.797	.796	.797	.796	.796	.793
.785	.784	.788	.790	.791	.792	.791	.796	.799	.799	.797	.800	.800	.797	.795	.795	.795	.794	.787
.786	.785	.787	.790	.791	.795	.796	.798	.800	.800	.797	.800	.800	.797	.795	.798	.797	.793	.787
.786	.786	.789	.790	.791	.793	.797	.798	.800	.800	.798	.798	.797	.797	.796	.795	.794	.788	.800
.785	.787	.787	.790	.791	.784	.800	.800	.800	.800	.798	.798	.797	.798	.797	.797	.797	.793	.795
.778	.785	.788	.790	.793	.793	.800	.800	.797	.801	.798	.798	.798	.797	.797	.797	.790	.792	.790
.783	.786	.787	.789	.792	.794	.797	.799	.801	.801	.800	.797	.798	.797	.796	.794	.795	.794	.792
.787	.790	.791	.791	.792	.795	.799	.797	.798	.803	.797	.798	.798	.799	.797	.795	.793	.794	.792
.787	.789	.790	.791	.793	.795	.800	.800	.796	.800	.798	.800	.800	.797	.796	.795	.795	.795	.794
.787	.790	.790	.791	.793	.795	.798	.799	.799	.799	.797	.798	.797	.798	.796	.796	.795	.792	.797
.789	.789	.790	.794	.794	.797	.799	.800	.786	.801	.797	.798	.800	.798	.799	.797	.796	.794	.787
.789	.790	.793	.795	.796	.800	.800	.801	.795	.802	.792	.797	.794	.796	.796	.794	.795	.794	.792
.783	.791	.792	.794	.795	.799	.800	.800	.801	.801	.790	.797	.799	.799	.797	.795	.793	.795	.794
.787	.790	.792	.792	.793	.797	.799	.797	.800	.801	.797	.796	.798	.797	.797	.795	.793	.794	.794
.786	.791	.790	.791	.794	.797	.798	.800	.800	.803	.800	.800	.800	.798	.799	.797	.797	.795	.794
.786	.794	.792	.794	.795	.800	.800	.801	.801	.801	.802	.800	.800	.800	.795	.793	.797	.794	.787
.784	.785	.791	.793	.795	.797	.800	.800	.801	.801	.797	.797	.798	.798	.799	.797	.796	.796	.783
.787	.791	.791	.792	.795	.800	.798	.798	.801	.800	.800	.798	.799	.799	.798	.798	.795	.795	.790
.784	.790	.793	.795	.795	.788	.800	.800	.801	.799	.789	.802	.799	.799	.798	.798	.798	.795	.790
.786	.790	.793	.794	.795	.796	.800	.800	.801	.800	.800	.800	.799	.799	.798	.797	.796	.796	.792
.784	.788	.790	.792	.796	.797	.799	.800	.798	.800	.805	.803	.800	.800	.791	.798	.798	.797	.792
.787	.787	.793	.792	.793	.795	.795	.797	.794	.800	.800	.802	.802	.802	.800	.800	.800	.800	.793
.788	.790	.790	.792	.793	.794	.795	.797	.798	.799	.803	.803	.805	.802	.802	.801	.800	.800	.794
.790	.790	.790	.791	.793	.797	.800	.798	.801	.800	.802	.805	.803	.807	.803	.801	.800	.800	.795
.785	.783	.790	.790	.793	.795	.799	.797	.798	.801	.799	.801	.799	.795	.800	.801	.800	.800	.798
.785	.783	.790	.791	.793	.795	.799	.798	.797	.800	.801	.805	.803	.801	.802	.800	.801	.800	.797
.785	.791	.790	.791	.795	.795	.796	.796	.800	.790	.796	.796	.802	.804	.802	.802	.801	.798	.798
.784	.785	.790	.790	.793	.795	.795	.796	.799	.799	.799	.800	.798	.799	.799	.800	.797	.797	.796
.782	.779	.788	.790	.790	.794	.798	.795	.796	.800	.798	.797	.798	.798	.799	.796	.797	.797	.794
.781	.782	.790	.790	.791	.794	.794	.795	.795	.796	.798	.800	.798	.798	.797	.796	.796	.797	.796
.785	.780	.784	.790	.795	.795	.796	.796	.796	.796	.800	.798	.802	.799	.798	.796	.795	.796	.794
.785	.786	.787	.790	.793	.792	.795	.796	.796	.797	.798	.799	.800	.798	.797	.795	.795	.796	.794
.784	.784	.789	.790	.791	.791	.793	.793	.796	.791	.799	.798	.798	.798	.798	.797	.796	.797	.795
.785	.780	.788	.790	.790	.791	.796	.796	.800	.800	.798	.797	.798	.798	.798	.797	.797	.797	.794
.784	.779	.783	.788	.791	.793	.794	.795	.795	.797	.800	.797	.797	.800	.798	.797	.797	.796	.794
.785	.785	.785	.785	.785	.791	.795	.794	.796	.796	.798	.797	.798	.798	.798	.797	.797	.797	.780
.785	.786	.784	.783	.791	.793	.794	.793	.795	.795	.800	.800	.796	.797	.795	.796	.797	.794	.770
.785	.785	.788	.790	.790	.793	.795	.796	.797	.797	.795	.795	.797	.797	.797	.797	.797	.796	.793
.786	.786	.788	.790	.791	.793	.795	.795	.797	.797	.798	.798	.798	.800	.798	.794	.795	.795	.793
.785	.786	.788	.790	.791	.790	.794	.795	.797	.794	.798	.798	.798	.797	.797	.797	.796	.796	.795
.781	.781	.785	.786	.788	.790	.791	.793	.793	.795	.798	.797	.797	.797	.796	.795	.795	.790	.791
.780	.782	.789	.788	.790	.790	.789	.793	.795	.795	.795	.797	.795	.797	.796	.794	.795	.796	.787
.781	.780	.789	.790	.789	.791	.795	.794	.795	.795	.900	.800	.800	.800	.796	.790	.795	.796	.787
.782	.785	.789	.789	.795	.793	.794	.796	.793	.798	.794	.798	.795	.793	.792	.794	.795	.793	.787
.784	.786	.790	.790	.793	.792	.797	.798	.797	.798	.798	.797	.797	.797	.796	.797	.797	.792	.786
.784	.786	.788	.788	.788	.789	.789	.795	.792	.796	.794	.795	.797	.794	.795	.794	.794	.790	.786

TABLE VI - HEAT 8 PLATE, PLATE NO. 2
ULTRASONIC THICKNESS TRAVERSE DATA

2.7.1 Dimensional, Soundness and Hardness Inspection (Cont'd.)

Plate surfaces were characterized by a rather tenacious, crazed mill scale which was not readily removed by grit blasting. The thickness of the scale was approximately 0.001 inches. Occasional laps and surface imbedded inclusions were found in Heat B plate. These surface defects apparently resulted during plate rolling.

Occasionally, such defects behaved as initiation sites for cracks for cracks induced during fatigue cracking of the PTC specimens. Figures 11 through 14 illustrate the visual defects found in the Heat B plates.

The hardness of the as-received Heat A plate averaged 34 Rockwell C, and ranged from 32 to 34.5 Rockwell C. These values are at the limit specified in DMS 1835. The hardness of the as-received Heat B plate averaged 30.3 Rockwell "C" and ranged from 28.5 to 32.1. These values are well within the requirements.

2.7.2 Metallographic Examination

Metallographic specimens were examined from plate in the as-received mill-annealed condition. Both transverse and longitudinal sections were examined. Figures 15 and 16 illustrate characteristic microstructures for the 18Ni-7Co-5Mo alloy. Banding is more pronounced on transverse than on longitudinal sections. The Figures illustrate types of inclusion typically observed in the 18-7-5 alloy. The type illustrated in Figure 15 is often gold colored and predominately occurs within light etching bands. The extremities of the inclusions appear to be bounded by sharp cornered voids. The voids may have been

Diagram of HEAT-B, PLATE 1 - SIDE 1. The diagram shows a rectangular plate with dimensions 120" (width) and 348" (height). The corners are labeled CORNER A, CORNER B, CORNER C, and CORNER D. The top edge is labeled CORNER B and the right edge is labeled CORNER C. The bottom edge is labeled CORNER A and the left edge is labeled CORNER D. The diagram includes several defects and dimensions:

- Top Edge (CORNER B):**
 - Defect 1: 5" vertical, 0.01 horizontal.
 - Defect 2: 25" vertical, 10" horizontal, 0.01 horizontal.
 - Defect 3: 20" vertical, 15" horizontal, 0.01 horizontal.
 - Defect 4: 60" vertical, 0.01 TO 0.02 horizontal.
 - Defect 5: 5" vertical, 0.02 horizontal.
- Right Edge (CORNER C):**
 - Defect 6: 20" vertical, 10" horizontal, 0.01 TO 0.02 horizontal.
- Bottom Edge (CORNER A):**
 - Defect 7: 10" vertical, 0.01 horizontal.
- Interior Defects:**
 - Defect 8: 40" vertical, 30" horizontal, 0.01 TO 0.02 horizontal.
 - Defect 9: 25" vertical, 0.01 horizontal.
 - Defect 10: 7" vertical, 0.03 horizontal.
- Dimensions:**
 - Top edge: 170" (left), 150" (right).
 - Right edge: 90" (top), 25" (middle), 10" (bottom).
 - Bottom edge: 130" (left), 150" (right).
 - Interior: 70" (top), 55" (bottom), 40" (left), 30" (right).

26

DIAGRAM SHOWING VISUAL DEFECTS, PITS AND SCARS
HEAT-B, PLATE 1 - SIDE 2

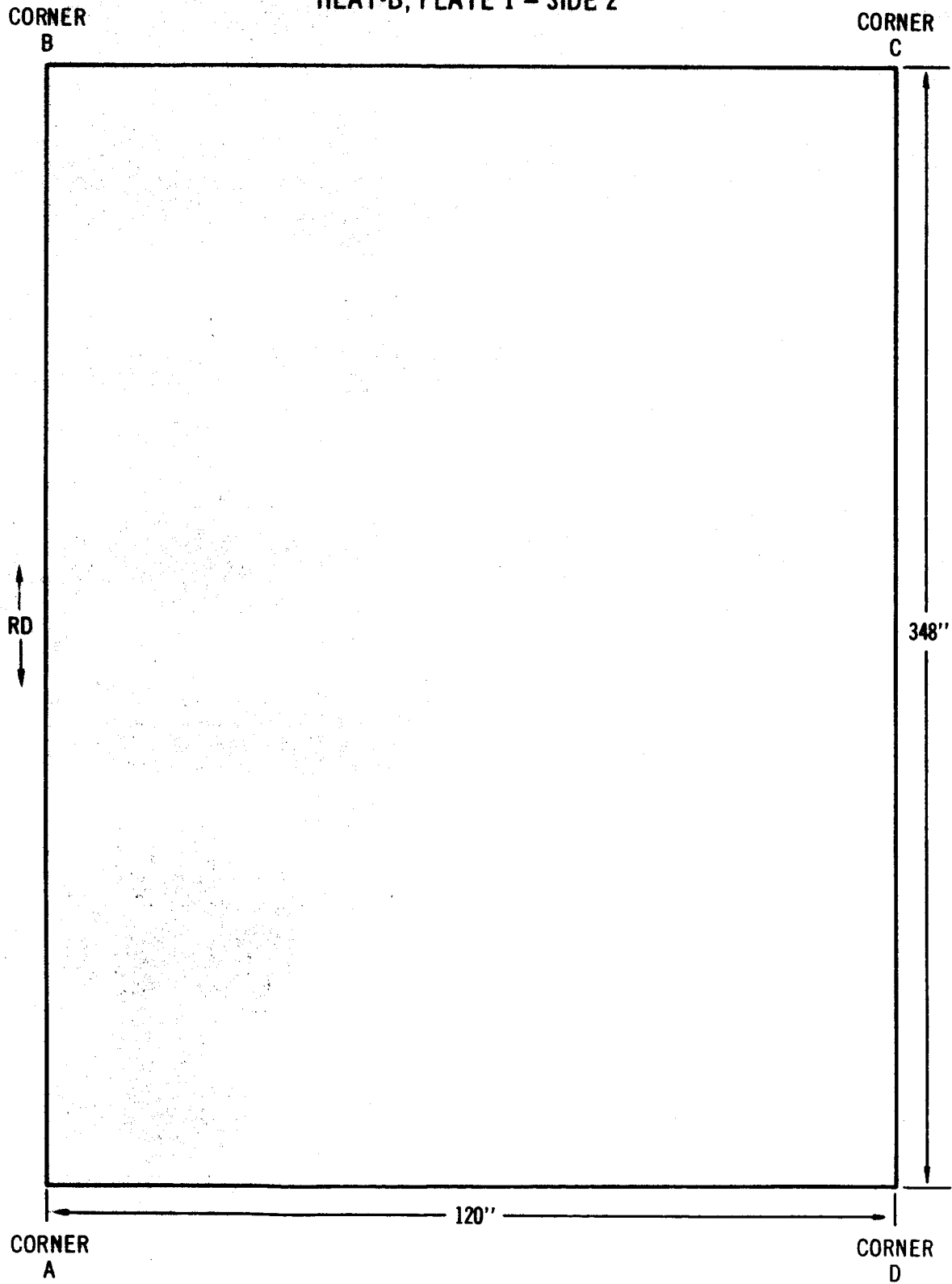


FIGURE 12

DIAGRAM SHOWING VISUAL DEFECTS, PITS AND SCARS
HEAT-B, PLATE 2 - SIDE 1

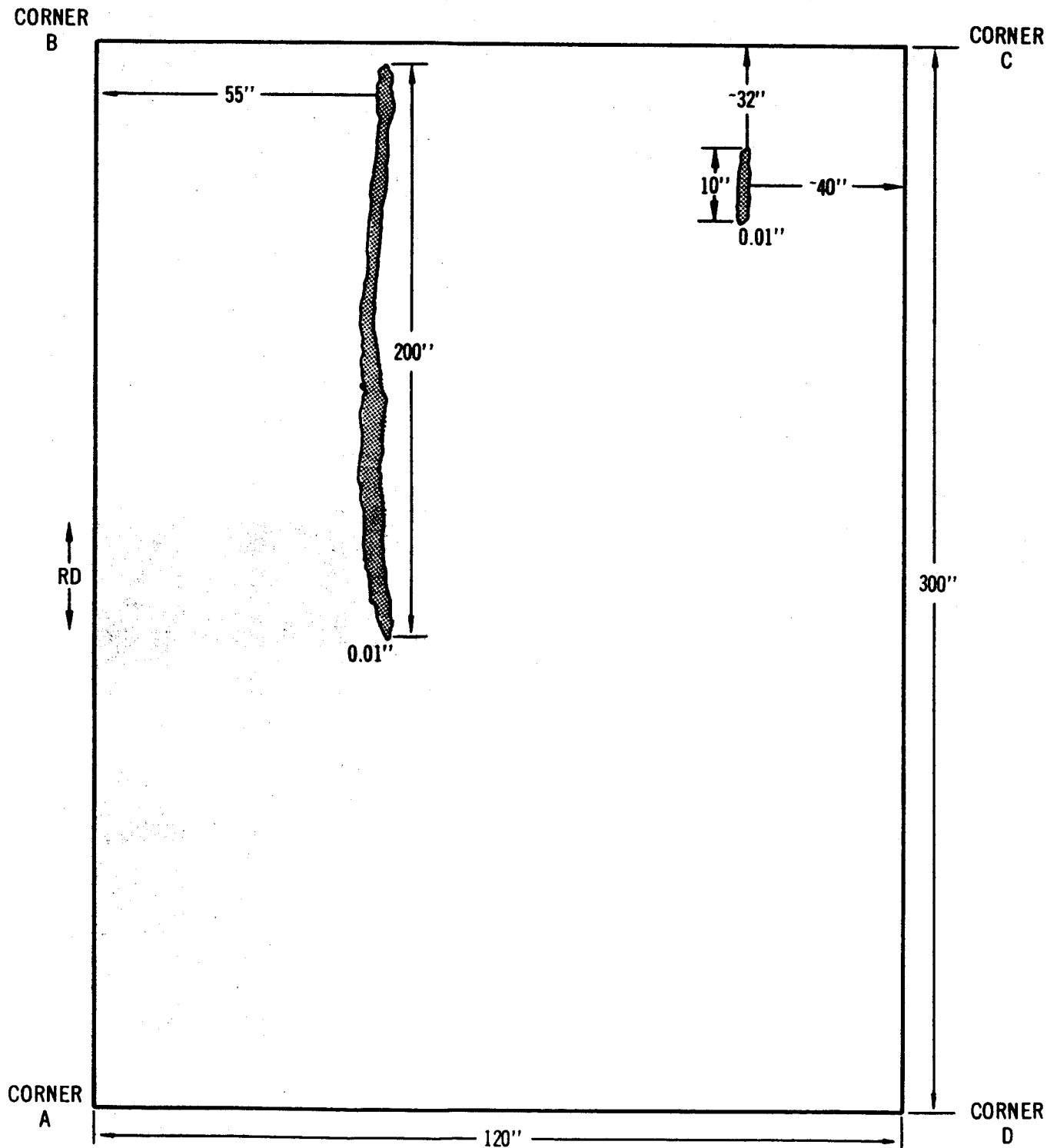


FIGURE 13

DIAGRAM SHOWING VISUAL DEFECTS, PITS AND SCARS
HEAT-B, PLATE 2 - SIDE 2

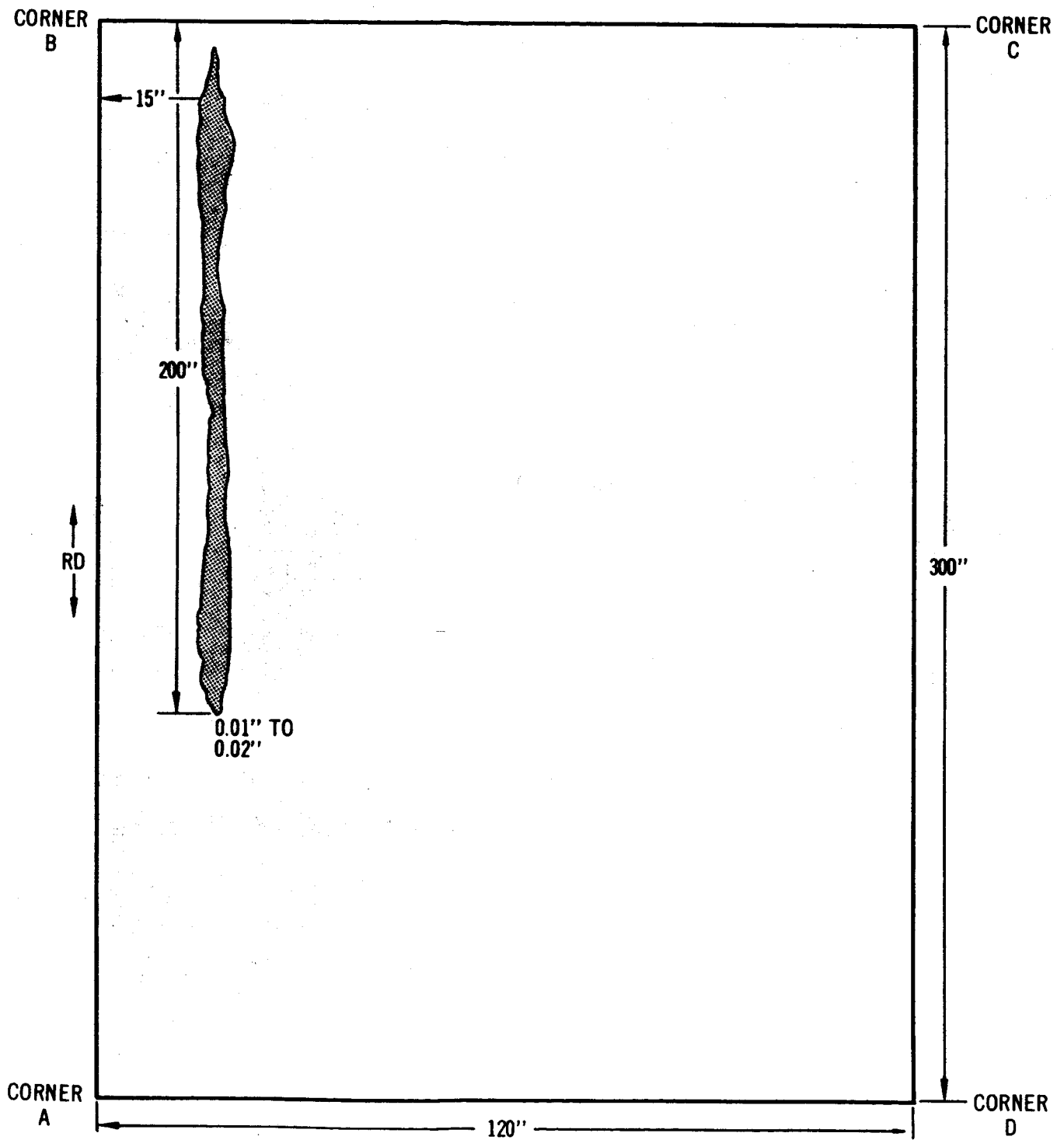
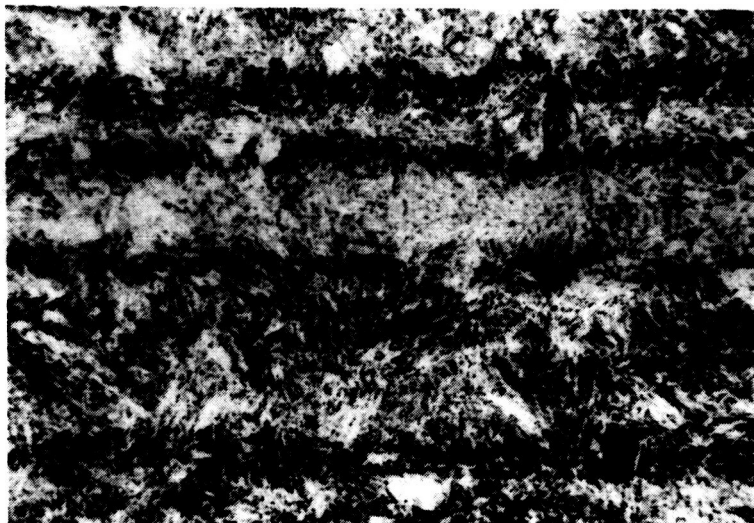
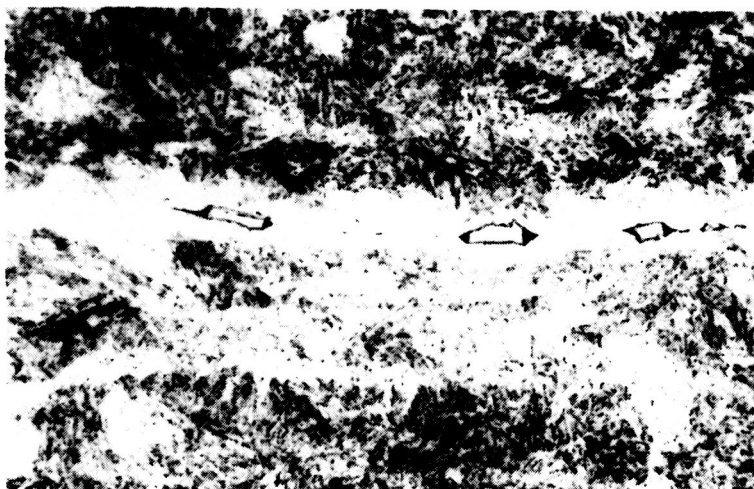


FIGURE 14



TYPICAL TRANSVERSE SECTION ILLUSTRATING
CHARACTERISTIC BANDED APPEARANCE

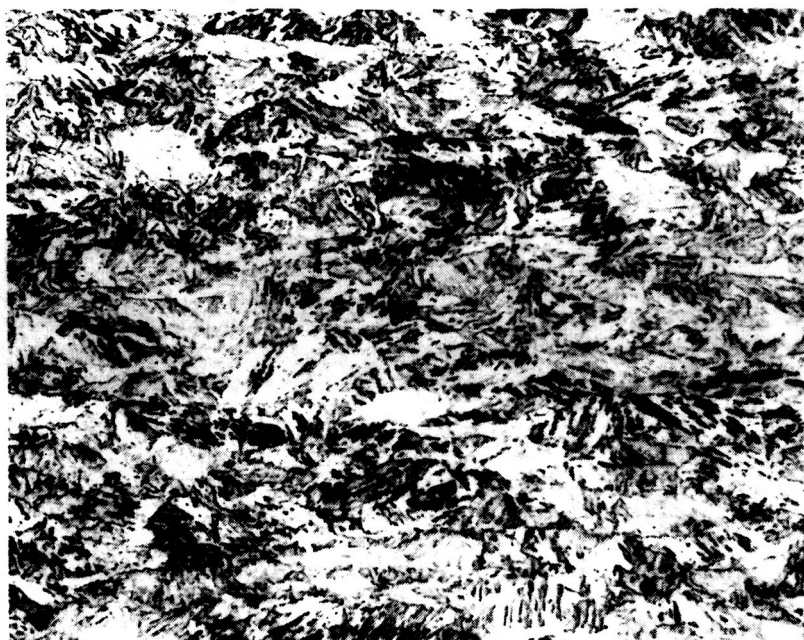


SECTION SHOWING INCLUSIONS
AS RECEIVED HEAT-A PLATE

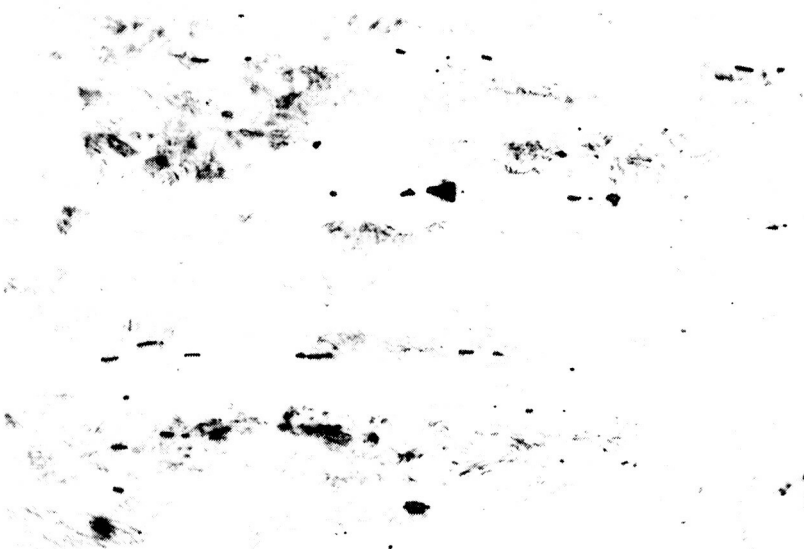
250X

ETCH: 50 ML HCL
25 ML HNO₃
1 GR CuCl₂
150 ML H₂O²

FIGURE 15



TYPICAL TRANSVERSE SECTION - HEAVY ETCH



SECTION SHOWING INCLUSIONS - LIGHT ETCH

AS RECEIVED HEAT-B PLATE

FIGURE 16

250X

ETCH: 50 ML HCl
25 ML HNO₃
1 GR CuCl₂
150 ML H₂O

2.7.2 Metallographic Examination (Cont'd.)

produced by selective etching; however, in all probability they were induced during plate rolling when the inclusions failed to deform and elongate in the same way as the surrounding material. This type of inclusion is tentatively identified in a later section as titanium nitride. As will be seen, titanium nitride inclusions represent a major detriment to toughness in this alloy, especially in welds. Typical smaller inclusions are illustrated in Figure 16.

Inclusion content determinations were made on Heats I, A and B plate in accordance with ASTM Designation E-45, Method A. Table VII presents the average values determined by the suppliers, Newport News, and Douglas. The values are within the limits specified with the exceptions of the thin series for Type B and D. The majority of the inclusions were the angular type presumed to be primarily titanium nitrides. Some differences in the inclusion counts are indicated. However, the limited data prohibit the formulation of decisive conclusions concerning the apparent differences.

2.7.3 Tensile Property Check

Twelve 0.505 tensile specimens aged at 900°F for 3 hours, were tensile tested to determine whether or not Heats A and B plate possessed the minimum property requirements specified in DMS 1835. The results are presented in Table VIII. The properties exceed the minimum requirements of the specifications.

TABLE VII

INCLUSION CONTENT DETERMINED IN ACCORDANCE WITH ASTM DESIGNATION E-45 METHOD A

HEAT I

SOURCE	TYPE A		TYPE B		TYPE C		TYPE D	
	Thin	Heavy	Thin	Heavy	Thin	Heavy	Thin	Heavy
Douglas	1.0	0	1.0	0	0	0	1	0
	2.0	0	0	0	0	0	2	0
Avg.	1.5	0	0.5	0	0	0	1.5	0

HEAT A

Newport	0	0	0.14	0	0	0	1.88	0
Douglas	1.0	0.75	1.2	1.0	0	0	1.0	0
U.S.S.	1.0	0	1.5	0	0	0	1.5	0
Avg.	0.7	0.25	0.9	0.3	0	0	1.6	0

HEAT B

Newport	0	0	1.75	0	0	0	2.75	1.0
Douglas	0	0	1.50	0	1.50	0.5	0.5	0.5
Avg.	0	0	1.6	0	0.75	0.25	1.6	0.75

TABLE VIII

TENSILE DATA ON HEATS A AND B PLATE
TO CHECK SPECIFICATION CONFORMANCE

SPEC. No.	SPECIMEN ORIENTATION	0.2% YIELD STRESS, (KSI)	ULTIMATE STRESS, (KSI)	% ELONG. (2 in. GAGE)	% RED. IN AREA
HEAT-A PLATE TENSILE DATA					
AP 31	L	253.0	259.0	11.0	45.5
AP 32	L	252.0	258.5	11.0	44.9
AP 33	L	253.6	258.8	11.0	44.0
AP 34	T	255.0	260.8	8.0	32.5
AP 35	T	252.0	260.0	10.0	36.6
AP 36	T	254.0	260.3	9.0	38.8
HEAT-B PLATE TENSILE DATA					
P-31	L	254.5	264.0	9.0	41.9
P-32	L	257.0	265.0	11.0	41.3
P-33	L	253.5	263.0	8.0	38.5
P-34	T	265.5	270.0	8.0	33.4
P-35	T	264.0	267.5	8.0	33.4
P-36	T	259.0	269.0	7.0	34.4

NOTES:

1. L = Longitudinal

T = Transverse

2. All results obtained with 0.505-in. diameter specimens

3. Aged at 900°F for 3 hours

2.7.4 Effect of Rolling Direction and Aging Treatment on Tensile Properties

Figures 17 through 22 show the effect of aging time and temperature on the uniaxial tensile properties of both transverse and longitudinal 0.505-in. diameter specimens from the Heats A and B plate.

Data shown are for aging temperatures of 875, 900 and 950°F and aging times of 1, 3, 6, and 12 hours. Each point represents an individual test specimen. Data for Heat I are shown in Figure 23. Specimens were aged for times of 1, 3, 8, or 15 hours. Yield stress data are not illustrated in Figure 23 since values for the range were not obtained.

Figures 24 and 25 illustrate the comparative strength and ductility of the three plate heats. Ultimate strength alone is plotted in Figure 24 since the alloy is characterized by yield-to-ultimate strength ratios generally exceeding 0.9. Tabulated data on Heats I, A, and B are presented in Appendix IV.

The data may be summarized as follows:

1. Aging at 875°F is characterized by a monotonic increase in tensile strength with increasing aging time (Figure 24) for the three plate heats. The absolute strengths that are achieved and the rates of strengthening differ. A maximum difference of approximately 20 KSI exists between Heat I, the lowest strength, and Heat B. Heats I and A differ by about 5 KSI over the entire aging time range examined. Heat B appears to strengthen at a more rapid rate than either Heats I or A. Unexpectedly high strength, approaching 300-KSI, was attained by Heat-B plate

after a 12 hour aging exposure.

2. Heats I and A, after 900°F aging, exhibit about the same strengthening response (Figure 24). The strength levels are approximately equivalent and appear to reach a relative plateau after 6 hours. Heat B exhibits substantially higher strength over the entire range of aging times. Heat B overages at 900°F as indicated by the drop in strength after 6 hours. Overaging does not occur for Heats I or A at the 900°F aging temperature.
3. At 950°F all heats reach a peak strength after 3 hours, (Figure 24). After 3 hours, overaging occurs as depicted by a steady drop in strength with increasing aging time. Again Heat B exhibits the highest tensile strength. Heat I, which was lower in strength than Heat A after 875°F aging and about equal after 900°F, exhibits intermediate strength after 950°F aging.
4. Two other temperatures were investigated for Heat I. These were 925°F and 1000°F. The 925°F aging cycle very nearly produces the same strengths as the 900°F cycle. The 1000°F cycle exhibits immediate overaging (Figure 23).
5. Ductility (as measured by per cent elongation and reduction in area) for Heats I and A are similar for all aging times and temperatures and are slightly higher than the values for Heat B. Ductility in the transverse direction is generally inferior to that in the longitudinal direction.

2.7.4

Effect of Rolling Direction and Aging Treatment on Tensile Properties (Cont'd.)

Figure 25 shows a scatterband plot showing the effect of aging times and temperatures on ductility for Heats A and B. If Heat I were shown, it would be within the values drawn for Heat A.

6. Although transverse strengths are generally greater than longitudinal, some notable exceptions were observed: Heat B, 900°F for 12 hours, (Figure 21) and 950°F for all aging times (Figure 22). Thus orientation effects are not definitive.
7. The above observations demonstrate that rather striking differences can exist in the aging response of nominally 18Ni-7Co-5Mo plate.

2.7.5

Effects of Aging Treatment on Hardness

The dependence of hardness on the aging treatment is depicted graphically in Figure 26 for plate from the three heats. Each point represents the average of four to eight indentations. As may be seen, hardness remains very nearly constant over a wide range of aging times and temperatures. Heats I and B are slightly harder than Heat A. This agrees with the relative strength of Heat B plate, which had the highest tensile properties. However, Heat I generally exhibited the lowest strength. Hardness does not appear to correlate very well with tensile strength.

EFFECT OF AGING TIME AT 875°F ON THE UNIAXIAL TENSILE
PROPERTIES OF HEAT-A 18Ni-7Co-5Mo AIRMELTED PLATE

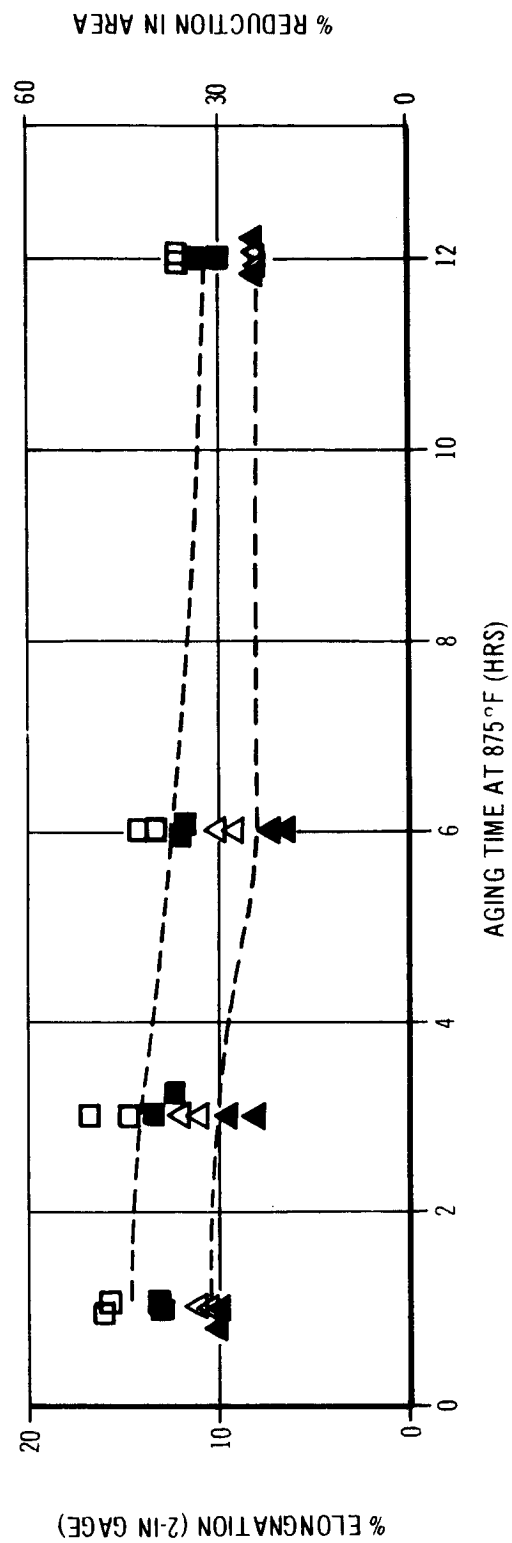
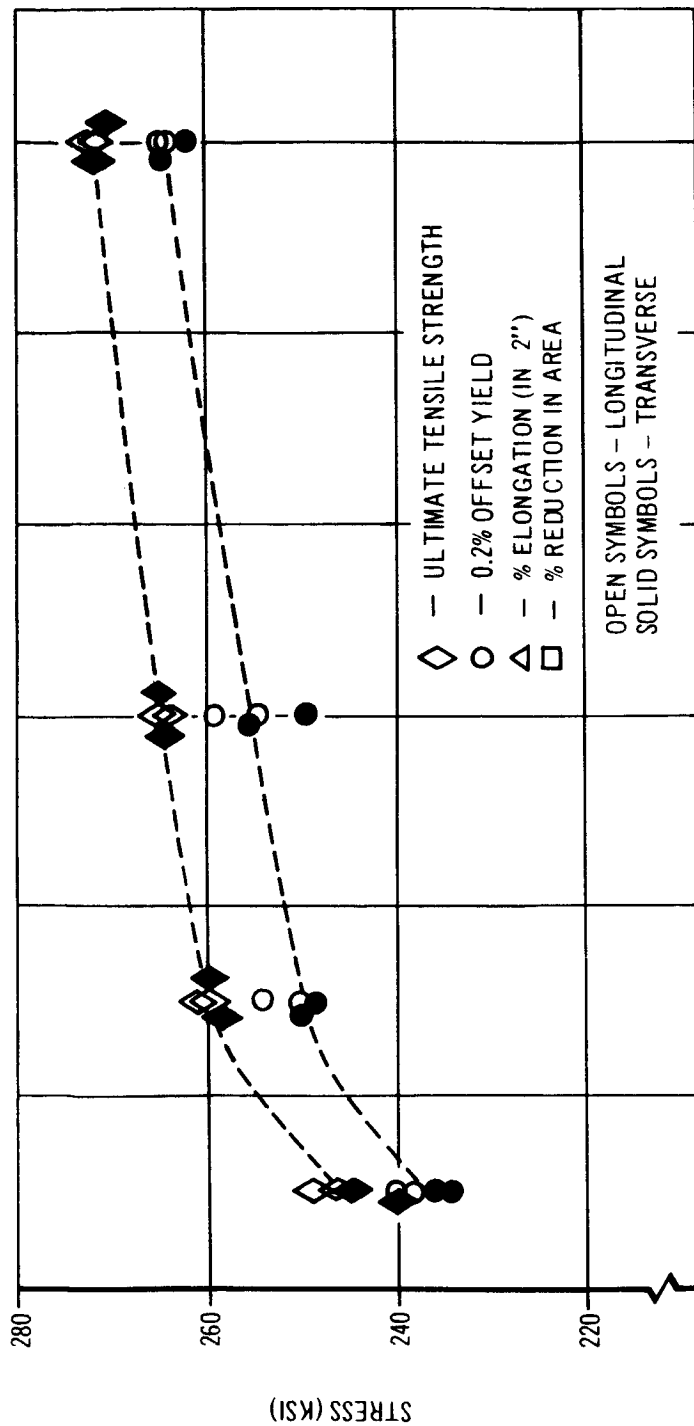


FIGURE 17

EFFECT OF AGING TIME AT 900°F ON THE UNIAXIAL TENSILE
PROPERTIES OF HEAT - A 18Ni-7Co-5Mo AIRMELTED PLATE

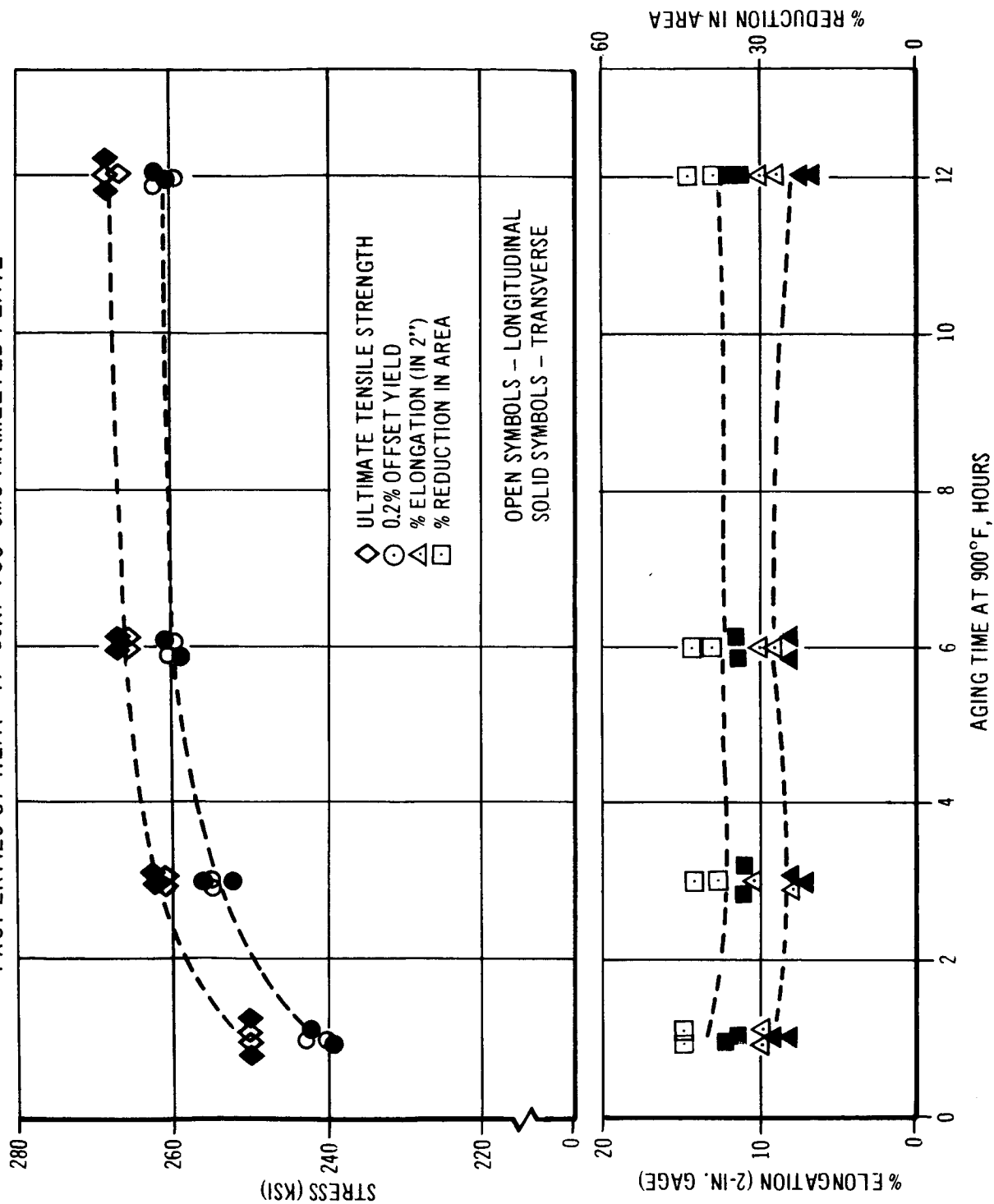


FIGURE 18

EFFECT OF AGING TIME AT 950°F ON THE UNIAXIAL
TENSILE PROPERTIES OF HEAT - A 18Ni-7Co-5Mo AIRMELTED PLATE

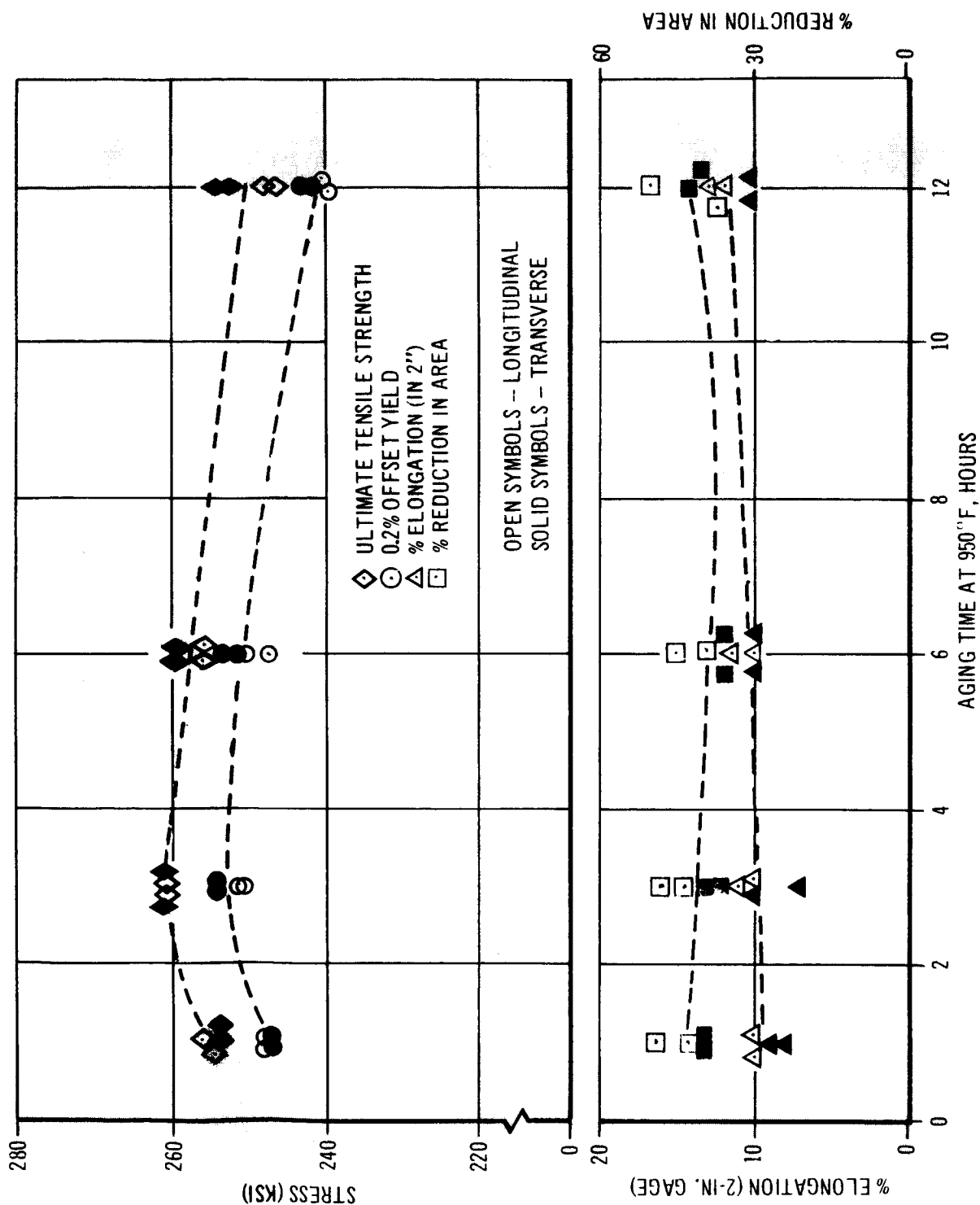


FIGURE 19

EFFECT OF AGING TIME AT 875°F ON THE UNIAXIAL TENSILE
PROPERTIES OF HEAT B 18Ni-7Co-5Mo AIRMELTED PLATE

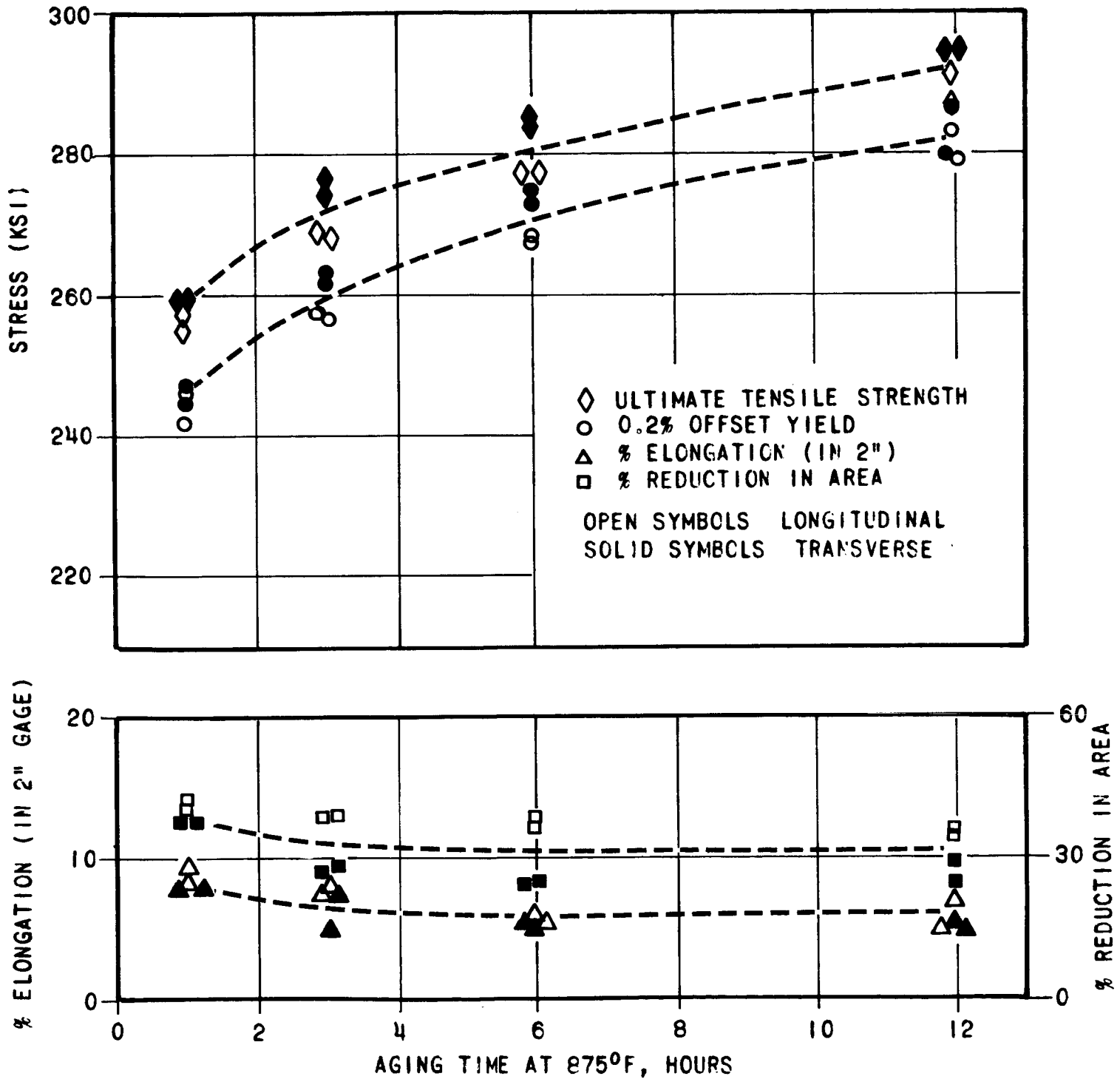
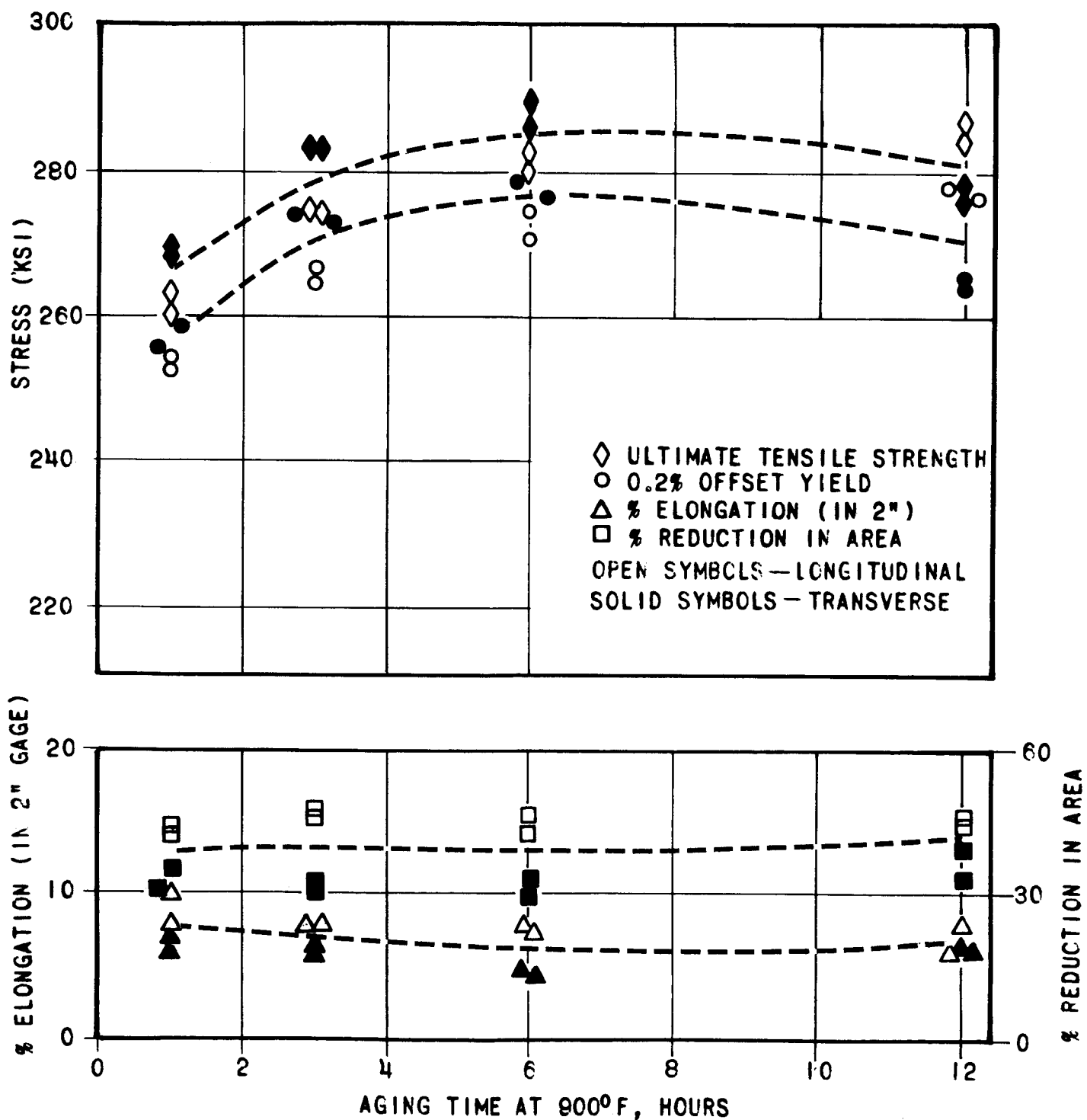


FIGURE 20

EFFECT OF AGING TIME AT 900°F* ON THE UNIAXIAL TENSILE
PROPERTIES OF HEAT B 18Ni-7Co-5Mo AIRMELTED PLATE



* 3 HOUR SPECIMENS INADVERTENTLY AGED AT 915°F.

FIGURE 21

EFFECT OF AGING TIME AT 950° F ON THE UNIAXIAL TENSILE
PROPERTIES OF HEAT B 18Ni-7Co-5Mo AIRMELTED PLATE

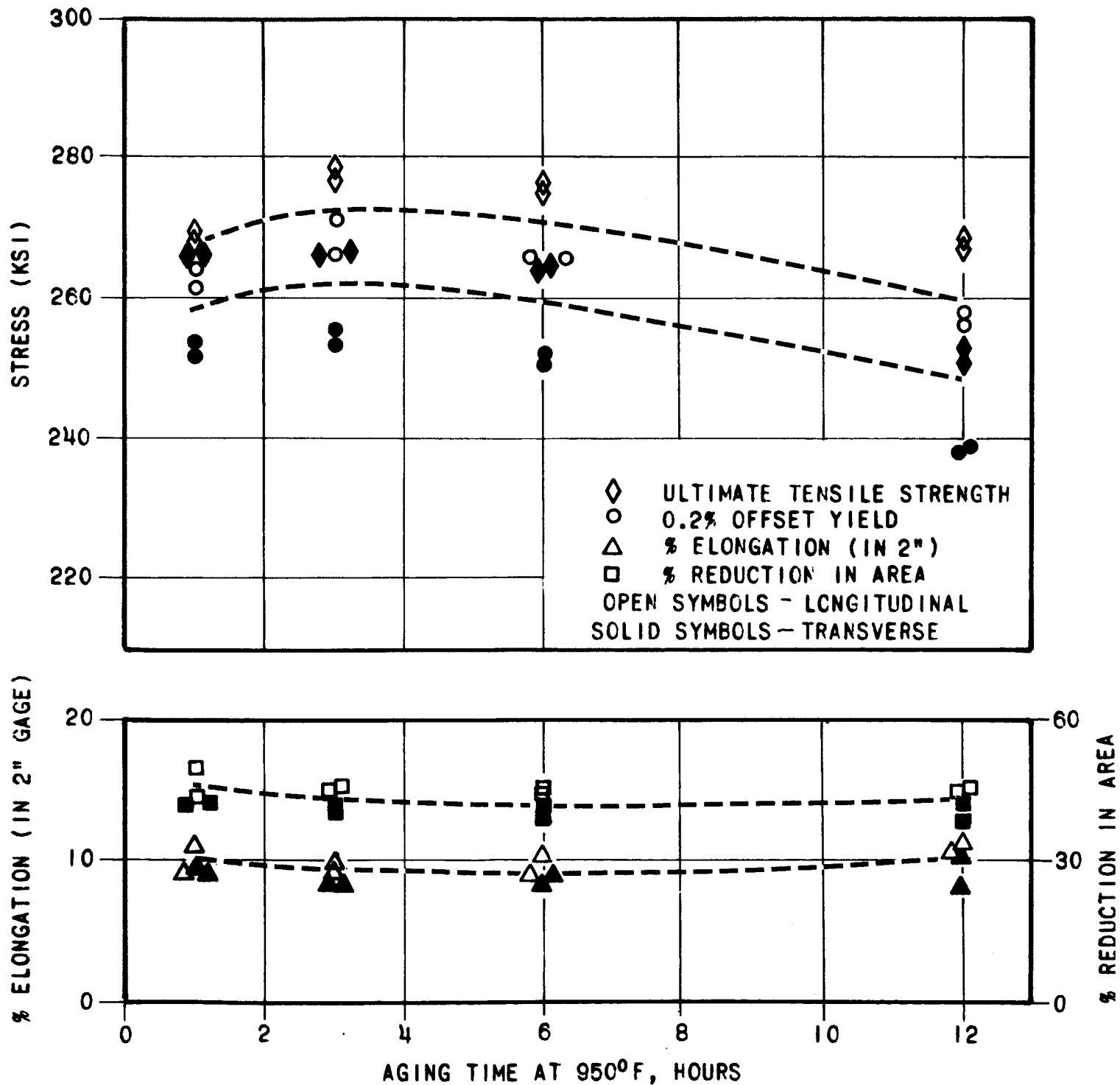


FIGURE 22

EFFECT OF AGING TIME AT TEMPERATURES
FROM 875 TO 1000 °F ON THE UNIAXIAL
TENSILE PROPERTIES OF HEAT-1 18Ni-7Co-5Mo
AIRMELTED PLATE

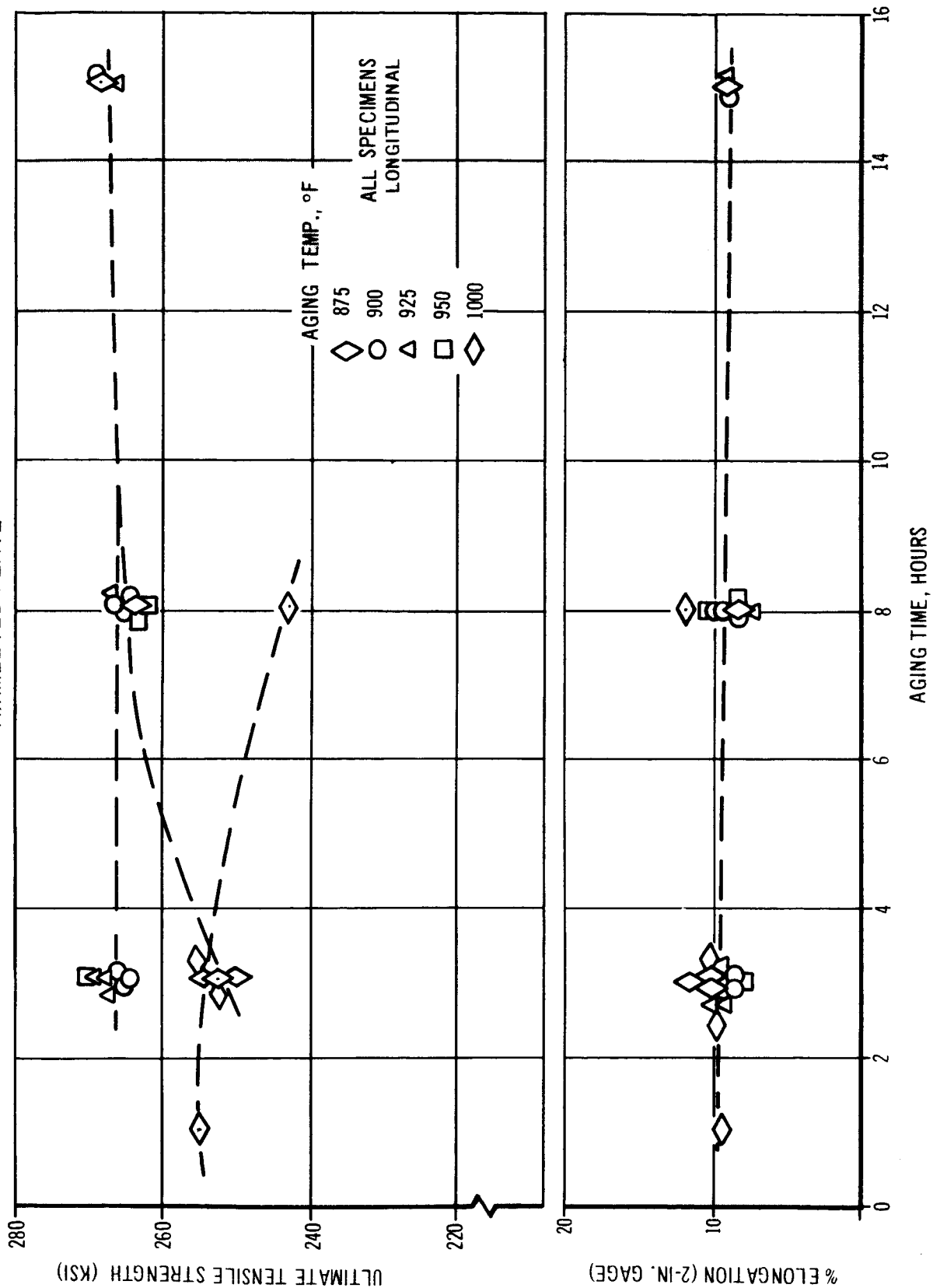


FIGURE 23

EFFECT OF AGING TIME AND TEMPERATURES ON ULTIMATE TENSILE STRENGTH OF HEATS 1, A, AND B PLATE

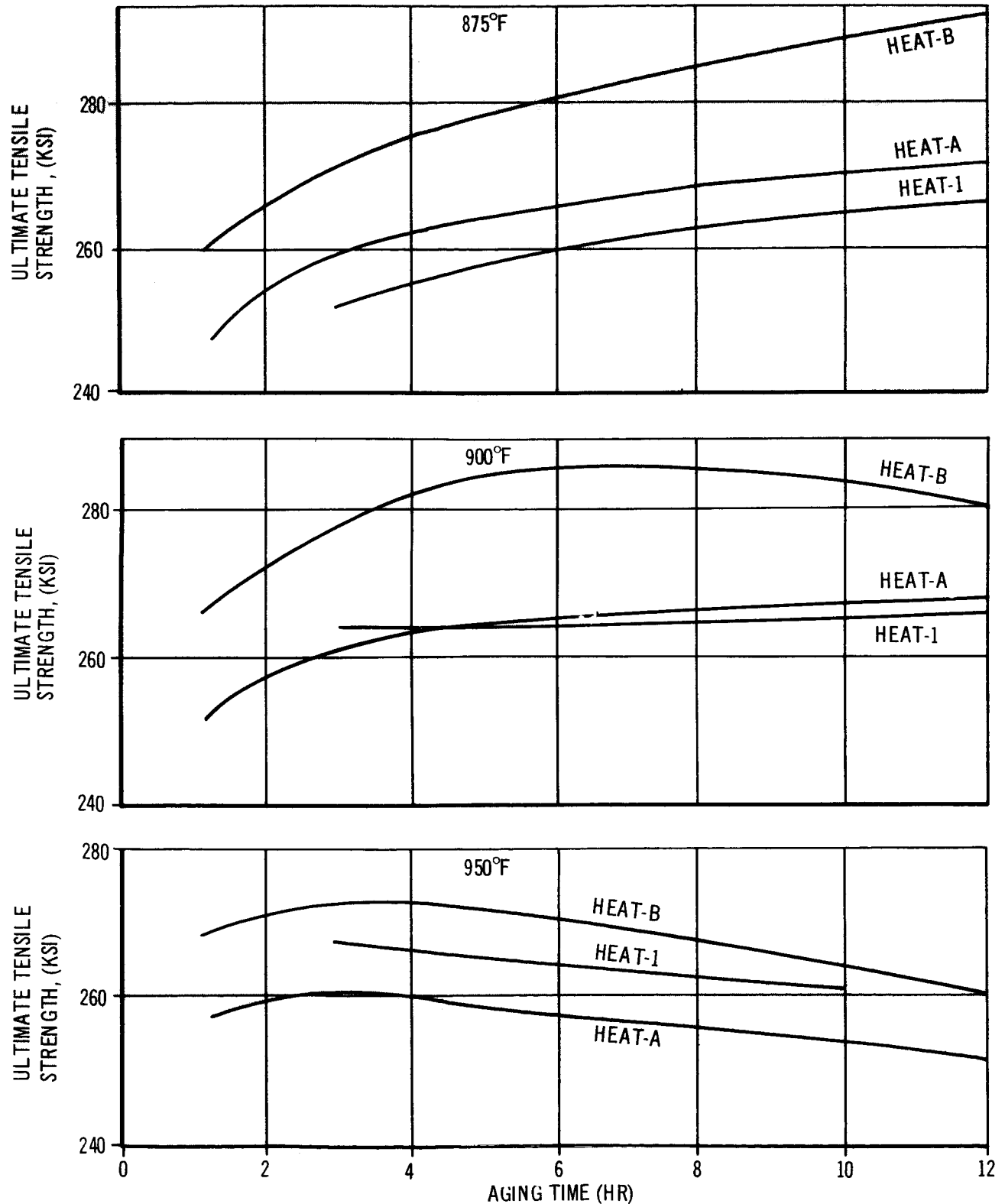


FIGURE 24

EFFECT OF AGING TIME ON PERCENT
REDUCTION IN AREA AND PERCENT ELONGATION FOR HEATS A AND B PLATE

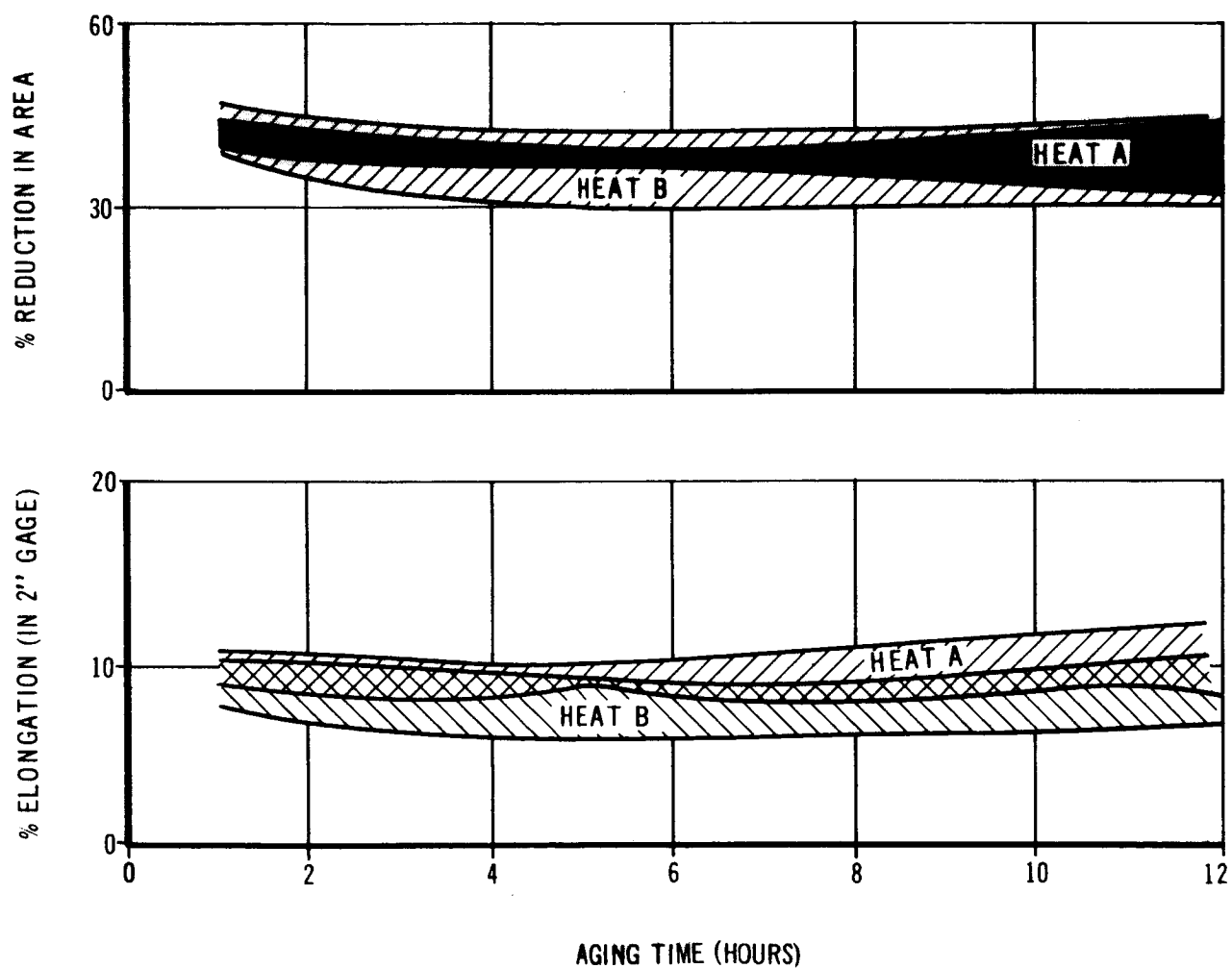


FIGURE 25

EFFECT OF AGING TEMPERATURES AND TIME ON HARDNESS FOR HEATS 1, A AND B PLATE

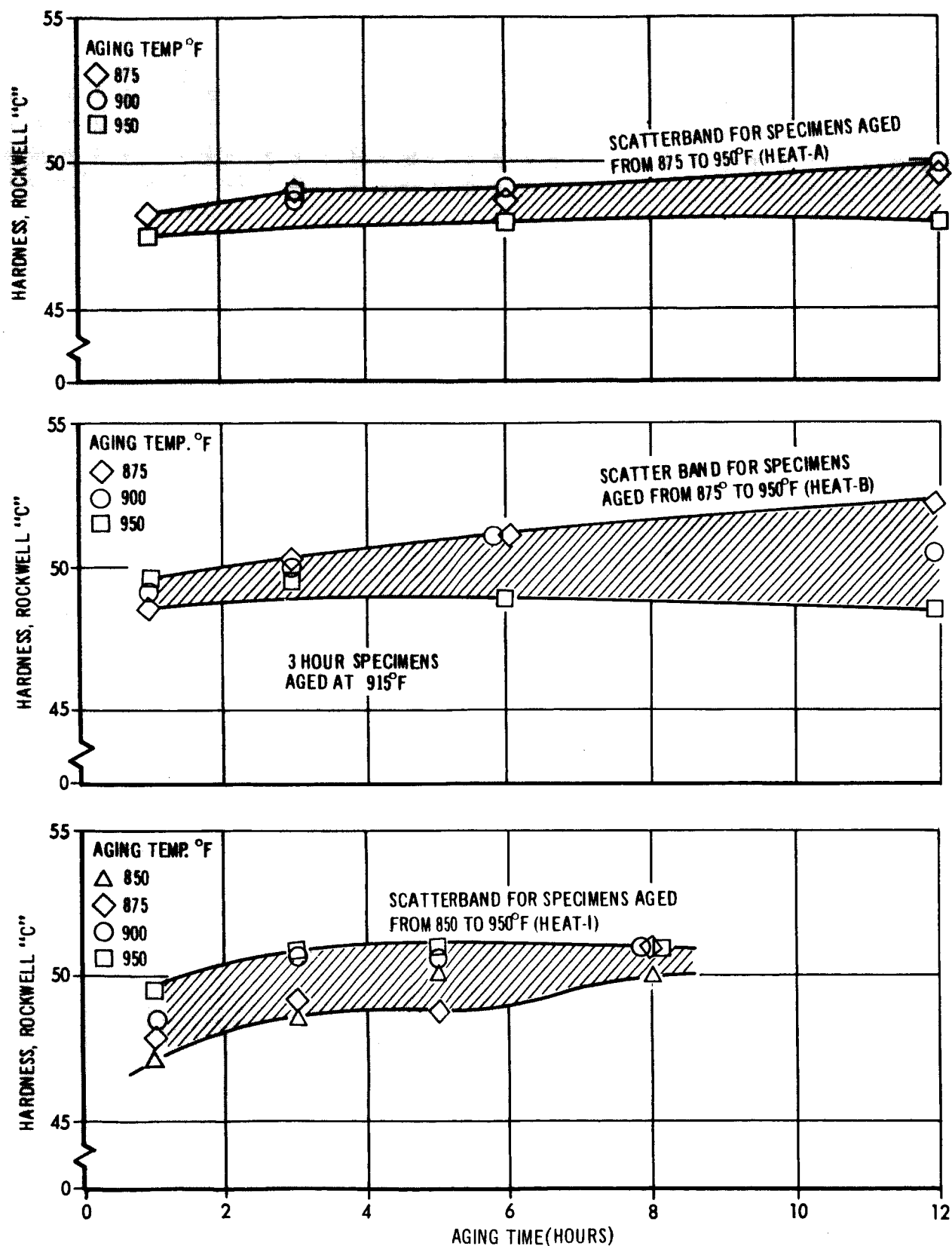


FIGURE 26

2.8 Fracture Toughness of Plate

This section describes the plane strain fracture toughness properties of plate from the three heats. All results discussed in this section pertain to full thickness plate specimens. Results obtained using a subsize specimen are discussed in a subsequent section, wherein specimen size effects are described.

Heat 1 plate was evaluated using the 48-in PTC test specimen (Figure 7) exclusively, and only in the longitudinal (parallel to the rolling) direction. One aging temperature (900°F) and two aging times (3 and 12 hours) were evaluated. Heat A and B plates were evaluated using the 24-in specimen (Figure 8). Heat A plate was tested after 900°F , 3 hour aging only. Two aging temperatures (875°F and 900°F) and two aging times (3 and 12 hours) were employed for Heat B. Longitudinal and transverse specimens were tested for Heats A and B plate. The dependence of net-fracture stress on shallow-crack depth was studied. (Crack depth, rather than length or some other crack-shape parameter, was selected as the independent variable. However, it should be recognized that depth may not be the most significant crack-shape parameter. Studies are currently in progress at Douglas to define the most significant crack-shape parameter). Net stress is calculated on the basis of original crack size as displayed on the fracture surface. The area is calculated from length and depth measurements by assuming the crack to be a semi-ellipse. Figure 27 illustrates the excellent agreement between calculated and actual area for several specimens. The actual area was determined by a planimetric

2.8 Fracture Toughness of Plate (Cont'd.)

measurement of a photographically enlarged image of the crack on the fracture surface. The results for the three plate heats are discussed in the following three paragraphs. Tabulated data, including crack depth and length, are presented in Appendix V.

2.8.1 Heat I

The results depicted in Figure 28 show that the net-fracture stress of Heat I plate, after 3 hour aging at 900°F, remains constant until a crack depth of approximately 0.110 inches (the "critical depth") is reached. Thereafter, the net-fracture stress decreases steadily with increasing crack depth. Similar behavior is observed after a 12 hour age. However, the critical crack depth after 12 hours may be somewhat less (perhaps as low as; 0.080-in; however, the data are not decisive). The net stress for a given crack depth is 10 to 20 KSI less after 12 hour aging than it is after 3 hours.

2.8.2 Heat A

Heat A data exhibit very close agreement with that for Heat I plate aged for 3 hours. The longitudinal properties of Heat A may be slightly superior to those for Heat I, but the differences appear to be small. The transverse properties of Heat A plate appear to be somewhat inferior to the longitudinal properties. This may be ascertained by comparing the net-fracture stresses for approximately identical crack sizes.

2.8.3 Heat B

Figure 29 illustrates the net fracture stress dependence on crack depth after 12 hour aging at 875°F. Figure 30 presents the dependence after 3 and 12 hour aging at 900°F. Both longitudinal and transverse orientations are depicted. The behavior is similar to that observed for Heats I and A plate. Notably, however, the critical crack depth is less, ranging from about 0.050 inches to 0.075 inches. As in the cases of Heats I and A plate, both the critical crack depth and the net-fracture stress (for a given crack depth) appear to decrease upon extended aging treatment.

2.8.4 Plane Strain Fracture Toughness Parameter, K_{IC}

Plane strain fracture toughness values, K_{IC} * were calculated from Irwin's equation (Reference 1), as follows:

$$K_{IC} = \sqrt{\frac{3.77\sigma^2 b}{\phi^2 - 0.212 \left(\frac{\sigma}{\sigma_{YS}}\right)^2}}$$

where,

$$\phi = \int_{\theta=0}^{\theta=\pi/2} \sqrt{1 - \left(\frac{a^2 - b^2}{a^2}\right) \sin^2 \theta} \, d\theta$$

* K_{IC} is an analytically derived expression related to a material's resistance to premature failure in the presence of a flaw. For a given tensile strength level, resistance to failure is directly proportional to K_{IC} .

2.8.4 Plane Strain Fracture Toughness Parameter, K_{IC} (Cont'd.)

$2a$ = Crack length

b = Crack depth

σ = Gross-fracture stress

$\sigma_{y.s.}$ = 0.2% offset yield strength

The following sections pertain to the dependence of K_{IC} on thermal treatments and orientation.

2.8.5 Effect of Aging Duration and Temperature on K_{IC}

Figure 31 presents a bar chart depicting the spread in K_{IC} for the various aging treatments evaluated. Tabulated values are presented in Appendix V. The results show that transverse properties are somewhat inferior to longitudinal, and that prolonged aging tends to degrade K_{IC} . Heat 1 plate exhibits the latter trends most markedly. (As will be seen in subsequent sections, the differences attributable to specimen size are inconsequential.)

2.8.6 Comparison of Experimental and Theoretical Dependence of Fracture Stress on Crack Size

Figure 32 illustrates the comparative net fracture stress versus crack depth dependencies for both experimental data (Heat B plate) and theoretical curves derived from Irwin's equation. The theoretical curves (calculated using $\sigma_{y.s.} = 280$ KSI and $K_{IC} = 98$ KSI $\sqrt{\text{in}}$) are depicted for a range of crack length-to-depth ratios from two to eight. The theoretical curves are extrapolated to intersection with the ultimate strength plateau so as to approximate critical

RELATIONSHIP BETWEEN MEASURED CRACK AREA, AND CALCULATED CRACK AREA

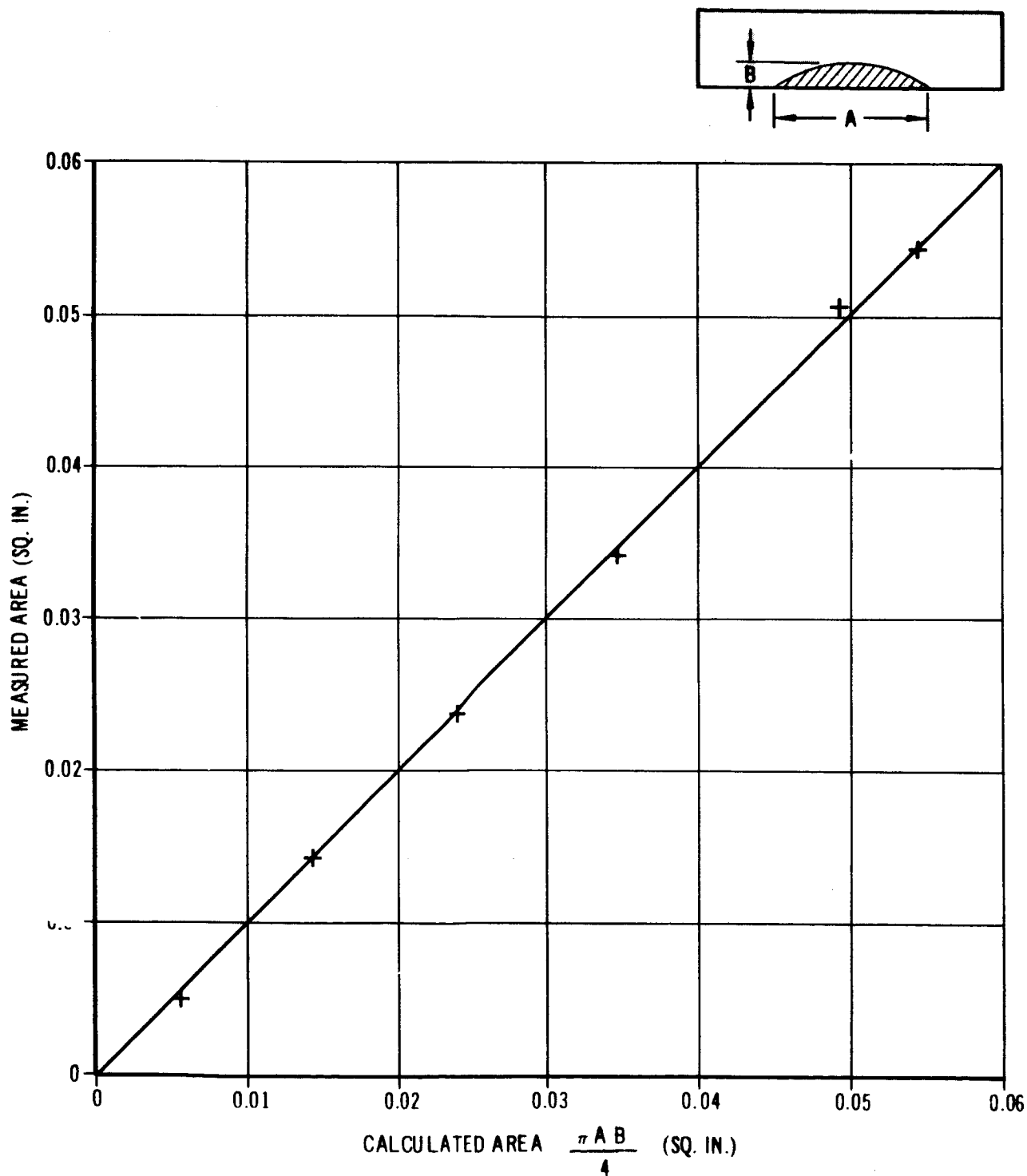


FIGURE 27

EFFECT OF CRACK DEPTH ON THE NET FRACTURE
STRESS OF 3/4 IN. THICK AIRMELTED 18Ni-7Co-5Mo PLATE

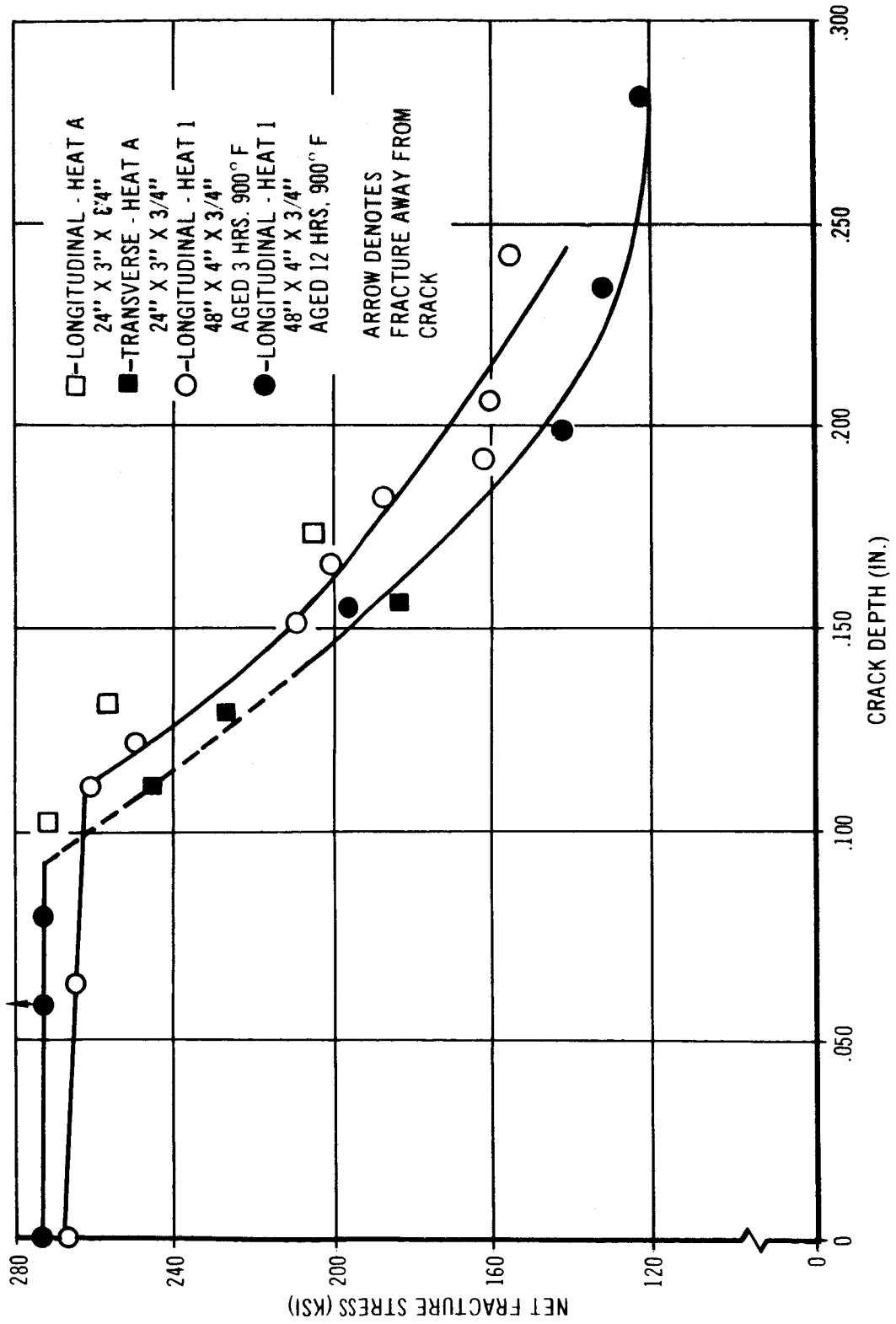


FIGURE 28

EFFECT OF CRACK DEPTH ON
THE NET FRACTURE STRESS OF
HEAT-B
18 Ni-7 Co-5 Mo PLATE

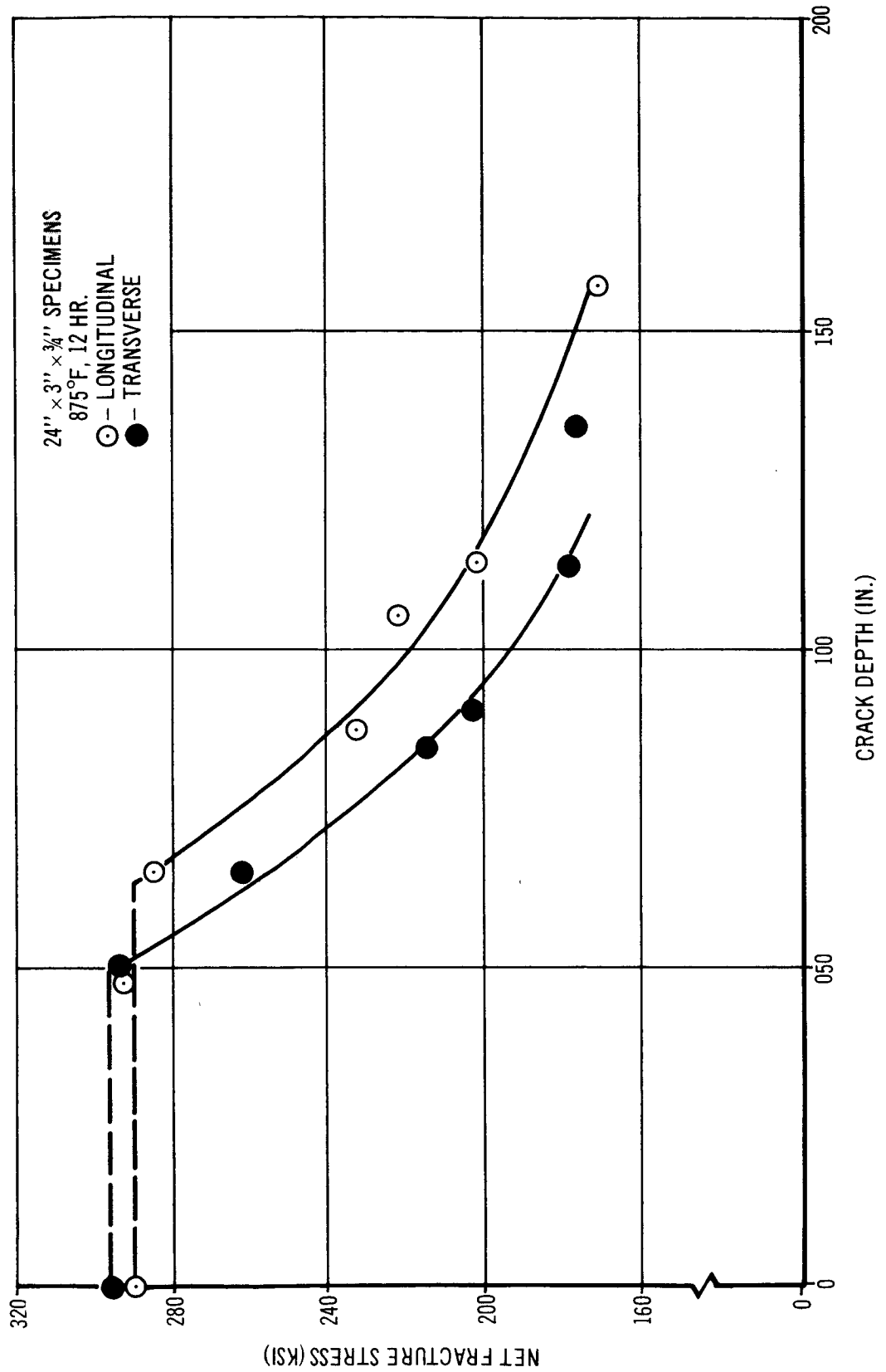


FIGURE 29

EFFECT OF CRACK DEPTH ON THE NET
FRACTURE STRESS OF HEAT-B
18 Ni-7 Co-5 Mo PLATE

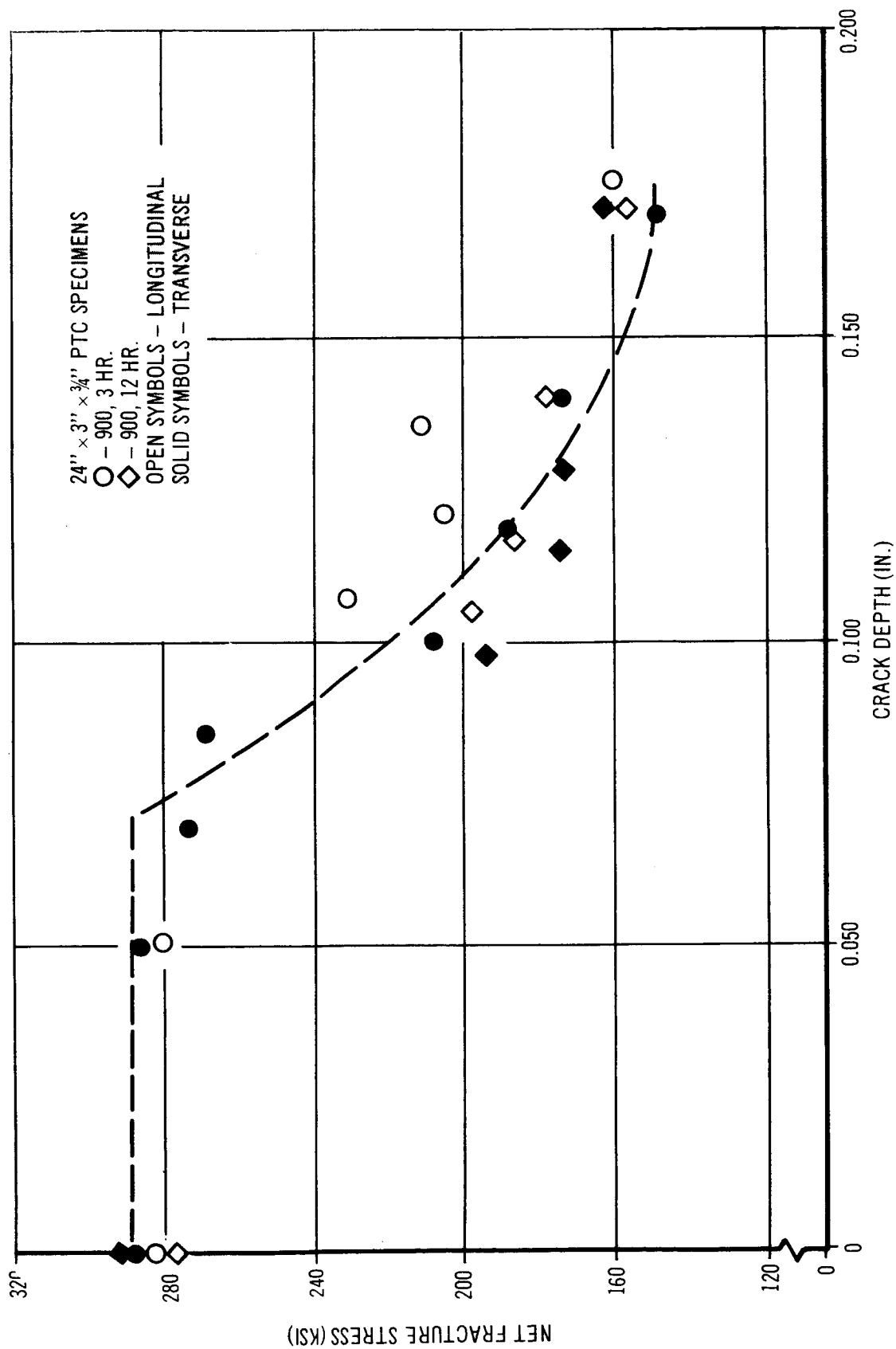


FIGURE 30

EFFECT OF AGING HEAT TREATMENT ON K_{IC} OF THE THREE PLATE HEATS

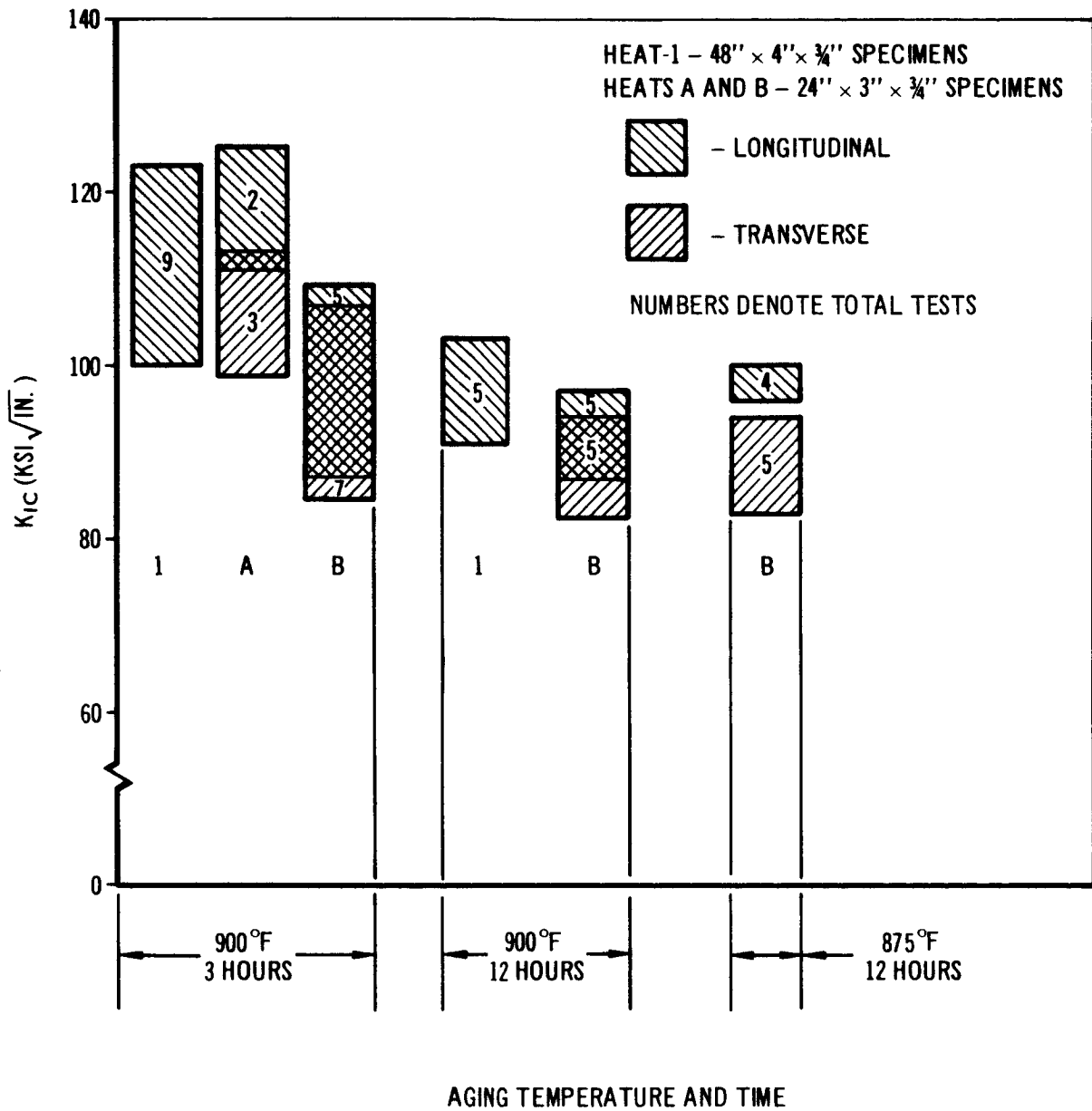


FIGURE 31

2.8.6 Comparison of Experimental and Theoretical Dependence of Fracture Stress on Crack Size (Cont'd.)

crack depths. Since the 18Ni-7Co-5Mo plate under study is characterized by yield-to-ultimate strength ratios exceeding 0.9, such an extrapolation is not unreasonable.

The experimental data fall within the calculated theoretical range (i.e., $2a/b$ equal from about 2 to 4). The actual critical crack depth range is reasonably approximated by the intercept of the theoretical curve for $2a/b = 2$ with the ultimate strength plateau. However, such approximations may not always be accurate enough for process control requirements. Nonetheless, these data demonstrate that theoretical plane strain fracture toughness values may portray the actual behavior with reasonable accuracy. More comprehensive comparisons are necessary to fully establish the generality of the theoretical correlations with experimental data.

2.9 Evaluation of Small PTC Specimen

The measurement of plane strain fracture toughness of high-strength alloys has been approached in many ways. Generally, if edge-cracked or center-cracked specimens (References 2 and 3) are used, rather expensive and elaborate techniques are required for the determination of the onset of rapid crack propagation. The partial thickness crack specimen (References 1 and 4) now commonly designated as the PTC specimen, has the virtue of being much simpler to test and to analyze. Perhaps even more important is the fact that this test yields information (i.e., net-fracture stress versus crack size)

COMPARISON OF EXPERIMENTAL AND THEORETICAL DEPENDENCE OF FRACTURE STRESS ON CRACK SIZE

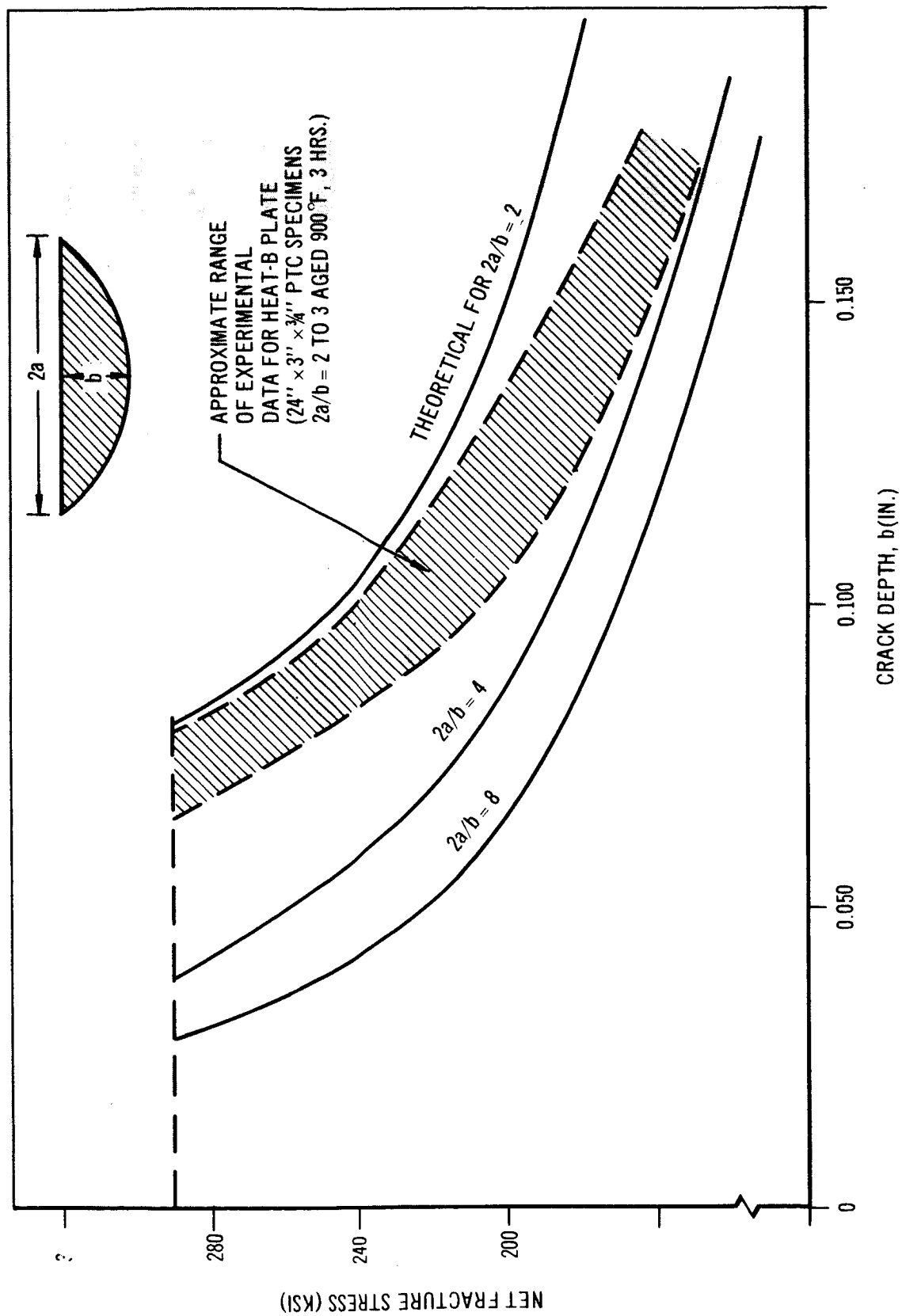


FIGURE 32

2.9

Evaluation of Small PTC Specimen

which may be used directly for design and inspection purposes. Also plane-strain fracture toughness values, K_{IC} , may be directly calculated from the results using Irwin's analysis assuming negligible slow crack extension. The latter assumption is often questioned; however, sustained load data presented later show that this assumption, at least for these maraging alloys, is reasonable.

The PTC test has often been objected to, however, because of the belief that large specimens were required to obtain valid results. Data presented in this section provide the justification for the use of a small, economical, plane strain PTC specimen.

2.9.1

Background

During the initial stages of the 18Ni-7Co-5Mo maraging steel investigations at Douglas, the large 48" x 4" x 3/4" specimen was employed to measure the fracture toughness of the 3/4-inch thick plate and welds (Figure 7). Obviously, this specimen consumed much material, was expensive from the standpoint of machining and testing, and because of its weight (108 lb) was rather difficult to handle. Testing of welds with this type of specimen further requires a one foot long weld for each specimen (assuming a transverse test), which thus pyramids the cost of gathering sufficient data needed for research-type investigations. For the latter reasons, and based on earlier data on AISI 4340 (Reference 5), a small PTC specimen was evaluated for welds (Figure 33). Figure 34 compares results obtained with the two specimen types in evaluating

2.9.1 Background (Cont'd.)

the fracture toughness of weldmetal (Reference 7). (Discussions concerning welding procedures and compositional effects are presented in a later section.) The results indicate rather close correlation between the two specimen sizes. It should be noted that the ratio of crack length to depth is about the same for the two PTC specimen sizes (length = $2\frac{1}{2}$ to $3 \times$ depth). Otherwise, such good agreement would not be expected.

On the basis of the weld test results, a far more comprehensive evaluation of the effects of specimen size was undertaken on Heat B plate using the configurations illustrated in Figures 8 and 9. One specimen, the $24" \times 3" \times \frac{3}{4}"$, was used to test full plate thickness with the crack plane perpendicular to the plate surface (results described previously). The orientations used for the $8" \times 11/16" \times 5/16"$ specimens are illustrated in Figure 35. The geometry of the latter specimen was selected on the basis that the largest crack to be tested would not exceed one-half the specimen thickness (thus fulfilling Irwin's criteria for K_{IC} calculations). The small $8" \times 11/16" \times 5/16"$ PTC specimens were subjected to aging treatments identical to those investigated for the previously discussed $24" \times 3" \times \frac{3}{4}"$ PTC specimens.

2.9.2 Effect of Specimen Size and Orientation on Net Fracture Stress

To fully compare the 8-in PTC specimens with the larger type, specimens were removed in the three orientations shown in Figure 35. Two are designated "thickness" types, and are the most economical

2.9.2 Effect of Specimen Size and Orientation on Net Fracture Stress (Cont'd.)

to machine. The specimens were all aged at a constant temperature (900°F) for two different times (3 hours, 12 hours).

Examination of the net fracture stress data, illustrated in Figure 36, shows that substantially the same results are obtained with the three specimen configurations. The results obtained with surface-type 8" PTC correlate closer with the 24" PTC specimen than with the results from the thickness-type 8" specimen. This might have been anticipated since the crack propagation direction for the 8" PTC surface type and 24" PTC specimens coincides.

The principal crack propagation direction for the thickness-type 8" x 11/16" x 5/16" specimen is 90 degrees to that for the surface type (i.e., approximating short transverse). Thus, the differences that are seen apparently reflect this orientation difference rather than that of specimen geometry. Generally, the data from the 8" are slightly more conservative than those from the 24" specimens. (Tabulated data for the 8-in specimens are presented in Appendix VI). The good agreement between the two specimen geometries would not have been expected had not the crack ellipticity ratio (crack length-to depth ratio) been about the same. Figure 37 illustrates the relative constancy of the ellipticity ratio for a variety of the two specimen types (welds are also included and will be discussed in detail later).

SHALLOW CRACK FRACTURE TOUGHNESS TEST SPECIMEN
 $8'' \times 1\frac{1}{2}'' \times \frac{1}{8}''$

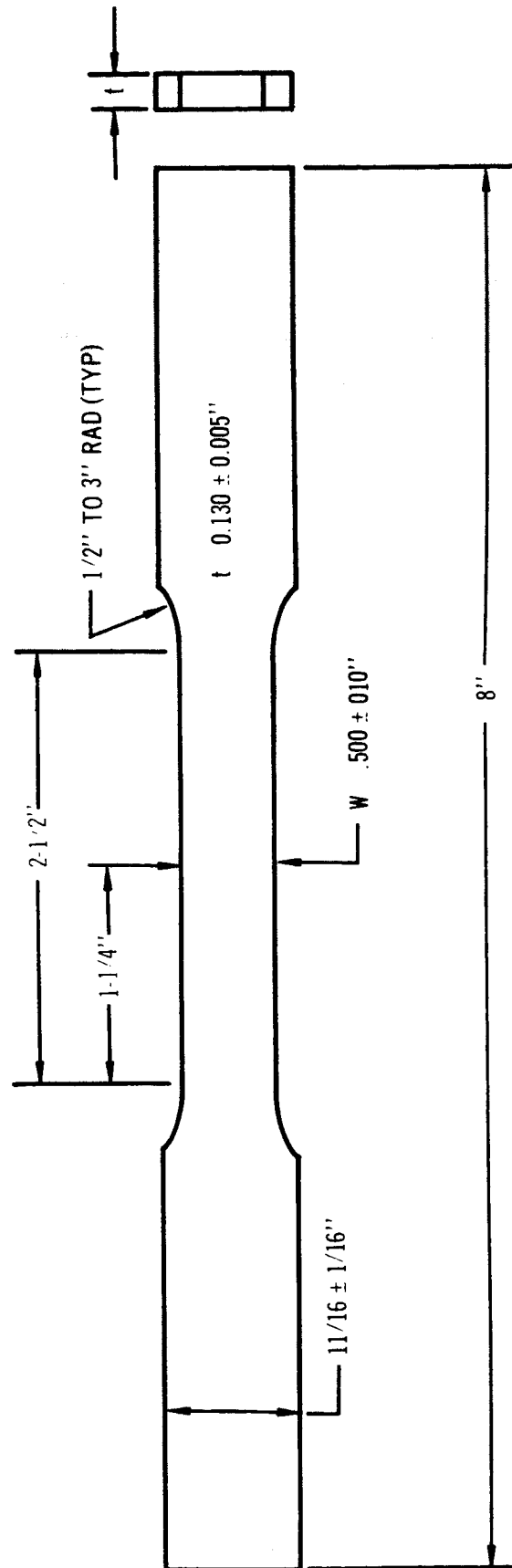


FIGURE 33

FRACTURE STRENGTH VS CRACK DEPTH
 TYPE W2 WELDS IN 3/4" 18 Ni-7 Co-5 Mo
 AIRMELTED PLATE

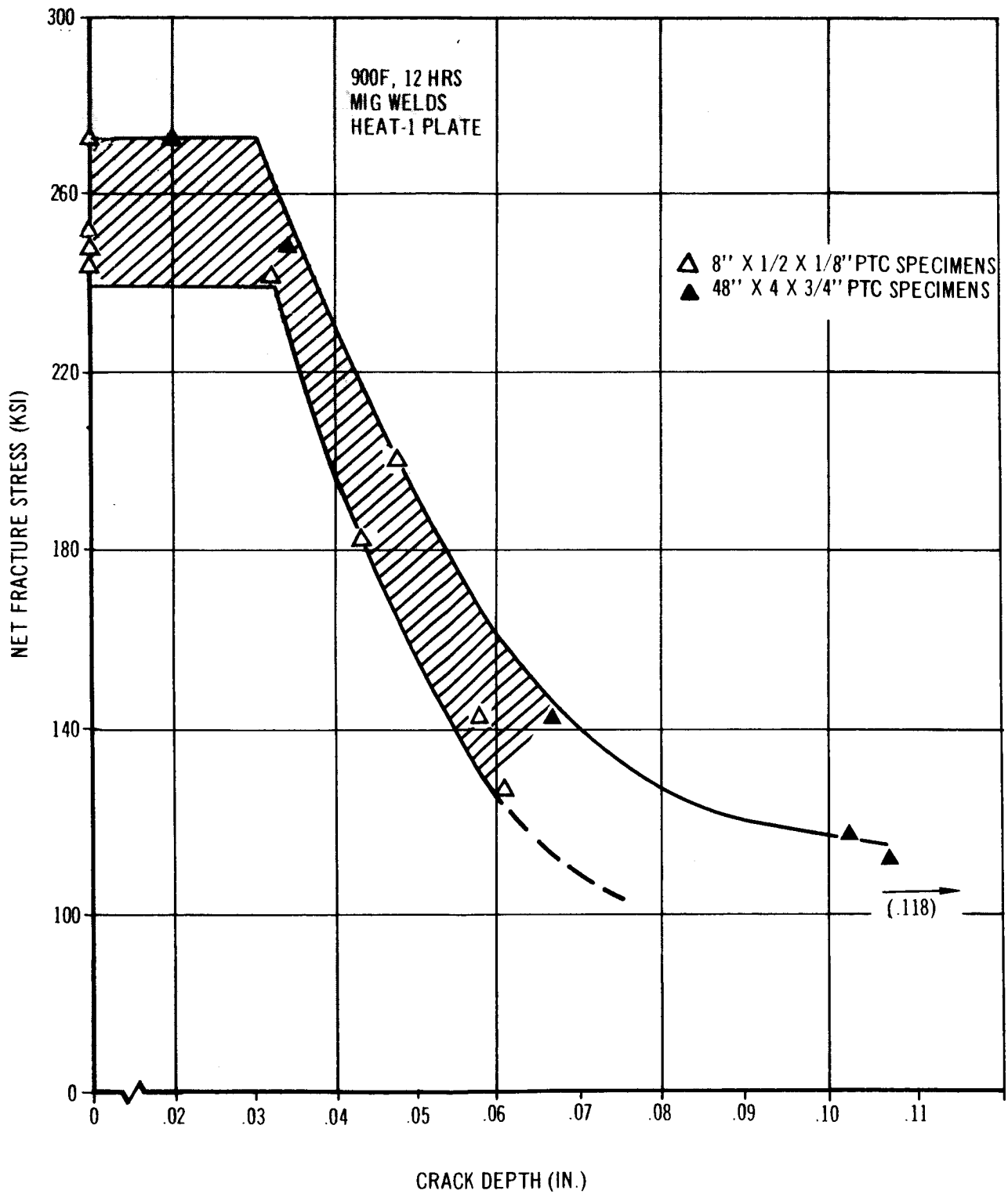


FIGURE 34

ORIENTATIONS OF THE 8" X 11/16" X 5/16" PARTIAL THICKNESS CRACK SPECIMEN

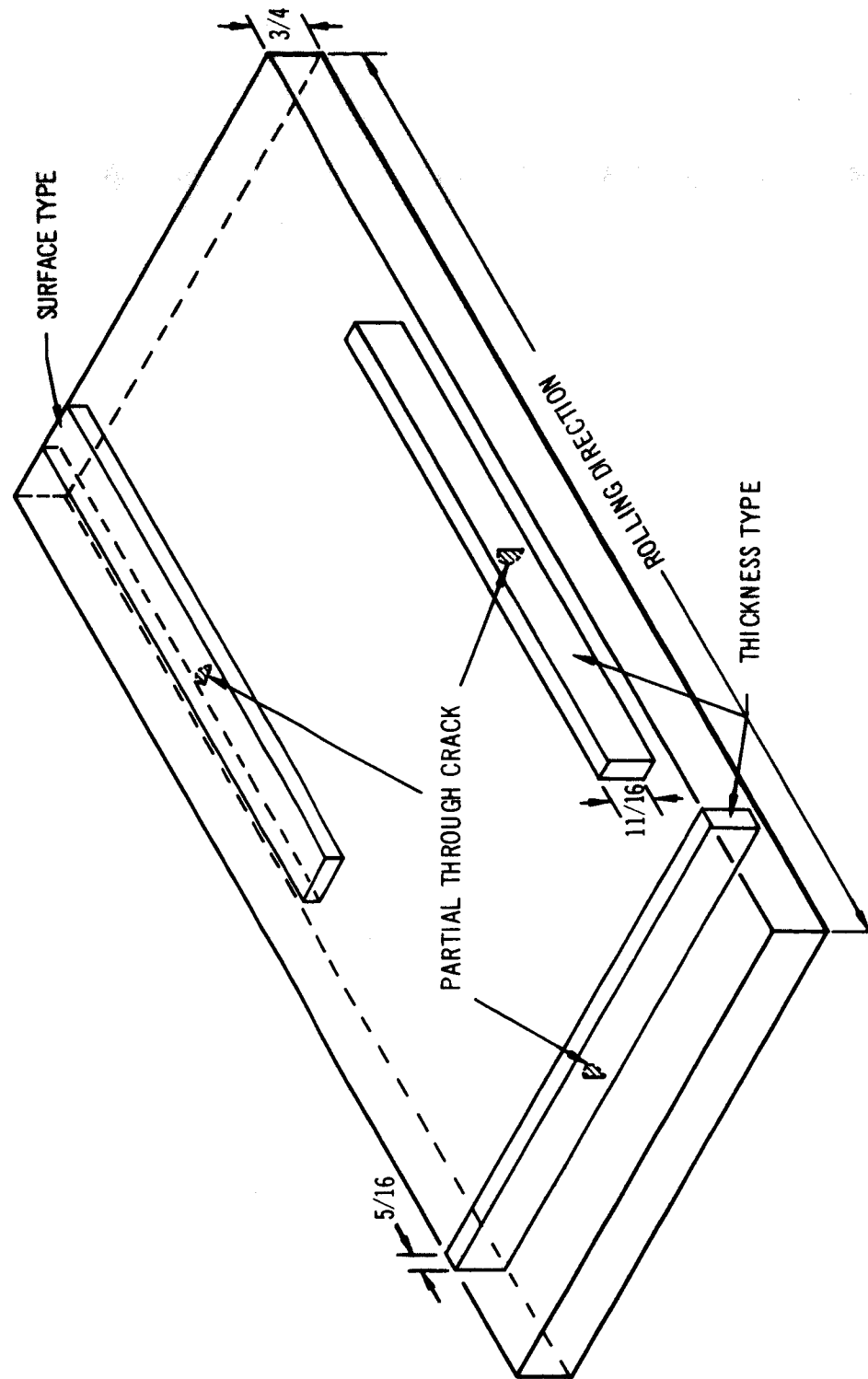


FIGURE 35

EFFECT OF CRACK DEPTH ON NET FRACTURE STRESS FOR TWO SPECIMEN CONFIGURATIONS,
SEVERAL ORIENTATIONS AND AGING TREATMENTS - HEAT B PLATE

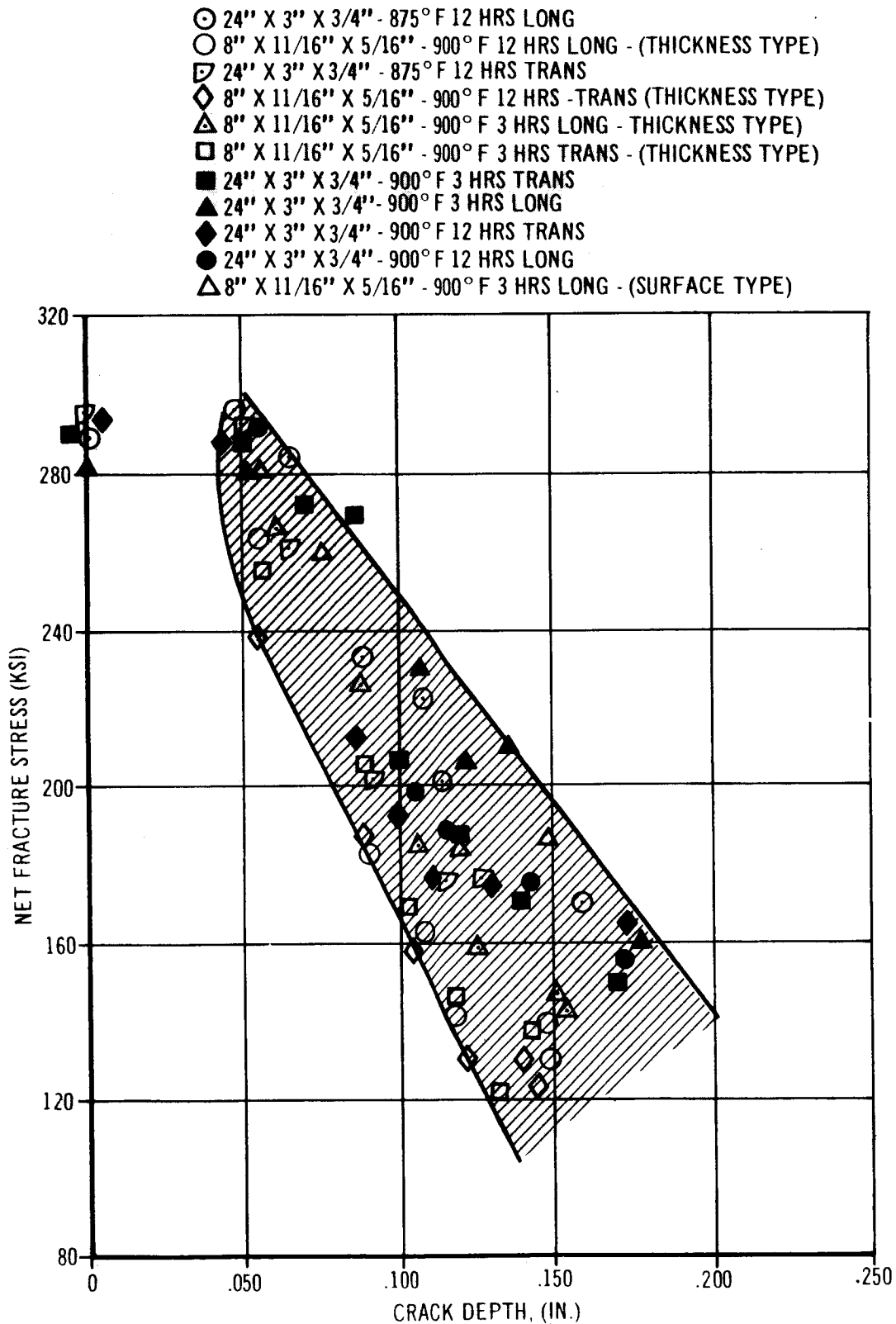


FIGURE 36

RELATIONSHIP BETWEEN CRACK LENGTH AND DEPTH IN PARTIAL THICKNESS CRACK SPECIMENS

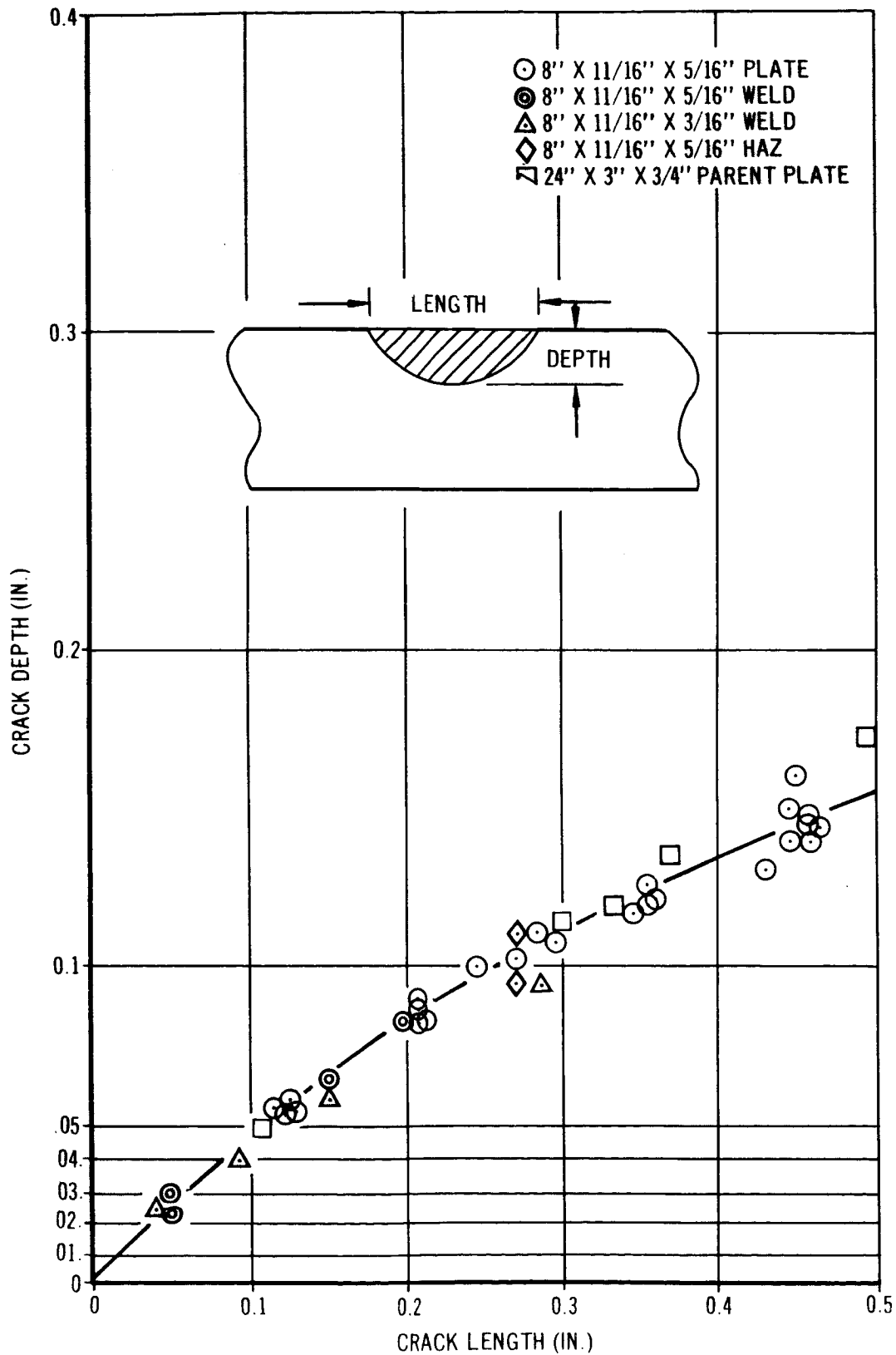


FIGURE 37

2.9.3 Effect of Specimen Size on K_{IC}

The calculation of K_{IC} from the data generated using the 8-in. PTC specimens presented a special problem. In the case of these specimens, the area occupied by the partial thickness crack was a relatively substantial fraction (approaching 30 per cent for the largest cracks) of the total cross sectional area of the specimen. Partial thickness cracks in the 24-in. specimens occupied a relatively negligible area fraction of the total cross section. Therefore, the calculation of K_{IC} for the 8-in. specimens on the basis of gross stress resulted in a geometrically induced bias. In an effort to overcome this geometrical bias, "quasi" K_{IC} values were also calculated on the basis of net, rather than gross, fracture stress. Net stress represents a convenient, albeit arbitrary, weighting function which tends to compensate for the geometry effects. Obvious theoretical justification for the use of net fracture stress in the K_{IC} equation is lacking.

Figure 38 illustrates the result of the net stress correction on K_{IC} (complete tabulations of K_{IC} calculations based on net and gross fracture stress are presented in Appendix VI). The figure illustrates the effects of calculating K_{IC} from gross and net stress for the surface type 8-in PTC specimens (longitudinal, aged 900°F, 3 hours). Results for identically treated 24-in. PTC specimens are shown for comparison. The data demonstrate that the net stress weighting function brings the K_{IC} values for the 8-in and 24-in. specimens into approximate equivalence (as expected since orientations are identical). Furthermore, for the crack size range

2.9.3 Effect of Specimen Size on K_{IC} (Cont'd.)

evaluated, K_{IC} becomes relatively constant. (However such constancy would not have arisen had not the crack length-to-depth ratios been virtually constant and identical for both specimen sizes). The data shown in Figure 38 are characteristic of the remainder of the data tabulated in Appendix VI.

A comprehensive comparison of the 8-in and 24-in specimens is given in Figure 39 on the basis of K_{IC} versus the ratio of total cross-sectional area to net cross-sectional area. This ratio represents a convenient parameter of the relative size of the crack and specimen cross sectional area and is in fact equivalent to the ratio of net-fracture stress to gross-fracture stress. K_{IC} was calculated on the basis of net fracture stress for all the 8-in specimens. A direct comparison of the two specimen configurations can be made by symbols without tails (24") to like symbols with tails (8"). The "surface" type coupons correlate closer to the 24-in coupons, than the "thickness" type. Maximum differences of about 10 percent are seen. The 8-in "thickness" type specimens exhibit somewhat lower K_{IC} values than the "surface" type, but as reported in a previous section, this might be expected.

The small specimens tend to favor the right side of the graph. This trend is due to the dependence of the ratio of net stress to gross stress on specimen size. For the 24-in specimens, the net and gross stresses are very nearly equivalent, while for the 8-in specimens substantial differences exist. Relative size differences are illus-

2.9.3 Effect of Specimen Size on K_{IC} (Cont'd.)

trated in Figure 40. Regardless of the value of the ratio, the K_{IC} values are in good agreement for both types of specimens. Especially good agreement persists when crack propagation directions are identical.

The results show that plane strain K_{IC} values and net fracture stress data generated using either specimen are substantially the same. From the standpoint of economics, the 8-in "thickness" type specimen is favored even though the values obtained are somewhat more conservative than those obtained from the 24-in. specimens. On the basis of these results, the 8" x 11/16" x 5/16" PTC specimen was used extensively for the weld studies to be described in the forthcoming sections.

The approach represented by these results should not be generalized for all alloys unless specifically demonstrated to be applicable. Theoretical analysis of specimen geometry and relative crack size effects are also required.

2.9.4 Fracture Surface Appearance

Figure 41 illustrates the fracture surfaces typical of transverse and longitudinal 24-in PTC specimens from Heats A and B plate. The transverse specimens exhibit surfaces characterized by striations parallel to the rolling direction. Striations are far less prevalent on the fracture surfaces of the longitudinal specimens. The striations are probably related to the banded microstructure

EFFECT OF K_{IC} METHOD OF CALCULATION ON THE DEPENDENCE OF
 K_{IC} ON CRACK SIZE FOR 8-IN AND 24-IN. PTC SPECIMENS

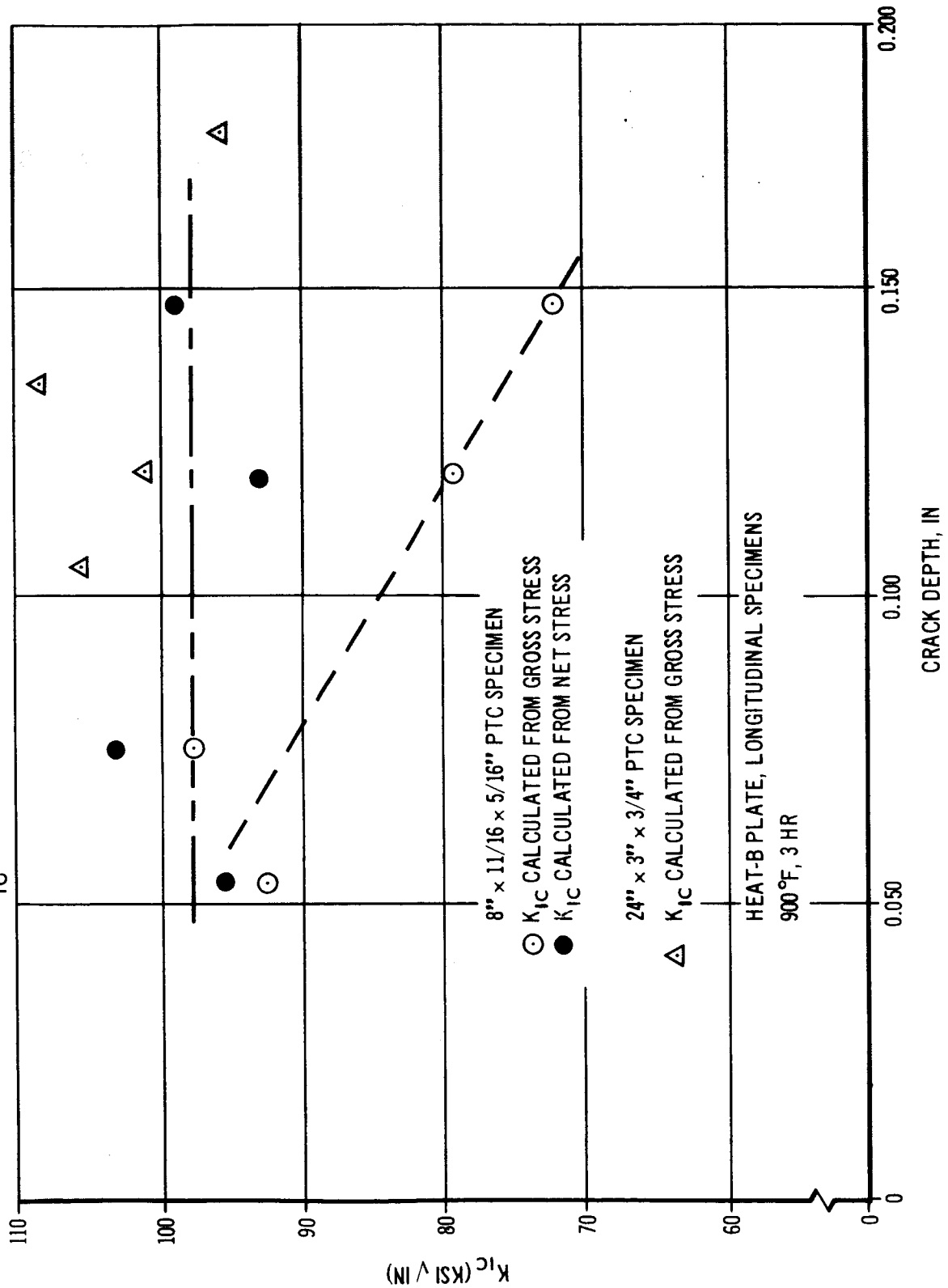


FIGURE 38

EFFECT OF RELATIVE CRACK AREA, SPECIMEN
ORIENTATION AND AGING TREATMENT ON K_{IC}
HEAT - B PLATE

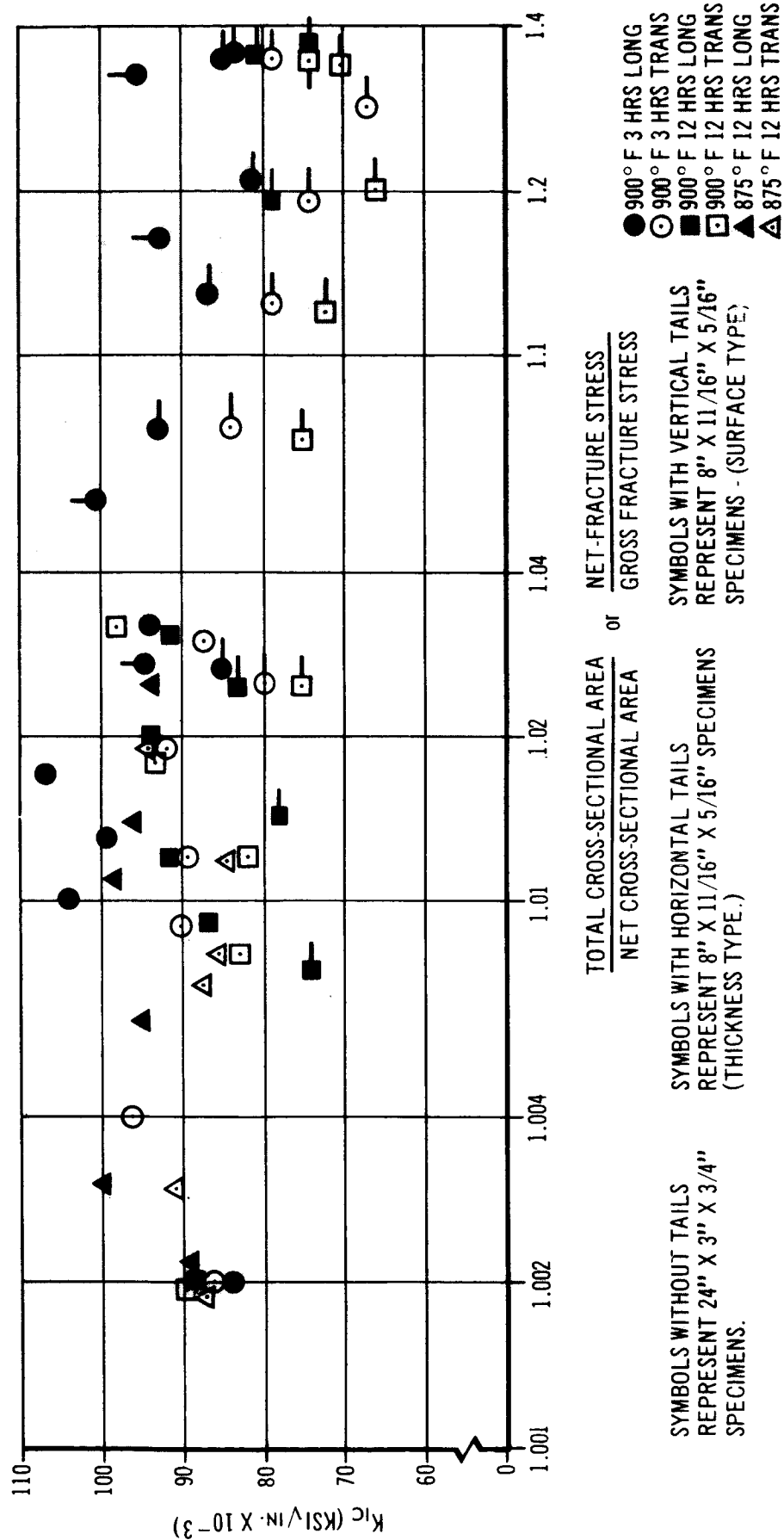
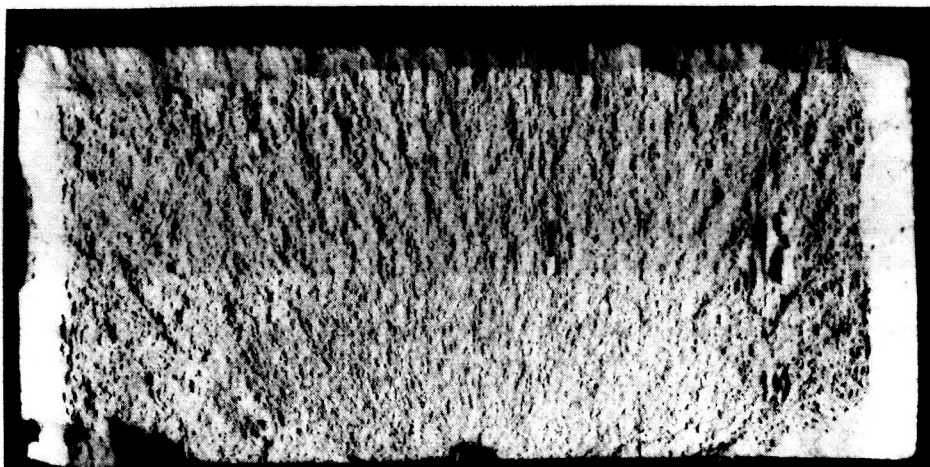
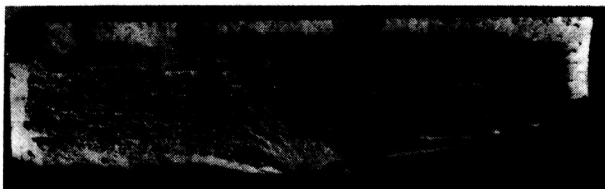


FIGURE 39



5/16" X 11/16" FRACTURE SURFACE. CRACK LENGTH = 0.446", CRACK DEPTH = 0.143".
 ELOX STARTER NOTCH AT BOTTOM IS ABOUT 0.030" LONG AND 0.015" DEEP.
 FATIGUE CRACK EXTENDS UPWARD FROM LOWER SURFACE.
 APPROX 8X



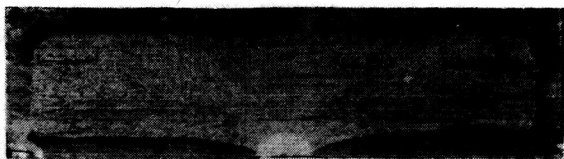
3/4" X 3" FRACTURE SURFACE. CRACK LENGTH = 0.290",
 CRACK DEPTH = 0.114. ELOX STARTER NOTCH IS BARELY EVIDENT
 FATIGUE CRACK EXTENDS UPWARD FROM LOWER SURFACE.
 APPROX. FULL SIZE

FRACTURE SURFACE OF 8" X 11/16" X 5/16" AND 24" X 3" X 3/4"
 PTC SPECIMENS ILLUSTRATING REPRESENTATIVE APPEARANCE.

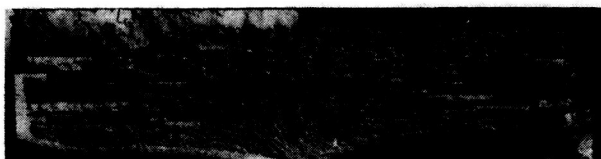
FIGURE 40

2.9.4 Fracture Surface Appearance (Cont'd.)

illustrated in Figure 15. Electron fractography failed to reveal any differences between longitudinal and transverse specimens. However, potentially damaging inclusions were disclosed. The significance of these inclusions and their characteristics are described in subsequent sections.



AP 4-5



P 16

TRANSVERSE



AP 4-2



P 125

LONGITUDINAL

HEAT-A

HEAT-B

MAGN.: APPROX. 1:1

TYPICAL 24" \times 3" \times $\frac{3}{4}$ " PTC FRACTURE SURFACES
HEATS-A AND B PLATE

FIGURE 41

3. PROPERTIES OF WELDED PLATE

3.1 INTRODUCTION

The following sections present observations relating to welding procedures and to the mechanical properties of welds deposited in plates from Heat I and B. All data presented on welds made in Heat I plate were acquired in the previous Douglas sponsored programs (References 5-7). All data on welds deposited in Heat B plate were obtained from tests performed under this contract.

The majority of the welding was performed under laboratory conditions employing flat plate specimens. However, an evaluation of welding under simulated production conditions using special fixtures and contoured plate segments was also undertaken.

Heat B plate welds were made by personnel at both Douglas Aircraft Co., and Newport News Shipbuilding and Dry Dock Co. (performing as a subcontractor). Comparison of the results obtained at the two laboratories provides a basis for evaluating the reproducibility of the welding procedures.

Mechanical property data on weldments include across-the-joint tensile, all weldmetal tensile, and weldmetal and heat-affected zone fracture toughness.

The results presented in this section relate the mechanical behavior of weldments with respect to chemical composition, thermal treatments and welding procedures. Mechanical properties and the effects of compositional and thermal variables are in turn related, insofar

3.1 INTRODUCTION (Cont'd.)

as presently possible, to metallurgical observations.

3.2 Flat Plate Welding - Specimen Preparation

Almost all of the welding performed during these investigations was accomplished using the inert-gas shielded metal-arc (MIG) process. Very limited work on Heat I plate was done using electron beam welding.

The chemical compositions of the three consumable electrode weldwires that were employed for the MIG welding are tabulated in Table IX. The weldwires were produced by Armetco Inc., using vacuum induction melting procedures; and after drawing, vacuum annealing. The wire procurement specification is presented in Appendix II.

Wire A1 was used exclusively for all welding done under this contract, while wires A2 and A3 were used for the previous Douglas sponsored work. The chemical composition of wire A1 was selected on the basis of preliminary evaluations of weld deposited with wires A2 and A3 and using titanium implant methods (References 5-7).

Welds were deposited in a variety of plate blank sizes. The welds in Heat I plate were made in 9-in. x 10-in. x 3/4-in. and 72-in x 48-in. x 3/4-in blanks. The deposits in Heat B plate were made in either 20-in. x 10-in. x 3/4-in. or 52-in. x 26-in. x 3/4-in. blanks. Figures 1-5 present the specimen blank layout used for the plate blanks. Specimen codings are also shown on the layout, and may be referred to in subsequent sections to identify the locations of weld

TABLE IX

CHEMICAL COMPOSITION OF WELD WIRE
CHEMICAL COMPOSITION, WT. PER CENT

CODE	ARMETCO HEAT NO.	C	Mn	P	S	Si	Cu	Ni	Mo	Al	Ti	Co	B	Zr	N ₂	H ₂	O ₂	SOURCE OF ANALYSIS
		0.01	0.04	0.004	0.005	0.04	NA	18.29	4.96	0.10	1.03	9.40	0.003	0.014	0.002	0.0001	0.0015	Armetco
A1	07867	0.01	0.008	0.003	0.005	NIL	NA	17.30 18.7*	5.35*	0.17	0.92*	9.78*	NA	NA	0.001	NA	NA	Douglas
A2	06919	0.02	0.04	0.006	0.009	0.09	NA	17.94	4.75	0.002	0.60	9.74	NA	NA	0.0023	0.0001	0.0016	Armetco
A3	V-192	0.02	0.04	0.003	0.004	0.01	NA	17.95	4.50	0.06	1.20	9.80	NA	NA	0.0033	0.0001	0.0025	Armetco

* Spectrographic Analysis
NA No Analysis

TABLE X - TABULATION OF MECHANICAL TEST SPECIMENS MACHINED FROM HEAT-B WELDED TEST PLATES

<u>PLATES WELDED TOGETHER</u>	<u>MECHANICAL TEST SPECIMENS MACHINED FROM WELDED PLATES</u>
3W1, 3W3	AA-1, AA-2, AA-3, AA-4, AA-5, AA-6
W-22, W-26	BB-1, BB-2, BB-3, BB-4, BB-5, BB-6
W-32, W-34	CC-1, CC-2, CC-3, CC-4, CC-5, CC-6
W-38, W-40	DD-1, DD-2, DD-3, DD-4, DD-5, DD-6
W-5, W-9	GG-1, GG-2, GG-3, GG-4, GG-5, GG-6
W-21, W-25	HH-1, HH-2, HH-3, HH-4, HH-5, HH-6
W-31, W-33	JJ-1, JJ-2, JJ-3, JJ-4, JJ-5, JJ-6
W-42, W-45	KK-1, KK-2, KK-3, KK-4, KK-5, KK-6
4W-39, 4W-49	4A-1 through 4A-12, 4A-31
4W-31, 4W-7	4E-1 through 4E-7, 4E-31
4W-41, 4W-52	4F-1 through 4F-10, 4F-31
4W-42, 4W-54	4G-1 through 4G-7, 4G-31
4W-43, 4W-53	4H-1 through 4H-10, 4H-31
4W-51, 4W-55	4J-1 through 4J-12, 4J-31
2W-3, 2W-1	2A-1 through 2A-12, 2A-31
2W-5, 2W-7	2B-A1 through 2B-A6, 2B-1 through 2B-6, 2B-31
6W-5, 6W-6	6W-1, 6W-2, 6W-3, 6W-4
6W-7, 6W-8	6AW-1, 6AW-2, 6W-5, 6W-6
5W-2, 5W-4	7A-1 through 7A-9, 7A-13, through 7A-25
5W-10, 5W-12	7B-32, 7B-33, 7B-34, 7B-35, 7B-36, 7B-37, 6AW3, 6AW4, 7B-1, 7B-2, 7B-3
5W-6, 5W-8	7C-1 through 7C-6, 7C-32, 7C-33, 7C-34, 7C-35, 7C-36, 7C-37, 7C-10, 7C-11, 7C-12
W-3, W-7	211G-1, 211G-2, 211G-3, 211G-4, 211G-5, 211G-6
W-11, W-19	211H-1, 211H-2, 211H-3, 211H-4, 211H-5, 211H-6
W-1, W-23	211J-1, 211J-2, 211J-3, 211J-4, 211J-5, 211J-6
W-27, W-39	211K-1, 211K-2, 211K-3, 211K-4, 211K-5, 211K-6
W-4, W-8	211A-1, 211A-2, 211A-3, 211A-4, 211A-5, 211A-6
W-12, W-20	211B-1, 211B-2, 211B-3, 211B-4, 211B-5, 211B-6
W-2, W-24	211C-1, 211C-2, 211C-3, 211C-4, 211C-5, 211C-6
W-28	211D-1, 211D-2, 211D-3, 211D-4, 211D-5, 211D-6
2W2, 2W4	212A-1, 212A-2
2W6, 2W8	212B-1, 212B-2
4W8, 4W50	214A-1 through 214A-12
4W9, 4W36	213D-1, 214D-1 through 214D-8
4W10, 4W21	213E-1, 214E-1 through 214E-8
4W11, 4W33	213F-1, 214F-1 through 214F-8
4W12, 4W22	213G-1, 214G-1 through 214G-8
4W23, 4W34	213H-1, 214H-1 through 214H-8
4W24, 4W35	213J-1, 214J-1 through 214J-8
5W9, 5W11	215A-1, 215A-2, 215A-3
5W1, 5W3	215B-1, 215B-2, 215B-3
5W13, 5W15	215C-1, 215C-2, 215C-3
5W5, 5W7	215D-1, 215D-2, 215D-3
8W2, 8W4	222A-1, 222A-2, 222A-3, 222A-4, 222A-5, 222A-6, 222A-7, 222A-8
	222B-1, 222B-2, 222B-3, 222B-4, 222B-5, 222B-6, 222B-7, 222B-8
8W1, 8W3	222C-1, 222C-2, 222C-3, 222C-4, 222C-5, 222C-6, 222C-7, 222C-8
	222D-1, 222D-2, 222D-3, 222D-4, 222D-5, 222D-6, 222D-7, 222D-8

test blanks. Table X designates the sections that were welded together to provide the welded test specimens for mechanical evaluation.

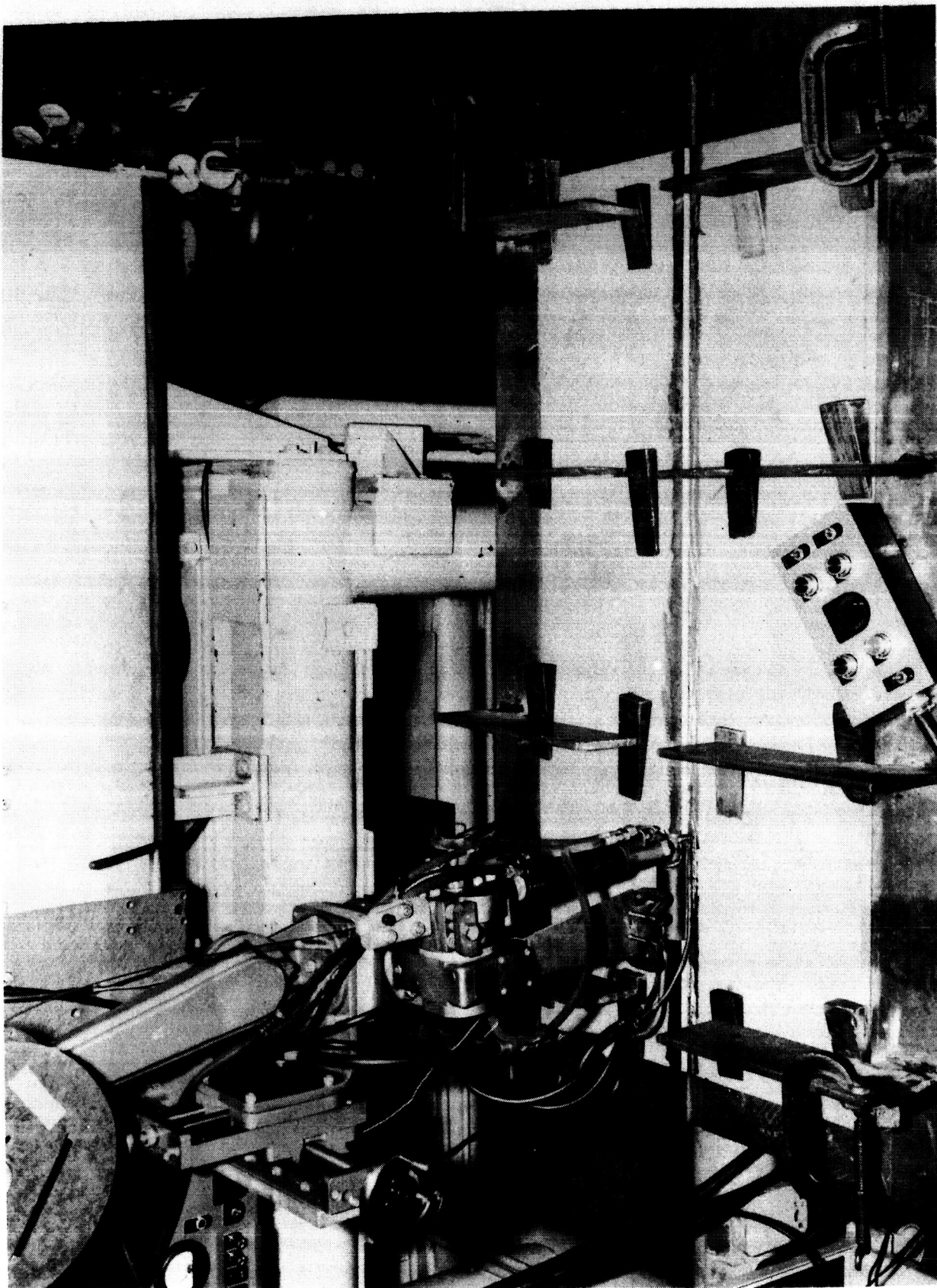
Most of the welds were deposited perpendicular to the plate rolling direction, although several test welds were also made parallel to the rolling direction. Welds were deposited primarily in the as-received mill annealed plate, although a few welds were also deposited in aged plate.

Prior to welding, the plates were usually grit blasted and always ground with a portable grinder adjacent to the weld joint preparation. This procedure served to remove any mill scale that might otherwise have contaminated the weld deposit. Stainless steel wire brushing was employed between passes to remove heat tint and excessive weldmetal scale.

The test plates were restrained in the flat position while welding to prevent lateral distortion. Neither preheat nor postheat was employed, and the interpass temperature never exceeded 300°F.

All welds were deposited with standard commercial welding equipment. Arc current and voltage were continuously recorded for each weld. The dewpoint of the argon shielding gas was periodically monitored both at the bottle outlet and welding torch nozzle (employing a special fitting). The dewpoint was always minus 70°F or lower.

Figure 42 shows a typical arrangement used for the welding of flat



SETUP FOR WELDING FLAT PLATE

FIGURE 42

TABLE XI

WELDING PROCEDURES AND WELDMETAL CHEMICAL COMPOSITIONS

CODE NO.	WELDING PERFORMED BY	BASE PLATE HEAT	WELDING PROCEDURE	APPROX KILO JOULES PER INCH OF WELD PER PASS	WELD WIRE	CHEMICAL COMPOSITION, WT. PERCENT														H ₂	O ₂	
						C	Mn	P	S	Si	Cu	Ni	Mo	Al	Ti	Co	B	Zr	N ₂			
W1	Douglas	I	Two-Pass MIG	120	A2	0.03 0.03	0.03			0.10		17.54 17.40	4.68		0.48 0.45	9.04 9.04			0.03 0.02			
W2	Douglas	I	Two-Pass MIG	120	A2	0.03 0.03	0.04			0.11		17.90 17.90	4.88		1.13 1.09	9.08 8.98			0.02 0.02			Ti IMPLANT USED FOR ALLOYING (SEE REF. 4)
W3	Douglas	I	Two-Pass MIG	130	A3							17.60			1.0	9.35						
W4	Douglas	I	15-Pass MIG	40	A3							NO ANALYSIS PERFORMED										DEPOSIT CHEMISTRY WOULD BE ABOUT THE SAME AS WIRE A3
W5	Douglas	I	C - Pass MIG	50	A2							NO ANALYSIS PERFORMED										DEPOSIT CHEMISTRY WOULD BE ABOUT THE SAME AS WIRE A2
W6	Douglas	I	1-Pass Electron Beam	20	None							NO ANALYSIS PERFORMED										DEPOSIT CHEMISTRY WOULD BE ABOUT THE SAME AS HEAT-1 PLATE
W7	Douglas	B	Two-Pass MIG	105	A1	0.02 0.01						18.75 18.10	4.46 4.45		0.97 0.90	8.9 8.1			0.006 0.006			
W8	Newport News	B	Two-Pass MIG	120	A1	0.015 0.02	0.03 0.02	0.005	0.003	0.06	0.04	18.33 18.52	4.74 4.75	0.16	0.75 0.81	8.14 9.15			0.007			
W9	Douglas	B	Two-Pass MIG	155	A1	0.01							4.50 4.75		0.91 0.85	8.05 8.60			0.008			

3.2

Flat Plate Welding - Specimen Preparation (Cont'd.)

plate at Douglas. The Newport News arrangement was similar. Table XI describes in a general way the different welding procedures that were employed and designates each weld type by means of a code number. These weld type codes will be referred to in subsequent sections. Weld deposit chemical compositions are also presented and will be discussed in subsequent sections.

Weld types W1 through W6 were evaluated in the previous Douglas sponsored programs and types W7 through W9 were prepared and evaluated in fulfillment of this contract. As may be seen from the tabulated characteristics in Table XI, the welding procedures included principally two-pass MIG deposited welds (about 120,000 joules per inch of weld per pass). However, multipass MIG (about 50,000 joules per inch of weld per pass) and electron beam welds (about 20,000 joules per inch of weld) are also included.

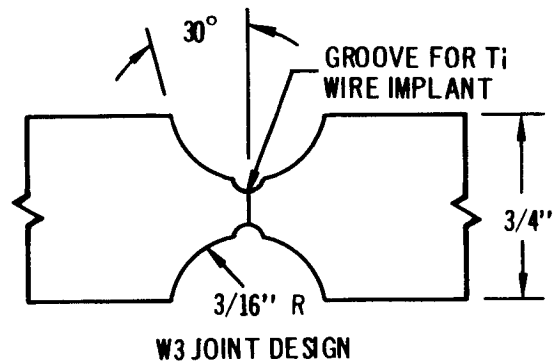
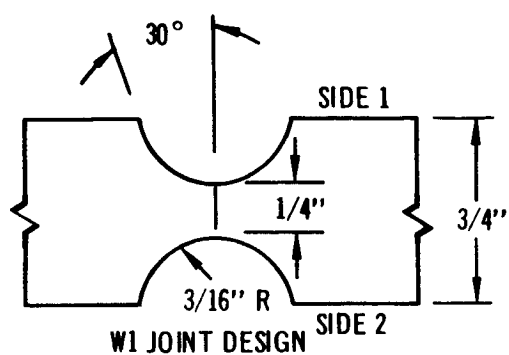
Figures 43 through 48 present the details of the welding procedures and joint preparations that were used for each type of weld listed in Table XI.

3.3

Inspection of Weldments

All weldments were radiographically inspected, and most were also surface dye penetrant inspected. Radiographic quality was rated per MIL-R-11468. Welds or weld sections were judged to be acceptable for testing only if the quality conformed to Class-I Standards. Dye penetrant was employed to detect surface cracks in weldmetal and heat-affected regions.

JOINT CONFIGURATION AND WELDING CONDITIONS FOR TYPES - W1 AND W2 WELDS



SIDE 1

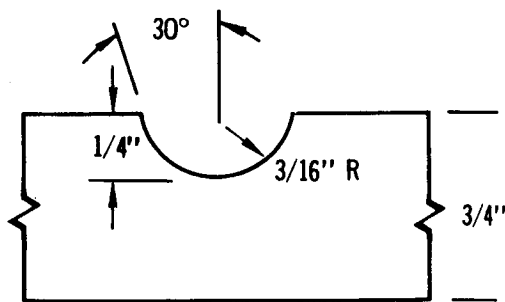
CURRENT - 475 AMPERES
VOLTAGE - 32 VOLTS
TRAVEL SPEED - 7.5 INCHES PER MIN (ipm)
PROCESS: MIG, DCRP
ELECTRODE: 0.093 - IN. DIAMETER TYPE A2
TORCH GAS: 80 CFH ARGON
TRAIL SHEILD: 190 CFH ARGON
TORCH ANGLE: 3° FOREHAND
POWER SOURCE; CONSTANT POTENTIAL
BASE PLATE: HEAT 1, 3/4 - IN THICK 18 Ni-7Co-.5Mo PLATE

SIDE 2

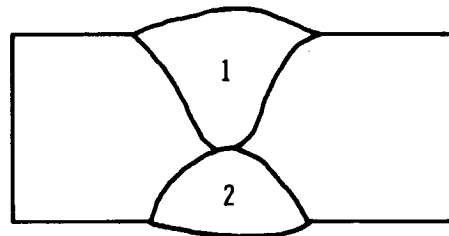
CURRENT - 475 AMPERES
VOLTAGE - 32 VOLTS
TRAVEL SPEED - 7.5 INCHES PER MIN.

FIGURE 43

JOINT CONFIGURATION AND WELDING CONDITIONS FOR TYPE - W3 WELDS



JOINT DESIGN



SIDE TWO BEVELED AFTER WELDING
SIDE ONE (SAME GROOVE AS SIDE ONE)

SIDE 1

CURRENT - 540 AMPERES
VOLTAGE - 31 VOLTS
TRAVEL SPEED - 7.5 (ipm)

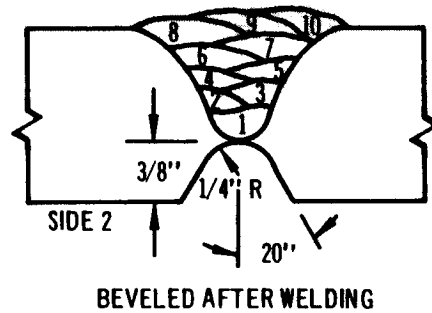
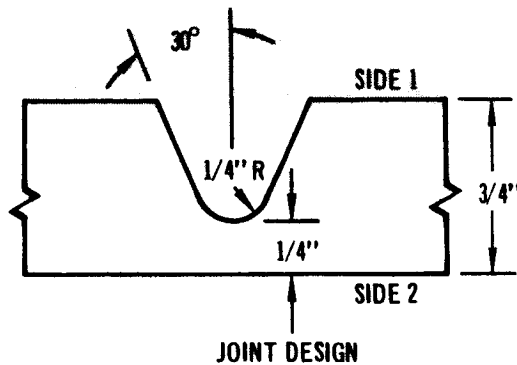
SIDE 2

CURRENT - 490 AMPERES
VOLTAGE - 33 VOLTS
TRAVEL SPEED - 7.5 (ipm)

PROCESS: MIG DCRP
ELECTROD: 0.093 - IN. DIAMETER TYPE A3
TORCH GAS: 80 CFH ARGON
TRAIL SHEILD: 190 CFH ARGON
TORCH ANGLE: 3° FOREHAND
POWER SOURCE: CONSTANT POTENTIAL
BASE PLATE: HEAT-1, 3/4-IN THICK 18Ni-Co-5Mo PLATE

FIGURE 44

JOINT CONFIGURATION AND WELDING CONDITIONS FOR TYPE- W4 WELDS



SIDE 1				SIDE 2			
PASS NO.	CURRENT AMPERES	VOLTS	TRAVEL SPEED i.p.m	PASS NO.	CURRENT AMPERES	VOLTS	TRAVEL SPEED, i.p.m.
1	580	29	18.5	1	420	26.5	18.5
2	510	29	18.5	2	465	26.5	14
3	500	26.5	18.5	3	465	26.5	14
4	450	26.5	18.5	4	465	26.5	14
5	470	26	18.5	5	465	26.5	14
6	450	26.5	18.5				
7	460	26	18.5				
8	455	26	18.5				
9	450	26	18.5				
10	455	26	18.5				

PROCESS: MIG, DCRP

ELECTRODE: 0.093 -IN. DIAMETER TYPE A3

TORCH GAS: 80 CFH ARGON

TRAIL SHIELD: 190 CFH ARGON

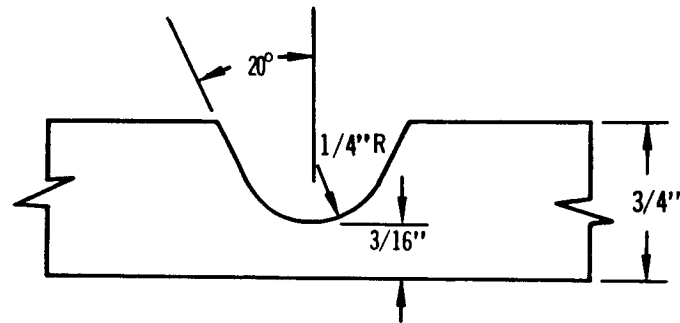
TORCH ANGLE: 3° FOREHAND

POWER SOURCE: CONSTANT POTENTIAL

BASE PLATE: HEAT-1, 3/4-IN. THICK 18Ni-7Co-5Mo PLATE

FIGURE 45

JOINT CONFIGURATION AND WELDING CONDITIONS FOR TYPE - W5 WELDS



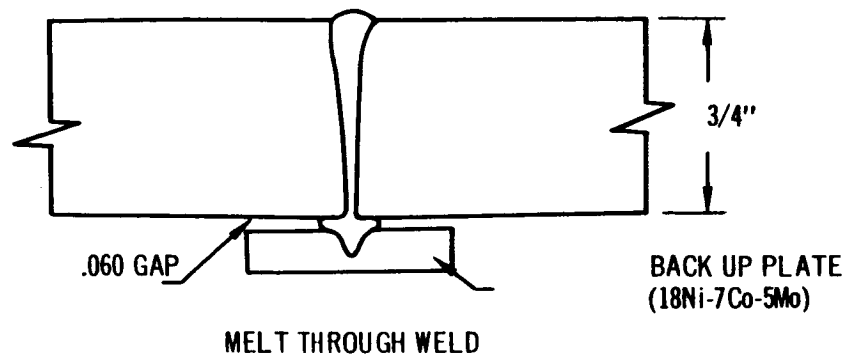
JOINT DESIGN

PASS NO.	CURRENT AMPERES	VOL TS	TRAVEL SPEED i.p.m.
1	350	30	10
2	315	29	12
3	350	29	12
4	350	29	12
5	350	29	12
6	350	29	13
7	350	29	13
8	350	29	13

PROCESS: MIG DCRP
ELECTRODE: 0.062-INCH DIAMETER TYPE A2
TORCH GAS: 60 CFH ARGON
TRAIL SHEILD: 60 CFH ARGON
POWER SOURCE: CONSTANT POTENTIAL
TORCH ANGLE: 3° FOREHAND
BASE PLATE: HEAT-1, 3/4-IN. THICK 18Ni-7CO-5MO PLATE

FIGURE 46

**JOINT CONFIGURATION AND WELDING
CONDITIONS FOR TYPE - W6 WELD**

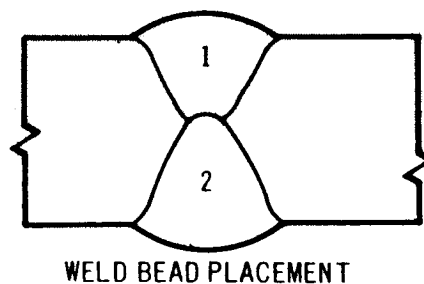
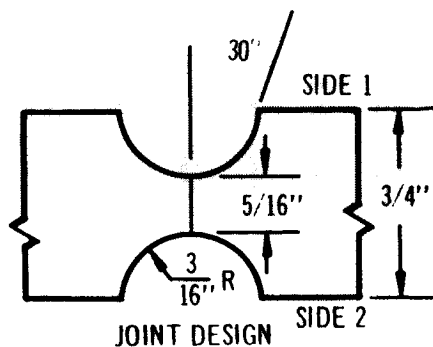


ELECTION BEAM WELD CONDITIONS:

BEAM VOLTAGE	30 Kv
BEAM CURRENT	370 Ma
TRAVEL SPEED	34 ipm
GUN TO WORK DISTANCE	1.5 IN
WELDOR-SCIACKY	150KV, .15ma
BASE PLATE: HEAT-1, 3/4-IN THICK 18Ni-7Co-5Mo PLATE	

FIGURE 47

JOINT DESIGN AND WELDING CONDITIONS FOR TYPES W7, W8, AND W9 WELDS



W-7 WELDING CONDITIONS

SIDE 1			SIDE 2		
CURRENT	-	425 AMPERES	CURRENT	-	570 AMPERES
VOLTAGE	-	24 VOLTS	VOLTAGE	-	25 VOLTS
TRAVEL SPEED	-	7.5 ipm	TRAVEL SP	-	7.5 ipm

SIDE

W-8 WELDING CONDITIONS

SIDE 1			SIDE 2		
CURRENT	-	420 AMPERES	CURRENT	-	460 AMPERES
VOLTAGE	-	32.5 VOLTS	VOLTAGE	-	32.5 VOLTS
TRAVEL SPEED	-	7.5 IPM	TRAVEL SPEED	-	7.5 IPM

W - 9 WELDING CONDITIONS

SIDE 1			SIDE 2		
CURRENT	-	485 AMPERES	CURRENT	-	525 AMPERES
VOLTAGE	-	36 VOLTS	VOLTAGE	-	37 VOLTS
TRAVEL SPEED	-	7 ipm	TRAVEL SPEED	-	7 ipm

PROCESS: MIG DCRP

ELECTRODE: 0.093-IN. DIAMETER TYPE A1
TORCH GAS: 70-80 CFH ARGON
TRAIL SHEILD: 90 CFH ARGON (TYPE W7 AND W9), 170 CFH ARGON (TYPE W8)
TORCH ANGLE: 3" FOREHAND
POWER SOURCE: CONSTANT POTENTIAL
BASE PLATE: HEAT-B, 3/4-IN. THICK 18Ni-7Co-.5Mo PLATE

FIGURE 48

3.4 Post-Weld Heat Treatment

Following welding and inspection, the welded plates were machined to provide the required test specimens. These specimens were then aged in accordance with the procedures described for the parent plate.

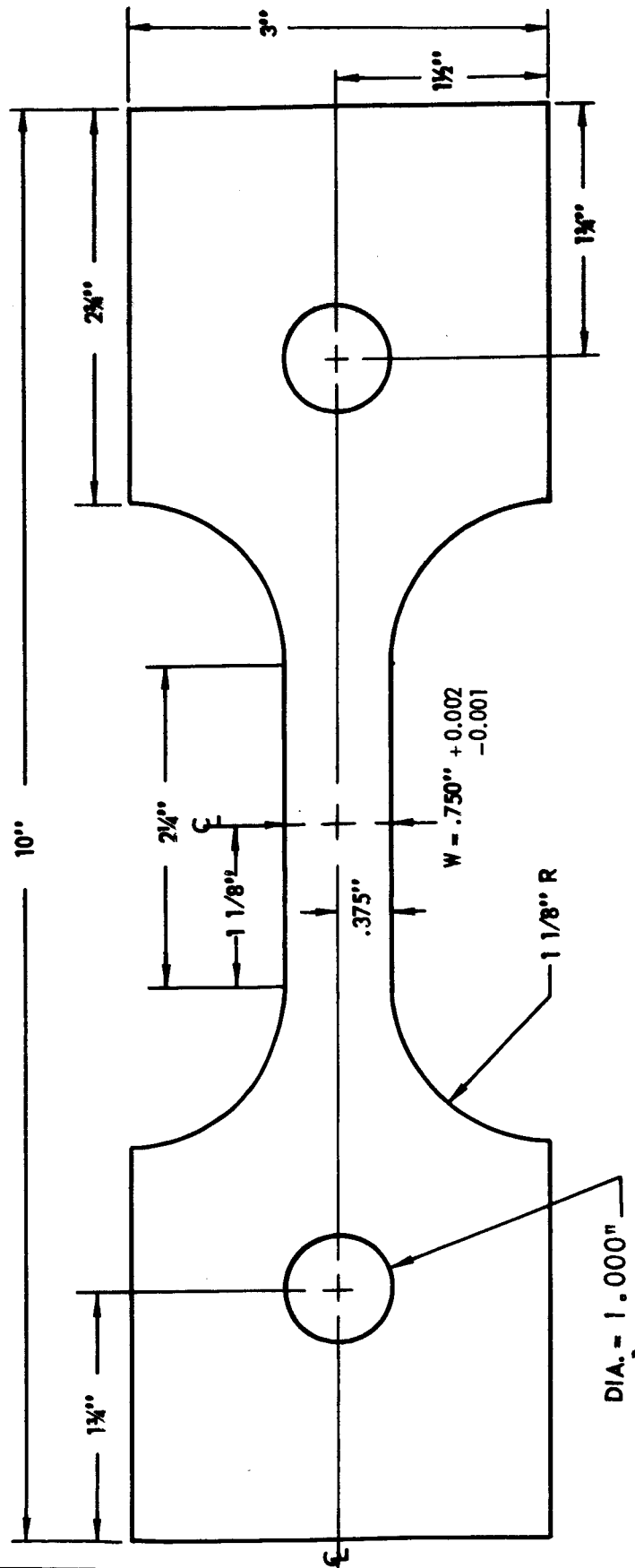
3.5 Mechanical Testing

Most tensile and fracture toughness testing of weldments was performed in accordance with the procedures described for parent plate. Any exceptions will be described in the appropriate sections. Table X details the locations of welded mechanical test specimens with respect to the individual welded test plate from which the specimens were machined.

Across-the-joint (i.e., transverse to the welding direction) tensile properties were measured using 0.505-in diameter round bars (Figure 6) and by means of 10" x 3/4" x 3/4" square bars (Figure 49). The latter type of specimen was also occasionally employed to determine longitudinal weldment properties. All-weldmetal tensile properties were measured using 0.250-inch diameter round bars (Figure 10). These specimens were carefully machined entirely from the second pass weld for all evaluations presented herein. The longitudinal axis of the 0.250-in diameter specimen was parallel to the longitudinal axis of the weld. Figure 50 illustrates the location of the specimen in the weld.

Fracture toughness evaluations were performed using the 8-in, 24-in.,

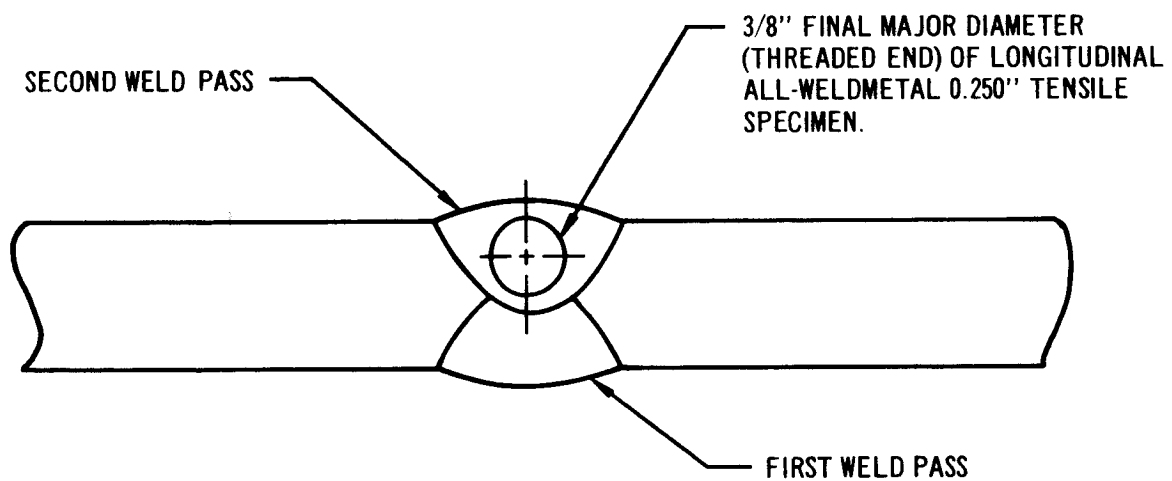
10" X $\frac{1}{2}$ " X $\frac{1}{4}$ " TENSILE SPECIMEN



NOTE
WHEN USED IN WELD EVALUATION,
WELDS WILL BE GROUND FLUSH
WITH PLATE SURFACE.

FIGURE 49

TRANSVERSE CROSS-SECTION ILLUSTRATING
THE LOCATION OF THE 0.250-INCH DIAMETER
ALL-WELDMETAL TENSILE SPECIMEN



TRANSVERSE CROSS SECTION

FIGURE 50

3.5 Mechanical Testing (Cont'd.)

and 48-in PTC specimen types illustrated previously in Figures 7, 8, 9 and 33. Several different specimen orientations with respect to the welding and plate rolling directions were investigated for weld-metal and heat-affected zone regions. Details of the various orientations will be described in the appropriate forthcoming sections.

3.6 Weldment Soundness

Some unexpected difficulty was encountered initially in producing welds of the required quality. An unusually high incidence of porosity developed in the first test welds made using the W9 conditions (See Tables XI and Figure 48). The incidence of porosity was sporadic and efforts to establish the cause or causes were not successful. Since a systematic study of porosity formation was not an objective of this contract, empirically guided modifications in the welding procedure were employed to eliminate the problem. The W7 and W8 conditions were capable of producing sound welds complying with the specified requirements.

The reasons for the improvement in weld quality produced by the change in welding conditions are not fully explainable. Work on the mechanisms of porosity formation in maraging alloys is worthy of further study.

Radiographic and dye-penetrant inspections failed to reveal significant weldmetal or heat-affected zone cracking in any of the welds.

3.6 Weldment Soundness (Cont'd.)

However, occasional crater cracking produced by inadequate crater fill was observed. Such cracking may be controlled by the automated adjustment of welding conditions upon termination of a weld. Microscopic examination of several weld sections failed to reveal any subsurface crack-like defects.

3.7 Effects of Welding and Heat Treatment Variables on Aging Response

This section presents data pertaining to the effects of post-weld aging treatments on the tensile and hardness properties of welds. The behavior of several weld types are described and compared. Both all-weldmetal and across-the-joint properties are discussed.

3.7.1 Effects of Aging Heat Treatment on the Aging Response of Type W9 Weldmetal

Although, as previously discussed, Type W9 welds were often characterized by unacceptable porosity, it was possible to machine specimens from porosity-free regions. All-weldmetal 0.250-in diameter specimens were machined from welds made both in as-received and in aged plate. The tensile specimens were aged at 875, 900, and 950°F for times ranging from 1 1/2 to 12 hours. Tensile property data are tabulated in Table XII and Appendix VII. The remarks column describes significant features of the fracture surface (as observed visually) in terms of a letter code. This letter code is defined in Table XIII and will be referred to frequently throughout the remainder of this report. The data are presented graphically in Figures 51, 52 and 53. The data are not

3.7.1

Effects of Aging Heat Treatment on the Aging Response of Type W9 Weldmetal (Cont'd.)

distinguished in terms of prior plate condition since this factor did not affect the results. The dependence of tensile strength properties on aging time at 875 and 900°F are quite similar. Both ultimate and yield strength tend to increase with increasing time. However, peak strength appears to be achieved after six hours at 900°F, while no peaking is evident at 875°F. Ductility appears to decrease drastically with increasing aging time at 875°F. Aging for 6 or 12 hours resulted in virtually nil ductility. The same trend is apparent for the 900°F specimens. However, scatter in the results makes the trend much less decisive. The low ductility upon prolonged aging is also manifested by the coincidence of yield and ultimate for one specimen aged for 6 hours at 900°F and another aged for 12 hours that failed at relatively low strength without measurable 0.2% yield.

The tensile strength of specimens aged at 950°F appears to be virtually independent of aging time. Ductility is uniformly low, although strengths equivalent to that achieved only after six hours aging at 875° and 900°F are attained after only 1 1/2 hours at 950°F.

Table XII describes a majority of the type W9 weldmetal specimens as being characterized by columnar appearing fracture surfaces. Figure 54 illustrates this typical columnar appearance. This structure resembles that resulting from fracture along the grain boundaries of large columnar grains produced in a very slowly

TABLE XII - LONGITUDINAL ALL WELDMETAL TENSILE DATA, SUMMARY
TYPE W9 WELDS IN HEAT-B PLATE

SPEC. NO.	CONDITION OF PLATE PRIOR TO WELDING	ORIENTA- TION	AGING TEMP., (°F)	AGING TIME (HRS)	0.2% YIELD STRENGTH (KSI)	ULTIMATE STRENGTH (KSI)	% ELONG (1" GAGE)	% REDUC- TION		REMARKS
								IN	AREA	
2IAA1	As Rec'd.	L-AWM	875	1.5	223.5	240.6	8.0	22.3		H
2IBB1	As Rec'd.	L-AWM	875	3.0	231.0	247.3	6.0	16.8		H
2ICC1	As Rec'd.	L-AWM	875	6.0	250.7	256.3	1.0	2.5		G
2IDD1	As Rec'd.	L-AWM	875	12.0	255.1	268.0	1.0	4.1		G
2IGG1	Aged	L-AWM	875	1.5	217.6	234.5	8.5	29.6		H
2IHH1	Aged	L-AWM	875	3.0	224.4	239.7	6.0	22.8		H
2IJJ1	Aged	L-AWM	875	6.0	254.5	263.3	1.0	3.1		G
2IKK1	Aged	L-AWM	875	12.0	260.8	276.2	2.0	3.2		G
2IAA3	As Rec'd.	L-AWM	900	1.5	232.4	247.7	1.0	5.5		G, H
2IBB3	As Rec'd.	L-AWM	900	3.0	240.8	258.7	4.5	18.3		G, H
2ICC3	As Rec'd.	L-AWM	900	6.0	257.4	257.4	1.0	6.3		G
2IDD3	As Rec'd.	L-AWM	900	12.0	NA	249.3	BOGM	1.6		H
2IGG3	Aged	L-AWM	900	1.5	225.7	241.1	6.0	24.6		H
2IHH3	Aged	L-AWM	900	3.0	240.1	249.3	1.0	1.6		G
2IJJ3	Aged	L-AWM	900	6.0	261.7	274.1	3.0	6.3		G
2IKK3	Aged	L-AWM	900	12.0	261.8	275.6	1.0	3.3		G
2IAA5	As Rec'd.	L-AWM	950	1.5	268.7	274.7	4.0	6.3		G
2IBB5	As Rec'd.	L-AWM	950	3.0	268.1	282.4	2.0	9.7		G
2ICC5	As Rec'd.	L-AWM	950	6.0	NA	265.6	1.0	3.1		G
2IDD5	As Rec'd.	L-AWM	950	12.0	265.3	276.0	1.0	0.8		G
2IGG5	Aged	L-AWM	950	1.5	253.9	268.6	4.0	14.1		H
2IHH5	Aged	L-AWM	950	3.0	262.2	273.5	1.0	2.3		G
2IJJ5	Aged	L-AWM	950	6.0	254.6	273.5	3.0	10.9		G
2IKK5	Aged	L-AWM	950	12.0	266.5	269.8	1.0	3.3		G

NOTES:

1. L-AWM - Longitudinal all weldmetal specimen; 0.250-in. diam.
2. See Table XIII for definition of Remark codes.
3. BOGM - Broke outside gage marks
4. NA - not available
5. Plates aged prior to welding were aged at 900°F for 3 hours.

TABLE XIII

CODE DEFINITIONS FOR VARIOUS TYPES OF OBSERVED FAILURES

<u>Code</u>	<u>Special Features of Failure</u>
A	Failure through weldmetal
B	Failure through heat-affected zone eyebrow
C	Failure through heat-affected zone between eyebrow and fusion line
D	Mixed failure - weldmetal and heat-affected zone
E	Failure through weldmetal - porosity on fracture surface (See Fig. 89)
F	Lack of fusion evident on fracture surface (See Fig. 88)
G	Columnar structure predominant on fracture surface (See Fig. 54)
H	Cup and cone fracture
J	Gold flakes on fracture surface - possible fracture initiation sites
K	Possible prior defect on fracture surface

EFFECT OF AGING TIME AT 875°F ON TYPE W9
ALL WELDMETAL UNIAXIAL TENSILE PROPERTIES

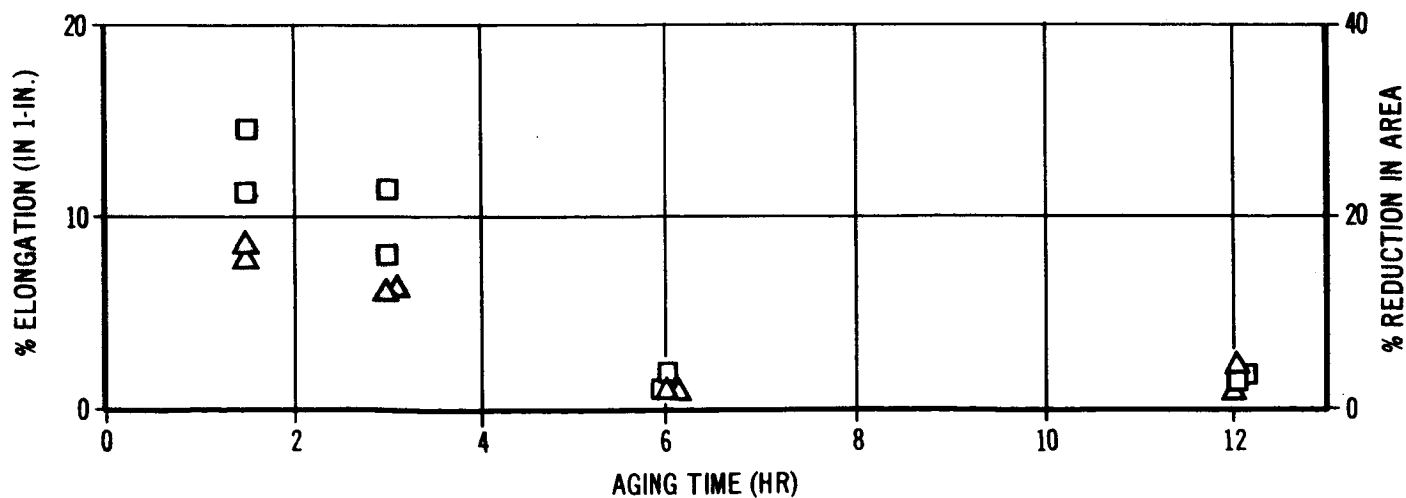
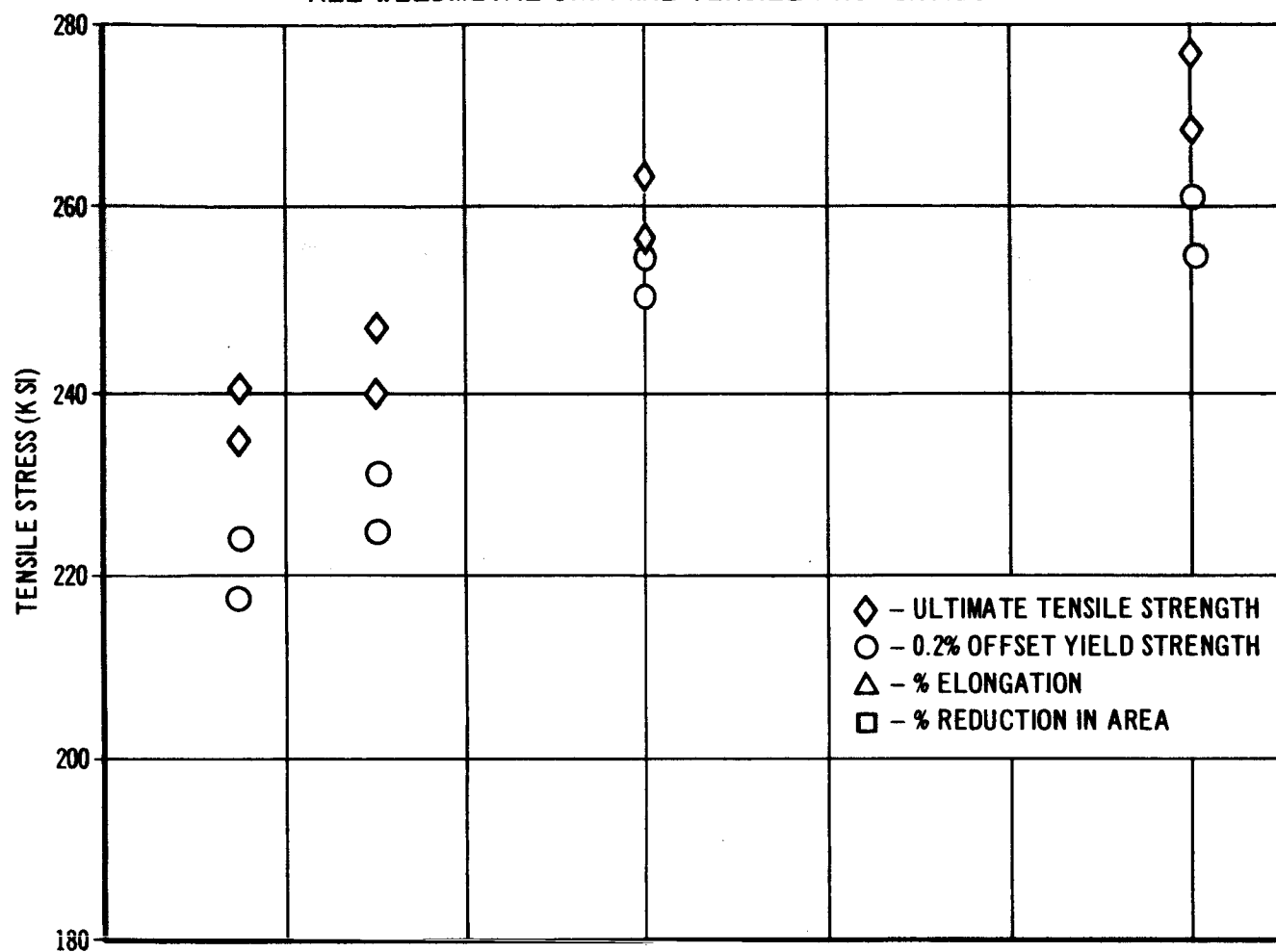


FIGURE 51

EFFECT OF AGING TIME AT 900°F ON TYPE W9
ALL WELDMETAL UNIAXIAL TENSILE PROPERTIES

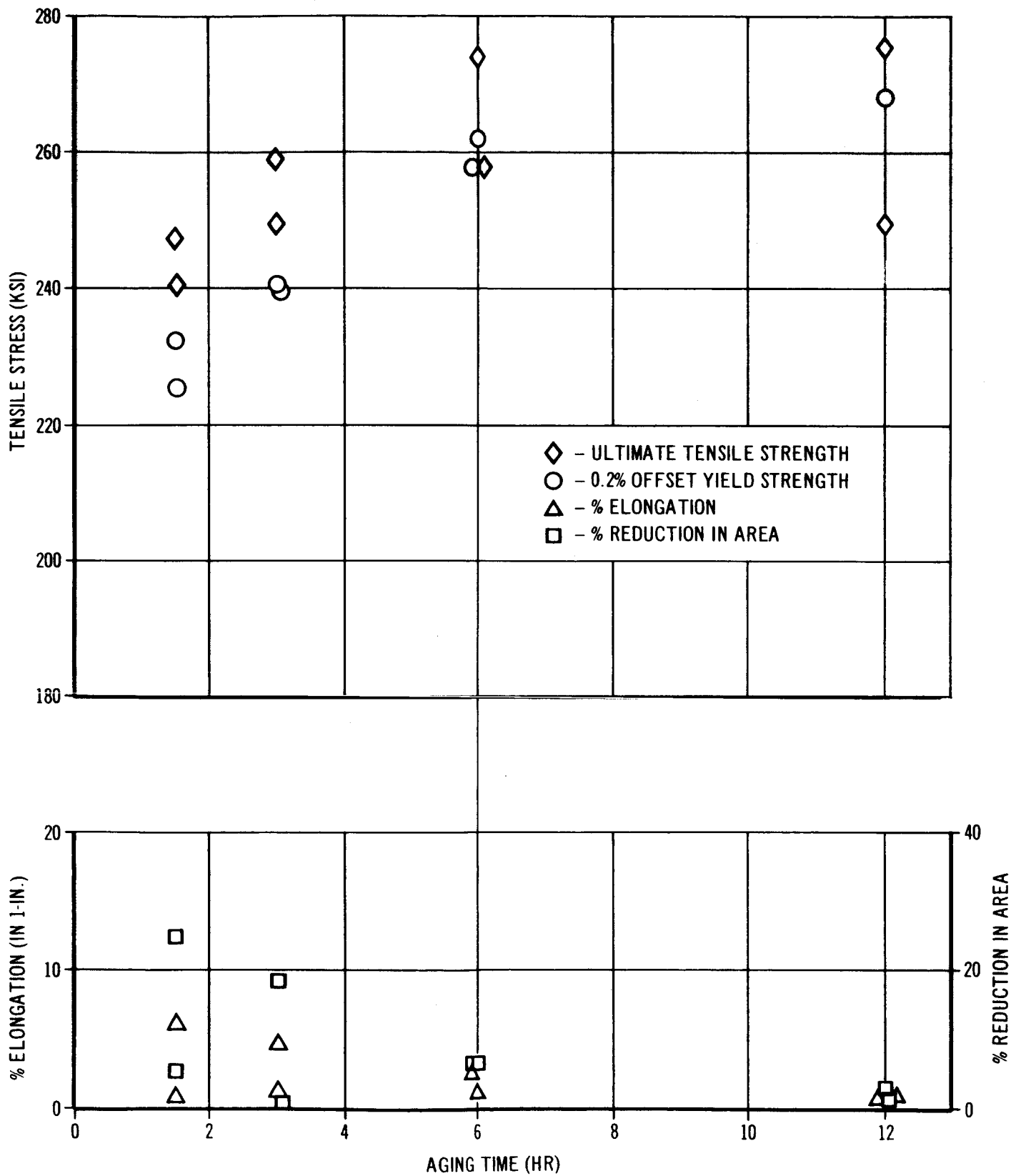


FIGURE 52

EFFECT OF AGING TIME AT 950°F ON TYPE W9
ALL WELDMETAL UNIAXIAL TENSILE PROPERTIES

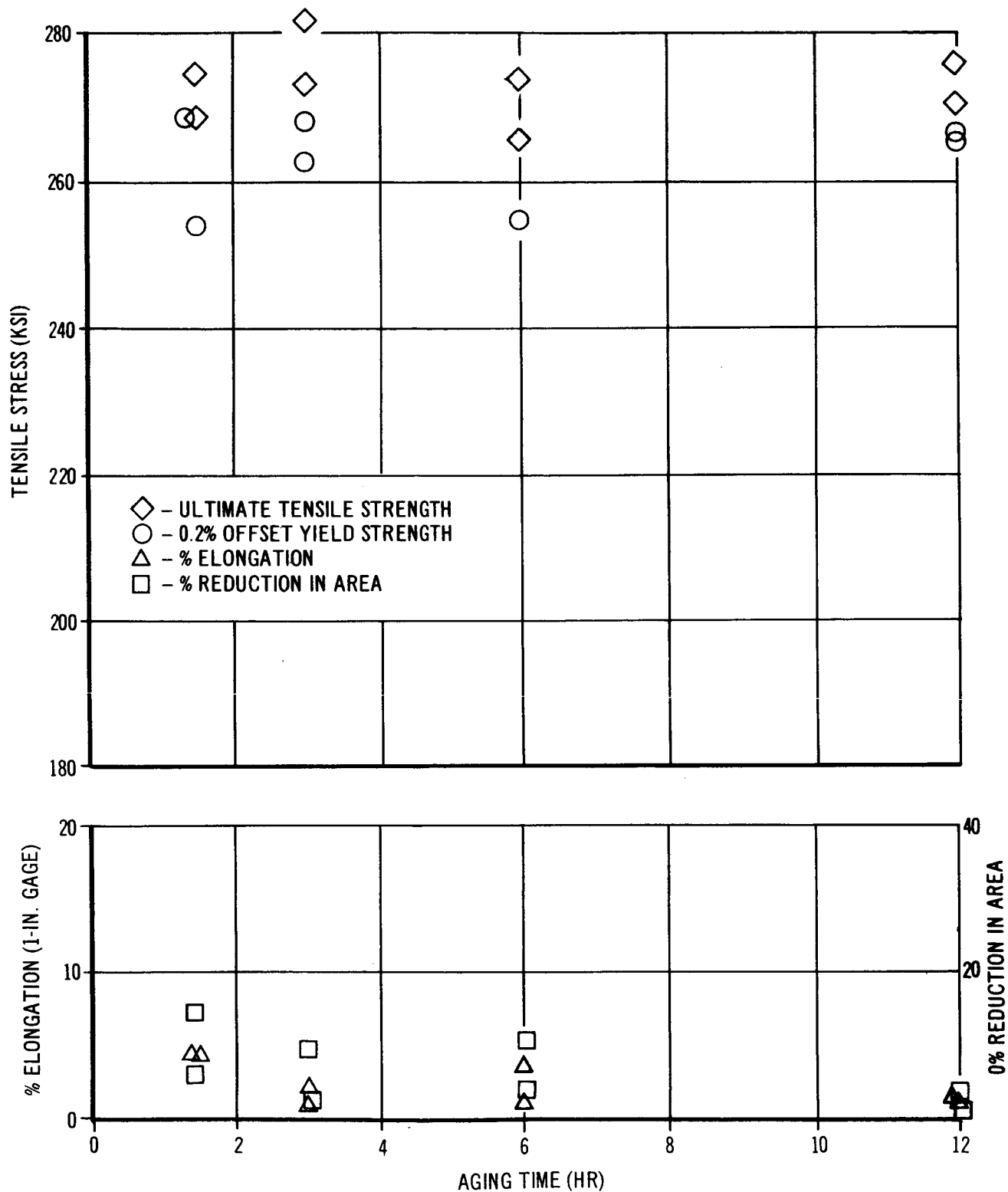


FIGURE 53

3.7.1 Effects of Aging Heat Treatment on the Aging Response of Type W9 Weldmetal (Cont'd.)

solidifying weld deposit. The type W9 welds were deposited using the highest unit energy investigated (approximately 150 Kilo Joules per inch of weld per pass), and would be expected to possess the coarsest grain structure. Electron fractographic examinations, described in a subsequent section indicate that the columnar fracture surfaces were laden with what is believed to be a damaging phase. This phase, identified as TiN, could substantially degrade ductility. It is not known whether the high concentration of TiN resulted from the high welding energy input or other unknown factors. The data do indicate, however, that the effects of welding energy input, and its attendant affect on weldmetal microstructure and properties, deserves further investigation.

3.7.2 Effects of Aging Heat Treatment on the Aging Response of Types W7 and W8 Weldmetal

Figures 55, 56 and 57 depict the dependence of types W7 and W8 all-weldmetal tensile properties on post weld aging heat treatment. Appendix VIII summarizes the same data. Figure 58 presents hardening response data for Type W8 weldmetal.

Examination of Figures 55-57 reveals that strength is significantly affected by aging time and temperature (Type W7 and W8 weldmetal respond similarly). Aging at 875 and 900°F produces continuously increasing strength up to 12 hours. Aging at 950°F produces peak strength at about 6 hours and a slight decrease after 12 hours. The weldmetal strength ranges from about 85 to approximately 100



TYPICAL COLUMNAR FEATURES ON TYPE W9
ALL WELDMETAL TENSILE SPECIMEN FRACTURE SURFACE

FIGURE 54

3.7.2 Effects of Aging Heat Treatment, on the Aging Response of Types W7 and W8 Weldmetal (Cont'd.)

per cent of that possessed by the Heat-B parent plate (compare Figures 55-57 to Figures 21-22). Aging at 950°F produced virtually equivalent strength in the weldmetal and parent plate for the full range of aging times investigated. Hardening response (Figure 58) parallels the strengthening response behavior. Ductility (as measured by both per cent elongation and per cent reduction in area) is relatively unaffected by aging treatment, although it appears to decrease slightly as aging time increases. Ductility values are generally slightly lower than for plate.

Unlike the W9 welds, columnar fracture surfaces were not observed on W7 and W8 all weldmetal tensile fracture surfaces. Both W7 and W8 type welds were deposited at significantly lower specific energy inputs than type W9. Thus it appears that the welding energy input may be an important factor influencing mechanical properties. However, as will be discussed later, welding energy input is probably significant only insofar as it may influence the dispersion of TiN in weldmetal.

3.7.3 Effects of Welding Procedure and Aging Heat Treatment on the Aging Response of Heat-Affected Regions

The aging response of heat-affected zones has been investigated by means of hardening response measurements and across-the-joint tensile properties. The data presented in this section indicate that although some strength impairment does prevail in heat-affected regions, the problem does not appear to be a major one.

EFFECT OF AGING TIME AT 875°F ON ALL-WELDMETAL UNIAXIAL TENSILE PROPERTIES OF DEPOSITS IN HEAT-B PLATE

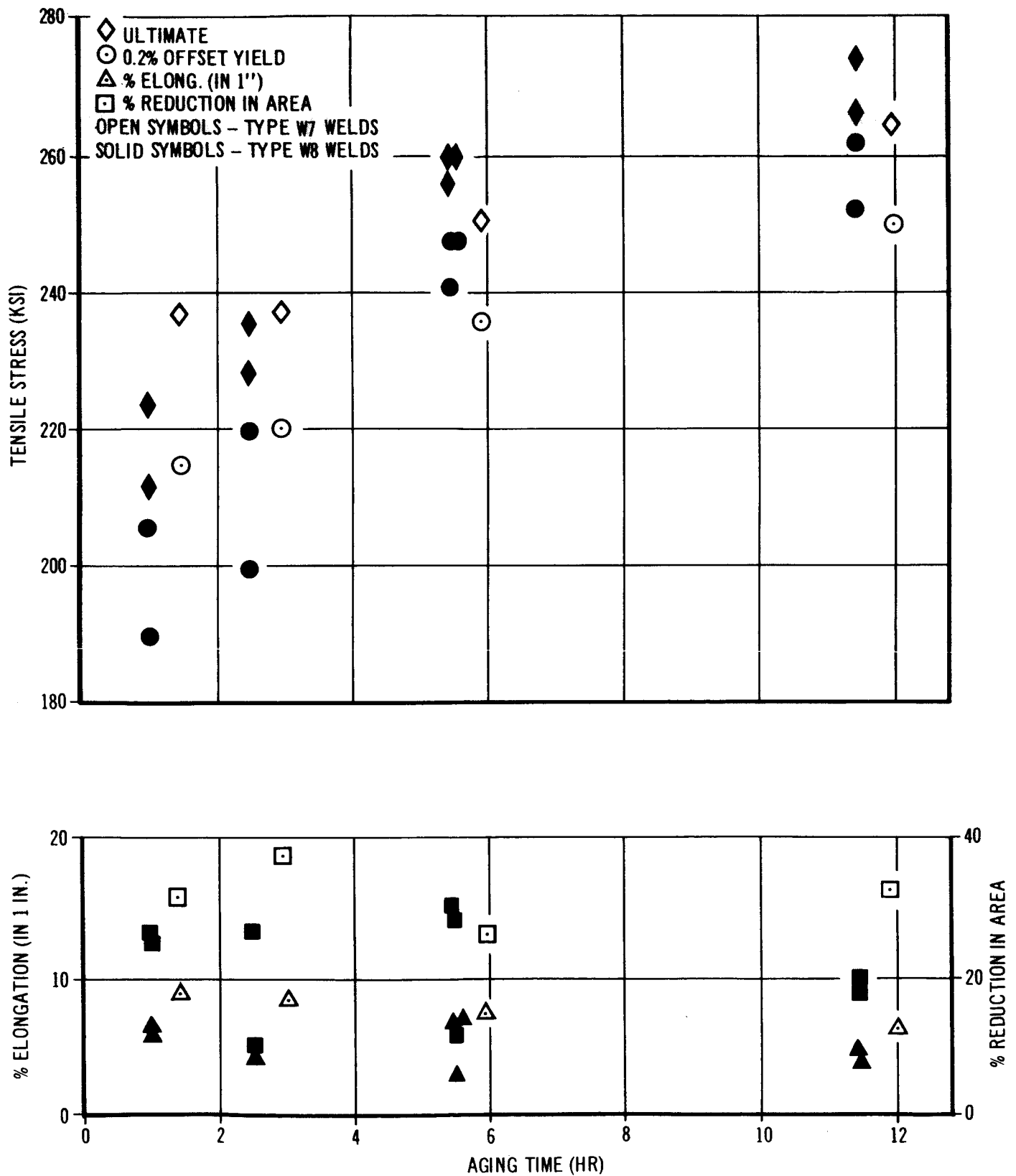


FIGURE 55

**EFFECT OF AGING TIME AT 900°F ON ALL-WELDMETAL
UNIAXIAL TENSILE PROPERTIES OF DEPOSITS IN HEAT-B PLATE**

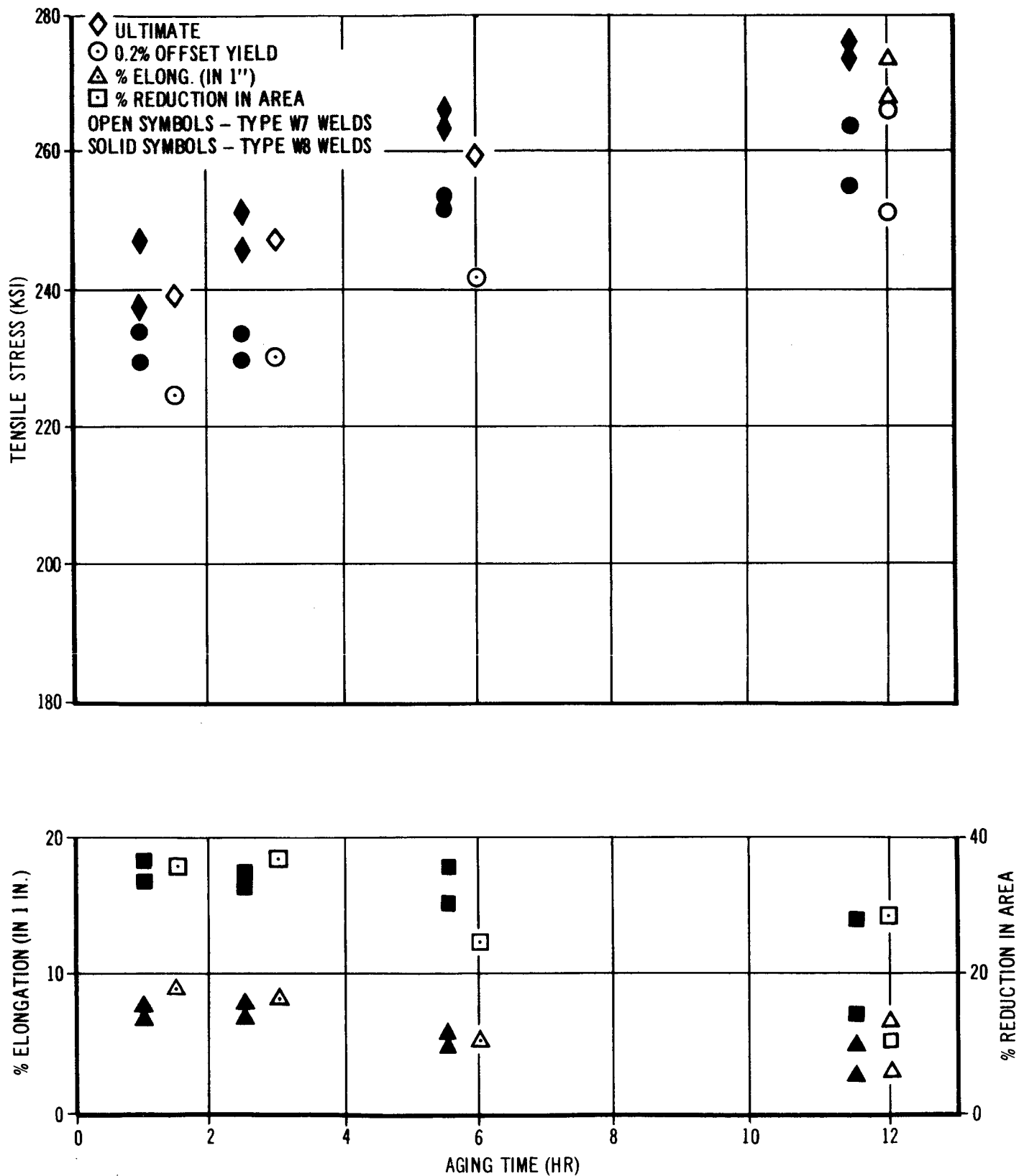


FIGURE 56

**EFFECT OF AGING TIME AT 950°F ON ALL-WELDMETAL
UNIAXIAL TENSILE PROPERTIES OF DEPOSITS IN HEAT-B PLATE**

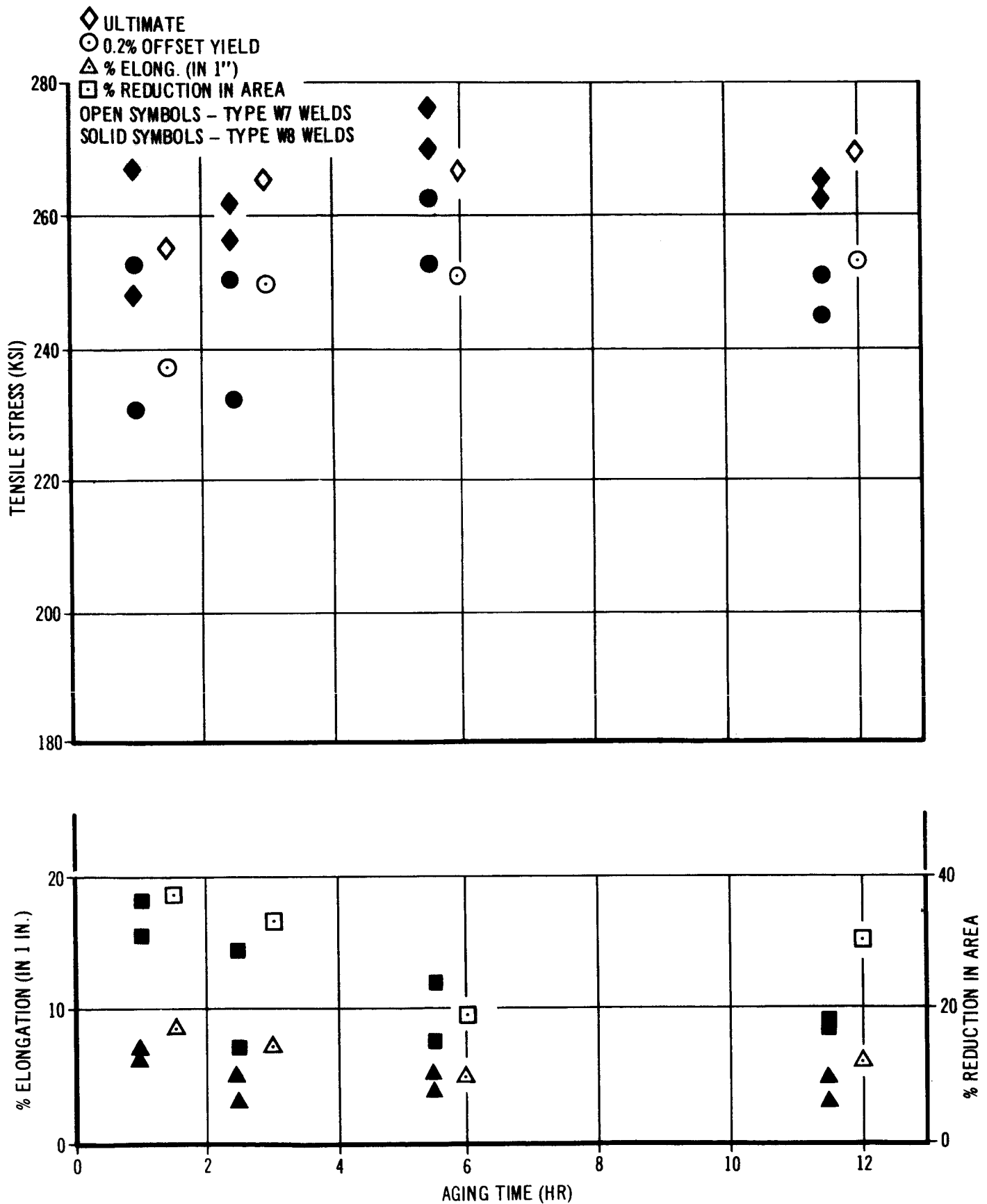


FIGURE 57

EFFECT OF AGING TIME AND TEMPERATURE ON
WELDMETAL HARDNESS

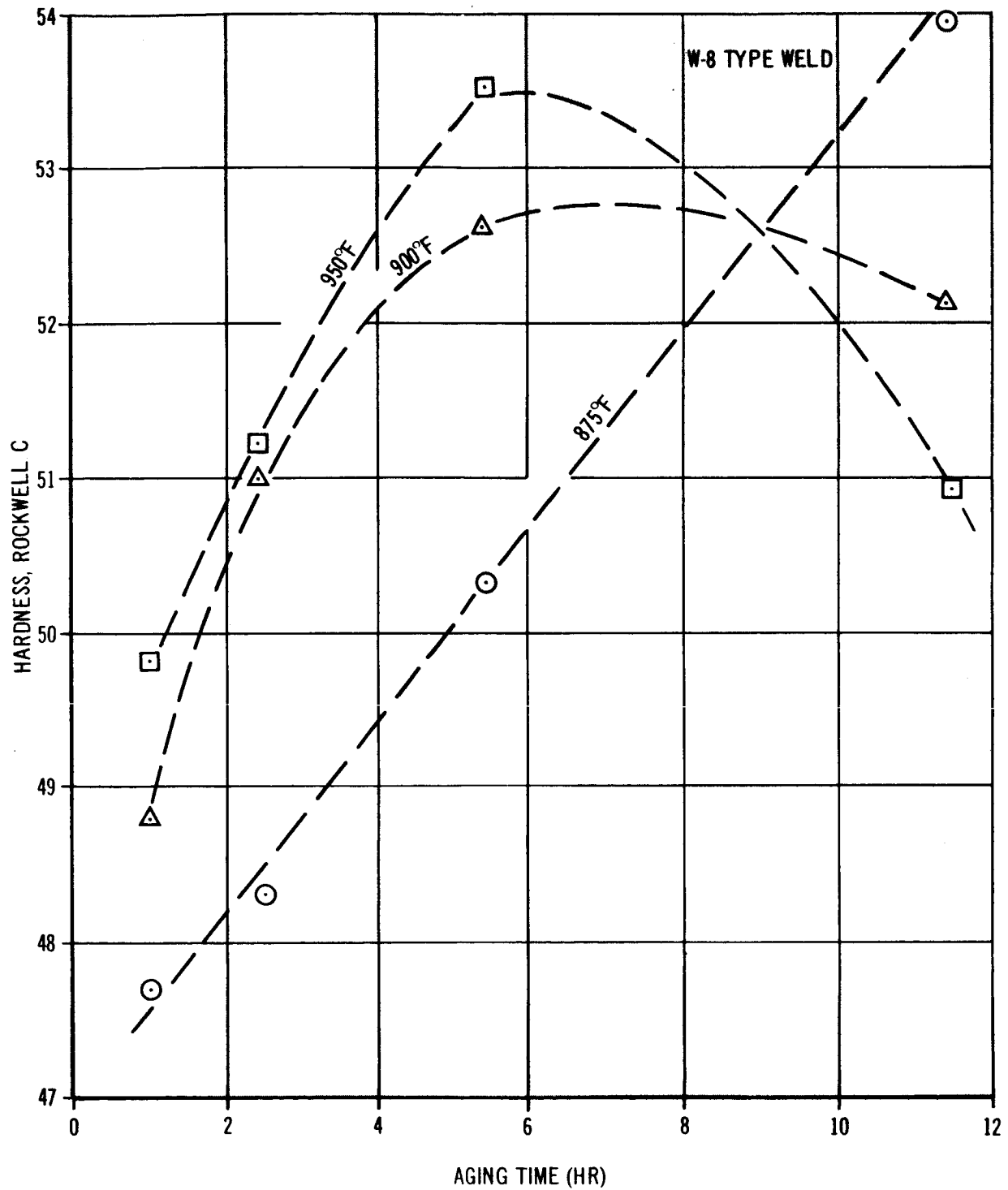


FIGURE 58

3.7.3 Effects of Welding Procedure and Aging Heat Treatment On the Aging Response of Heat-Affected Regions (Cont'd.)

Previous work (References 5-7) demonstrated that heat affected zone softening is produced in regions where brief exposures between about 1,200 and 1300°F occur. This softening has been shown to result from partial reversion and stabilization of austenite which does not respond fully to subsequent aging treatments, (References 8-11). Figure 59 illustrates the softening which occurs in the heat-affected zone as a result of austenite reversion.

Figure 60 depicts the effect of specific welding energy input on the minimum heat-affected zone strength of several types of welds previously described. Specific welding energy (i.e., energy per inch of weld per weld pass) was selected arbitrarily, and total integrated energy input could also be used. In either case the conclusions presented below would be the same. Tensile specimens (0.505-inch round bars) were machined transverse to the welding direction (the welding direction paralleled the rolling) and aged for 12 hours at 900°F. Under these conditions all failures occurred through heat-affected zones. Figure 61 illustrates a typical failure location for the two-pass welds. Fracture occurs substantially through the "eyebrow" regions as illustrated in the figure (where partial austenite reversion has occurred). It is noteworthy that the failure generally did not propagate through the coarsest-grained regions of the heat-affected zone adjacent to the fusion line. The strength data presented in Figure 60 may thus be interpreted to represent the minimum heat-affected zone ultimate tensile

3.7.3

Effects of Welding Procedure and Aging Heat Treatment On the Aging Response of Heat-Affected Regions (Cont'd.)

strength for the given welding procedures and the single postweld aging treatment.

The data presented in Figure 60 demonstrate that up to about 10 per cent loss in strength may occur in heat-affected regions. No decisive dependence on the specific welding energy input (joules per inch of weld per pass) may be ascertained from the data. Thus, it appears that over a wide range of welding thermal conditions, the heat-affected zone behavior remains relatively constant.

Figures 62 through 65 present additional data on the aging response of heat-affected zones in weldments of Type W2, W7, W8 and W9. Tabulated data are presented in Appendices VII and VIII. The data represent properties of across-the-joint specimens (0.505-inch diameter round bars) the majority of which failed through the "eyebrow" regions. Some W9 types failed through weldmetal exhibiting the columnar appearance previously described. Welds made in as-received as well as aged plate (900°F, 3 hours) are presented in Figures 63-65 for type W7 and W8 welds. Welds made in as-received or aged plate are not differentiated in the figures to simplify the presentation. However, welds deposited in aged plate generally exhibited slightly higher strengths after aging than those deposited in as-received plate. Apparently, previously aged plate is not impaired quite as much as as-received plate by the thermal effects of welding. Perhaps less austenite reversion occurs in the eyebrow regions of previously aged plate. The presence of a precipitate,

3.7.3 Effects of Welding Procedure and Aging Heat Treatment On the Aging Response of Heat-Affected Regions (Cont'd.)

containing austenite stabilizing elements, could also retard the rate of austenite reversion since additional time would be required for precipitate solution and subsequent reversion.

As may be seen from the tabulation in Appendices VII and VIII some of the tensile failures propagated through heat-affected zones away from the eyebrow. Thus it appears that some strength degradation may occur in other heat-affected zone regions as well. The tensile strength data, nonetheless, may be regarded as being a measure of the minimum heat-affected zone strength values. Reduction in area data give an indication of the relatively ductile nature of this region. Somewhat suprisingly, the data indicate that type W8 welds did not strengthen upon aging as well as the type W7. Additional across-the-joint and longitudinal specimens from type W7 and W8 welds were tested employing 10" x 3/4" x 3/4" specimens (Figure 49). Table XIV presents the tensile results after the specimens were aged for 3 hours at 900°F. The data indicate, as before, that the aging response of the type W7 welds was somewhat superior to that of type W8 welds. No satisfactory explanation can be offered to explain this difference. It is very unlikely that the small difference in specific energy input could account for the variation.

The data presented in Figures 62 through 65 also show that the impaired heat-affected zone regions may be strengthened by prolonged aging at the lower aging temperatures (875 and 900°F). The strength after prolonged aging approaches approximately 95% of the parent-

HARDENING RESPONSE IMPAIRMENT IN PLATE HEAT-AFFECTED ZONE TYPE W2 WELDS-HEAT-1 PLATE

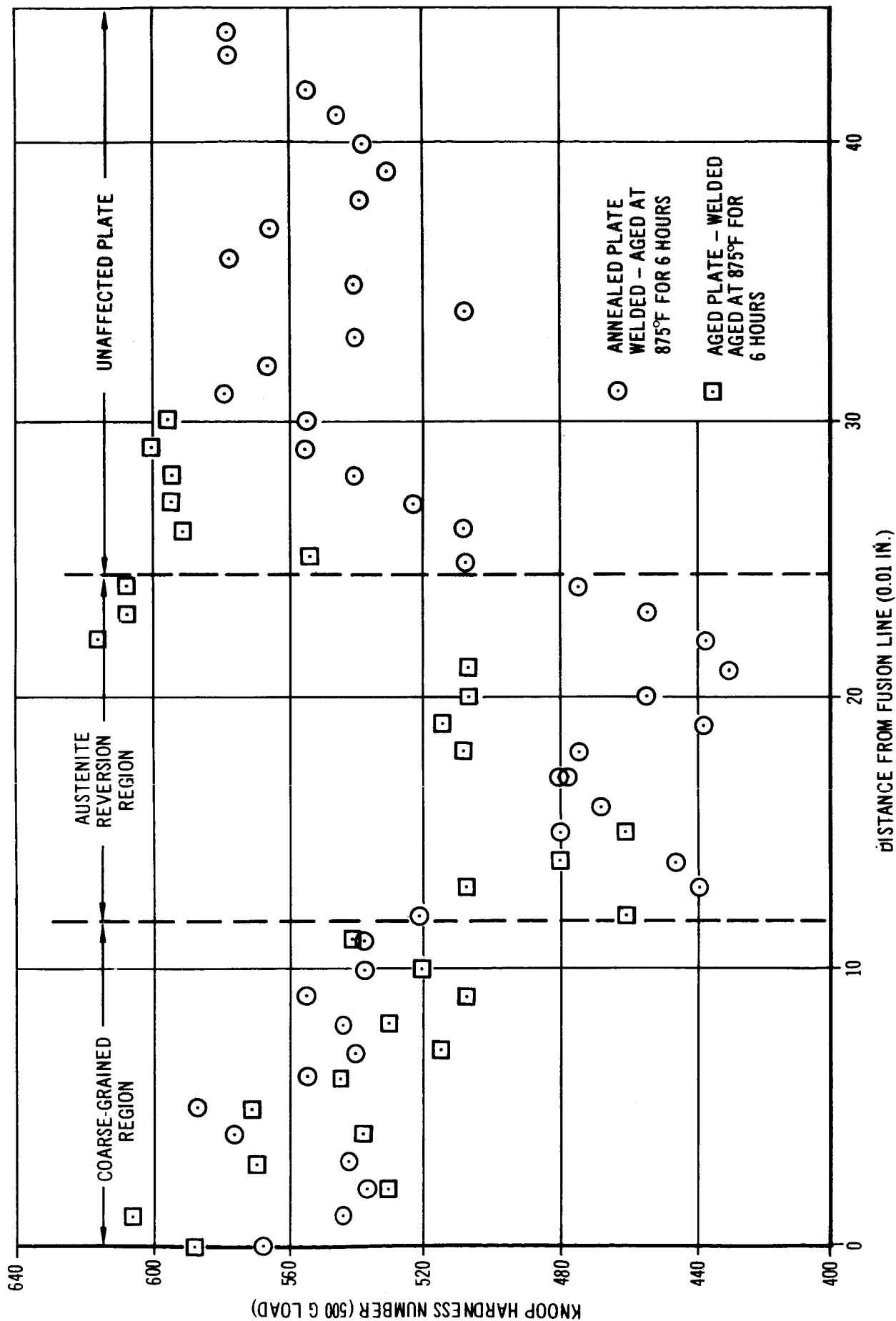


FIGURE 59

EFFECT OF WELDING ENERGY INPUT ON MINIMUM
HEAT-AFFECTED ZONE TENSILE STRENGTH AFTER 900F, 12 HR AGING

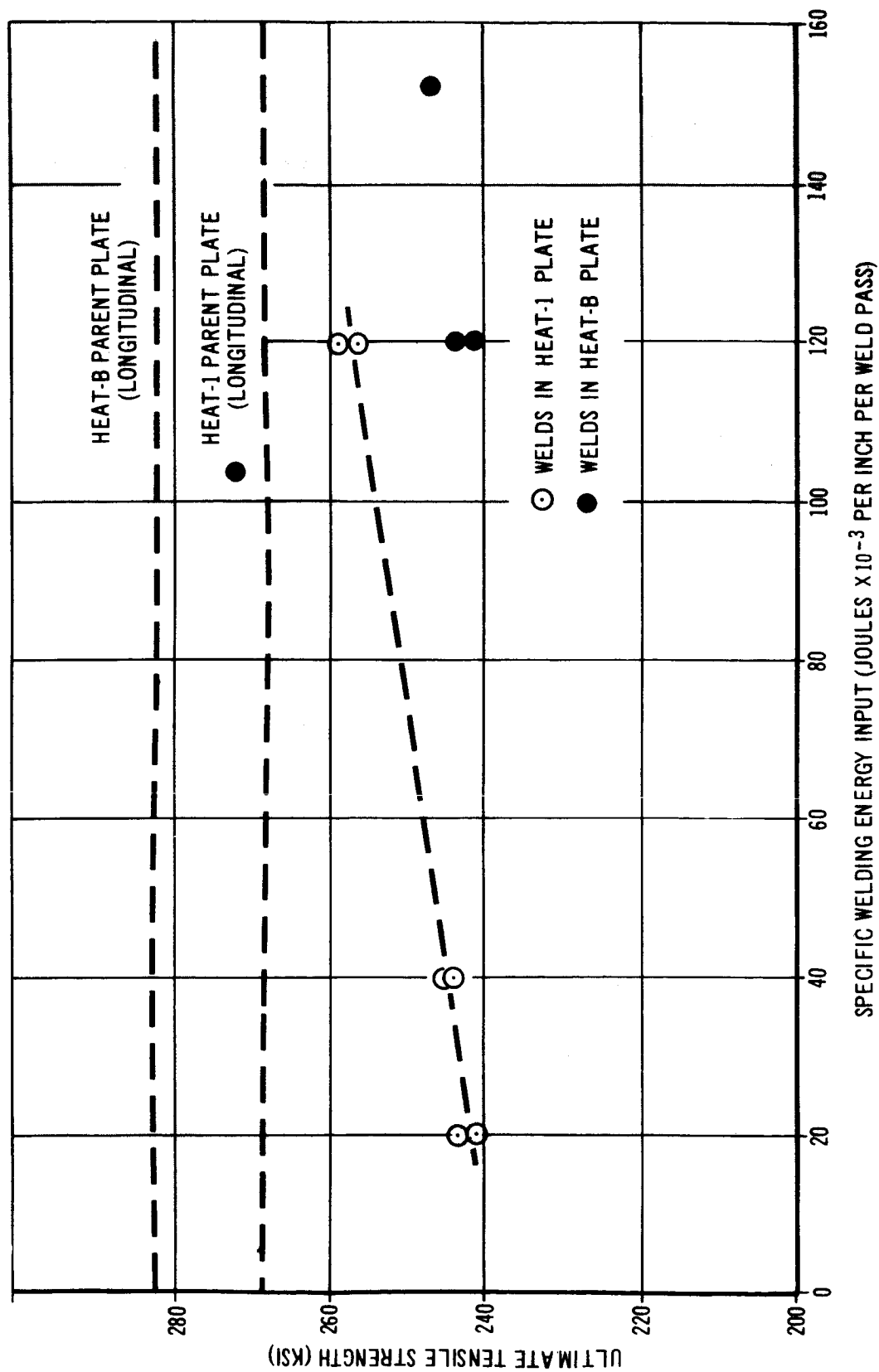


FIGURE 60

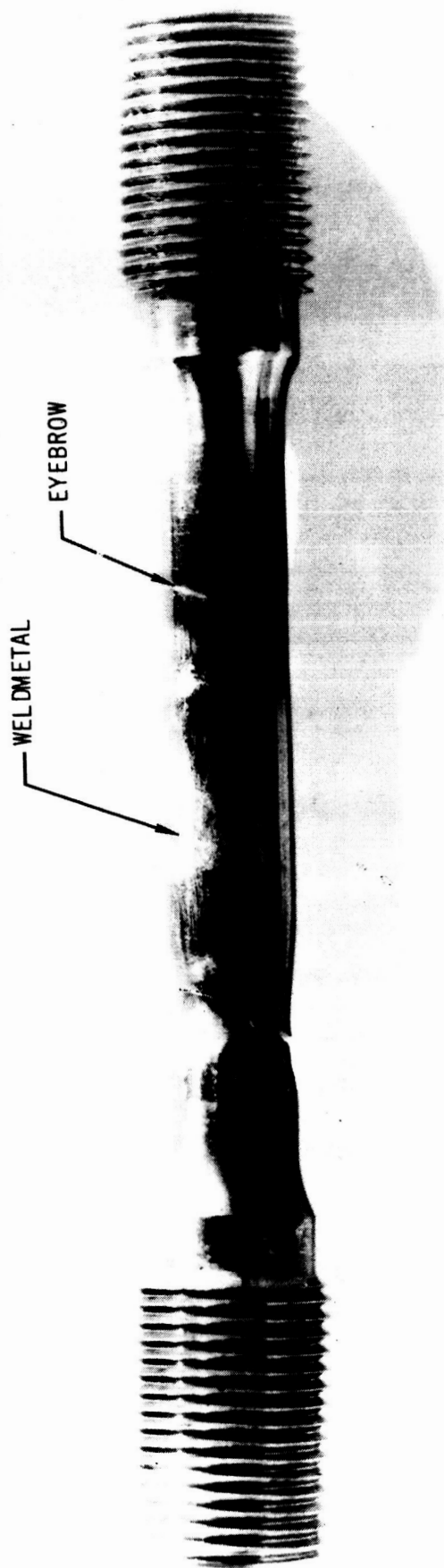


FIGURE 61

ACROSS-THE-JOINT TENSILE SPECIMEN
ILLUSTRATING TYPICAL LOCATION OF TENSILE
FRACTURE IN VICINITY OF HEAT-AFFECTED ZONE EYEBROW
(SPECIMEN ETCHED TO DELINEATE WELDMETAL AND EYEBROW REGIONS)

**EFFECT OF AGING TIME AT 875°F, 900, AND 950°F ON
THE ACROSS-THE-JOINT TENSILE PROPERTIES OF
TYPE W2 WELDS DEPOSITED IN HEAT-1 PLATE**

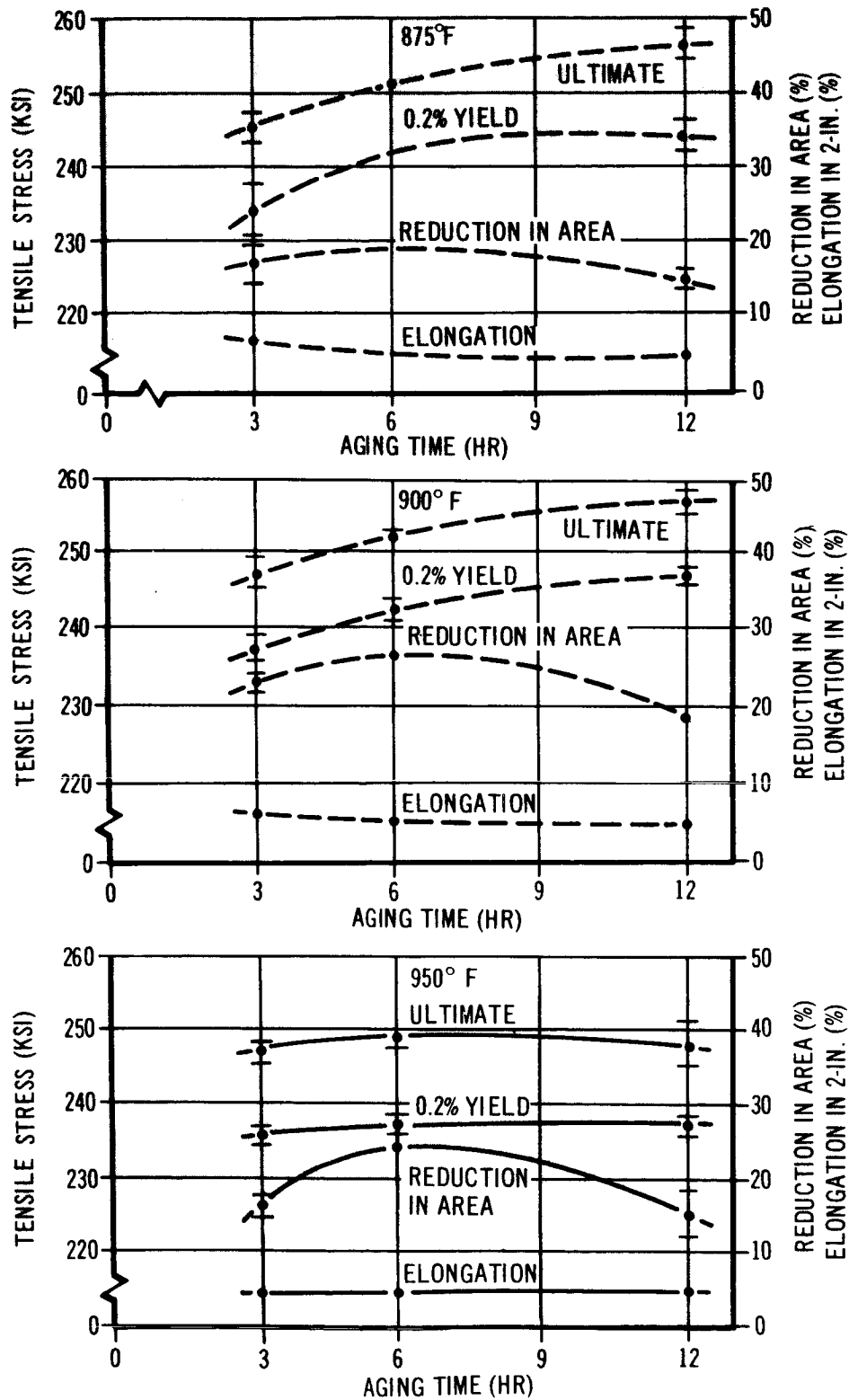


FIGURE 62

EFFECT OF AGING TIME AT 875°F ON THE ACROSS-THE-JOINT TENSILE PROPERTIES OF TYPES W-8 AND W-9 WELDS DEPOSITED HEAT-B PLATE

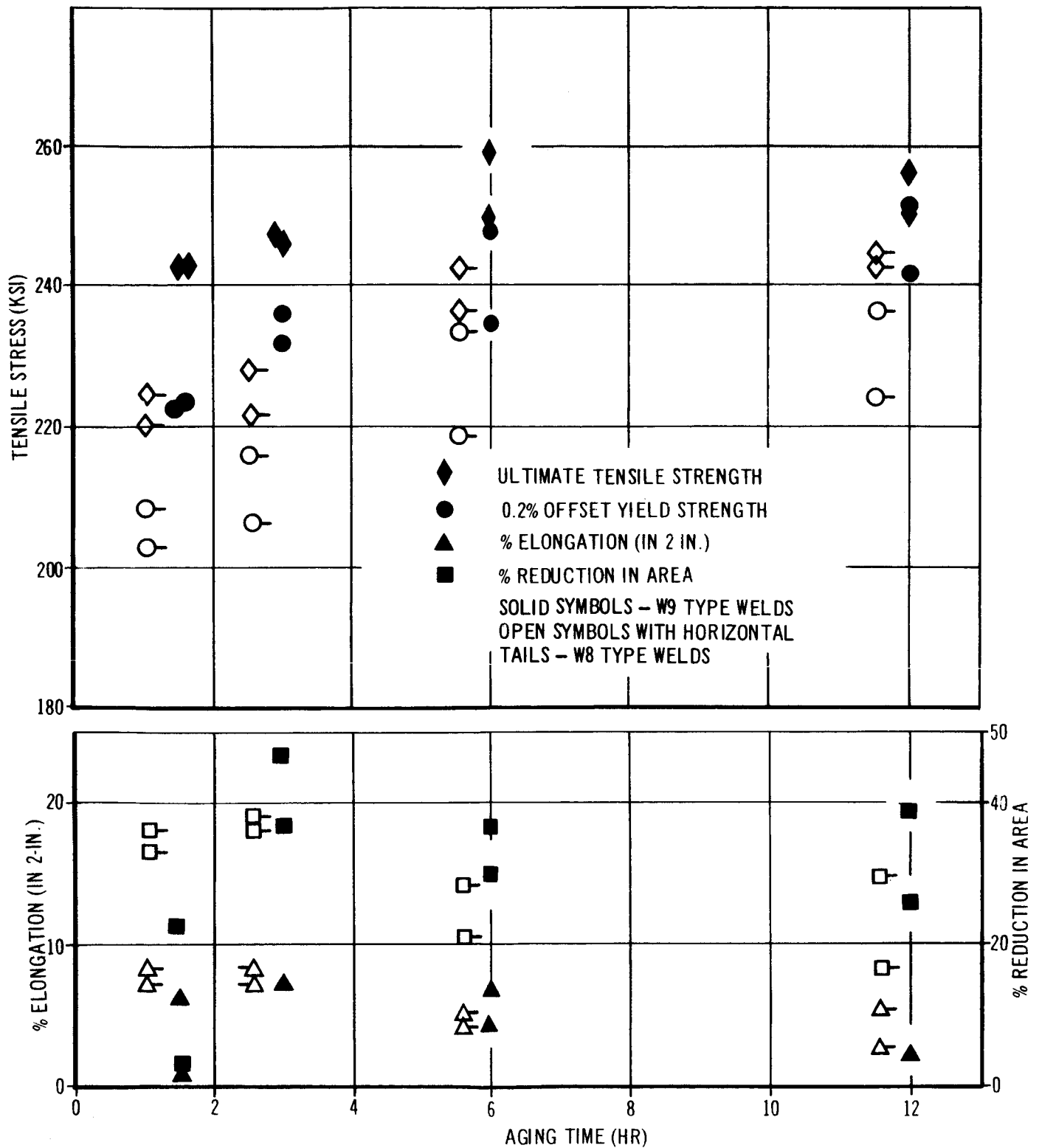
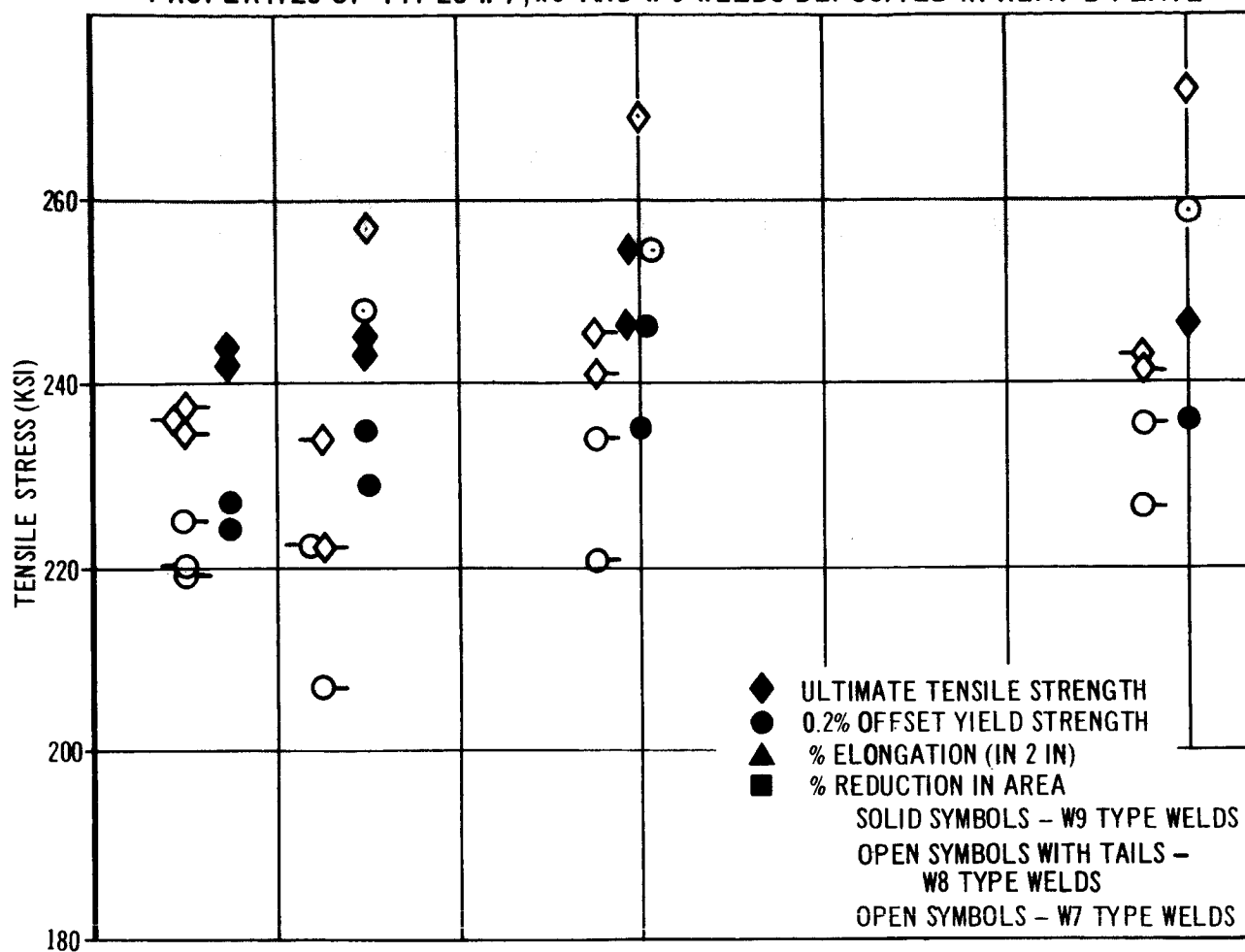


FIGURE 63

EFFECT OF AGING TIME AT 900°F ON THE ACROSS-THE-JOINT TENSILE PROPERTIES OF TYPES W-7, W8 AND W-9 WELDS DEPOSITED IN HEAT-B PLATE



EFFECT OF AGING TIME AT 950°F ON THE ACROSS-THE JOINT TENSILE PROPERTIES OF TYPES W-7, W-8 AND W-9 WELDS DEPOSITED IN HEAT-B PLATE

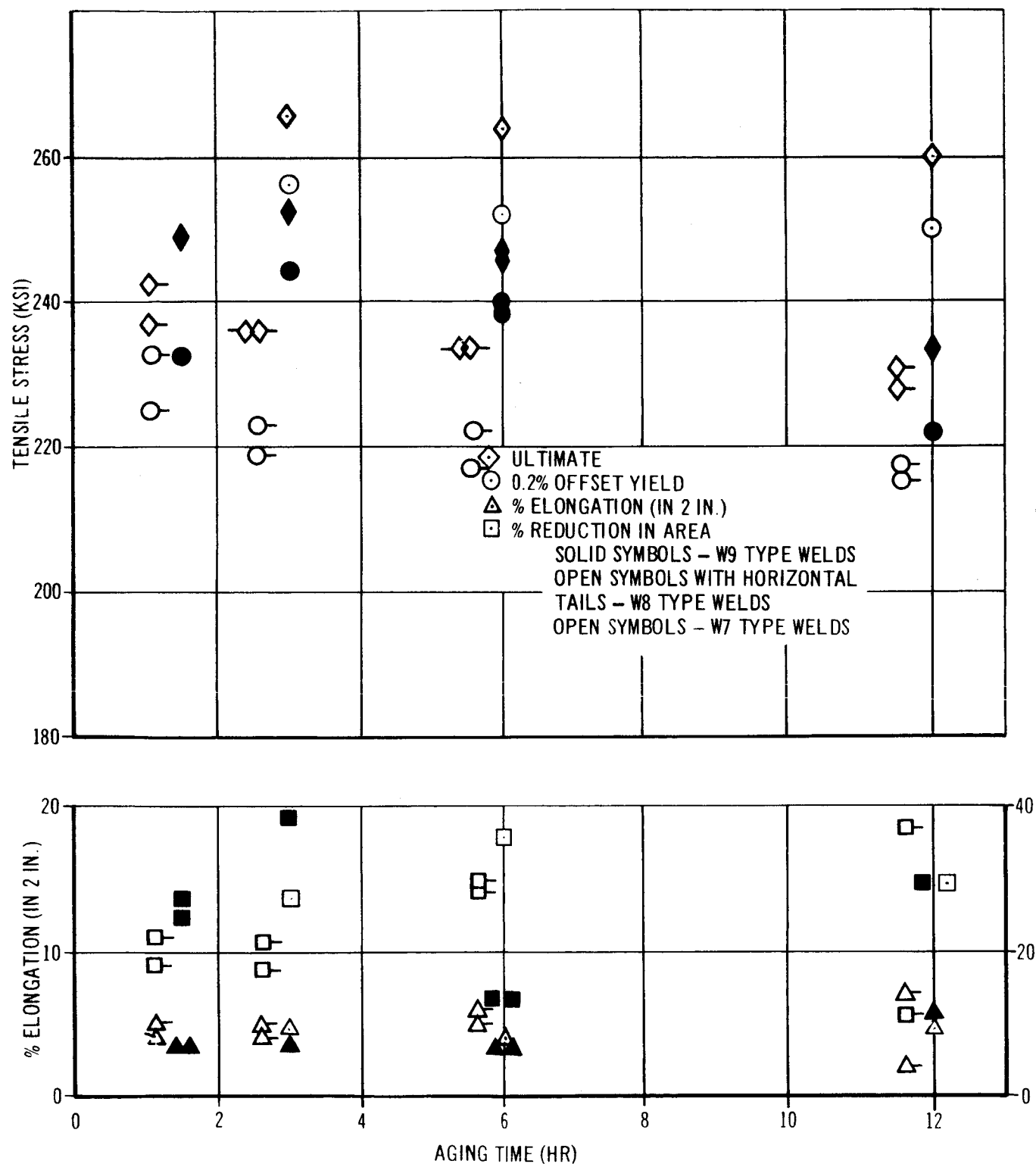


FIGURE 65

TABLE XIV TENSILE PROPERTY DATA ON TYPES W7 AND W8 WELDS

10" x 3/4 x 3/4" SPECIMENS

SPEC. NO.	WELD TYPE	PLATE CONDITION PRIOR TO WELDING	SPEC ORIENTATION	AGING TEMP. (°F)	AGING TIME (HRS)	0.2% YIELD STRENGTH (KSI)	ULTIMATE STRENGTH (KSI)	% ELONG (2- IN.)	REMARKS
6AW1	W7	As Rec'd.	L	900	3	245.8	264.5	7.0	J
6AW3	W7	Aged	L	900	3	252.7	263.9	5.5	
212A1	W8	As Rec'd.	L	900	3	255.0	258.0	7.0	
212B1	W8	As Rec'd.	L	900	3	262.0	267.0	8.0	
6AW2	W7	As Rec'd.	T	900	3	248.6	261.1	5.0	C
6AW4	W7	Aged	T	900	3	254.7	266.2	4.0	D
212A2	W8	As Rec'd.	T	900	3	243.0	247.0	5.0	C
212B2	W8	As Rec'd.	T	900	3	237.0	252.0	7.0	C

NOTES:

1. See Tables XI for definition of weld types
2. Plate aged before welding was aged at 900°F for 3 hours
3. See Table XII for definition of remark code numbers.

3.7.3 Effects of Welding Procedure and Aging Heat Treatment On The Aging Response of Heat-Affected Regions (Cont'd.)

plate strength, with little loss in ductility.

3.8 Effect of PTC Specimen Type and Orientation on the Net Fracture Stress of Weldmetal

As previously noted, during the initial stages of the 18Ni-7Co-5Mo maraging steel investigations at Douglas, a large (48" x 4" x 3/4") specimen was employed to measure the fracture toughness of the 3/4-inch thick plate and welds.

Results described in a previous section demonstrated that 18Ni-7Co-5Mo plate fracture toughness data obtained with 8" x 11/16" x 5/16" PTC specimens was essentially equivalent to that obtained with 24" x 3" x 3/4" PTC specimens. Data already presented, demonstrated that weldmetal would be expected to behave in a similar manner. This belief was further confirmed by tests performed on welds deposited in Heat B plate.

Figure 66 illustrates the specimen orientations used for the determination of weldmetal fracture toughness of deposits in Heat I plate.

Figure 34 (section 2.9.2) compares results obtained with the two specimen types in evaluating the fracture toughness of type W2 weldmetal (discussions concerning welding procedures and compositional effects will be presented in a later section).

Figure 67 depicts data on types W7 and W8 deposits in Heat B plate. In addition to the two specimen orientations employed for welds in Heat I plate, a third orientation was employed. The third specimen

3.8

Effect of PTC Specimen Type and Orientation on the Net Fracture Stress of Weldmetal (Cont'd.)

orientation consisted of a 8-in long, longitudinal, all weldmetal specimen. This type of specimen had to be machined to a thickness of 3/16-inch to assure an all-weldmetal coupon. The plane of the partial thickness crack is transverse to the longitudinal axis of symmetry of the weld and perpendicular to the plate surfaces.

The results indicate that rather close correlation exists among the different specimen sizes and crack orientations. The results obtained with the nominally 8" x 11/16" x 5/16" PTC specimens, regardless of crack orientation, are substantially in agreement with those obtained with the larger full 3/4-inch thickness specimens. These results must be qualified, however, since the ratio of crack length to crack depth is about the same for the various specimen sizes and orientations (crack length = 2 1/2 to 3 times depth; see Figure 37, Section 2.9.2). Had this not been the case, such good agreement would not have been obtained.

As a result of these findings, the small 8" x 11/16" x 5/16" PTC specimen was employed, almost exclusively, for the remainder of the weld evaluations conducted in fulfillment of this contract.

3.9

Effects of Weld Deposit Chemical Composition, Welding Procedure, and Post-Weld Aging Treatment on Weldmetal Fracture Toughness

This section summarizes experimental results concerning the dependence of weldmetal fracture toughness on a variety of welding, compositional and heat treatment variables. These observations,

PTC SPECIMENS AND CRACK LOCATIONS USED FOR
WELDMETAL FRACTURE TOUGHNESS EVALUATIONS

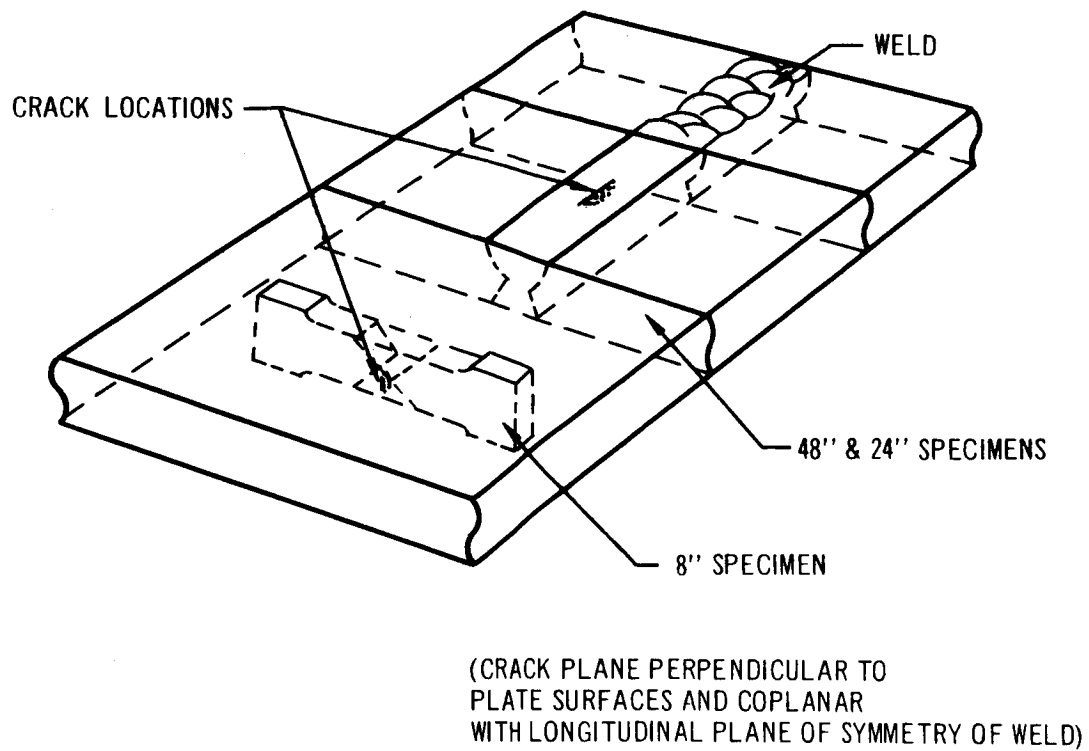


FIGURE 66

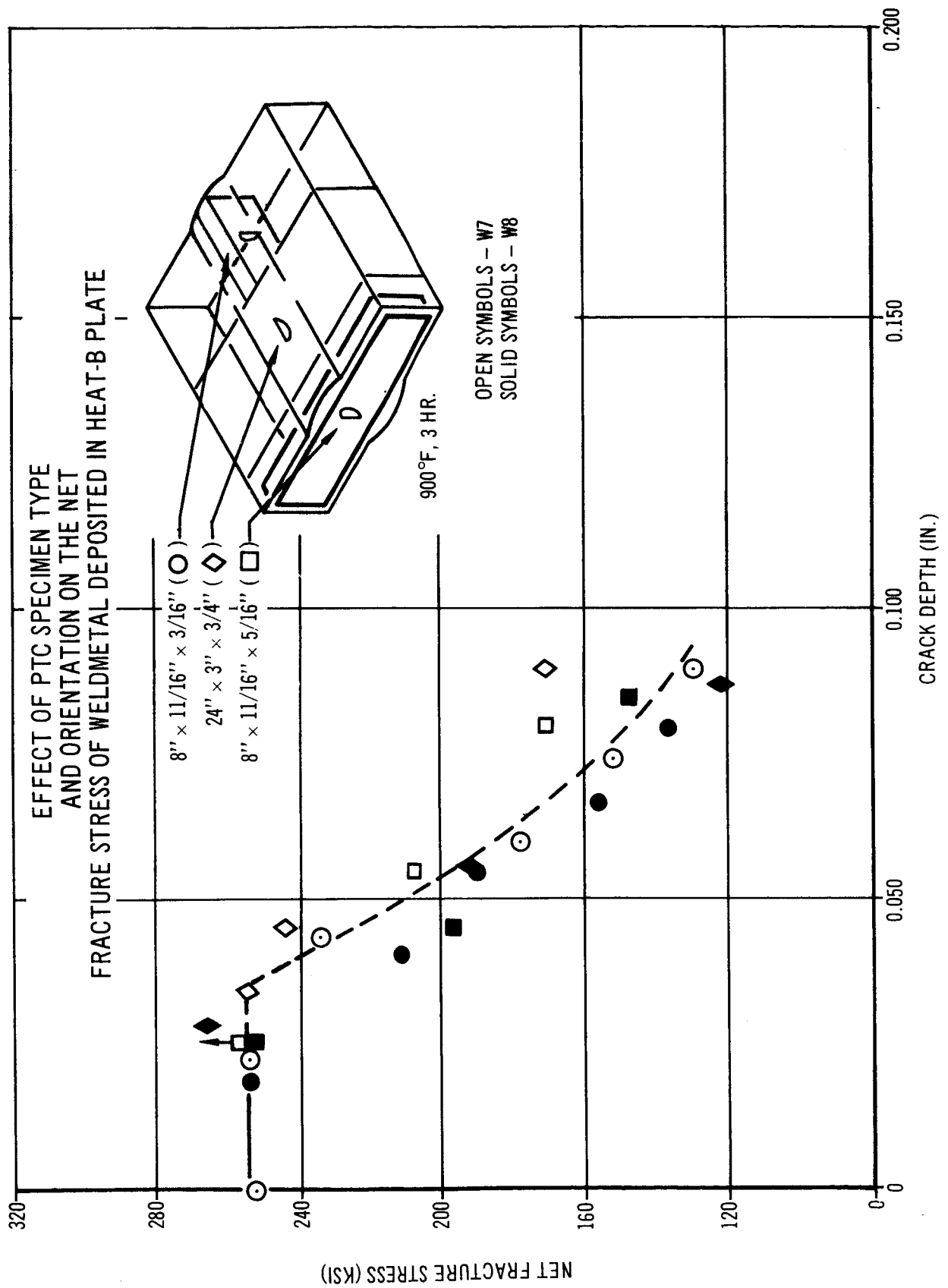


FIGURE 67

viewed in relationship to the metallurgical observations described in a later section, permit the formulation of an hypothesis relating the cause of inferior weldmetal toughness to a possible microstructural invariant.

3.9.1 Welds in Heat 1 Plate

As may be seen from the tabulated characteristics in Table XI, Section 3.2, the welding procedures included principally two-pass MIG deposited welds (about 120,000 joules per inch of weld per weld pass). However, multipass MIG (about 50,000 joules per inch of weld per weld per weld pass) and electron beam welds (about 20 joules per inch of weld) are also included. Figures 68 through 71 illustrate typical macrosections of some of the types of welds presented in Table XI. The differences in gross macrostructure are clearly evident. The two pass welds (Figures 70 and 71) are characterized by a pair of intersecting "eyebrows" which demark regions of partially reverted and retained austenite. The multipass welds (Figure 69) exhibit a multitude of intersecting "eyebrows", whereas the electron beam weld (Figure 68) exhibits single eyebrow paralleling each fusion line.

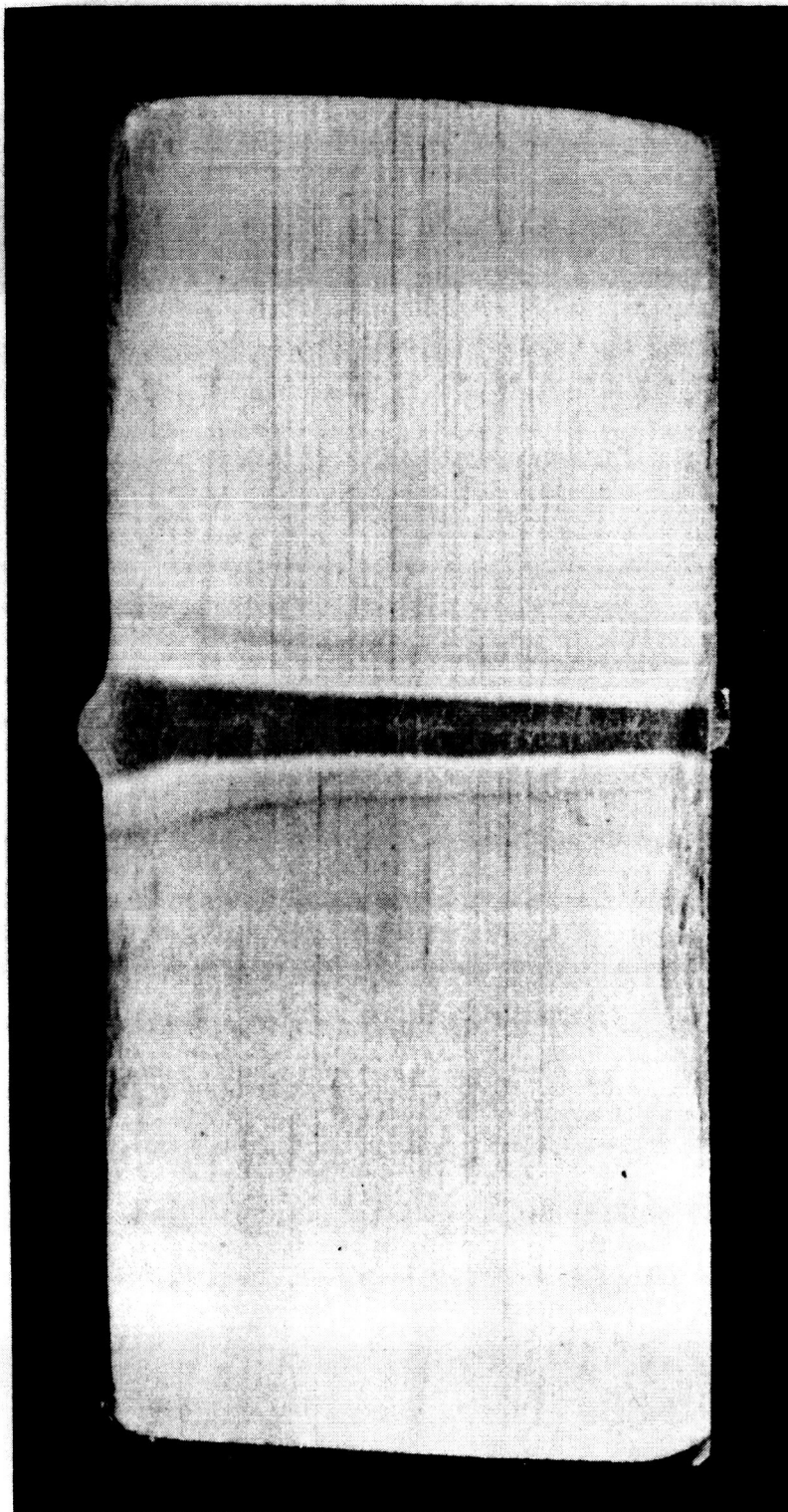
Figure 72 depicts the net-fracture strength characteristics for the various types of welds deposited in Heat 1 plate. The plane of the partial thickness cracks is illustrated in Figure 72, along the longitudinal axis of symmetry of the weld deposit and perpendicular

3.9.1 Welds in Heat I Plate (Cont'd.)

to the original plate surface. Post-weld aging treatments of 3 hours duration at 900°F appear to be somewhat less damaging than those of 12 hours duration. Because of the limited data, decisive conclusions concerning the effects of aging time cannot be stated. By comparing Figure 72 to Figure 28 (Section 2.8.3) (pertaining to Heat I plate), the weld deposits are observed to be substantially inferior to the parent plate. For example, the critical crack depth for Heat I plate and weld deposits in Heat I plate are about 0.100 and 0.035 inches, respectively. A most striking observation, however, is that despite the different welding procedures and weld deposit chemical compositions, the dependence of net fracture strength on crack size remains substantially constant (i.e., approximately constant $K_{IC} = 55-70 \text{ KSI}\sqrt{\text{in}}$, See Appendix IX). Furthermore, the differences in the specific welding energy inputs used in depositing the welds evaluated produce vastly different rates of solidification. Consequently, these observations also indicate that the rate of weldmetal solidification and the attendant differences in solidification pattern (partially illustrated in Figures 60 and 70), weld deposit grain size (prior austenitic grain size), and dendrite cell size have little, if any, effect on weldmetal toughness.

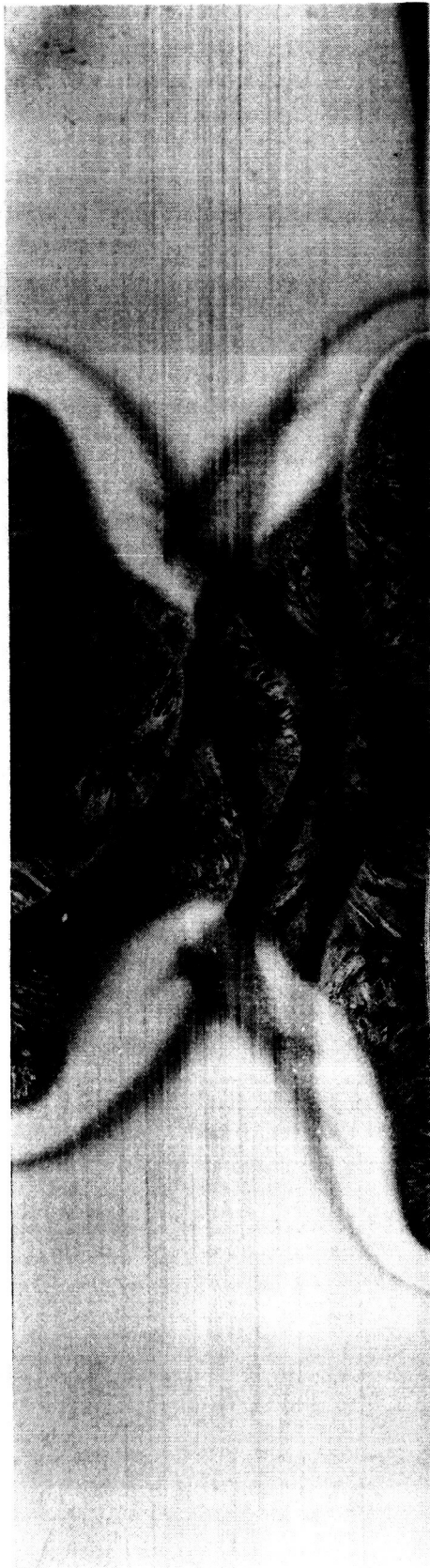
3.9.2 Welds in Heat B Plate

The rather surprising relative invariance of fracture toughness of weldmetal was again demonstrated by an evaluation of weld deposits in Heat B plate. Types W7 and W8 welds were evaluated using 8" x 11/16" x 5/16" PTC specimens. The partial cracks were located



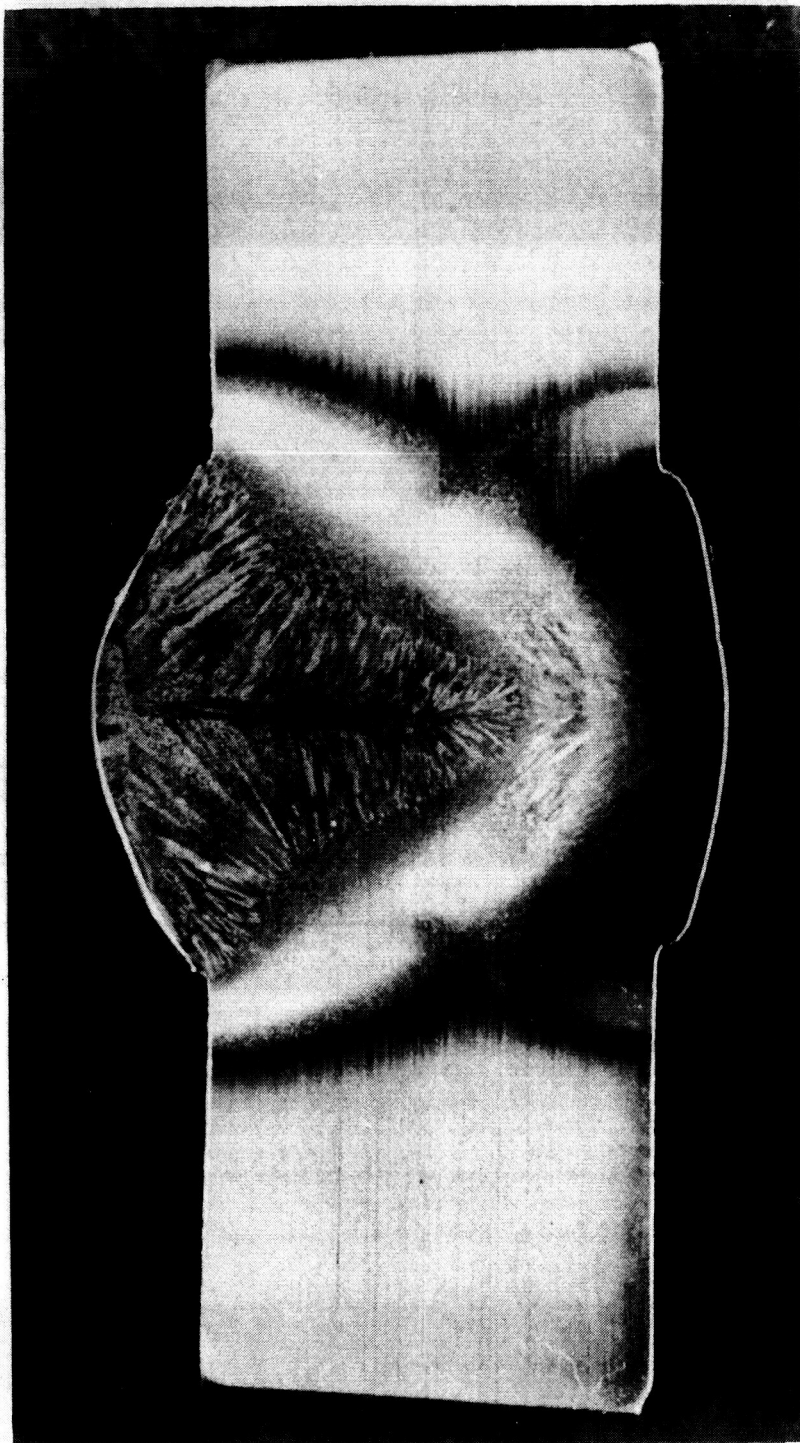
MACROSECTION OF TYPE W6 WELD
(20,000 JOULES PER INCH OF WELD).
ETCHED WITH CARAPELLAS REAGENT 4X

FIGURE 68



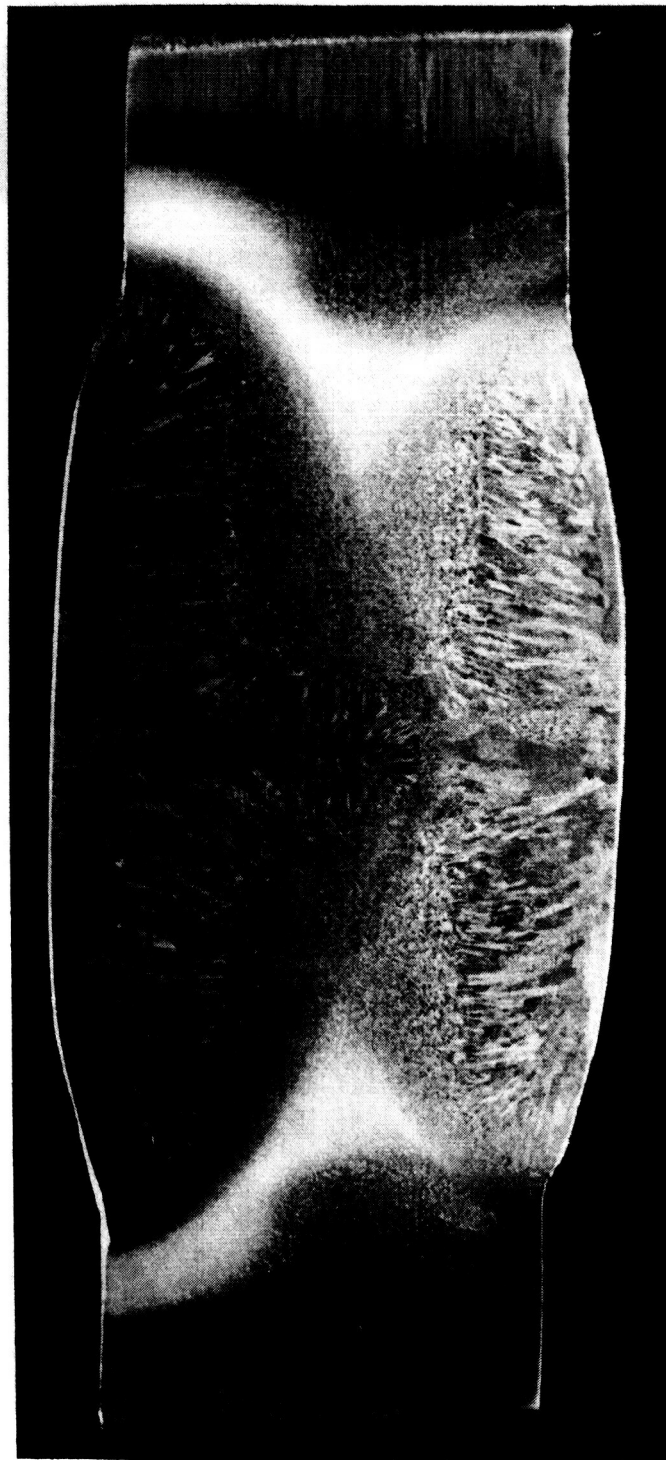
MACROSECTION OF TYPE W4 WELD
(40,000 JOULES PER INCH OF WELD PER PASS).
ETCHED WITH CARAPELLAS REAGENT. APPRX 3X.

FIGURE 69



MACROSECTION OF TYPE W7 WELD
(120,000 JOULES PER INCH OF WELD PER PASS).
ETCHED WITH CARAPELLAS REAGENT. APPRX 3X

FIGURE 70



MACROSECTION OF TYPE W9 WELD
(150,000 JOULES PER INCH OF WELD PER PASS).
ETCHED WITH CARAPELLAS REAGENT. APPRX 3X

FIGURE 71

EFFECT OF WELDMETAL COMPOSITION AND
DEPOSITION TECHNIQUE ON THE NET
FRACTURE STRENGTH OF WELD DEPOSITS IN
3/4"-18 Ni-7Co-5 Mo AIRMELTED STEEL (HEAT 1)
8" X 1/2" X 1/8" PTC SPECIMEN

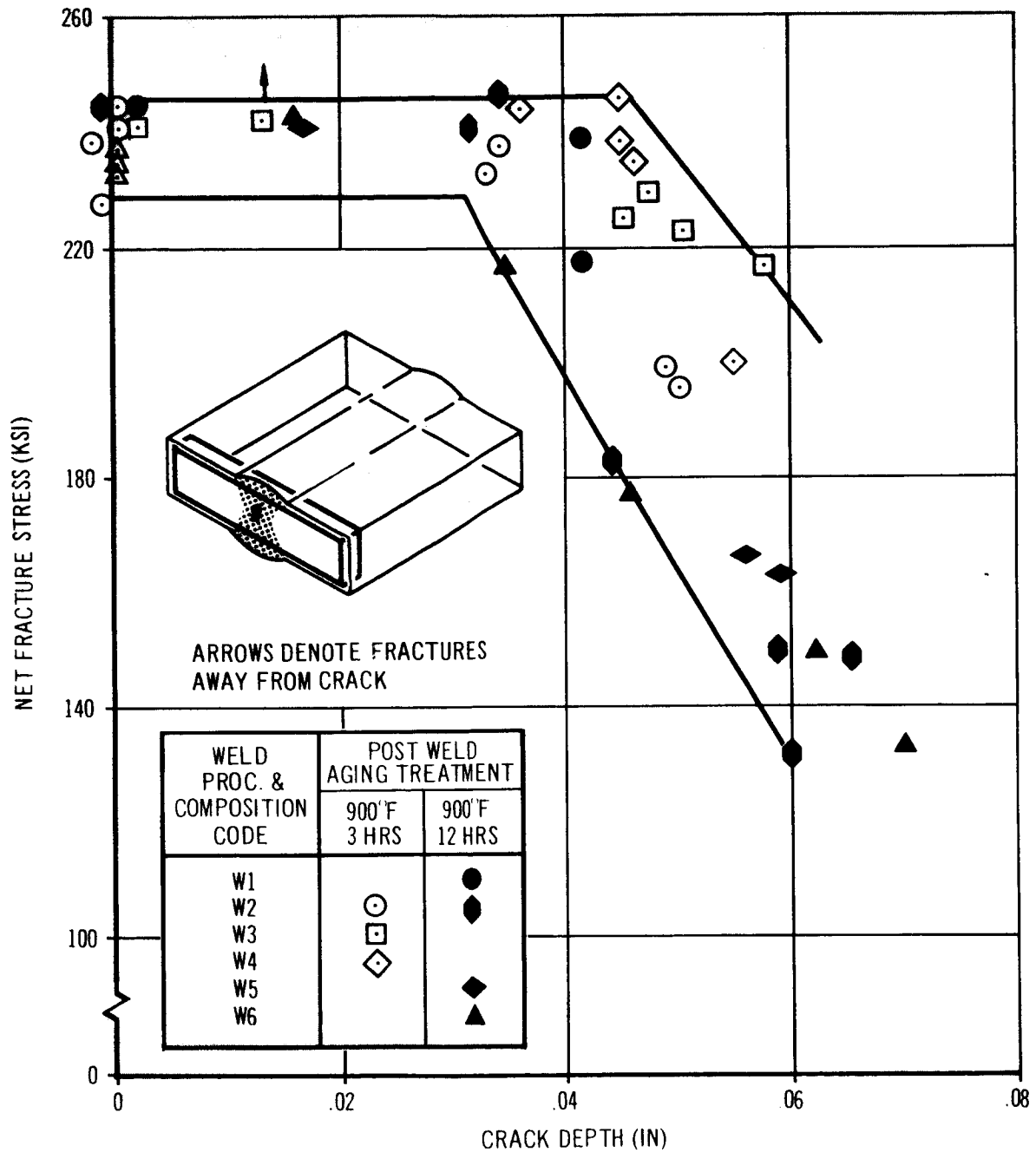


FIGURE 72

3.9.2 Welds In Heat B Plate

as illustrated, entirely within weldmetal. The crack plane was perpendicular to the plate surfaces and coplanar with the longitudinal plane of symmetry of the weld. Figures 73 through 75 depict the dependence of weldmetal net-fracture stress on post-weld aging treatment (for times ranging from 1-1/2 to 12 hours at 875, 900, $950^{\circ}\text{F} \pm 5^{\circ}\text{F}$) for the two types of welds. The data are summarized in Appendix IX. The results obtained with the two types of welds are in good agreement. Comparison of the longest (6 and 12 hours) exposure to the shortest (1-1/2 and 3 hours) indicates that some degradation does occur upon prolonged aging especially at 875 and 900°F . This latter point is further demonstrated by Figures 76 through 78 in which K_{IC} (calculated on the basis of net fracture stress as described earlier) is plotted as a function of aging time. Plane-strain fracture toughness, K_{IC} , tends to decrease somewhat with increasing aging time (especially at 875°F and 900°F), although the changes are small. The striking observation, as for the weld deposits in Heat 1 plate, is the relative constancy of fracture toughness properties. This very significant point is elaborated upon in subsequent sections where metallurgical observations are related.

Considering these fracture toughness data along with the all weld-metal tensile data presented in a previous section, the following observations may be made: (a) the metallurgical changes (precipitation, ordering, and possibly austenite reversion) responsible for producing substantial tensile strength and hardness changes during

3.9.2 Welds in Heat B Plate, (Cont'd.)

aging do not produce proportional concomitant changes in plane-strain fracture toughness, K_{IC} . (b) Ductility and plane-strain fracture toughness tend to remain relatively invariant over a wide range of aging temperature and times. These two observations suggest that the principal metallurgical factors influencing toughness and ductility properties are different from those which are responsible for the strengthening and hardening kinetics. One must conclude either that some microstructural invariant is responsible for the relative constancy of toughness and ductility, or that complicated compensating mechanisms are interacting. Metallurgical observations related in a later section favor the former conclusion.

3.9.3 Effect of Re-Solution Heat Treatments on Weldmetal Toughness

A limited evaluation of the effect of re-solution heat treatment prior to aging on weldmetal toughness has been undertaken (reference 7). Type W2 welds were re-solution heat treated at 1500°F for one hour following welding and then aged at 900°F for three or 12 hours. Plane strain fracture toughness was evaluated using the 8" x 1/2" x 1/8" PTC specimen. Figure 79 shows the effects of re-solution treatment on the net-fracture stress behavior. Re-solution heat treatment failed to improve fracture toughness, and for the 12 hour 900°F aging treatment produced some additional degradation. Thus, once again relative constancy is demonstrated in fracture behavior. This further suggests that some "microstructural invariant" may be responsible for the inferior toughness properties of weldmetal.

DEPENDENCE OF NET-FRACTURE STRESS ON CRACK DEPTH
 FOR WELDMETAL AGED AT 875° F FOR TIMES
 RANGING FROM 1 1/2 TO 12 HOURS.
 WELD DEPOSITS IN HEAT-B PLATE

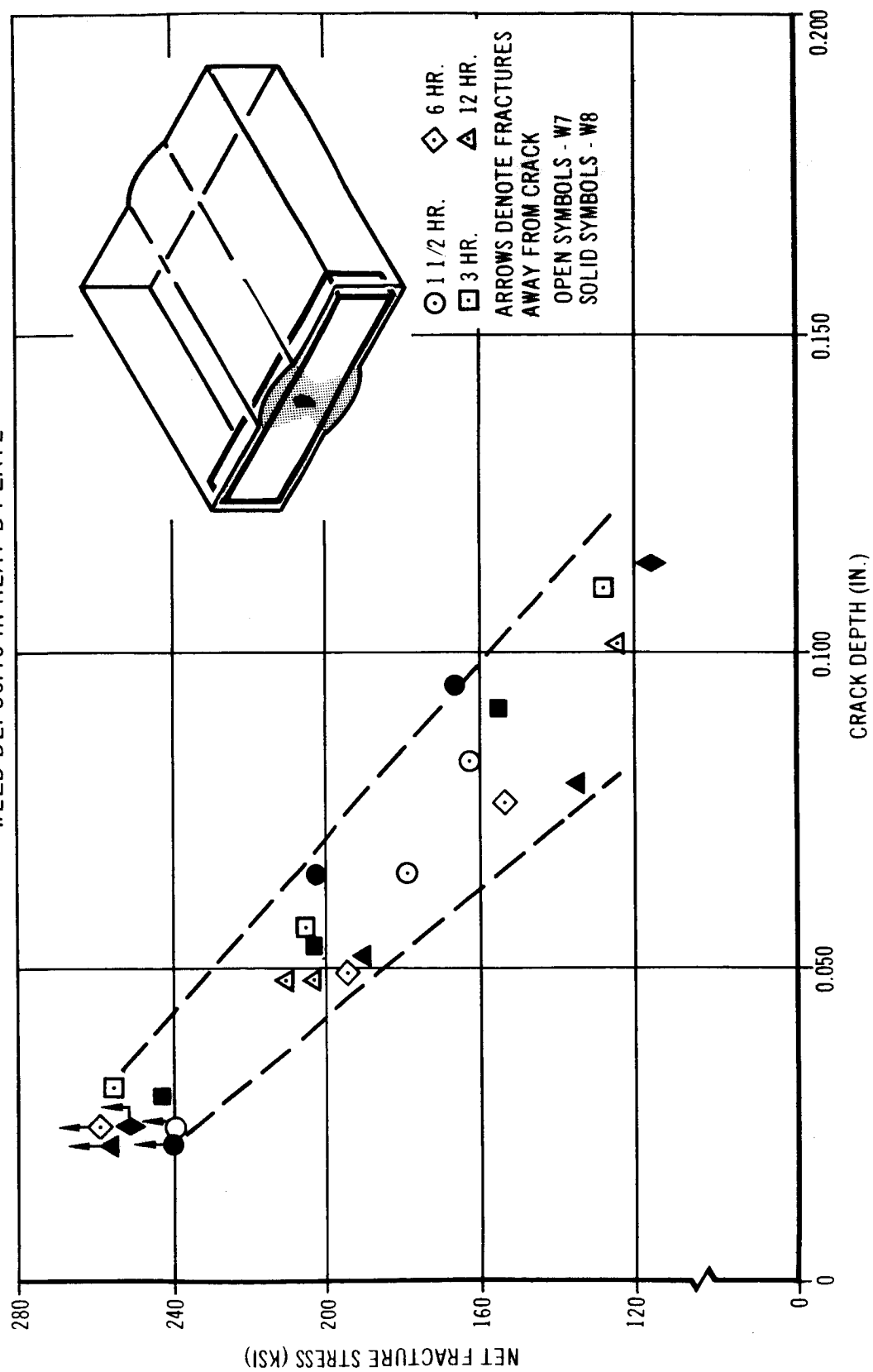


FIGURE 73

DEPENDENCE OF NET-FRACTURE STRESS ON CRACK DEPTH
FOR WELD METAL AGED AT 900° F FOR TIMES RANGING FROM
1 1/2 TO 12 HOURS WELD DEPOSITS IN HEAT-B PLATE

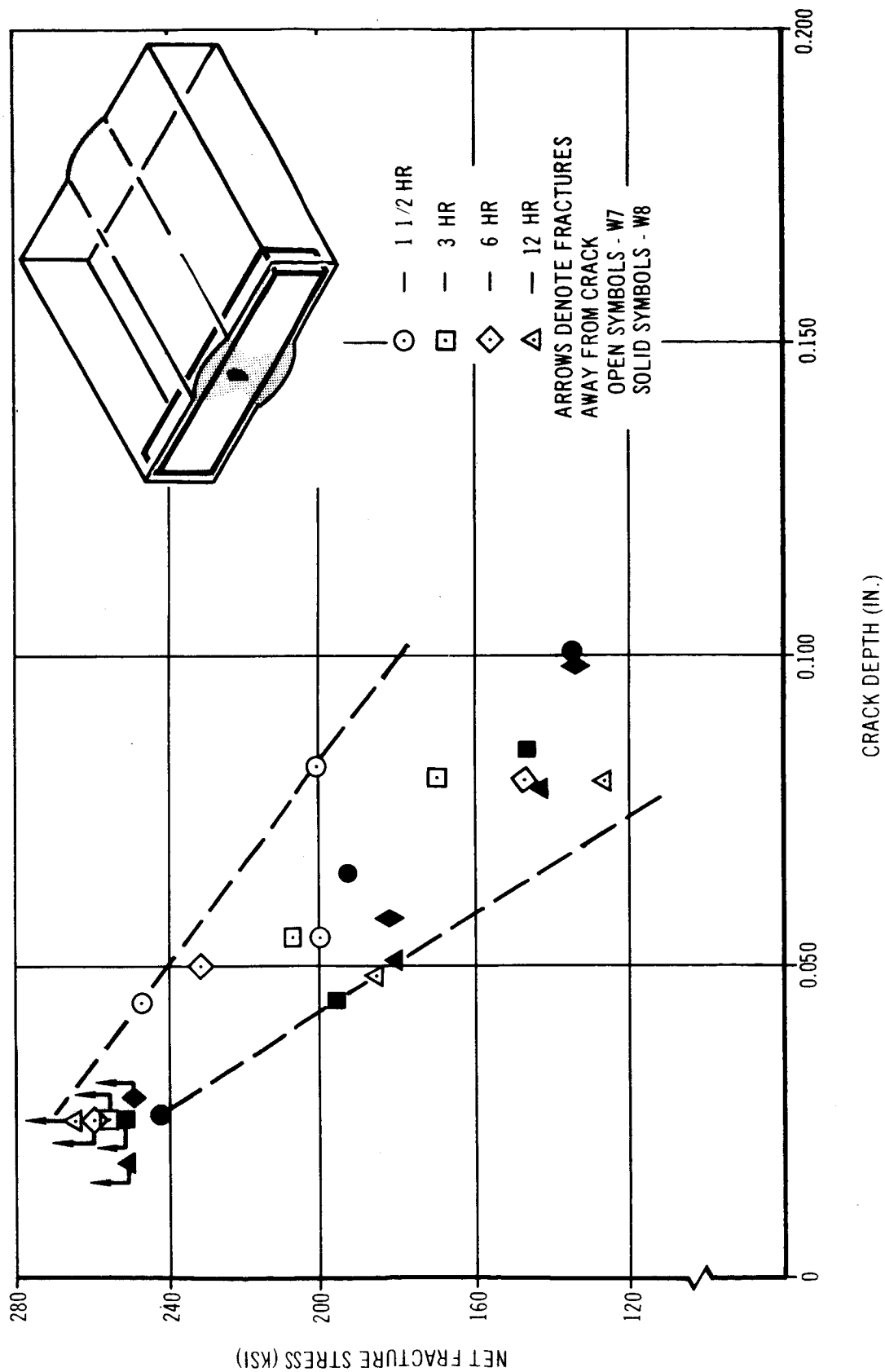


FIGURE 74

DEPENDENCE OF NET-FRACTURE STRESS ON CRACK DEPTH
 FOR WELD METAL AGED AT 950° F FOR TIMES
 RANGING FROM 1 1/2 TO 12 HOURS.
 WELD DEPOSITS IN HEAT-B B PLATE

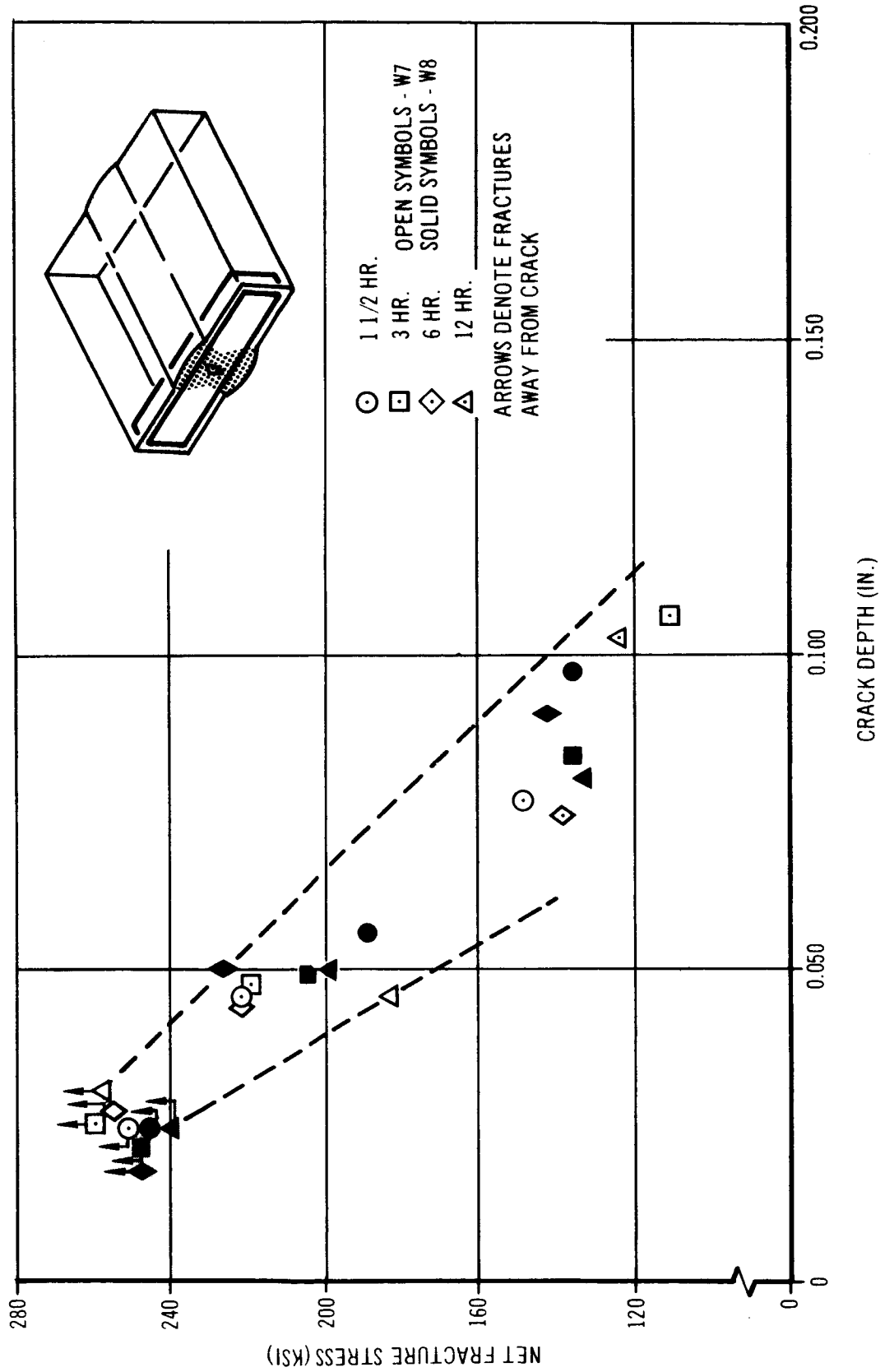


FIGURE 75

EFFECT OF 875°F AGING TIME ON K_{IC} OF WELDMETAL DEPOSITED IN HEAT-B PLATE

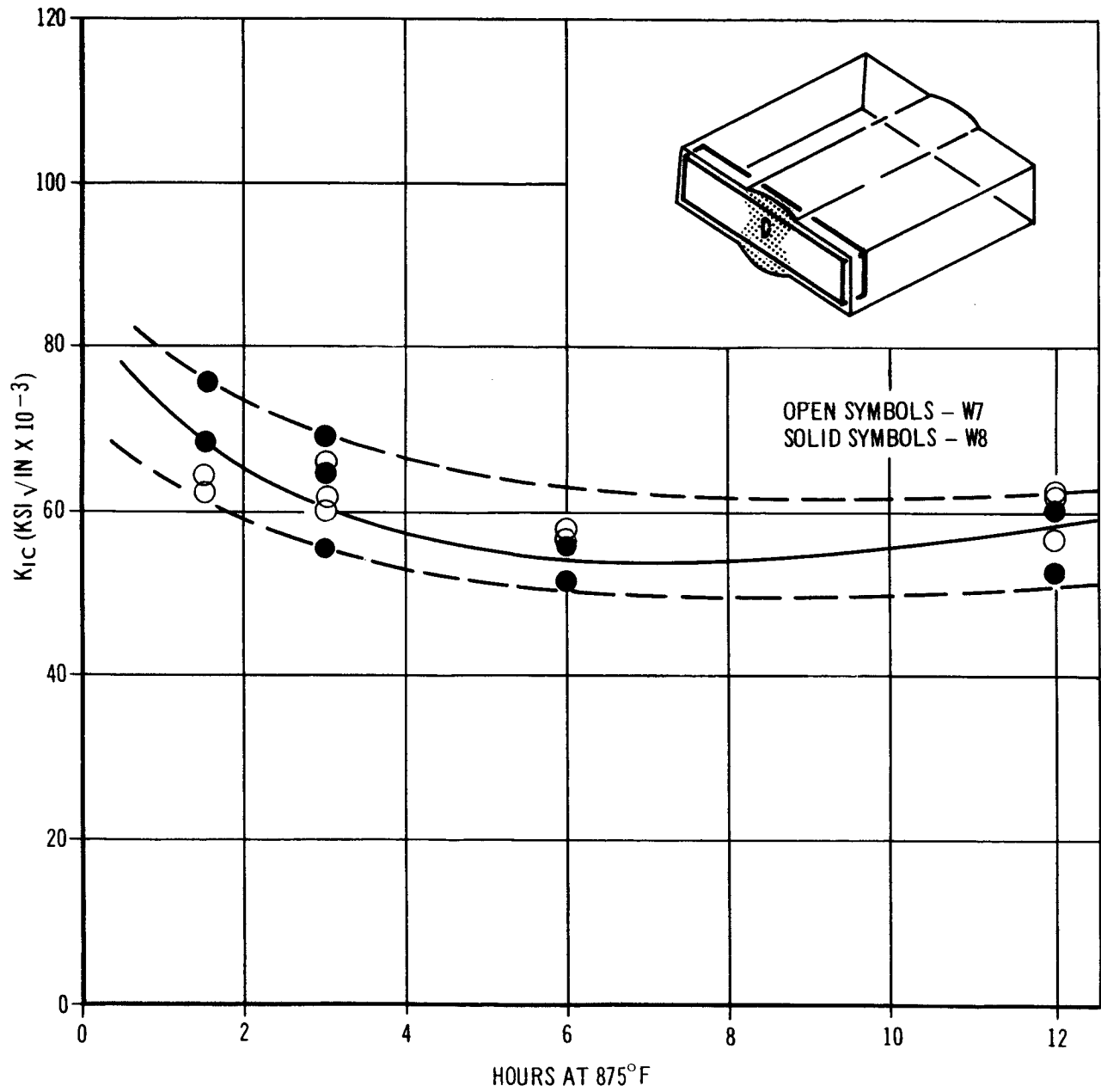


FIGURE 76

EFFECT OF 900°F AGING TIME ON K_{IC} OF WELDMETAL DEPOSITED IN HEAT-B PLATE

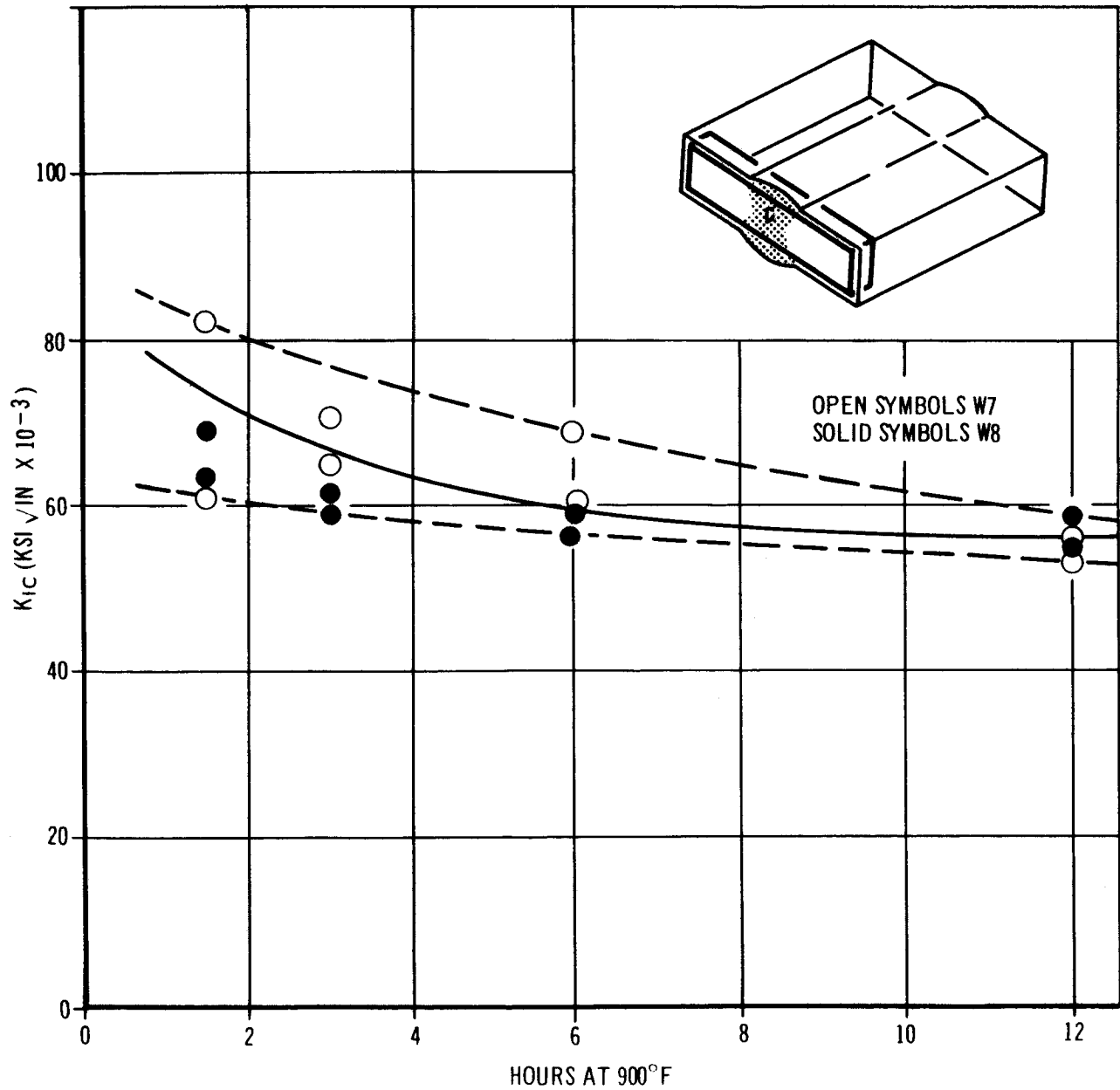


FIGURE 77

EFFECT OF 950°F AGING TIME ON K_{IC} OF WELDMETAL DEPOSITED IN HEAT-B PLATE

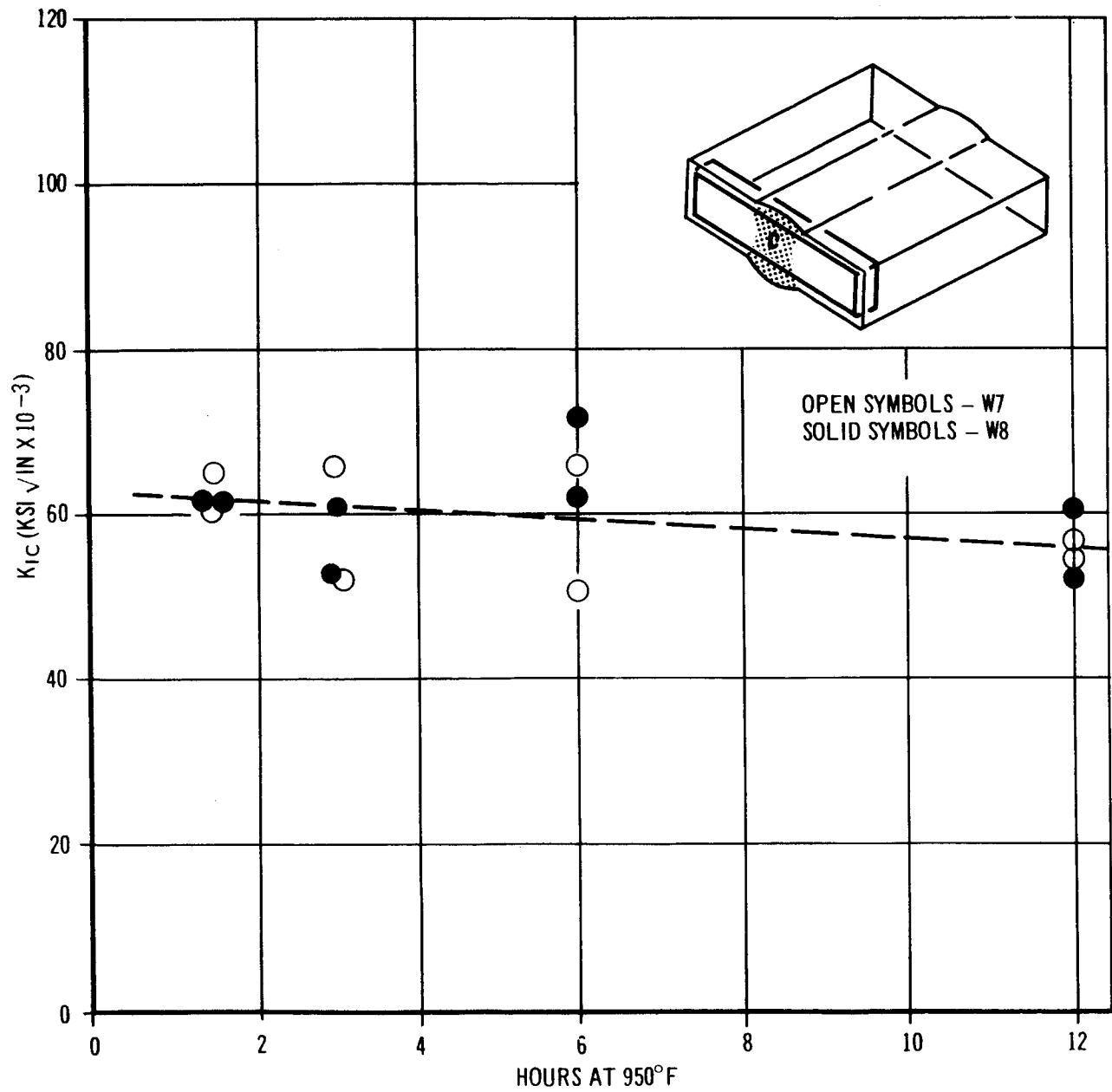


FIGURE 78

EFFECT OF CRACK DEPTH ON THE NET FRACTURE STRENGTH OF WELDMETAL AS INFLUENCED BY RE-SOLUTION HEAT TREATMENT

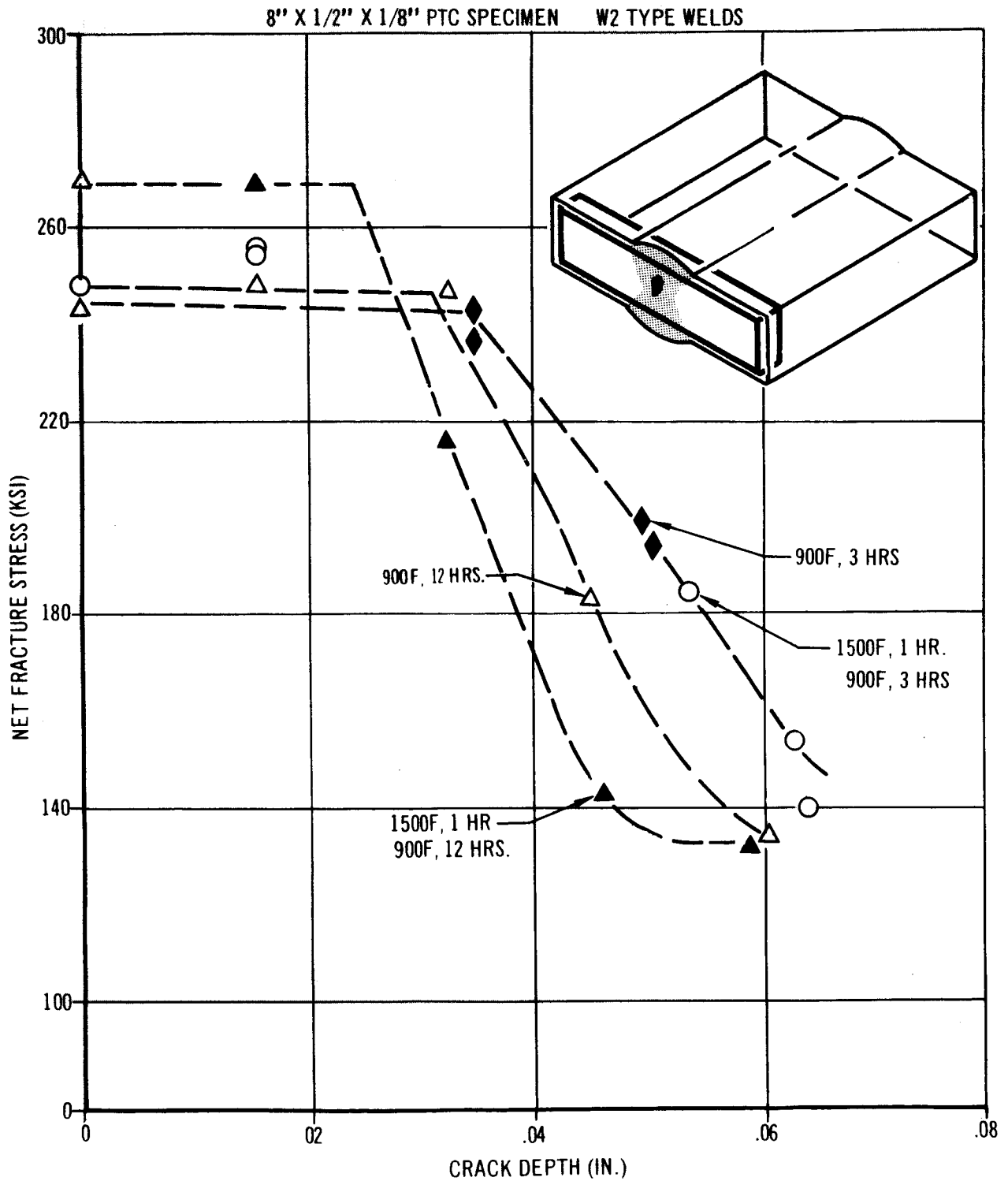


FIGURE 79

Fracture Toughness of Plate Heat-Affected Regions

This section presents data concerning the fracture toughness behavior of plate heat-affected zones. Heat-affected zone toughness deficiencies do not appear to be nearly as important a problem area as those represented by weldmetal toughness. However, metallurgical data to be presented in a subsequent section demonstrate that toughness impairment in both weldmetal and heat-affected regions could be produced by the same factors.

Figures 80, 81, and 82 depict net fracture strength behaviors for heat-affected regions in type W7 weldments in Heat B plate. Tabulated data are presented in Appendix V. Two crack propagation directions with respect to plate rolling direction and three specimen orientations were employed as illustrated in the figures. The weldments were subjected to postweld aging at 900°F for 3 hours.

Plane strain fracture toughness values, K_{IC} , are denoted in parentheses for applicable points. There are some difficulties involved in the interpretation of these data. First, crack propagation does not occur through a single microstructural region, but rather through a microstructural composite (the cracks were generally confined near coarse-grained regions and every effort was made to avoid the reverted austenite region). Second, the crack could not be identically located in all specimens. As a result of these limitations, some scatter would be anticipated. For the most part the results do not differ significantly from those obtained on parent plate for the same aging heat treatments (see Figure 36, Section 2.9.2

and identical specimen orientations).

The data do not disclose any striking deficiencies in heat-affected zone toughness, although some scatter does prevail especially for the Figure 82 data. Some of the scatter is undoubtedly due to the limitations previously discussed. However, several rather low K_{IC} values are apparent (especially the $K_{IC} = 63 \text{ KSI}\sqrt{\text{in}}$) for the specimens depicted in Figure 82 for which the crack propagation direction is parallel to the rolling direction. It would be unwarranted to attach much importance to these few low points on the basis of such limited data. However, metallurgical observations related in later sections lend support to the contention that degraded toughness may indeed prevail in some heat-affected regions. As will be seen, the possible degradation does not appear to be related to the heat affects of welding as much as it is to the chance concentration of a damaging type of inclusion.

Finally, it must be recognized that heat-affected zone toughness properties have not been exhaustively studied and that potential impairment may exist in other regions, or under other conditions of welding energy input. However, a rather comprehensive study reported by Peterson (Reference 8) showed that over a rather wide range of energy inputs, heat-affected zone toughness (as measured by Charpy impact specimens) remains essentially the same as unaffected parent plate. Compared to the weldmetal toughness problem, the heat-affected zone problem does not appear to be nearly as acute.

EFFECT OF CRACK DEPTH ON THE NET-FRACTURE STRESS OF WELDMETAL DEPOSITED IN HEAT-B PLATE

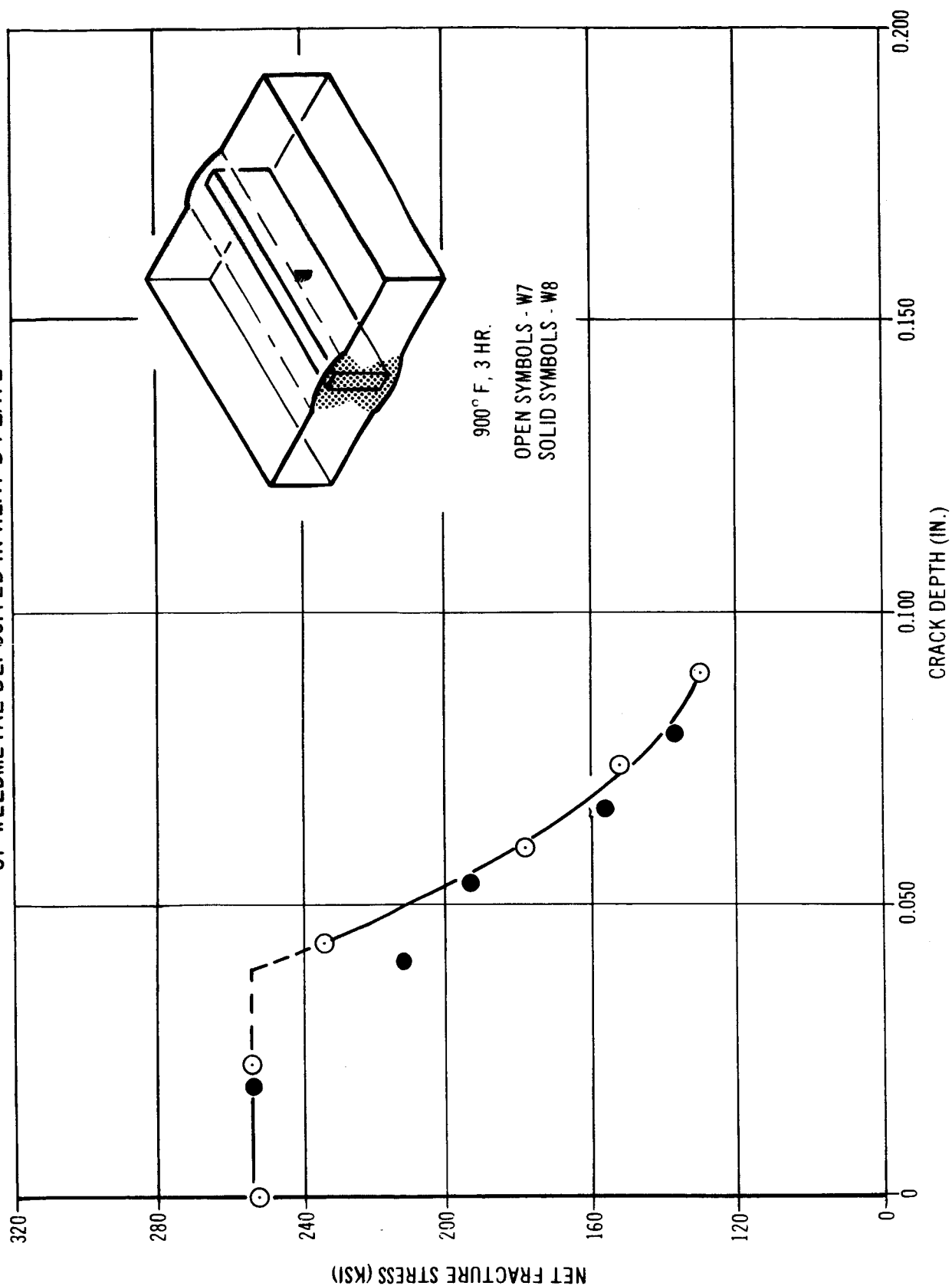


FIGURE 80

EFFECT OF CRACK DEPTH ON NET FRACTURE STRESS
IN HEAT - AFFECTED ZONE REGIONS OF
WELDMENTS DEPOSITED IN HEAT - B PLATE

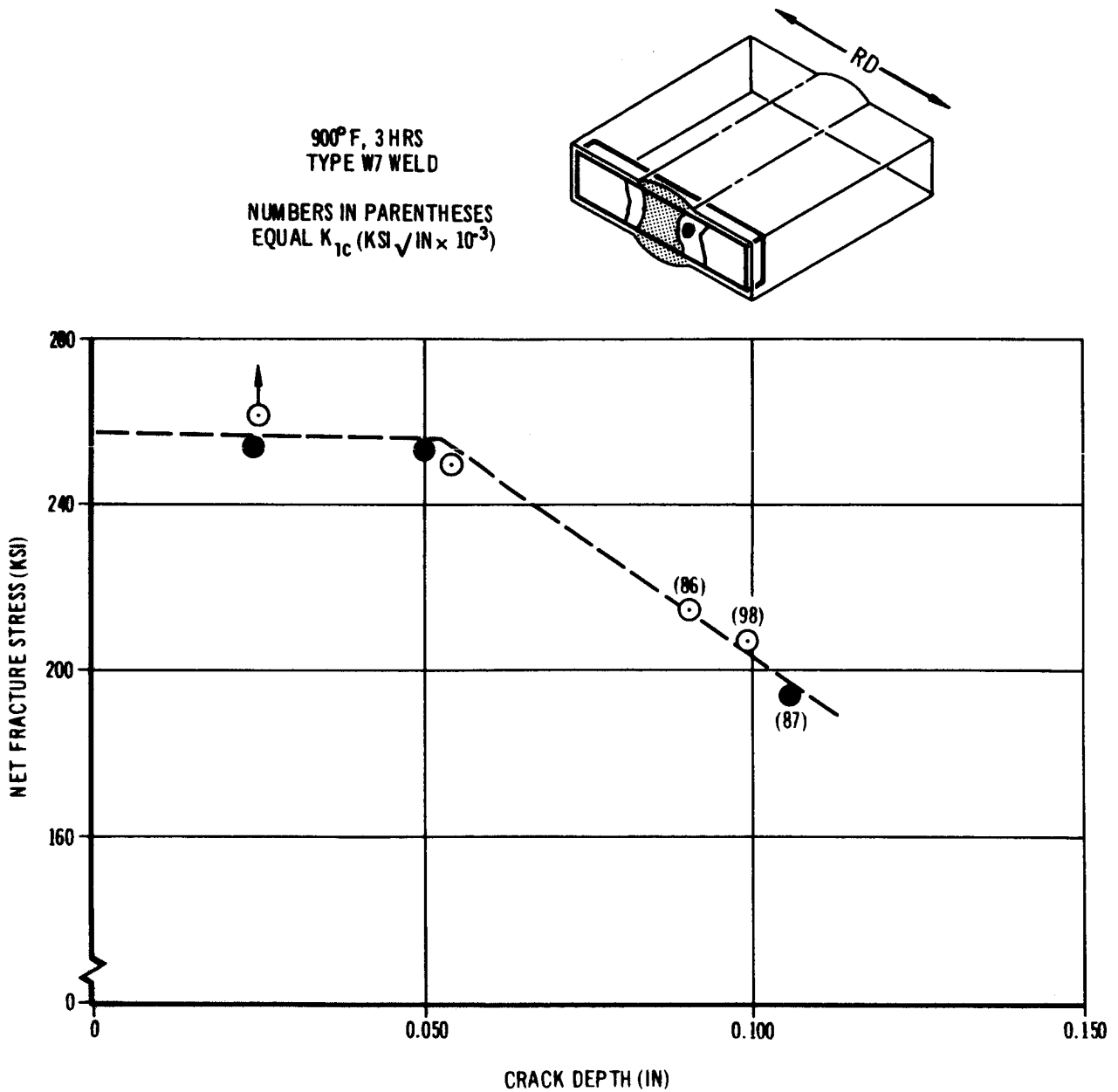


FIGURE 81

EFFECT OF CRACK DEPTH ON NET-FRACTURE STRESS
IN HEAT-AFFECTED ZONE REGIONS OF
WELDMENTS DEPOSITED IN HEAT-B PLATE

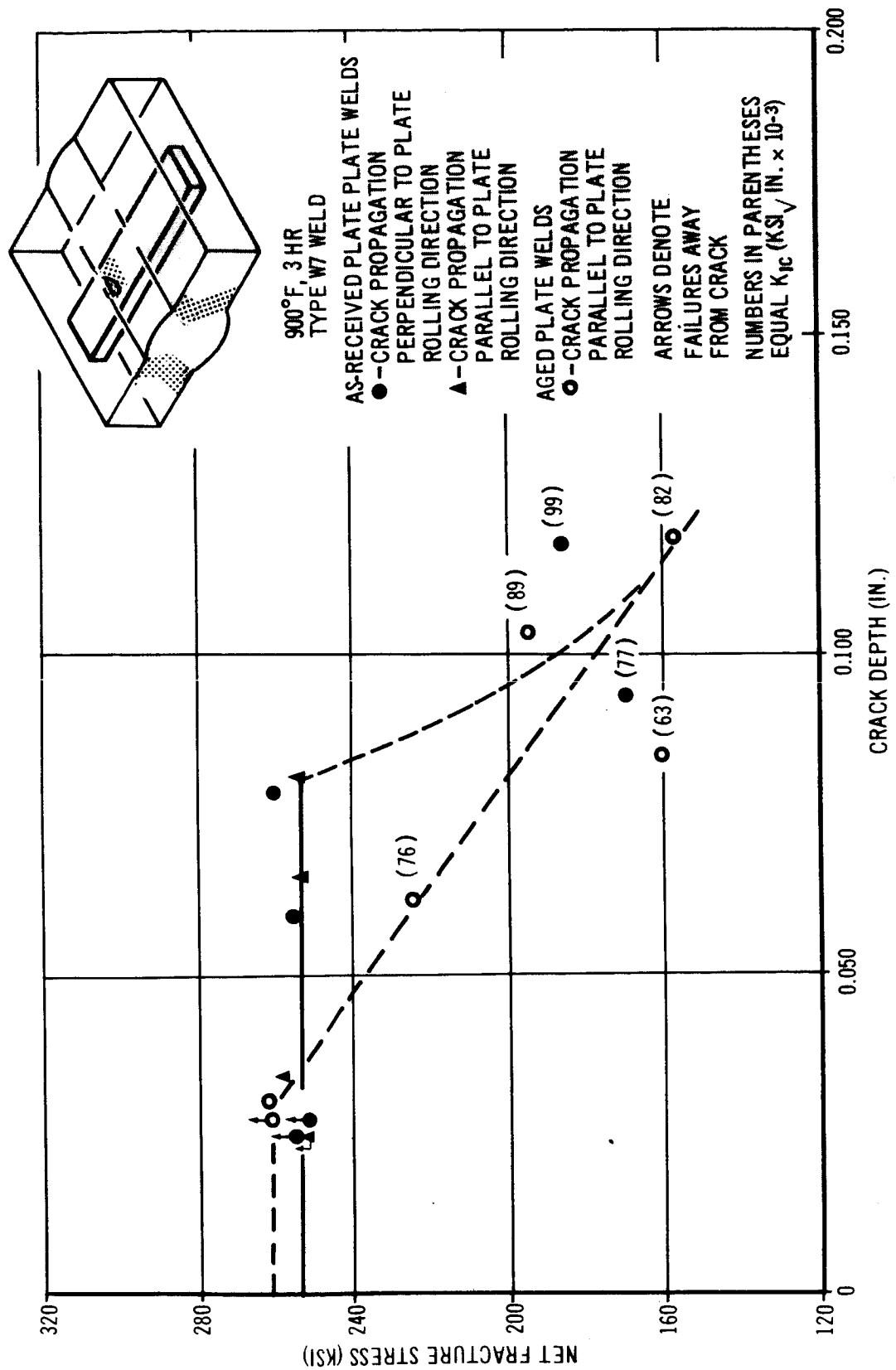


FIGURE 82

4. CONTOURED PLATE WELDING

This section describes the results of an evaluation of production prototype welding under conditions simulating possible fabrication procedures for actual space launch vehicles. Weld repair procedures were also evaluated.

4.1 Preparation of Test Plates

Newport News Shipbuilding and Dry Dock Co. performed the fabrication tasks for evaluation. Four 10-ft x 2-ft x 3/4-in. thick sections from Heat B plate were formed (in the as-received condition) into 10-ft radius, contoured sections. The forming was accomplished using a 600 ton hydraulic bending press as illustrated in Figure 83. The forming was accomplished after the joint preparations had been machined. One set of two contoured sections was aged at 900°F for 3 hours. The other set was maintained in the as-received and formed condition.

Two contoured sections, of identical thermal history, were joined along their 10-ft lengths (which was perpendicular to the plate rolling direction). Welding was performed employing two experimental welding fixtures available at Newport News Shipbuilding and Dry Dock Co.

Figure 84 presents the joint design and welding conditions that were employed. The conditions are modified W8 conditions. Preliminary testing indicated the need for the enacted changes. The side 1 weld was deposited using the fixture shown in Figure 85. After side 1

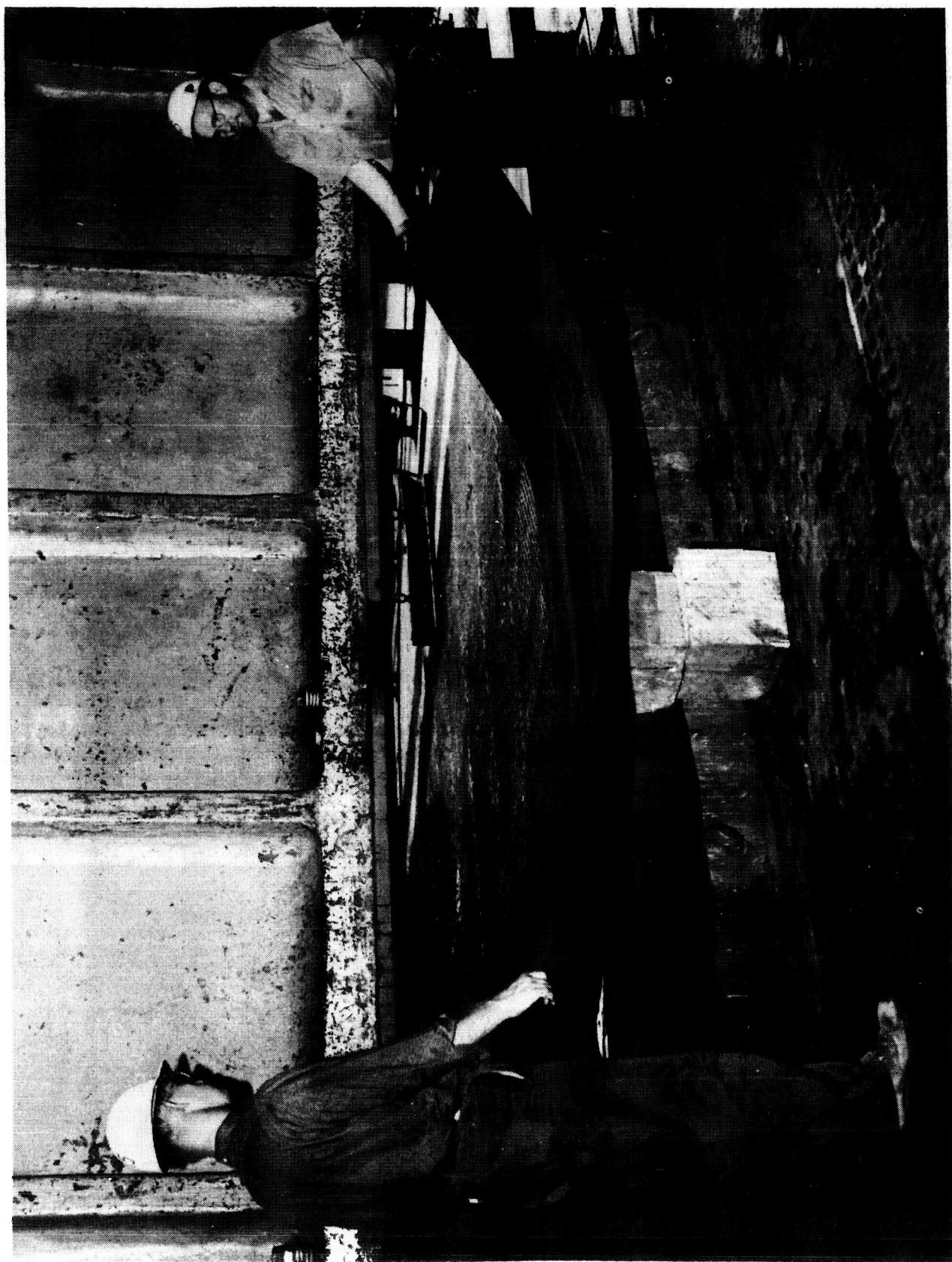
Preparation of Test Plate

was deposited the welded section was removed from the inside weld fixture and clamped on the outside weld fixture as illustrated in Figure 86. Manual carbon-arc gouging was employed to machine the side 2 groove. Manual grinding with a rotary abrasive wheel was employed to clean up the arc-gouged surfaces. The Side 2 weld was then deposited.

Repair welds were simulated in both the aged and as-received welded sections. This was accomplished by arc-gouging out a 5-ft length from the side 1 weld and rewelding as shown in Figure 84.

During this welding operation a very practical problem plagued the operation. During the flat plate welding (described in Section 3), spatter was often encountered. Because of the comparatively short weld lengths, no serious gas shielding problems resulted. However, during the 10-ft weld substantial time was available for the accumulation of spatter around the torch nozzle and on the underside of the trailing shield. Figure 87 illustrates typical accumulation after a 10-ft long weld. Such accumulation severely impaired gas shielding and very likely was the indirect cause of the lack-of-fusion defects revealed by testing.

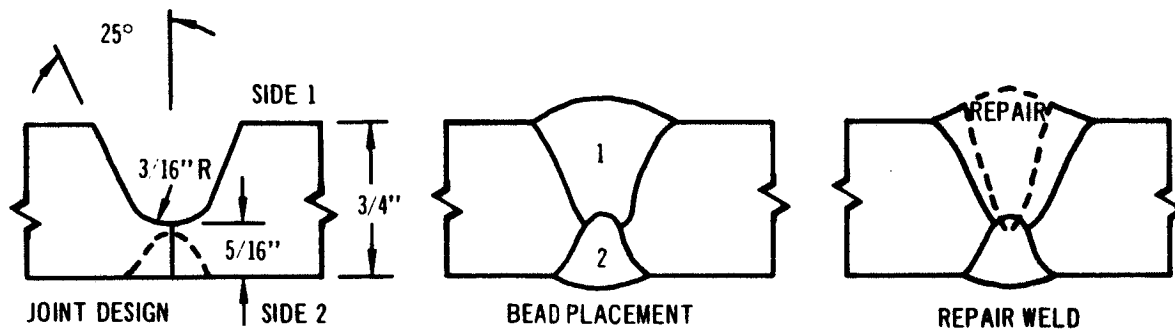
Following welding, the weldments were inspected radiographically. Although occasional porosity was evident, the amount was within the acceptable limit. No other defects were observed. The fact that no other defects were radiographically detected is quite striking in view of the prevalence of lack of fusion which was revealed on the fracture surfaces of tested specimens.



SETUP FOR FORMING OF TEN FOOT RADIUS CONTOURED SEGMENTS USING BENDING PRESS

FIGURE 83

JOINT CONFIGURATION AND WELDING CONDITIONS FOR CONTOURED PLATE WELDS



SIDE 1

CURRENT - 510 AMPERES
VOLTAGE 31.5 - 31.5 VOLTS
TRAVEL SPEED - 6 ipm

SIDE 2

CURRENT - 540 AMPERES
VOLTAGE - 31.5 VOLTS
TRAVEL SPEED - 9 ipm

REPAIR WELD

CURRENT - 540 AMPERES
VOLTAGE - 32 VOLTS
TRAVEL SPEED - 9 ipm

PROCESS: MIG, DCRP

ELECTRODE; 0.093-IN. DIAMETER TYPE A1

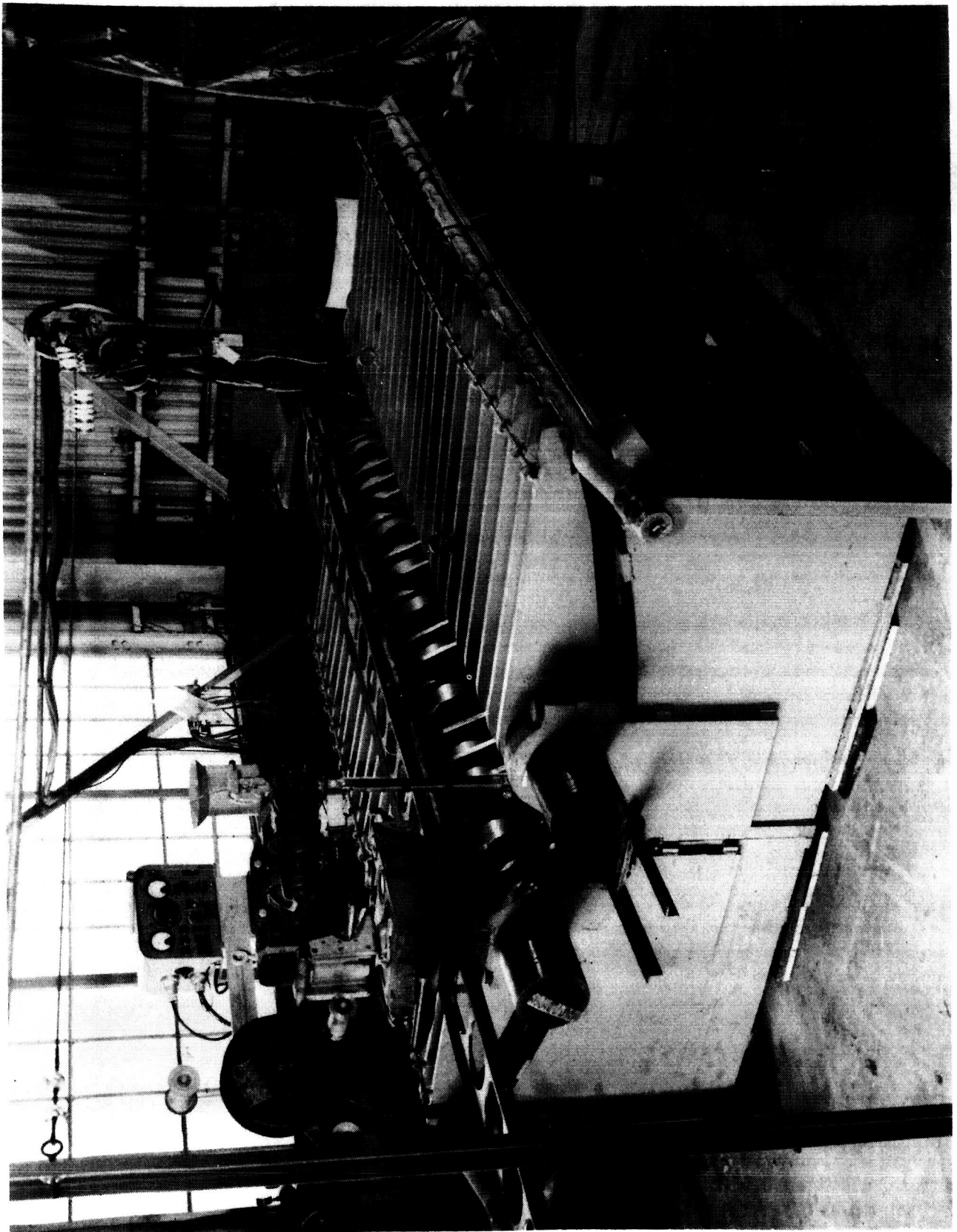
TORCH GAS: 85 CFH ARGON

TRAIL SHIELD: 185 CFH ARGON

TORCH ANGLE: 3° FOREHAND

BASE PLATE - HEAT-B, 3/4"-IN THICK 18Ni-7Co-5Mo PLATE

FIGURE 84



CONTOURED PLATE WELDING FIXTURE FOR INSIDE WELD

FIGURE 85



TYPICAL SPATTER ACCUMULATION ON THE UNDERSIDE OF THE TRAILING SHIELD AND
ON TORCH NOZZLE AFTER THE COMPLETION OF ONE CONTOURED PLATE WELD

FIGURE 87

4.2 Tensile Properties of Contoured Plate Welds

Tensile properties were evaluated using smooth 10" x 3/4" x 3/4" tensile specimens (Figure 49) oriented both transverse and parallel to the longitudinal axis of the weld. The specimens were aged at 900°F for 3 hours. The longitudinal axis of symmetry of the longitudinal specimen coincided with the longitudinal axis of symmetry of the weld and consisted of approximately 80 per cent weld and 20 per cent plate heat-affected zone. For the transverse specimen, the longitudinal axis of the weld was coincident with the transverse axis of symmetry of the specimen.

The tensile results are presented in Table XV. Numerous nil-ductility failures occurred, and after several extensometer accidents, the measurement of yield strength was abandoned. Ultimate strength values ranged from 143,500 psi to 273,400 psi, and per cent elongations varying from zero to 5.5 per cent were obtained. Fifteen of the sixteen specimens failed through weldmetal. The fracture surfaces of these specimens exhibited two predominant types of flaws. Figure 88 illustrates a typical lack of fusion defect on the weldmetal fracture surface of a transverse specimen (222-D2). Figure 89 illustrates a typical porosity defect on a weldmetal fracture surface of a longitudinal specimen. The oblique crescent sections along two edges delineate plate heat-affected zone.

Lack of fusion appears to be a far more serious type defect than porosity. Several specimens exhibiting lack of fusion failed at very low stress levels. For example, specimen 222-D2 which is

4.2 Tensile Properties of Contoured Plate Welds (Cont'd.)

depicted in Figure 88 failed at 173,400 psi. When the failing stress is calculated on the basis of net area, ultimate stress is approximately 185,000 psi. Apparently the lack of fusion defect affects mechanical behavior in a manner similar to that produced by a partial crack. No direct correlation with net fracture stress data was possible, however, because of the irregular geometry of the lack-of-fusion type defects.

The tensile data demonstrate that the weld quality was quite inferior to that obtained for the W7 and W8 flat plate welds. Nonetheless, the data also reveal that tensile properties equivalent to that obtained in flat plate welds can be achieved.

4.3 Fracture Toughness Properties of Contoured Plate Welds

Fracture toughness properties of weld metal deposited in the contoured plate sections were evaluated using the 8" x 11/16" x 5/16" PTC specimen. The specimens were aged at 900°F for 3 hours. Because of the lack of fusion type defects, secondary cracks often developed away from the starter notch during flexural fatiguing. One specimen failed during flexural fatiguing from a crack propagating through an area of gross lack of fusion.

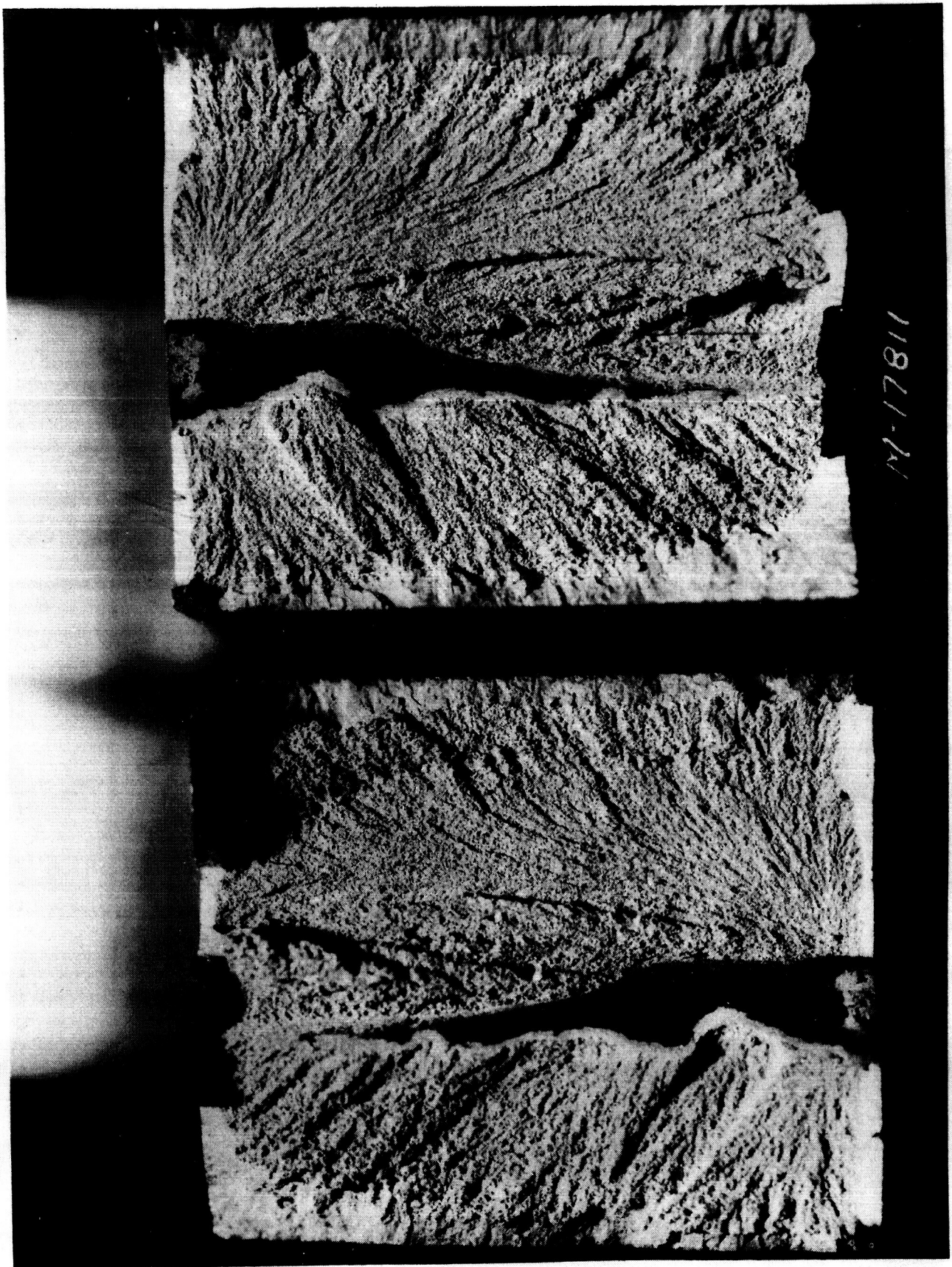
TABLE XV - TENSILE PROPERTY DATA FOR CONTOURED PLATE WELDS

10" x 3/4" x 3/4" SPECIMENS

SPEC. NO.	PLATE CONDITION PRIOR TO WELDING	SPEC. ORIENTATION	SPECIMEN TYPE	0.2% YIELD STRENGTH (KSI)	ULTIMATE STRENGTH (KSI)	% ELONG. (2-IN.)	LOCATION OF FAILURE & REMARKS
222-A1	As Rec'd.	L	As Deposited		256.9	3.0	WM-LOF
222-A7	As Rec'd.	L	As Deposited	220.8	261.7	5.5	WM-LOF
222-B1	As Rec'd.	L	Repaired	-----	260.4	2.0	WM-P
222-B7	As Rec'd.	L	Repaired	-----	254.4	2.0	WM-P
222-A2	As Rec'd.	T	As Deposited	-----	143.5	0.0	WM-LOF
222-A8	As Rec'd.	T	As Deposited	-----	213.0	0.0	WM-LOF
222-B2	As Rec'd.	T	Repaired	-----	229.2	0.0	WM-LOF
222-B8	As Rec'd.	T	Repaired	249.3	249.3	0.2	WM-LOF
222-C1	Aged	L	As Deposited	239.6	266.4	1.4	WM-P
222-C7	Aged	L	As Deposited	-----	256.2	2.0	WM-P
222-D1	Aged	L	Repaired	260.9	273.4	2.0	WM-P
222-D7	Aged	L	Repaired	-----	251.6	5.5	WM-P
222-C2	Aged	T	As Deposited	-----	247.2	1.0	WM-LOF
222-C8	Aged	T	As Deposited	-----	245.1	1.5	WM-LOF
222-D2	Aged	T	Repaired	-----	173.4	0.0	WM-LOF
222-D8	Aged	T	Repaired	240.0	262.0	2.0	HAZ

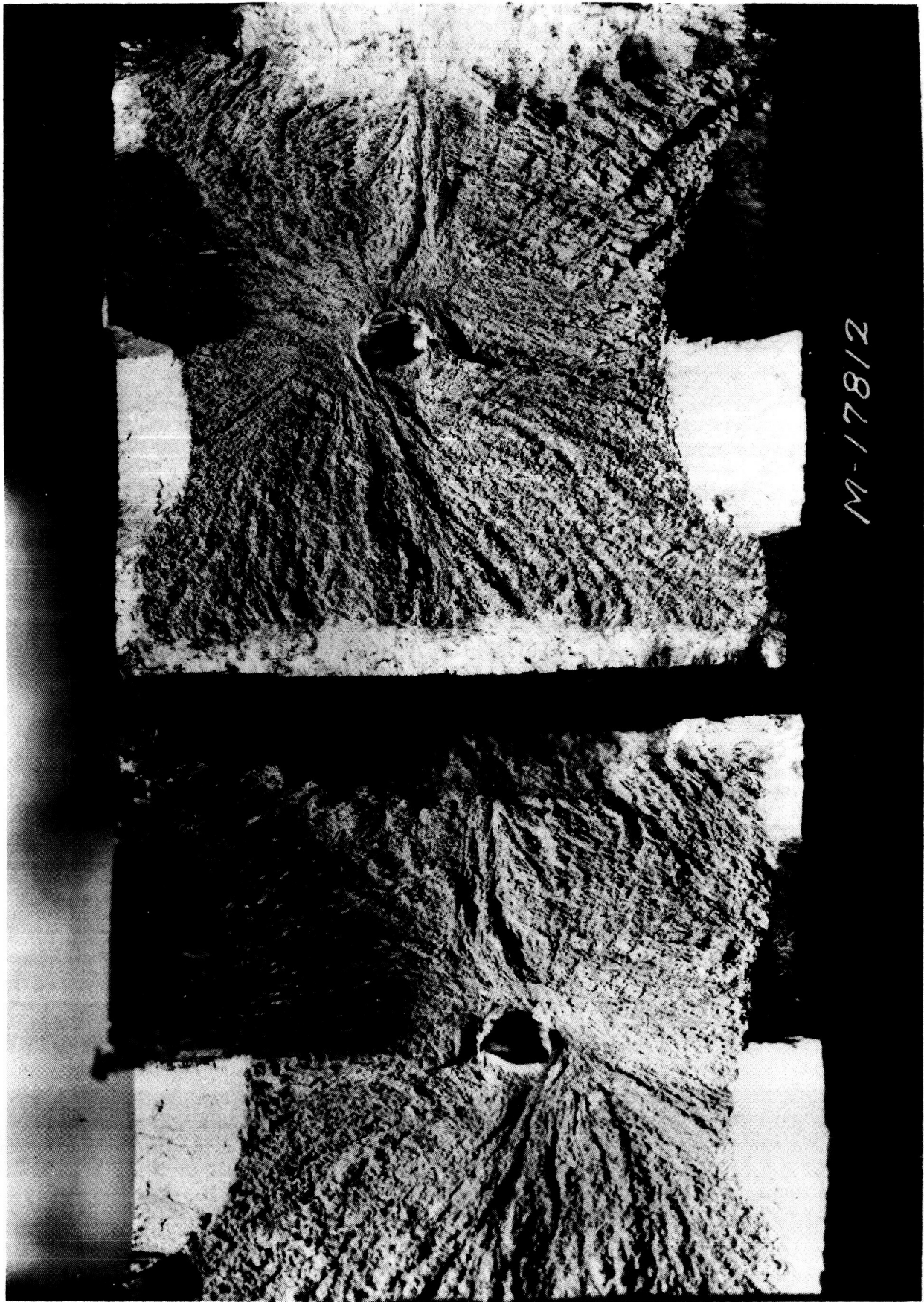
NOTES:

1. Plates aged prior to welding were aged at 900°F for 3 hours.
2. All tensile specimens aged at 900°F for 3 hours.
3. L = Parallel to weld; T = transverse, across-the-joint.
4. WM-LOF - Weldmetal, lack of fusion
5. WM-P - Weldmetal, porosity
6. HAZ - Heat-affected zone



MAGN 6½X – TYPICAL LACK OF FUSION DEFECT IN CONTOURED PLATE TENSILE SPECIMENS

FIGURE 88



MAGN 6½X - TYPICAL POROSITY DEFECT IN CONTOURED PLATE TENSILE SPECIMENS

FIGURE 89

4.3 Fracture Toughness Properties of Contoured Plate Welds (Cont'd.)

Table XVI presents the fracture toughness data on these specimens. More than half of the specimens developed secondary cracks during flexuring because of lack of fusion or porosity defects. As a result, crack propagation was often partially through weld and plate heat-affected zone. If such points are disregarded, the remainder of the data agrees reasonably well with the data generated on types W7 and W8 flat-plate welds. Figure 90 illustrates this comparison. Plane strain fracture toughness values, K_{IC} , also compare favorably with values for the flat plate welds (60-80 KSI $\sqrt{\text{in.}}$) subjected to the same post-weld aging treatment.

The data demonstrate the feasibility of transferring laboratory procedures into production procedures. However, significant practical problems must be overcome before such procedures could be performed with the necessary degree of confidence.

The results demonstrate that radiographic inspection may be totally inadequate for the detection of lack-of fusion defects in thick plate. Such defects may behave much like cracks and, therefore, they represent a very damaging type. More sensitive non-destructive inspection procedures should be explored for full scale space launch vehicle fabrication.

TABLE XVI - FRACTURE TOUGHNESS PROPERTY DATA FOR CONTOURED PLATE WELDS
8" x 11/16" x 5/16" SPECIMENS

Spec. No.	Plate Condition Prior to Welding	Spec. Orientation	Specimen Type	Crack Length (in.)	Crack Depth (in.)	Gross Fracture Stress (KSI)	Net Fracture Stress (KSI)	Applicable Yield Stress (KSI)	Gross K_{IC} (KSI√in)	Net K_{IC} (KSI√in)
222A3	As Rec'd.	T	As Deposited	0.123	0.057	245.6	252.0	---	**	**
222A4	As Rec'd.	T	As Deposited	0.112	0.050	198.3	202.5	246.6	59.6	61.1
222A5	As Rec'd.	L	As Deposited	0.080	0.038	234.5	237.4	246.6	60.4	61.2
222A6	As Rec'd.	T	As Deposited	Failed During Flexure Fatigue				---		
222B3	As Rec'd.	T	Repaired	*	---	250.0	250.0	---	---	---
222B4	As Rec'd.	T	Repaired	0.112	0.050	233.7	238.9	246.6	71.2	73.0
222B5	As Rec'd.	L	Repaired	0.069	0.025	231.3	232.0	246.6	54.8	55.1
222B6	As Rec'd.	T	Repaired	0.390	0.147	81.1	103.3	---	**	**
222C3	Aged	T	As Deposited	0.264	0.117	163.6	184.8	---	**	**
222C4	Aged	T	As Deposited	0.230	0.125	133.0	149.5	---	**	**
222C5	Aged	T	As Deposited	0.155	0.098	206.8	219.2	---	**	**
222C6	Aged	L	As Deposited	0.080	0.038	244.4	247.2	246.6	63.2	64.0
222D3	Aged	T	Repaired	0.112	0.085	211.6	215.5	---	**	**
222D4	Aged	T	Repaired	0.188	0.075	187.2	198.5	246.6	72.4	77.1
222D5	Aged	L	Repaired	0.076	0.031	228.2	230.0	246.6	57.0	57.5
222D6	Aged	L	Repaired	0.179	0.060	176.3	185.0	246.6	64.9	68.4

NOTES:

1. All specimens aged 900°F, 3 hours.
2. * Broke away from crack
3. ** Secondary cracks developed because of lack of fusion defects and crack propagation surface was composed of both weldmetal and heat-affected zone material in various proportions.
4. Gross Fracture Stress = Failing load divided by gage area
5. Net Fracture Stress = Failing load divided by gage area minus crack area.

DEPENDENCE OF NET FRACTURE STRESS
ON CRACK DEPTH FOR CONTOURED PLATE
WELDMETAL AGED AT 900°F FOR 3 HOURS

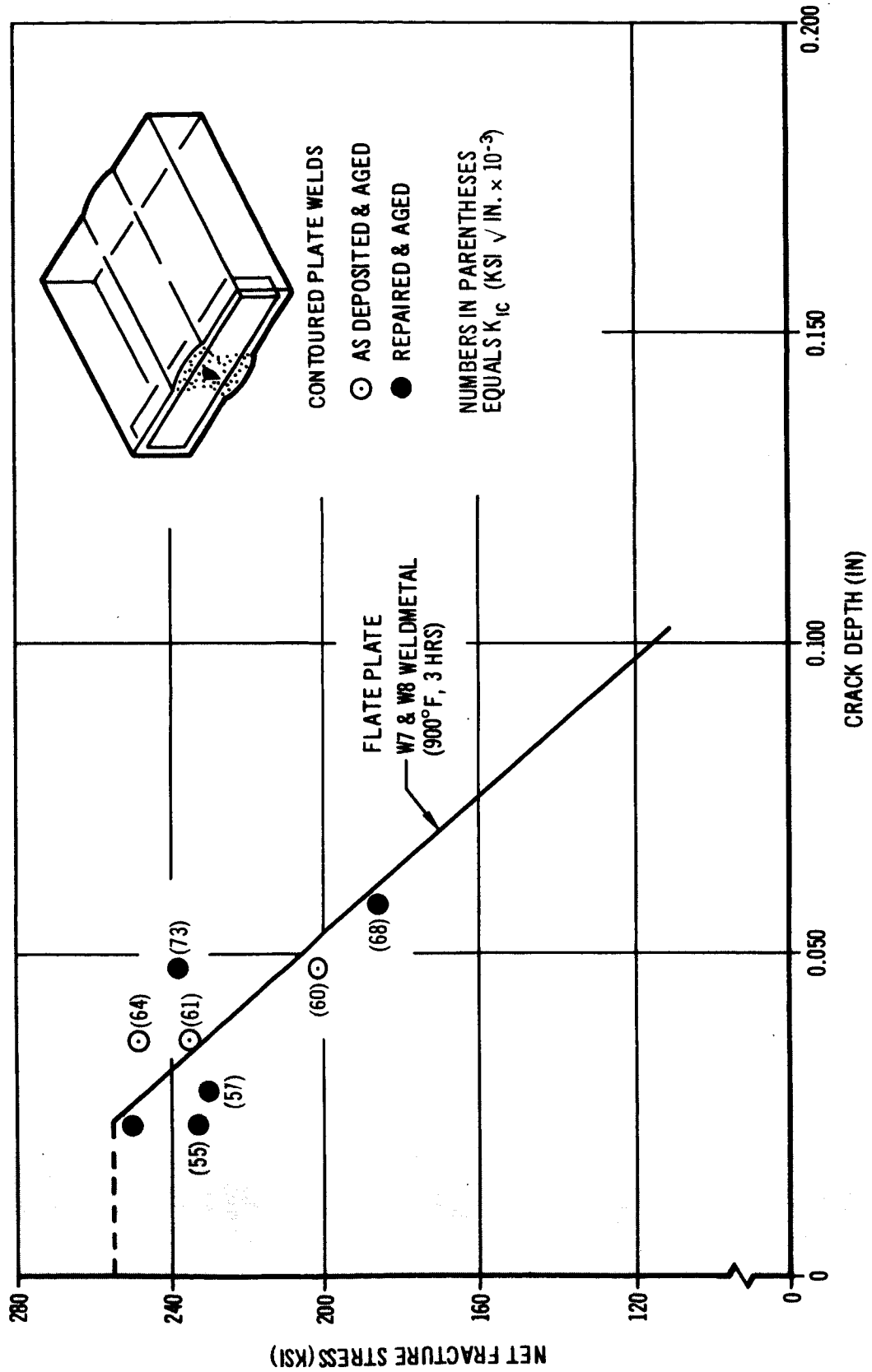


FIGURE 90

5. EFFECT OF ENVIRONMENT ON THE SUSTAINED LOAD BEHAVIOR OF PLATE AND WELDS

The reliability and performance of any pressure vessel fabricated from 18Ni-7Co-5Mo alloy steel will be significantly affected by the slow growth of cracks under sustained static loads. Previous studies performed at Douglas (Reference 12) demonstrated that cracks introduced in high strength AISI 4340 steel sheet resisted slow growth under sustained loads, equal to 98% of ultimate, when tested in air. However, the addition of moisture resulted in the rapid growth of cracks and catastrophic failure at low stress levels.

Short time sustained load conditions, under potentially damaging environmental conditions prevail when a pressure vessel is being tested. Present industry practice is to proof test steel pressure vessels with oil so as to avoid the possibility of failure induced by accelerated crack growth (of cracks or crack-like flaws that escaped detection during inspection).

This section presents data pertaining to the sustained load behavior of 18Ni-7Co-5Mo plate and welds. Caution in the selection of a proof testing media and the need for possible control of surface condition is indicated. Furthermore, weld behavior is inferior to plate and may require special attention.

5.1 Sustained Load Testing Procedure

Both plate and weldments were tested employing the 24-in PTC specimens, (Figure 8, Section 2.4) and the 8-in PTC specimen (Figure 9, Section 2.4). The thickness type 8-in PTC specimen

5.1 Sustained Load Testing Procedure (Cont'd.)

Figure 35, Section 2.9.2) was used. In the case of plate, the specimens were transverse to the rolling direction. Weld evaluations were performed using Type W7 welds (Table XI, Section 3.2) employing the specimen and crack orientations illustrated in Figure 66 (Section 3.8). Most of the specimens were aged at 900°F for 12 hours although a few were also aged for 3 hours. The 12 hours age was selected for the majority of the testing since such a treatment had previously been observed to produce toughness degradation. Therefore, the results might represent a potentially extreme condition.

All the specimens were tested containing partial thickness cracks. It was originally intended that all the cracks be approximately equal in size to that determined to be critical in the fracture toughness testing. Cracks of critical size were selected since failure would be expected to occur at tensile ultimate strength unless crack growth occurred. Any crack growth would thereby extend the crack beyond critical size and induce a lower strength failure. However, several exceptions prevailed because of spurious cracking in specimens.

Duplicate specimens were tested in each of four environments:

- a) ambient air ranging in relative humidity from 21 to 65 percent at dry bulb temperatures from 70 to 78°F, b) type "Texaco 519" corvus oil, c) NaCl solution 20%, by weight, prepared with deionized water ranging in p^H from 5.9 to 7.8 and having a specific electrical conductivity of $178 \text{ ohm}^{-1} \cdot \text{cm}^{-1}$ and d) distilled, deionized

5.1 Sustained Load Testing Procedure (Cont'd.)

water ranging in pH from 5.7 to 7.8 and specific electrical conductivity ranging from 0.001 to 0.002. The liquid testing environments were contained in plastic envelopes taped on the specimen. Approximately constant liquid volumes were used (about 30 c.c. for the 8-in PTC specimens and about 120 c.c. for the 24-in PTC specimens). Liquid contacted the specimen surfaces over a distance extending approximately 1-1/2 inches on either side of the crack. This extent of contact was deliberately selected so that liquid would come in full contact with heat-affected zone and weldmetal regions in the weld specimens.

The specimens were step-loaded in three intermediate steps of one hour duration each, unless failure occurred. A final step-load to failure was performed if the specimen survived the first three hours. The step loads were 90, 95, 97 per cent of estimated ultimate strength (based on previous data). Loads were maintained to within 1/2% of nominal.

Test results are described in the following two sections. Data are summarized in Table XVII.

5.2 Sustained Load Behavior of Plate

The tests performed on the four 24-in PTC specimens were conducted employing plate covered with the original crazed mill scale.

Previous fracture toughness tests were performed after the mill scale had been removed by grinding. As it turned out, the crazed mill

TABLE XV.11

EFFECT OF VARIOUS ENVIRONMENTS ON NET FRACTURE STRENGTH OF PLATE AND W7 TYPE WELDMENTS UNDER SUSTAINED LOAD

Spec. No.	Aging Time at (900°F) (Hours)	Crack Length (Inches)	Crack Depth (Inches)	Environment	ESTIMATED SUSTAINED STRESS (KSI) % of ULTIMATE				Actual Sustained Stress (KSI)	Time To Failure (Min)	Location of Failure if Not Through Specified Cracks
					90	95	97	100			
24" x 3" x 3/4" Parent Plate											
P-54	3	0.085 0.110	0.040 0.045	20% NaCl	259	274	279	288	285	180+	
P56	12	0.100	0.046	20% NaCl	266				279	60+	Failed through several spurious cracks
31W5	3	0.100	0.045	20% NaCl	259				272	60+	
31W8	12	0.100* (Plus Numerous Spurious Cracks)	0.045	20% NaCl					237	0	
24" x 3" x 3/4" Weldments W7 Type											
6W5	3	0.058	0.024	20% NaCl	235	247	250	260	250	121	Failed away from crack through apparent weld flaw.
6W6	12	0.058*	0.024	20% NaCl	235	247			247	68	
8" x 11/16" x 5/16" Parent Plate											
PP5	12	0.091	0.045	Air	260	274	280	289	294	180+	Failed away from crack Failed away from crack Failed away from crack Failed away from crack Failed away from crack
PP12	12	0.091	0.043	Air	260	274	280	289	289	180+	
PP6	12	0.060	0.030	20% NaCl	260	274	280	289	290	180+	
PP11	12	0.060*	0.030	20% NaCl	260	274			274	95	
PP7	12	0.060*	0.030	H ₂ O	260	274	280	289	288	180+	
PP10	12	0.060*	0.030	H ₂ O	260	274	280	289	288	180+	
PP8	12	0.060*	0.030	Oil	260	274	280	289	292	180+	
PP9	12	0.060*	0.030	Oil	260	274	280	289	292	180+	
8" x 11/16" x 5/16" Weldments W7 Type											
2B1	12	0.060*	0.030	Air	232	245	250	258	250	168	Failed away from crack (HAZ)
4E1	12	0.062	0.031	Air					230	0	
2B2	12	0.060*	0.030	20% NaCl	232	245			245	93	Failed away from crack (eyebrow region)
4E2	12	0.061	0.033	20% NaCl	232				232	43	
2B3	12	0.060*	0.030	H ₂ O	232	245	250	258	245	155	Failed away from crack (HAZ)
4E3	12	0.075	0.035	H ₂ O					228	0	
2B4	12	0.060*	0.030	Oil	232	245			245	103	Failed away from crack (eyebrow region) Failed through spurious crack
4E4	12	0.120	0.060	Oil					209	0	

NOTES:

- * Crack depth estimated on the basis of original crack length (See Figure 37)
- Zero time in time to failure column denotes failure during initial loading
- 180+ in time to failure column denotes failure immediately after the one hour, 97% stress condition, and following the final step load to failure.
- 60+ in time to failure column denotes failure immediately after the one hour, 90% stress condition, during the second step load to 95%.

5.2 Sustained Load Behavior of Plate (Cont'd.)

scale acted as an initiator for multiple cracks during flexural fatigue. The prevalence of multiple cracks makes some data interpretation somewhat difficult.

The four 24-in. transverse plate specimens were tested in 20% NaCl (Table XVII). Specimens were aged at 900°F for 3 and 12 hours, respectively. Only one of the four specimens sustained the full 3 hour test period. This specimen exhibited two separate cracks on the fracture surface. One specimen exhibiting multiple cracks failed upon initial loading. Two specimens, which did not exhibit spurious cracks, failed after 60 minutes upon being loaded from the 90 to 95% level.

The 8-in PTC plate specimens, which were fully machined on all surfaces, exhibited generally different behavior than that exhibited by the 24-in PTC specimens. Figure 91 portrays the results for the tests performed in the four different environments on plate and welds (welds will be discussed later). As may be seen, seven of the eight plate specimens survived the full 180 minute test duration, failing at the 100% level. The single early failure occurred in the 20% NaCl solution after a 35 minute exposure at the 95% level. Post-failure examination revealed that the specimen failed near a grip end probably through a stress riser induced by the grips.

Comparison of the behavior of the 24 and 8-in specimens tested in the four environments is illustrated in Figure 92. The data indicate that the condition of the exposed surface (mill scale versus machined)

5.2 Sustained Load Behavior of Plate (Cont'd.)

may be an important factor, and that 18Ni-7Co-5Mo plate is capable of exhibiting rather remarkable resistance to slow crack growth in environments that are rather hostile to high-strength, low-alloy steels (e.g., AISI 4340).

5.3 Sustained Load Behavior of Welds

The data presented in Figures 91 and 92 show that the welds were substantially inferior to the plate. Not one of the two 24-in and eight 8-in PTC specimens survived the full 180 minute test duration. Three 8-in specimens failed during loading; however, one of these (tested in corvus oil) had an excessively large crack which accounts for the relatively low strength failure. Interestingly, all three of these initial-loading failures occurred in the 4E weld series (see Table XVIII). The remaining 4E specimen that was tested failed after 43 minutes at the 90% level. Four specimens tested from the 4B series all failed before completing 180 minutes exposures; however, their lives were much longer than those exhibited by the 4E specimens. Furthermore, while all of the 4E specimens failed through partial thickness cracks, none of the 4B series did so. Failures of all of the 4B specimens, surprisingly, were located in heat-affected zones, and no cracks were apparent on the fracture surfaces. No explanation for the differences in behavior is evident. Additional study of weldment behavior appears to be necessary.

EFFECT OF ENVIRONMENT ON NET FRACTURE STRESS OF PLATE
AND TYPE W7 WELDMENTS UNDER SUSTAINED LOAD
(AGED AT 900°F, 12 HOURS)

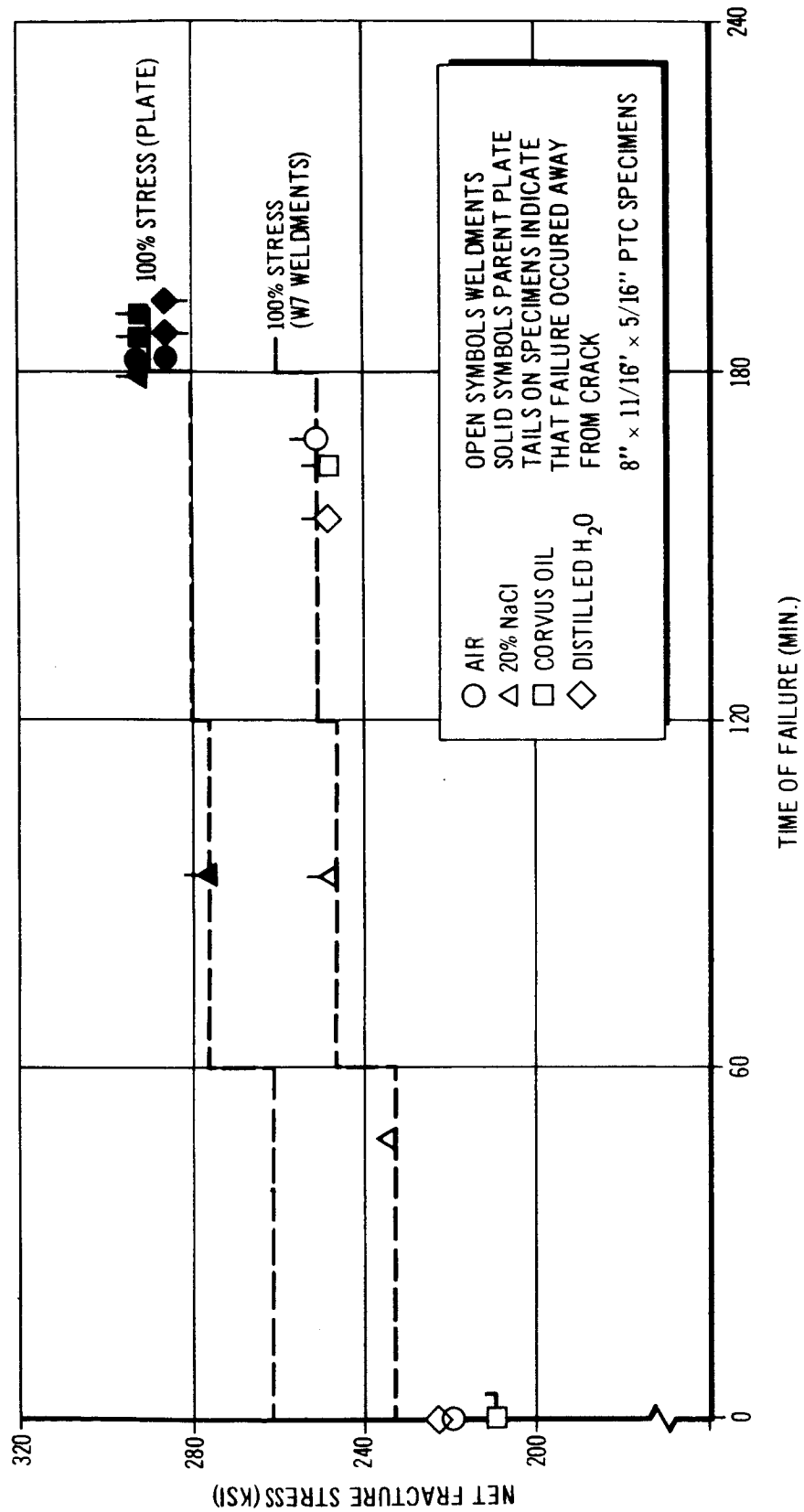


FIGURE 91

HISTOGRAM ILLUSTRATING FREQUENCY OF FAILURE IN VARIOUS TIME RANGES FOR SPECIMENS SUBJECTED TO SUSTAINED LOADS

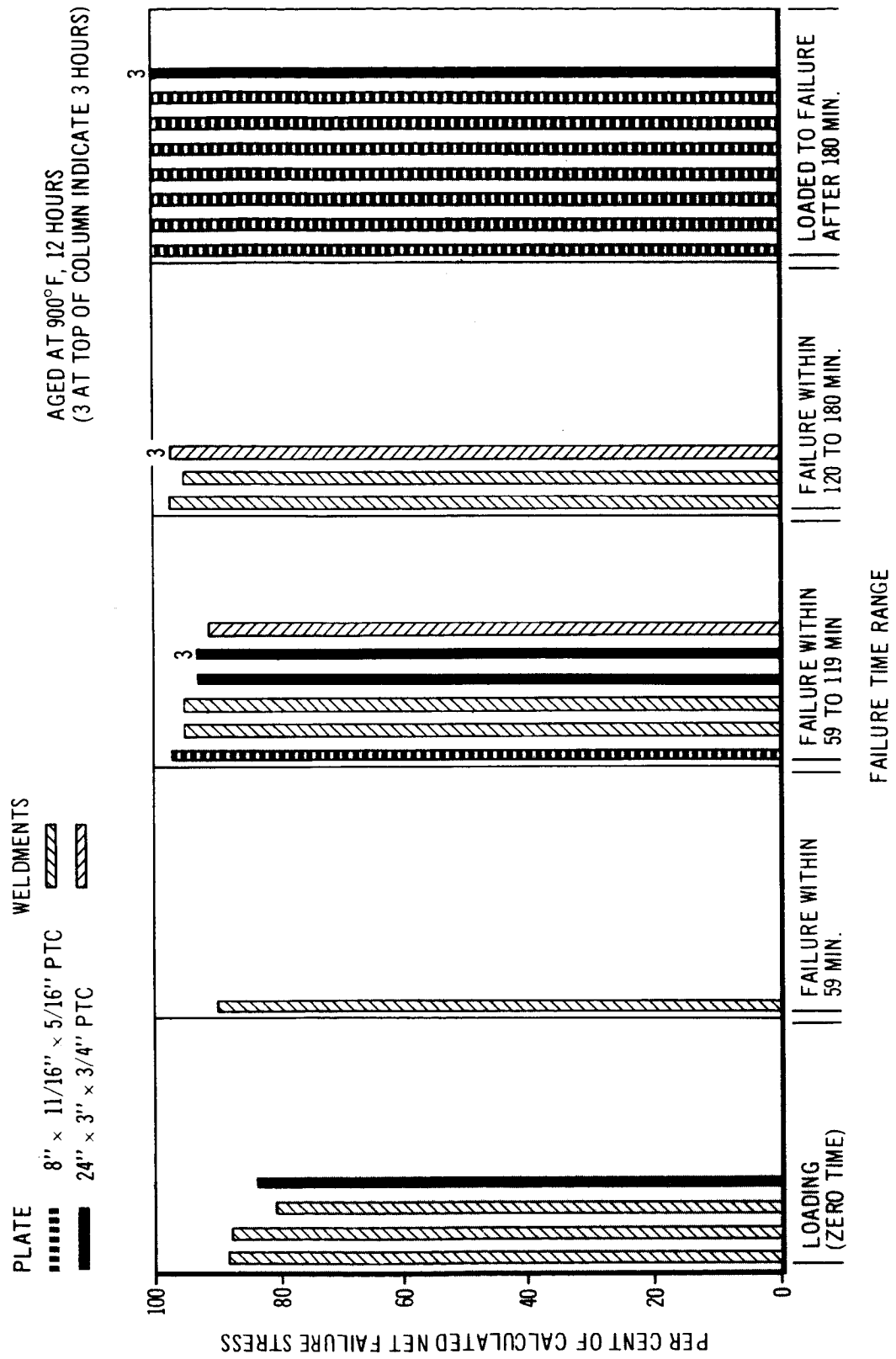


FIGURE 92

6. METALLOGRAPHIC OBSERVATIONS MADE BY OPTICAL AND ELECTRON MICROSCOPY AND ELECTRON FRACTOGRAPHY

The physical metallurgy and phase relationships of maraging alloys have been described in several publications (References 9-11, 13), but there remains much uncertainty concerning the exact strengthening mechanisms. No attempt will be made here to depict the numerous microstructural changes that are produced by thermal treatment.

This section instead presents a brief summary of a very intensive metallographic analysis which has been undertaken in fulfillment of this contract and as part of previous Douglas sponsored work. Particular emphasis is placed on metallurgical factors related to weldmetal fracture toughness, since this represents the principal mechanical property deficiency of maraging steel welds. The observation of a phase, which is identified in a later section as titanium nitride, is presented. Electron fractography has revealed this phase as a predominant feature on the fracture surfaces of weldmetal.

The metallographic evidence serves to support the hypothesis that titanium nitrides, either directly or indirectly, are responsible for the inferior fracture toughness of maraging steel weldmetal.

6.1 Parent Plate and Heat-Affected Zone Microstructure

Figures 15 and 16 (section 2.7.2) illustrates typical optical micrograph of 3/4" thick, 250 KSI grade, 18Ni-7Co-5Mo maraging plate. The banded structure illustrated is quite common and varies considerably in severity from heat-to-heat, and to some extent from region-

6.1 Parent Plate and Heat-Affected Zone Microstructure (Cont.'d.)

to region within a given plate. The sharp-cornered inclusions are common constituents in the banded zones. These types of inclusions are often observed to be gold colored. Table VII (Sec. 2.7.2) presented inclusion ratings for specimens taken from Heats I, A, and B plate. Angular inclusions of the type illustrated in Figures 15 and 16 represent the most conspicuous type present. These types of inclusions have been identified as titanium nitride or carbonitride in titanium bearing steels (References 14,15).

Figure 93 illustrates the appearance of angular inclusions on the rapid propagation fracture surface of a parent-plate plane-strain fracture toughness specimen. The matrix surrounding the inclusion consists of aged martensite. This fractograph was obtained using electron-fractographic techniques on an etched fracture surface employing a two-stage plastic-carbon replication technique. The inclusion appears to be fragmented as evidenced by replica seepage, and evidently fractured by cleavage mode. These types of inclusions were by no means heavily concentrated on such parent plate fracture surfaces, but were sufficiently common to be frequently encountered. Significantly, the surface immediately surrounding this type of inclusion is quite flat indicative of a low-ductility rupture (References 16, 17) or a highly localized state of triaxial stress. Figure 94 illustrates the more typical dimpled structure of rapid propagation regions in parent plate. This type of fracture surface structure is characteristic of ductile rupture (References 16, 17). The fractograph also illustrates, in the upper right-hand corner, a



ANGULAR INCLUSIONS OBSERVED ON THE FRACTURE SURFACE OF 3/4 INCH THICK 18Ni-7Co-5Mo PLATE
ETCHED SURFACE-2 STAGE PLASTIC CARBON REPLICA-45° CHROMIUM SHADOWED
ETCHANT-MIXED ACIDS PLUS CUPRIC CHLORIDE
MAG: 13,670 X

FIGURE 93



TYPICAL DIMPLED STRUCTURE
ON THE FRACTURE SURFACE OF
3/4 INCH THICK 18Ni-7Co-5Mo MARAGING STEEL PLATE
UNETCHED SURFACE - 2 STAGE PLASTIC-CARBON REPLICA
45° CHROMIUM SHADOWED
MAG: 6,500X

FIGURE 94



UNUSUALLY HIGH CONCENTRATION OF
ANGULAR INCLUSIONS ON THE RAPID PROPAGATION
FRACTURE SURFACE THROUGH A HEAT AFFECTED ZONE REGION
ETCHED SURFACE - 2 STAGE PLASTIC CARBON REPLICA
45° CHROMIUM SHADOWED
ETCHANT - CARAPELLAS REAGENT
MAG: 6,500 X

FIGURE 95

6.1 Parent Plate and Heat-Affected Zone Microstructure (Cont'd.)

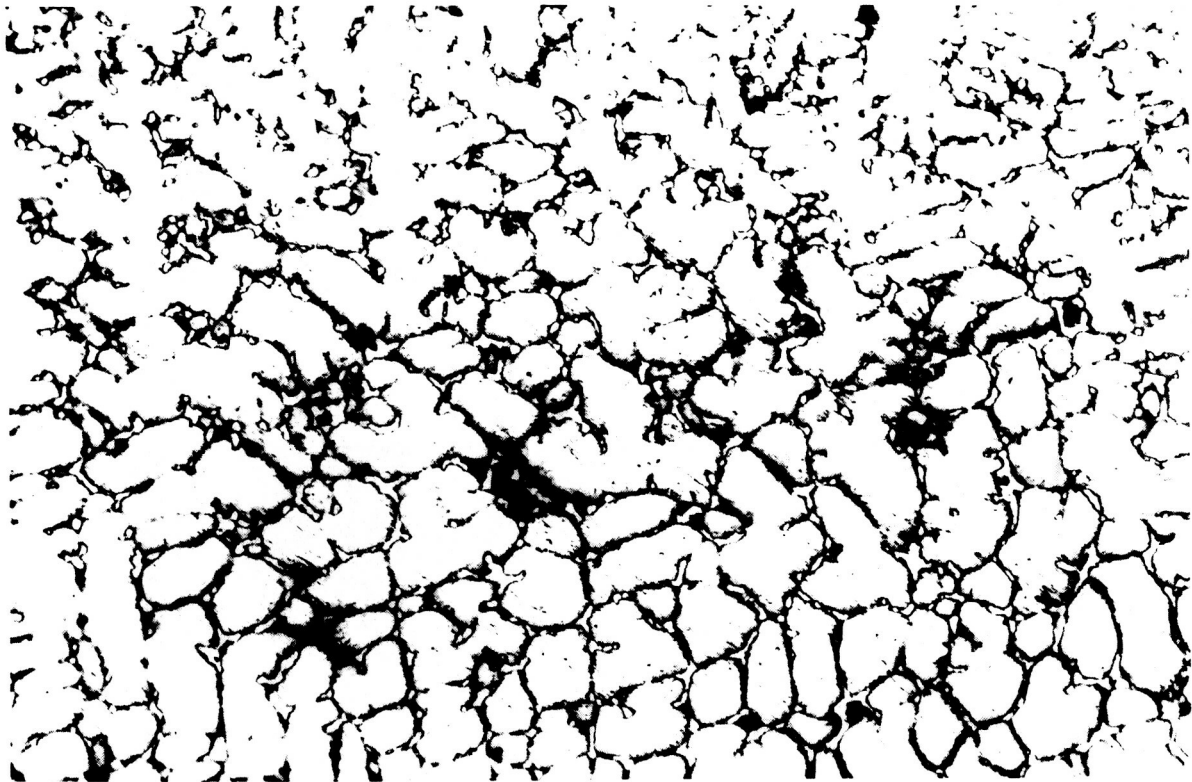
region containing angular inclusions of the type illustrated in Figure 93. The flat, non-dimpled surface in the vicinity of the inclusions is apparent.

Figure 95 illustrates a fractograph of a rapid propagation fracture surface through a heat-affected zone region. A rather high concentration of angular inclusions is observed, which is quite typical for this particular specimen. Rather low plane-strain fracture toughness ($K_{IC} = 63 \text{ KSI} \sqrt{\text{in}}$, see Section 3.10) also characterized this specimen. The relatively flat features of the fracture are evident. In general, heat-affected zone fracture surfaces through eyebrow regions were predominately dimpled and similar to that illustrated in Figure 94.

In summation, metallographic observations reveal that angular non-metallic inclusions, resembling titanium nitride, are prevalent in 18Ni-7Co-5Mo maraging steel plate. Fractographic analysis indicates that these angular inclusions tend to promote relatively flat fracture surfaces, and that the inclusions themselves fracture by apparent cleavage mode. Fractographic analyses thus far conducted have revealed that low fracture toughness is associated with an abundance of these inclusions on the fracture surface. These observations demonstrate the potential damaging influence of such inclusions in plate or heat-affected zone regions.

6.2 Weldmetal Microstructure

Figure 96 illustrates the typical microstructure prevalent in aged



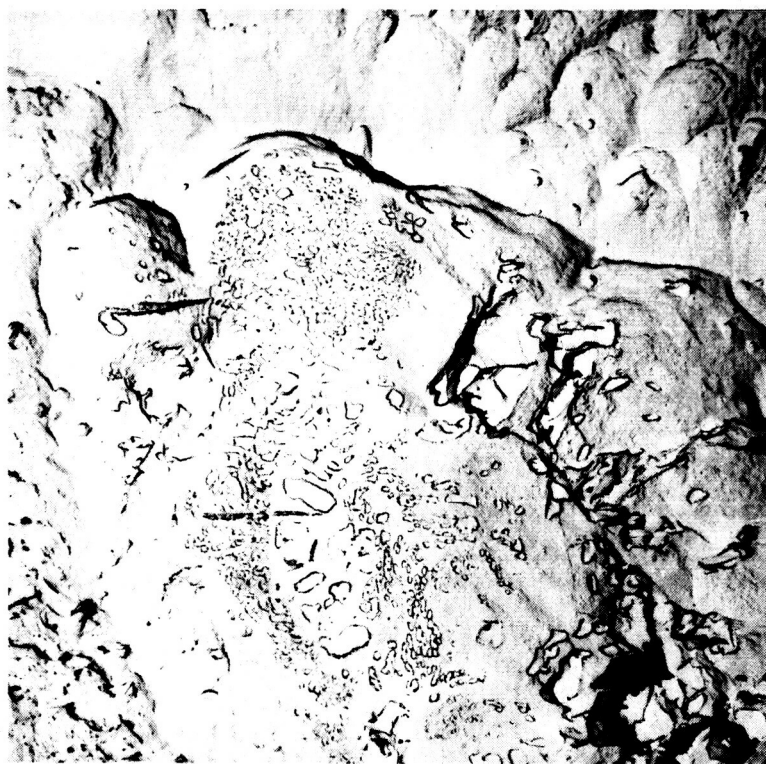
TYPICAL AGED WELDMETAL MICROSTRUCTURE
ETCHED - MIXED ACIDS PLUS CUPRIC CHLORIDE
MAG: 250X

FIGURE 96

6.2 Weldmetal Microstructure (Cont'd.)

maraging steel weldmetal. Light-etching islands form cell boundaries throughout an aged martensitic matrix. The light etching islands are believed to be reverted austenite enriched with austenite-stabilizing elements such as carbon, nickel, and nitrogen. Alloy segregation, which promotes the localized reversion to austenite in weldmetal, probably occurs during the non-equilibrium solidification and cooling of the weld deposit. Optical microscopy cannot reveal the fine details of structure which exist in such regions; however, electron microscopy is well suited for this task. The most revealing observations using the electron microscope were made by means of electron fractographic analyses.

Figure 97 illustrates a type of structure repeatedly observed on maraging steel weldmetal fracture surfaces. A very high concentration of an angular phase, closely resembling the inclusions observed in parent plate is shown. This phase was very abundant on the columnar regions of fracture surfaces of Type W9 all-weldmetal tensile specimens which exhibited such brittle behavior. Occasionally, relatively massive angular gold colored inclusion could be seen with the unaided eye. It will be shown later that preliminary work has resulted in the tentative identification of this constituent as TiN. Local concentrations of this angular phase vary considerably. As in the cases of parent plate and heat-affected zone regions, the fracture surface encompassing the angular phase is quite flat. The upper portion of Figure 97 illustrates a typical dimple structure in which the phase is absent.



AGED MARAGING WELD DEPOSIT FRACTURE SURFACE
ILLUSTRATING A HIGH CONCENTRATION OF ANGULAR INCLUSIONS

ETCHED SURFACE - 2 STAGE PLASTIC-CARBON REPLICA

45° CHROMIUM SHADOWED

ETCHANT - CARAPELLAS REAGENT

MAG: 6,500 X

FIGURE 97



AGED MARAGING WELD DEPOSIT FRACTURE SURFACE ILLUSTRATING
THE ANGULAR PHASE AND ITS ASSOCIATED MICROSTRUCTURE
ETCHED SURFACE-2 STAGE REPLICA-45° CHROMIUM SHADOWED
ETCHANT-CARAPELLAS REAGENT
MAG: 25,900X

FIGURE 98



AGED MARAGING WELD DEPOSIT FRACTURE SURFACE ILLUSTRATING
THE ANGULAR CONSTITUENT AND ITS ASSOCIATED MICROSTRUCTURE
ETCHED SURFACE-2 STAGE PLASTIC REPLICA-45° CHROMIUM SHADOWED
ETCHANT-CARAPELLAS REAGENT
MAG. 13,670 X

FIGURE 99

Figures 98 and 99 illustrate higher magnification fractographs depicting this angular phase, and the surrounding matrix. The fractured surfaces were etched prior to replication in order to reveal microstructural details. At the higher magnification the angular phase is seen to resemble the inclusions found in the parent material. The angular phase has apparently ruptured by cleavage (as evidenced by the very smooth, flat, surfaces) and is often fissured (as evidenced by replica seepage through several of the particles). This phase has always been observed to be virtually encircled by a clear-etching island within the aged, precipitation-laden matrix. The clear-etching islands seen on these fracture surfaces undoubtedly coincide with those observed in Figure 96. A rather pronounced interdependence appears to exist between the angular phase and the clear-etching phase within which it resides. Some hypothetical comments concerning this interdependency are presented in a later section.

The angular phase and the clear etching islands are a distinctive feature of aged weldmetal fracture surfaces. This duplex microstructural feature has not been observed in parent plate; however, angular inclusions closely resembling this constituent have been observed in parent plate. Furthermore, an unusually high concentration of angular inclusions in plate heat-affected zones has been associated with especially poor fracture properties. This, therefore, leads to the hypothesis that relatively high concentrations of the angular phase observed on weldmetal fracture surfaces must be

6.2 Weldmetal Microstructure (Cont'd.)

responsible, either directly or indirectly, for the poor fracture toughness properties of weldmetal.

7. IDENTIFICATION OF THE ANGULAR PHASE BY MEANS OF SELECTED AREA ELECTRON DIFFRACTION

This section describes preliminary work which has resulted in the tentative identification of the angular phase which appears to cause brittle behavior of maraging steel welds.

7.1 Carbon Extraction Replication Technique and Electron Diffraction

The technique employed to isolate the unknown angular phase is described in this section. First, the fracture surface to be examined is etched for approximately 60 seconds with Carapella's reagent. This is done to loosen the segregate. Then a direct carbon film is deposited on the fracture face using carbon vapor deposition. The carbon film is scribed into squares and then is removed by the application of Carapella's reagent. The unknown particles are thereby removed, attached to the carbon film. A gold film is deposited in a corner of the replica which is used to calculate the camera constant of the electron microscope. The extracted particles are identified by the use of electron diffraction techniques. A field limiting aperture was employed in the intermediate image plane, thereby restricting the diffraction area essentially to the particles isolated for identification (selected area diffraction). Unknown precipitates on the fracture surface can be analyzed by the electron diffraction pattern. Thus, important information can be obtained on influential factors affecting the path of the fracture.

7.2 Identification of the Angular Phase

In analyzing electron diffraction patterns, the following basic

7.2 Identification of the Angular Phase (Cont'd.)

relationship holds: $rd = L\lambda$, where r = radius of spot from the center, d = interplanar spacing, L = focal length of the microscope, λ = wavelength of the electron beam. The quantity $L\lambda$ is the camera constant, and may be used to evaluate the "d" value for any diffraction spot simply by measuring the corresponding "r".

Figure 100a is an electron fractograph illustrating the angular inclusion segregate on a fracture surface. This particular fractograph is characteristic of the fracture surface of a low toughness heat-affected zone specimen (Spec 7c2; $K_{IC} = 63 \text{ KSI} \sqrt{\text{in.}}$) Figure 100b shows a fractograph of a specimen from which the segregate has been successfully extracted by the aforementioned carbon extraction-replica technique. Figure 101 shows a typical extraction fractograph from weldmetal (Type W7, Spec. 4E31). The selected area diffraction pattern, from which the following data were obtained, is given in Figure 100c, with the reference diffraction rings of gold superimposed.

The "d" value lattice spacings corresponding to the various isolated diffraction spot of the segregate are presented in Table XVIII for diffraction patterns of inclusions from plate heat-affected zone and weldmetal regions, respectively. As may be seen, almost all the "d" values of cubic titanium nitride (ASTM card 6-0642) are apparent, although two of the values lie within two of the gold reference rings. Only one of the observed diffraction spot "d" values remains unidentified. Extra spots are not uncommon in electron diffraction patterns (Reference 18).

7.2 Identification of the Angular Phase (Cont'd.)

The identification of the angular inclusion as titanium nitride tends to be verified by electron microprobe x-ray analysis, as discussed later. This compound, as indexed, has a F.C.C. NaCl structure with lattice parameter $a_0 = 4.240 \text{ \AA}$.

TABLE XVIII

COMPARISON OF INTERPLANAR SPACINGS (\AA) CALCULATED FROM SELECTED AREA ELECTRON DIFFRACTION PATTERNS

Reference Ring Gold (ASTM Card 4-0784)	Replication Extraction Segregate		Titanium Nitride Ti N (ASTM Card 6-0642)	
	Heat-Affected Zone	Weldmetal		Miller Indices
	2.79	2.58		
	2.48	2.50	2.44	111
2.355				
	2.12	2.08	2.12	200
2.039				
	1.50	1.50	1.496	720
1.442				
	1.28	1.30	1.277	311
1.230		1.25	1.223	222
1.1774				
	1.06	1.09	1.059	400
	0.98	0.99	0.972	331
1.0196				
0.9358		0.96	0.948	420
0.9120				
	0.87	0.88	0.865	422
0.8325				
	0.82	0.83	0.816	333, 511

8. ELECTRON MICROPROBE X-RAY ANALYSIS

This section describes work done under Douglas sponsored research to evaluate the applicability of electron microprobe analysis for inclusion analysis. These exploratory results lend support to the electron diffraction data which demonstrated that TiN inclusions represent a significant feature of weldmetal fracture surfaces.

The electron microprobe X-ray analyzer employs a fine electron beam, approaching submicron diameter, to excite X-ray emission spectra within a localized area of a specimen. A quantitative analysis may then be made by analyzing the characteristic X-ray emitted for the presence of elements down to atomic number ten. Some preliminary work on maraging steel welds was conducted for Douglas in order to test the usefulness of the microprobe as an analytical tool. Sample runs were conducted at Materials Testing Laboratories, Division of Magnaflux Corporation.

8.1 Scanning Weldmetal Fracture Surfaces

Weldmetal fracture surfaces were examined on the ARL electron microprobe X-ray analyzer. Because of the surface roughness inherent in the fracture surface, the scanning images of back-scattered electrons, sample current, and even X-ray fluorescence, as shown on the cathode ray tube, reveal primarily the topology of the surface. Intensities are different for separate areas of identical chemical composition due to differences in absorption and the take-off angle caused by the irregular, non-parallel surface. One is sometimes able to detect rather large areas of gross compositional change by comparing back-

8.1 Scanning Weldmetal Fracture Surfaces (Cont'd.)

scattered electrons and sample current images of the same area. However, it is not readily possible to locate small area (approximately 1 micron) of even large compositional difference, or to locate large areas of small compositional differences, by this method. However, it was found quite possible to locate areas of the order of one micron with large compositional differences from the matrix by a technique of profile scanning.

If the X-ray intensity of a single element is sought, even a uniform distribution in the matrix of that element will result in a profile of varying intensities due to the effect of the rough surface mentioned before. However, if several elements are profiled for the same path and their intensities compared at various points of the path, it may be possible to detect large compositional variations even in micron or submicron areas. In the present case, titanium was profiled together with iron and nickel on weldmetal fracture surfaces. For this case, the change in intensities produced by the rough surface at a given point should be approximately the same for all three elements and in the same direction; thus, compositional variations are still detectable. In this manner, a number of areas were found where the ratios of titanium to both iron and nickel intensities were much higher than elsewhere, indicating an area considerably enriched with titanium, compared to the matrix value.

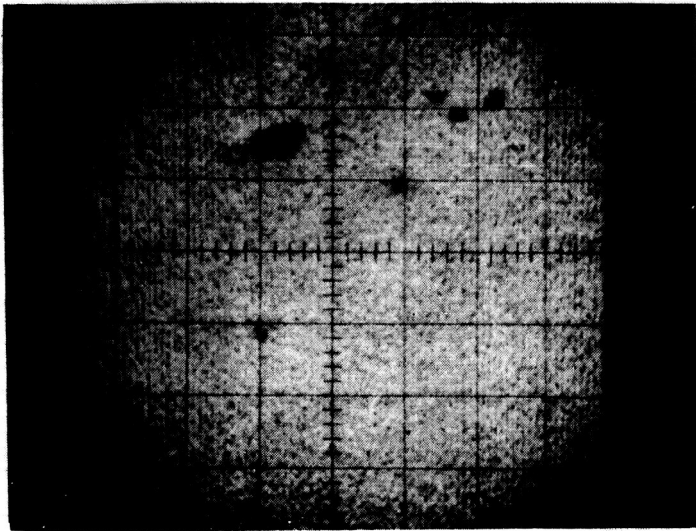
For the work to identify the titanium segregates in weldmetal, an electron beam of diameter less than 0.5 microns was used. The small specimen movement necessary to pass into and out of the high titanium

8.1 Scanning Weldmetal Fracture Surfaces (Cont'd.)

area leads to the conclusion that most of the areas were of micron and submicron dimensions. The segregates appeared to be uniformly distributed over most of the fracture surface. No reasonable attempt can be made at a quantitative analysis of these extremely small areas on the fracture surface. It can be said that the titanium concentration is considerably different from the matrix and from the 100 percent standard. A precise quantitative analysis should be easily accomplished on particles extracted by the extraction replica technique referred to earlier.

8.2 Scanning Polished Weldmetal Surfaces

With polished surfaces, cut perpendicular to the fracture surface, scanning images revealed numerous titanium-rich segregates. Quantitative measurements of such areas including the segregates were made. Back-scattering electron images were obtained on the cathode ray tube, showing numerous dark areas roughly several microns in diameter. A typical image is given in Figure 102. The dark areas indicate either the presence of an element of atomic number lower than that of the matrix or a void. Scanning the same area with the detector for a monochromator set for titanium gave an image with light areas (higher titanium than matrix) which corresponded to the dark areas. The other dark areas were shown to be voids in all cases examined. The presence of voids is determined by viewing the sample-current image and comparing it with the back-scattered electron image. For an element showing a dark spot on the latter, a corresponding bright spot will show on the sample-current image. A void will appear dark



BACK-SCATTERED ELECTRON SCANNING IMAGE
A NUMBER OF DARK AREAS ARE REVEALED, WHICH ARE EITHER
SEGREGATIONS OF AN ELEMENT OF ATOMIC NUMBER
LOWER THAN THAT OF THE MATRIX OR VOIDS.

(EACH SMALL DIVISION ON GRATICULE EQUALS 2.25 MICRONS)

888x

POLISHED SPECIMEN

FIGURE 102

on both images. It appears likely that the voids formerly contained segregates which were stripped out during the polishing process.

Quantitative analyses were made on a number of the titanium enriched areas, using integrated intensities. Raw intensity data must be corrected for several factors which include background, counter characteristics, absorption, enhancement by secondary fluorescence, electron deceleration in the specimen and back-scattering of electrons.

The elements determined were, Fe, Ni, Co, Mo, and Ti. Several determinations in the matrix compared very well with the corresponding values obtained by wet chemical methods. The areas of high titanium varied up to 38 weight per cent Ti, presumably due to size fluctuations which produced a dilution effect (to be discussed shortly). Each of the titanium-enriched areas had considerably less Fe, Ni, Co, and Mo, than the matrix; this decreased with increasing titanium concentrations, but maintained essentially the same ratios with respect to each other.

In all the quantitative measurements of titanium-enriched areas, the sum of the concentrations of the elements determined plus an estimate of the trace elements (made from matrix measurements or chemical analysis) did not total 100 weight per cent. The difference corresponds very well in each case to that which would be expected if the titanium were combined in an equi-molar stoichiometry with carbon, nitrogen, or oxygen. These three elements are not capable of direct determination by electron microprobe X-ray analysis. This is in

8.2 Scanning Polished Weldmetal Surfaces (Cont'd.)

good agreement with the data obtained by selected-area diffraction with the electron microscope, which revealed the extracted segregates as being titanium nitride.

8.3 Dilution Effects

It is important to realize that the effective volume of electron penetration of the specimen within which a given element will be excited (to emit fluorescent radiation) is not the same as the electron beam diameter, and varies with the element and electron-accelerating voltage. It is, of course, these areas to which the quantitative analysis applies for a given element. In general, the effective areas for the present determination were several microns in diameter, even at reduced accelerating voltage (25 reduced to 15 KV). Thus, generally, if the segregate in question is smaller than the effective areas of excitation, its true composition cannot be determined because of a dilution effect of the matrix. However, lower limits for each element in the segregate may be determined. Most of the segregates in the few specimens tested appear to be in this range, i.e., generally less than several microns.

As in the case of the segregates on the fracture surface, the size is often less than a micron, and the distribution of titanium enriched areas is rather uniform throughout the polished specimen surface. Quantitative data are strongly suggestive on TiN segregation, supplementing the electron diffraction findings.

9. THE INFLUENCE OF TiN AND RELATED FACTORS ON MARAGING STEEL WELD PROPERTIES

Results presented in previous sections show that a probable relationship persists between the angular phase recurrent on maraging steel fracture surfaces and low plane-strain fracture toughness. This appears to be especially true in weldmetal fracture surfaces. The preliminary work on the identification of this phase shows that the compound TiN is involved either directly or indirectly in this undesirable behavior. This section presents a brief discussion of the possible effects of TiN in the maraging class of alloys. A hypothesis is presented whereby the relative independence of fracture toughness on thermal treatments may be rationalized.

9.1 Properties of TiN and TiC

Titanium nitrides and carbides Ti (C,N,) are commonly present as inclusions in steels containing these alloying elements (References 21 and 22). The nitrogen is usually introduced as a result of melting practice. Once such particles have formed in the solid matrix, they cannot be readily eliminated because of their high chemical stability (References 15 and 19). In nickel alloys these particles have been shown to be stable up to the melting point of the alloy (Reference 20). Thus, it is unlikely that such inclusions in maraging steels could be eliminated by high temperature thermal treatment. TiC and TiN form a pseudo-binary isomorphous system, Figure 103. Both components are of the FCC-NaCl structure, and the anions substitutionally replace each other in the lattice. Some additional properties of interest are given in Table XIX. Both the carbide and

PHASE DIAGRAM OF TiC AND TiN
BASED ON AVAILABLE DATA

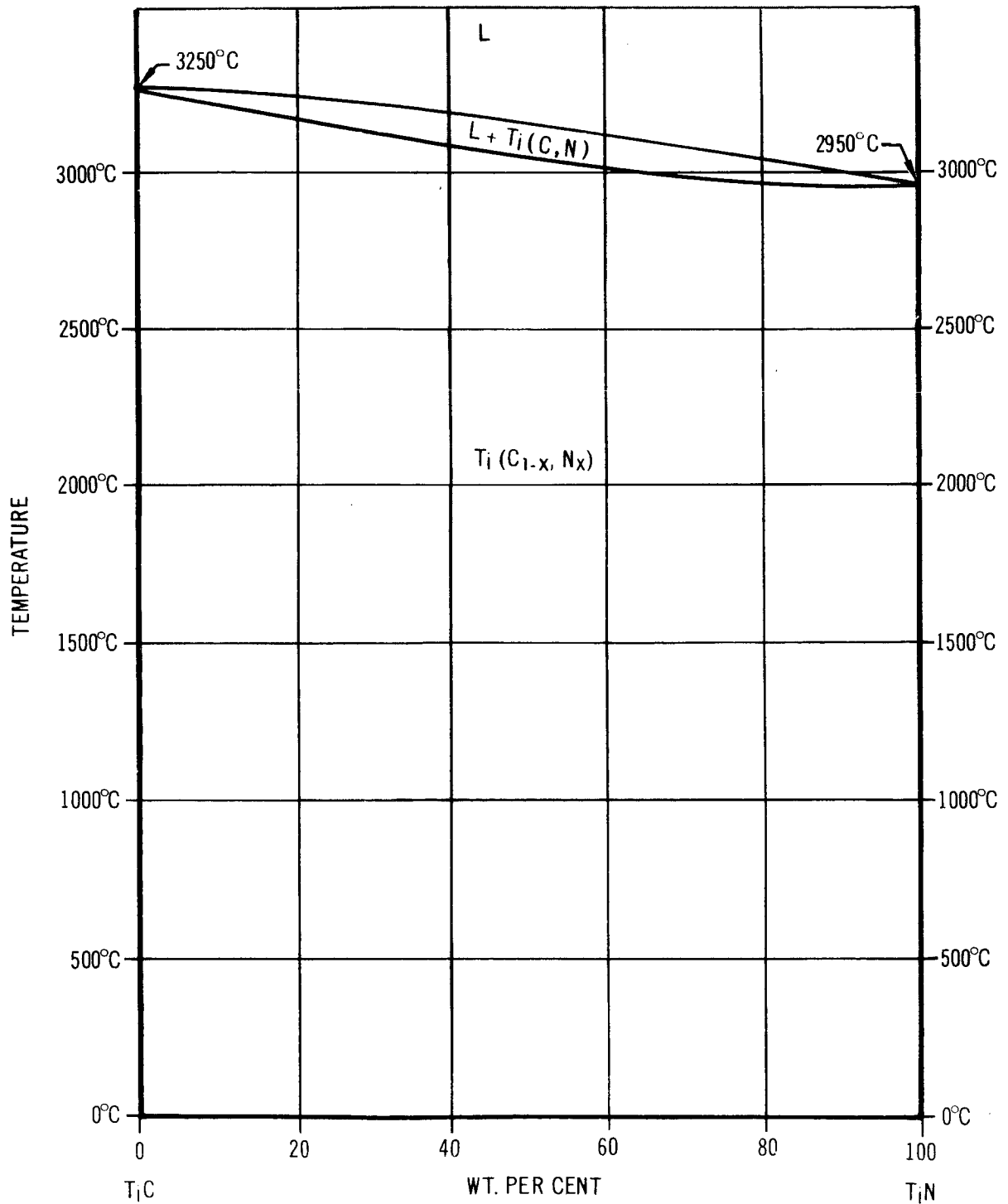


FIGURE 103

9.2 TiN in Weldmetal (Cont'd.)

Such reverted austenite may not transform to martensite upon cooling to room temperature until the localized concentration has decreased to the point where the M_s of the austenite is equal to or greater than room temperature, (Reference 21). Thus, until a critical nitrogen concentration is attained, the amount of austenite tends to increase with increasing aging time. Carbon probably has a similar effect.

9.3 Possible Effects of Austenite in Weldmetal

The austenite, retained or reverted during aging, may possess some interesting properties. Reverted austenite in 18 Ni-9Co-5Mo alloy and very likely also in 18Ni-7Co-5Mo, may be transformed back to martensite by plastic straining. The resultant martensite, despite the expected chemical non-homogeneity, is capable of a normal aging response (Reference 22).

This effect is of interest in weldmetal, since plastic deformation could possibly induce the transformation of austenitic islands to an alloy-enriched martensite and therefore change its mechanical properties. Such alloy-enriched martensite would be expected to be relatively brittle. Normally, the presence of austenite would be expected to increase the ductility of the weldmetal. However, the presence of relatively large concentrations of nitrogen could result in low fracture toughness arising from the nitrogen in solution as well as from the presence of the brittle TiN phase.

9.4. Toughness Degredation and TiN

In summation, the following hypothetical model relating to the formation and influence of titanium nitride appears to emerge.

1. Titanium nitrides present as inclusions in the parent plate, electrode wire, or originating from other sources find their way into molten weld puddle. Because of their high thermal stability, and the rapidity with which the weld puddle solidifies, the nitrides tend to remain essentially intact. Partial solution and re-precipitation upon cooling is possible.
2. The titanium nitrides tend to migrate to the liquid phase in the molten weld puddle. This leads to locally high concentrations of titanium nitride. Partial solution of the nitrides provides soluble nitrogen which tends to promote the formation of stable austenite. Such stable austenite may form upon direct solidification of the weld puddle or upon subsequent aging and re-cooling to room temperature.
3. As a result of the mechanisms postulated in (1) and (2) a semi-continuous dispersion of titanium nitrides, surrounded by alloy enriched austenite, may develop. Such semi-continuous networks found in aged weldmetal appear to provide favored propagation paths for fracture.

Several alternatives may be offered to explain the apparently damaging effects of the semi-continuous titanium nitride inclusions. First, damage may be produced simply because of the presence of the brittle TiN phase through which crack propagation may occur at a relatively

low energy expenditure. This effect is personally favored by the authors as the most important. As may be recalled, low toughness fractures were occasionally observed in heat-affected zone regions. These regions were characterized by high concentrations of titanium nitrides. However, unlike the weldmetal the nitrides were not surrounded by light etching islands (stable austenite or alloy enriched, unaged martensite). Thus it appears that the nitrides alone are responsible for the impairment of toughness. This conclusion is further supported by the observed effects of a variety of post weld thermal treatments.

As may be recalled, plane-strain fracture toughness of weldmetal was substantially unaffected by the duration or temperature of aging (as well as welding procedure). Nor did re-solution heat treatments change toughness significantly. The relative constancy is readily explainable in terms of the thermal stability of the titanium nitride network. Although precipitation, austenite reversion, and other reactions may occur as a result of the thermal treatments employed, very little change would be expected in the dispersion of titanium nitride. Thus the relative constancy of toughness may be explained by the thermal stability of the titanium nitride network.

A second mechanism may involve the presence of alloy-enriched (especially with nitrogen) austenite which may surround the titanium nitride inclusions. The possible spontaneous strain-induced transformation of such enriched austenite to relatively brittle martensite, during the course of crack propagation, could further

9.4 Toughness Degredation and TiN (Cont'd.)

degrade toughness.

As a third possibility, unaged alloy-enriched martensite surrounding the nitrides may produce additional damage.

Possibly all three mechanisms may be involved, however basic to all three is the predominant role of titanium nitride.

The precise effects of titanium nitride and the associated mechanisms responsible for the toughness degradation of welds cannot be positively stated at present. Critical testing of the postulated model is necessary. Such additional experimentation could lead to a clearer understanding of the phenomenon. Perhaps of even more importance, such work could provide methods of substantially improving the fracture toughness properties of welds.

SUMMARY, CONCLUSIONS, AND RECOMMENDATIONS

Significant observations, conclusions, and pertinent recommendations may be summarized as follows:

1. Different heats of nominally 250 KSI, 18Ni-7Co-5Mo 3/4-in thick airmelted plate have been shown to vary substantially in aging response. Both tensile and fracture toughness properties may exhibit significant differences, after identical aging treatments, despite relatively small chemical composition differences. The causes of these variations should be thoroughly investigated. Presently, plate from any heat must be individually tested to assure conformance with the required specifications. Compliance with chemical composition specifications, alone, cannot be relied upon.
2. Prolonged aging of plate tends to degrade toughness. The mechanisms responsible for the degradation are unknown and should be investigated. The decrease in toughness may not always be associated with a concomitant increase or decrease in strength.
3. Differences between transverse and longitudinal properties for plate were generally small. Tensile strength was usually higher and toughness lower for the transverse orientation.
4. Differences of 75°F in the aging temperature (875 versus 950°F) may produce tensile strength differences of up to 40,000 psi in plate. Special aging techniques may have to be developed for large space launch vehicle structures to assure the required temperature control.

SUMMARY, CONCLUSIONS, AND RECOMMENDATIONS (Cont'd.)

5. Plate hardness does not correlate very well with tensile strength.
6. A subsize partial thickness crack (PTC) fracture toughness specimen was developed and evaluated. The results showed that plane strain, K_{IC} (modified), and net fracture stress data generated using the subsize specimen correlated well with results obtained using substantially larger specimens. Theoretical analysis of specimen size effects is required.
7. Weldmetal and heat-affected zone cracking were not observed in welds deposited without preheat. Rigid control was, however, exerted on the hydrogen potential of the arc atmosphere.
8. Porosity problems were encountered in some of the welding studies. Although empirically guided modifications in welding procedures were able to eliminate the problem, the causes of porosity are not known. Work on the mechanisms of porosity formation in maraging alloys is worthy of study.
9. Tensile efficiency of weldmetal, deposited using a titanium enriched (about 1%) filler wire, generally exceeded 90 percent after most aging treatments and approached 100 percent after some.
10. Up to about 10 percent strength loss may occur in plate heat-affected regions of welds. The strength in these impaired heat-affected regions may be increased by prolonged aging to within 5 percent of the parent plate strength.

APPENDIX II (Cont'd.)

APPLICATION SPECIFICATIONS

The following specification, of issue in effect on date of invitation for bids, form part of this specification, as applicable:

Aeronautical Material Specification

AMS 2815-A	Identification and Packaging Welding Wire
------------	--

Military Specification

MIL-E-18193A	Steel, and Alloy Steel, Bare Coiled.
--------------	---

American Society for Testing Materials

ASTM E 45-51	Determining Inclusion Content of Steel
--------------	---

TECHNICAL REQUIREMENTS

Micro-Cleanliness

The micro-cleanliness shall be determined according to ASTM specification ASTM E 45-51 method A with ratings no poorer than:

	<u>Thin</u>	<u>Heavy</u>
A	1.0	1.0
B	1.0	1.0
C	1.0	1.0
D	1.0	1.0

Cast

Wire shall have imparted to it a curvature such that a specimen 10 to 12 feet long, when cut from the spool and suspended freely from its approximate midlength, shall form a circle not less than 20 inches and not greater than 36 inches in diameter. If

APPENDIX II (Cont'd.)

APPLICATION SPECIFICATIONS

The following specification, of issue in effect on date of invitation for bids, form part of this specification, as applicable:

Aeronautical Material Specification

AMS 2815-A	Identification and Packaging Welding Wire
------------	--

Military Specification

MIL-E-18193A	Steel, and Alloy Steel, Bare Coiled.
--------------	---

American Society for Testing Materials

ASTM E 45-51	Determining Inclusion Content of Steel
--------------	---

TECHNICAL REQUIREMENTS

Micro-Cleanliness

The micro-cleanliness shall be determined according to ASTM specification ASTM E 45-51 method A with ratings no poorer than:

	<u>Thin</u>	<u>Heavy</u>
A	1.0	1.0
B	1.0	1.0
C	1.0	1.0
D	1.0	1.0

Cast

Wire shall have imparted to it a curvature such that a specimen 10 to 12 feet long, when cut from the spool and suspended freely from its approximate midlength, shall form a circle not less than 20 inches and not greater than 36 inches in diameter. If

APPENDIX 11 (Cont'd.)

the curvature of the wire results in a coil of more than 1-1/2 turns, the excess shall be clipped off and the wire resuspended from its new approximate midlength.

Helix

A specimen cut and suspended as above and measured between adjacent turns shall show a separation not greater than 4 inches.

Layer Winding

Wire shall be closely wound in layers but adjacent turns within a layer need not necessarily be touching; shall be wound so as to avoid producing kinks, waves, and sharp bends; and shall be free to unwind without restriction caused by overlapping or wedging. The outside end of the spooled wire shall be so placed that it may be readily located.

Heat

Wire on each spool shall be of one continuous length from the same heat of material. Cut lengths in any one package shall be from the same heat of material.

Hardness

Wire hardness shall not exceed 34 Rockwell C or equivalent.

QUALITY

Material shall be vacuum melted. The product shall be uniform in quality and condition, clean, sound, smooth, and free from foreign materials and from internal and external imperfections detrimental to welding operations, operation of welding equipment, or properties of the deposited weld metal.

APPENDIX 11 (Cont'd.)

SIZES AND TOLERANCES

Unless other wise specified, wire shall be supplied in the following sizes and to the tolerances shown:

Diameter

Form	Nominal Diameter Inch	Tolerance, Inch plus and minus
Cut Length	0.045, 0.062, 0.093, 0.125	0.003
Spools	0.030, 0.035, 0.045, 0.062, 0.093	0.001
Spools	0.007, 0.010, 0.015, 0.020	0.0005

Length

Straight lengths shall be furnished in 18, 27, or 36-inch lengths as ordered, and shall not vary more than $\pm 1/4$ inch from the length ordered.

REPORTS

Unless otherwise specified, the vendor of the product shall furnish with each shipment three copies of a report of the results for chemical composition of each heat in the shipment and a statement that the product conforms to the technical requirements of this specification. This report shall include the purchase order number, material specification number, nominal size, and quantity from each heat.

Unless otherwise specified, when parts made of this wire or assemblies requiring the use of this welding wire are supplied, the part or assembly manufacturer shall inspect each lot of wire to determine conformance to this specification and shall furnish with each shipment three copies of a report stating that the wire conforms to the requirements of this specification. This report shall include the purchase order number, part or assembly number, and quantity.

APPENDIX II (Cont'd.)

PACKAGING AND MARKING

Packaging shall be accomplished in such a manner as to ensure that the wire, during shipment and storage, will be protected against machinical injury, contamination, and moisture.

Cut Lengths

Wire shall be furnished in standard containers of approximately 5, 10, 50, or 100 lb net weight, as specified.

Cut lengths shall be marked (code 615), cleaned, and packaged in accordance with the latest issue of AMS 2815.

Spooled Wire

Spools shall be of such materials and construction as to provide adequate strength and rigidity to prevent damage or distortion in normal handling and use, and to insulate the wire from the spindle. Unless otherwise specified, wire shall be furnished on spools of approximately 25 lbs \pm 1 lb net weight.

Marking

Both sides of each spool for spooled wire and each bundle and container for cut wire shall be permanently and legibly marked with the following information:

18% Maraging Steel Wire

DMS 1836 (revised 4/11/63)

Cobalt Content _____

Titanium Content _____

Carbon Content _____

Size _____

Quantity _____

Heat Number _____

APPENDIX II (Cont'd.)

Purchase Order Number _____

Manufacturer's Identification _____

REJECTIONS

Wire not conforming to this specification or to authorized modifications
will be subject to rejection.

APPENDIX III

PROCEDURE FOR CRACKING PTC COUPONS



Code 18355

AIRCRAFT COMPANY, INC.

DLP13.822**DOUGLAS LABORATORY PROCEDURE**

ISSUE OF 6-27-62

PAGE 1 OF 12

**TITLE: TECHNIQUE FOR MAKING SHALLOW-CRACKS IN
 SHEET METAL TENSILE SPECIMENS****A. SCOPE & USE:**

This Laboratory Procedure describes the method for making shallow-cracks in sheet metal tensile specimens.

B. EQUIPMENT:

1. 3600 RPM 50 lbs. capacity Krouse Sheet Flexure Fatigue Machine.
2. Two wedge type support blocks to clamp the specimen (Figures 1 and 2). These blocks should be made of a material that is as hard or harder than the specimen material. 4340 steel support blocks hardened to RC 53 have been used successfully for high-strength steel specimens.
3. Two adapter blocks to attach the specimen to the connecting rod of the fatigue machine. (Figures 3 and 4).
4. 40 power microscope with an eyepiece scale graduated in 0.001".

C. SPECIMEN PREPARATION:

1. The specimen used is a pin-loaded tensile specimen as shown in Figure 5.
2. The specimen which is to be cracked is ground or sanded so that the grinding or sanding striations are in the longitudinal direction of the specimen (normal to the crack length). It may be necessary to grind both sides of the specimen to maintain flatness. In grinding, not more than 0.001 inch thickness of material is removed with one pass. Preferably, high-strength steel is ground in the annealed condition to prevent grinding cracks and burning.
3. An electrical discharge machined starter notch (0.003 inch deep, 0.004 inch wide and 0.006 inch long) is made in the specimen at the desired location of the shallow-crack.

APPENDIX III (Cont'd.)

C. (Cont'd)

4. The specimen is then heat treated to the desired strength level, if required, using heat treat fixtures where necessary to maintain flatness.
5. The sharp corners and the specimen surface, on which the shallow-crack is to be introduced, are polished using No. 100 abrasive cloth first and finished with No. 1 abrasive polishing paper. The specimen is always polished in the longitudinal direction of the specimen.

D. PROCEDURE:

1. The specimen is placed (polished surface facing up) between the two wedge-shaped support blocks and its position adjusted so that the electrical discharge machined starter notch is located approximately 1/16 inch directly in front of the tip of the top wedge shaped block. (Figures 6 and 7).
2. The free end of the specimen is attached to the connecting rod of the fatigue machine by means of the two adapter blocks. (Figures 6 and 7).
3. By means of an adjustment screw near the fixed end of the specimen, the height of the specimen is adjusted so that the stress on the polished top surface of the specimen is always tension, never compression.
4. The eccentric of the fatigue machine is adjusted so that the initial crack occurs within a convenient time, about 3 to 5 minutes. An eccentricity of 16 to 20 divisions (deflection of 0.48 to 0.59 inch respectively) is satisfactory for high-strength steel.
5. The microscope is focused on the polished top surface of the specimen so that the electrical discharge machined starter notch is visible in the center of the field of view. (Figure 7).

APPENDIX III (Cont'd.)

D. (Cont'd)

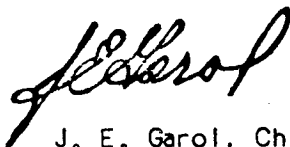
6. The fatigue machine is then turned on and allowed to run for a short time, one or two minutes. The fatigue machine is then stopped and the specimen surface viewed through the microscope to see if a crack has initiated from the starter notch. If there is no crack, the fatigue machine is run again for a short time and the specimen surface viewed again. This procedure is repeated until a crack has initiated from the starter notch. The crack length is then measured with the graduated eyepiece of the microscope. Cycling is continued until the desired crack length is obtained. Approximate relations between crack length and crack depth for 0.070 inch high-strength steel, 0.050 inch 6Al-4V Titanium, 0.050 inch 5Al-2.5 SN Titanium, 0.100 inch and 0.250 inch 2014-T6 Aluminum are presented in Figures 8 and 9.
7. The crack length and number of cycles are recorded and the specimen is removed from the fatigue machine.



J. L. Waisman
Assistant Chief Design Engineer
Materials Research & Production Methods
Missile & Space Systems Division



R. A. Simpson, Chief
Materials Research & Process Engineer
Aircraft Division



J. E. Garol, Chief
Materials & Process Engineer
Tulsa Division

SLP:bn

APPENDIX III (Cont'd.)

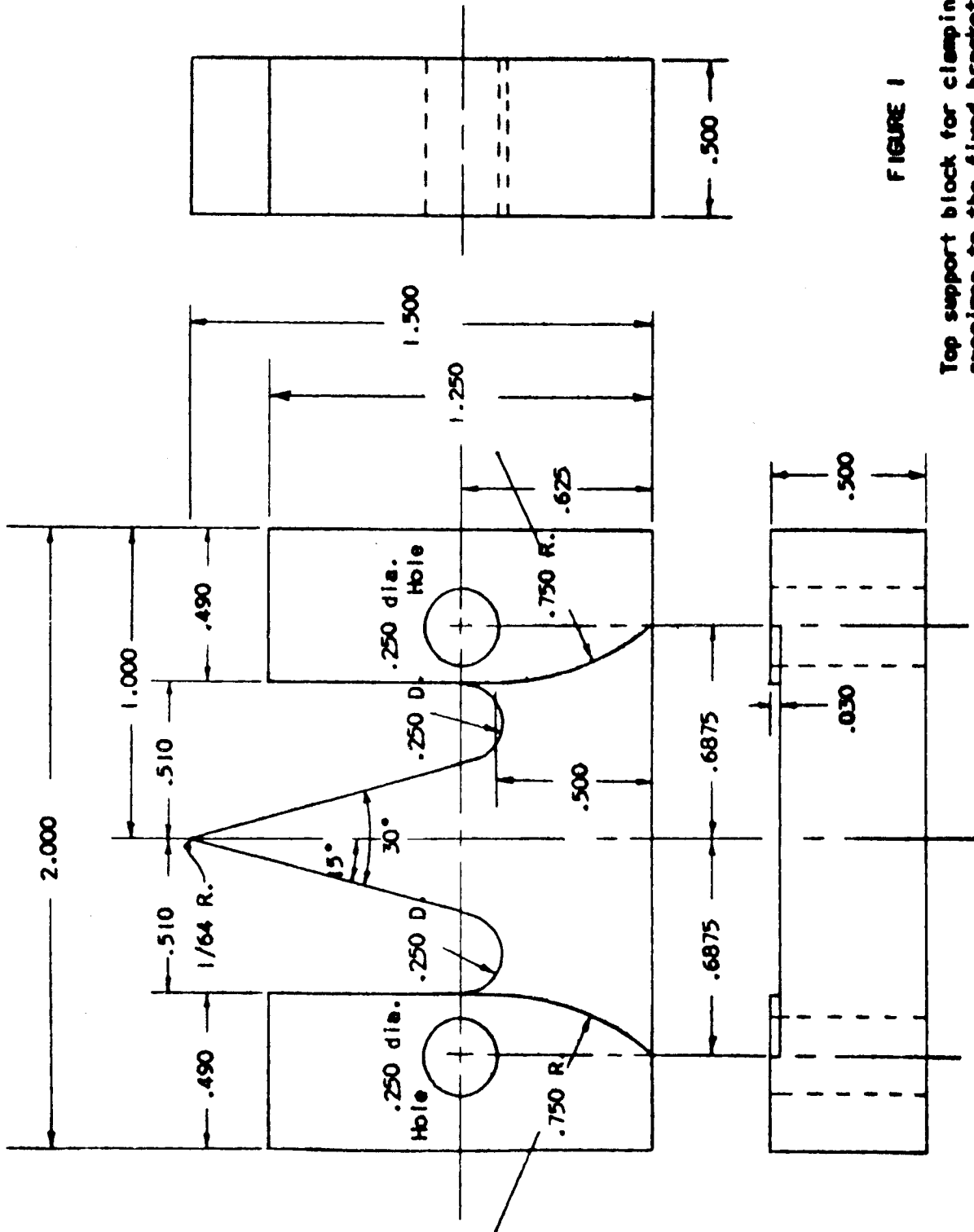


FIGURE 1

Top support block for clamping the specimen to the fixed bracket of the fatigue machine.

APPENDIX III (Cont'd.)

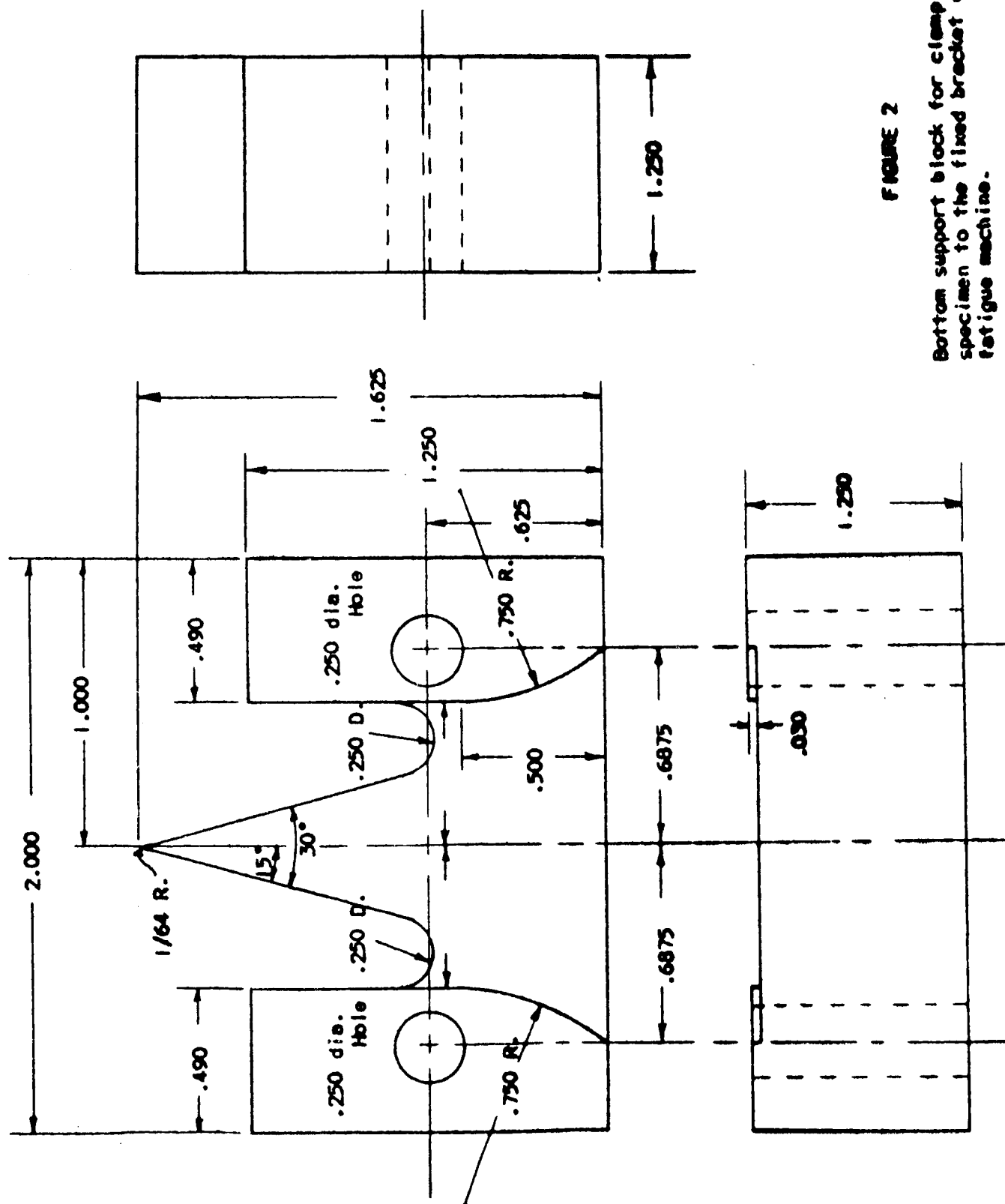


FIGURE 2

Bottom support block for clamping the specimen to the fixed bracket of the fatigue machine.

APPENDIX III (Cont'd.)

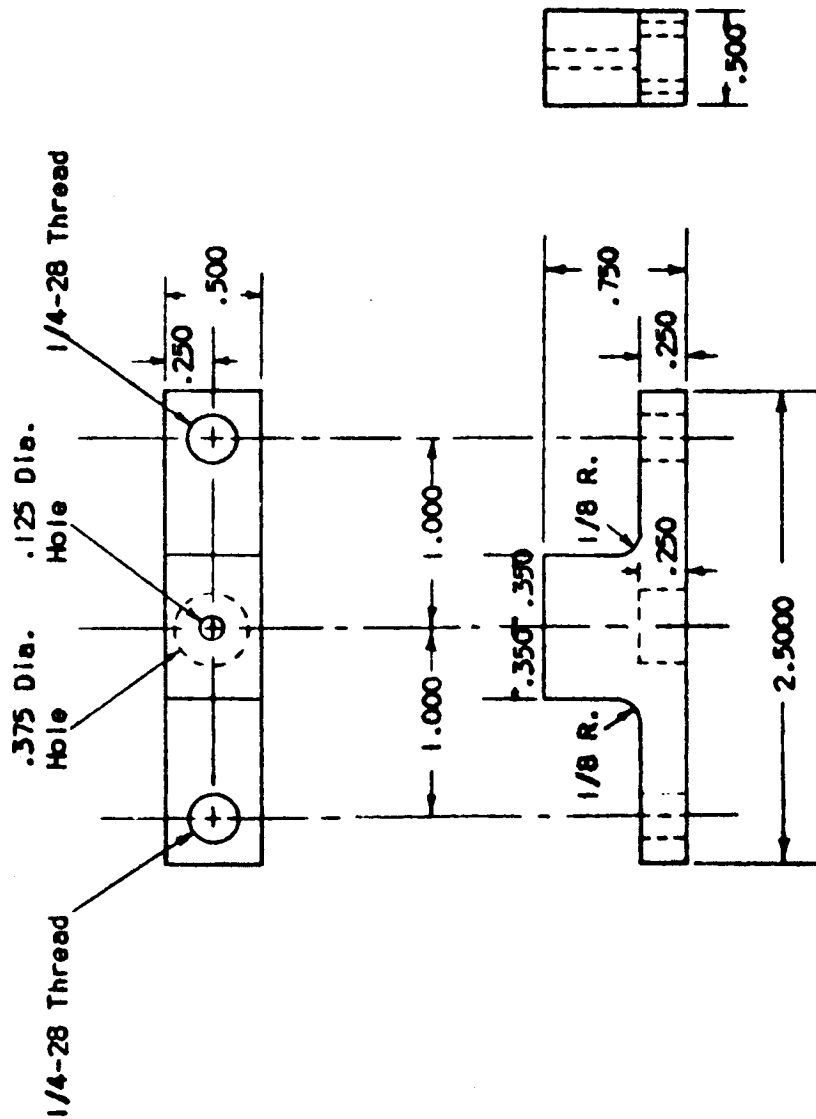


FIGURE 3

Top adapter block for attaching the specimen to the connecting rod of the fatigue machine.

APPENDIX III (Cont'd.)

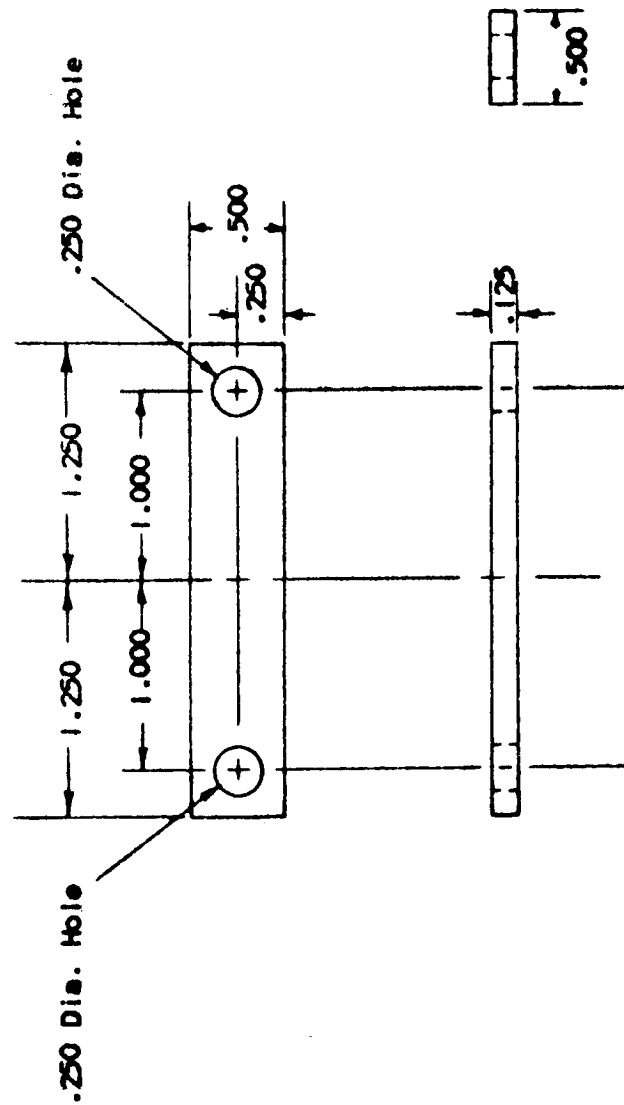
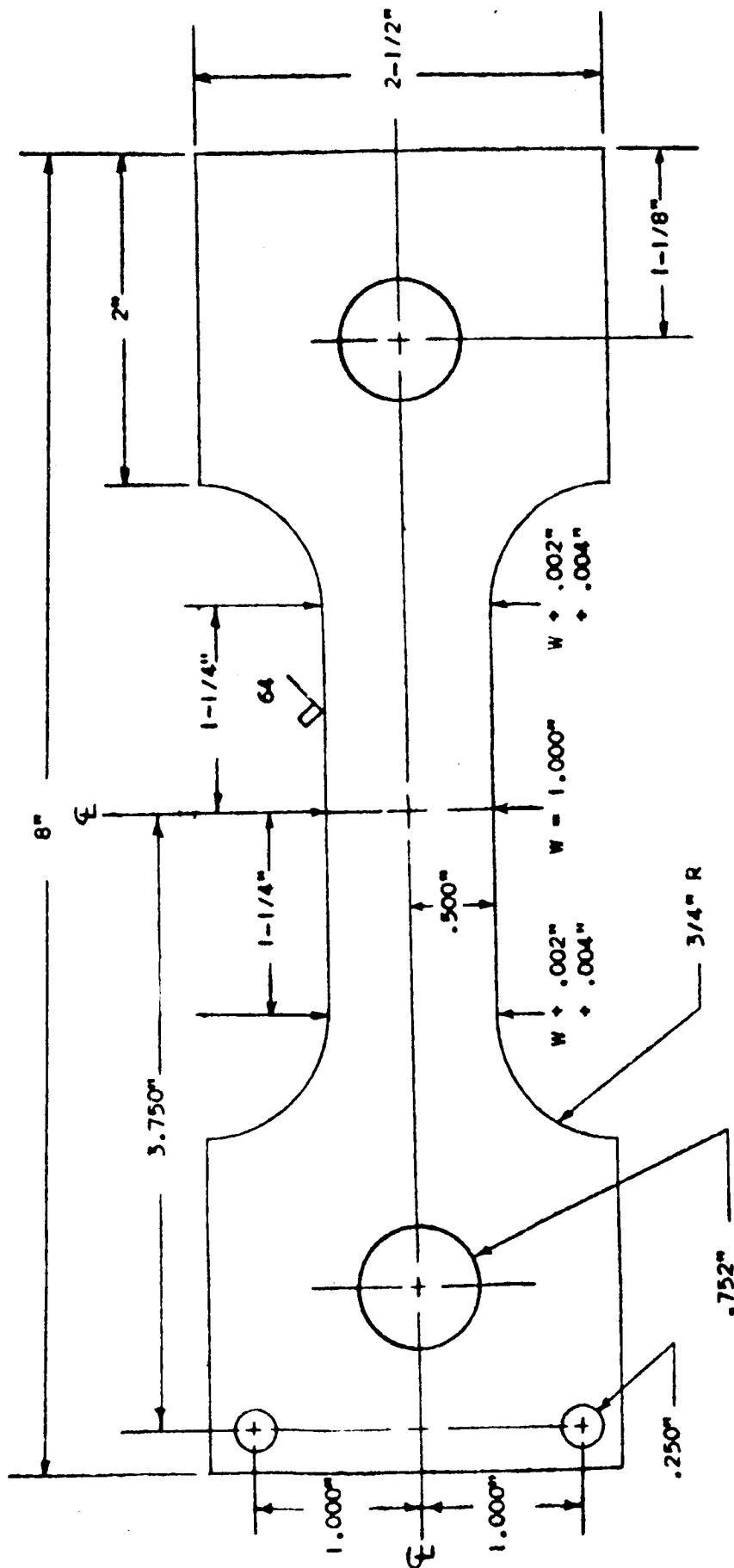


FIGURE 4

Bottom adapter block for attaching the specimen to the connecting rod of the fatigue machine.

FIGURE
SHALLOW CRACKED SHEET TENSILE SPECIMEN



TOLERANCES

Fractions $\pm 1/32^{\text{nd}}$

Decimal ± 0.002 "

Unless otherwise specified.

Notes

1. Gradual equal taper on both sides from outer ends of reduced section towards center as shown with no abrupt changes.
2. Edges of reduced section to be left sharp.
3. Finish is to be RMS 125 except as shown.
4. Holes must be on ϕ within 0.002".

APPENDIX III (Cont'd.)

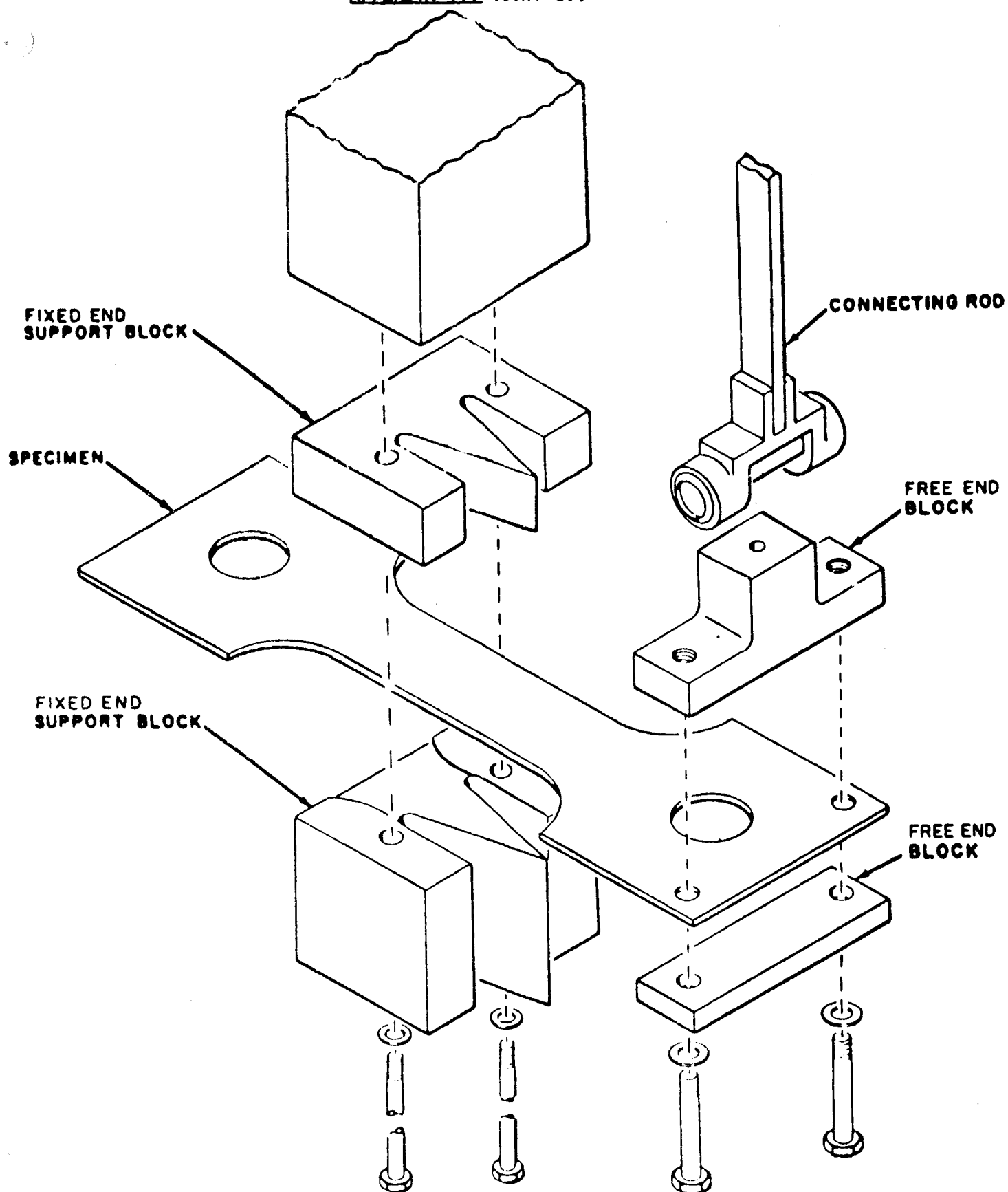
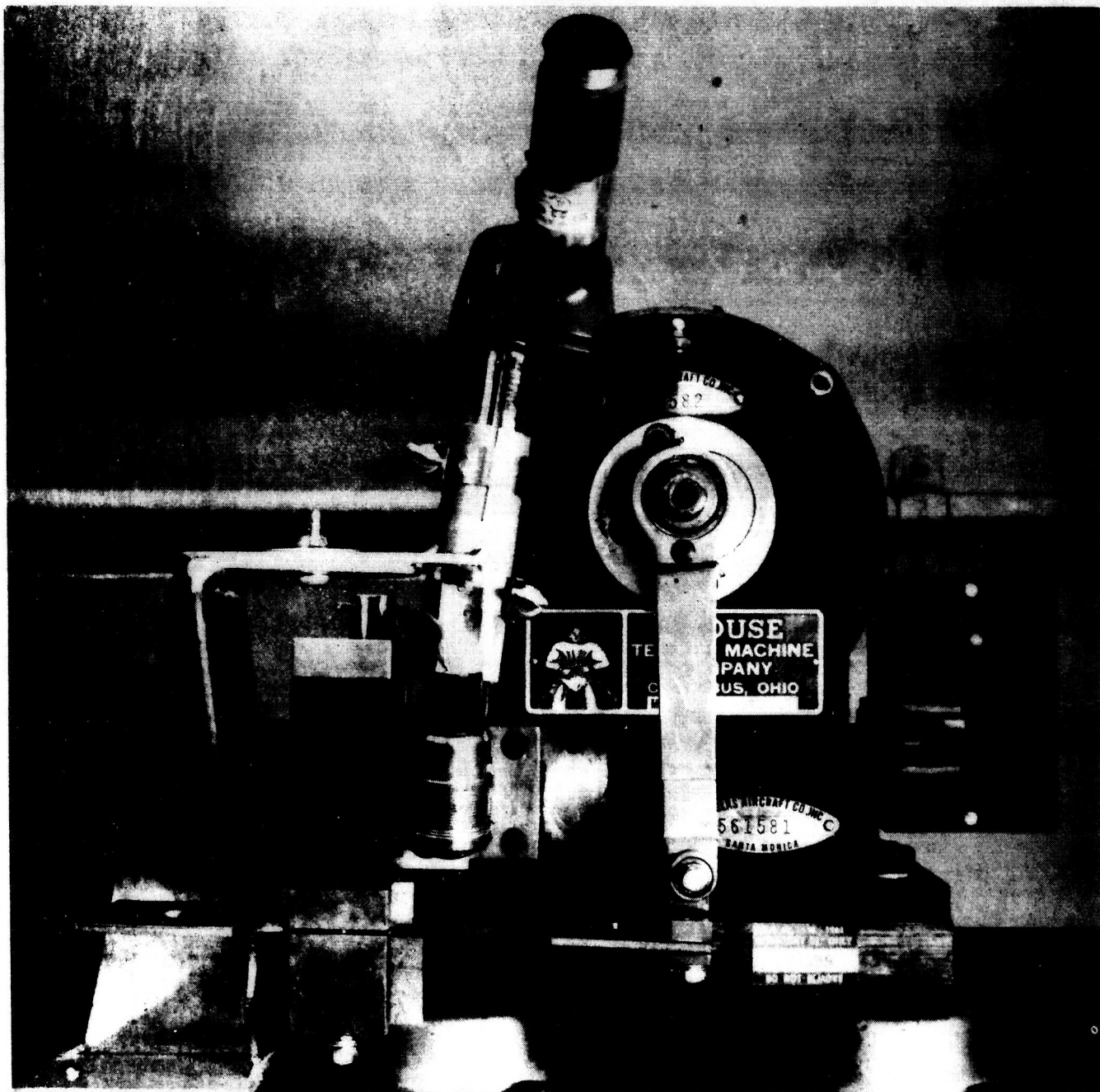


FIGURE 6

Set-up for making shallow crack (exploded view).

APPENDIX III (Cont'd.)



SM 350251

FIGURE 7

SET-UP FOR MAKING SHALLOW CRACKS (FRONT VIEW).

Relation between crack length and crack depth of shallow cracks in .070" thick 4340 and H-11 steels H.T. 260 to 280 ksi.

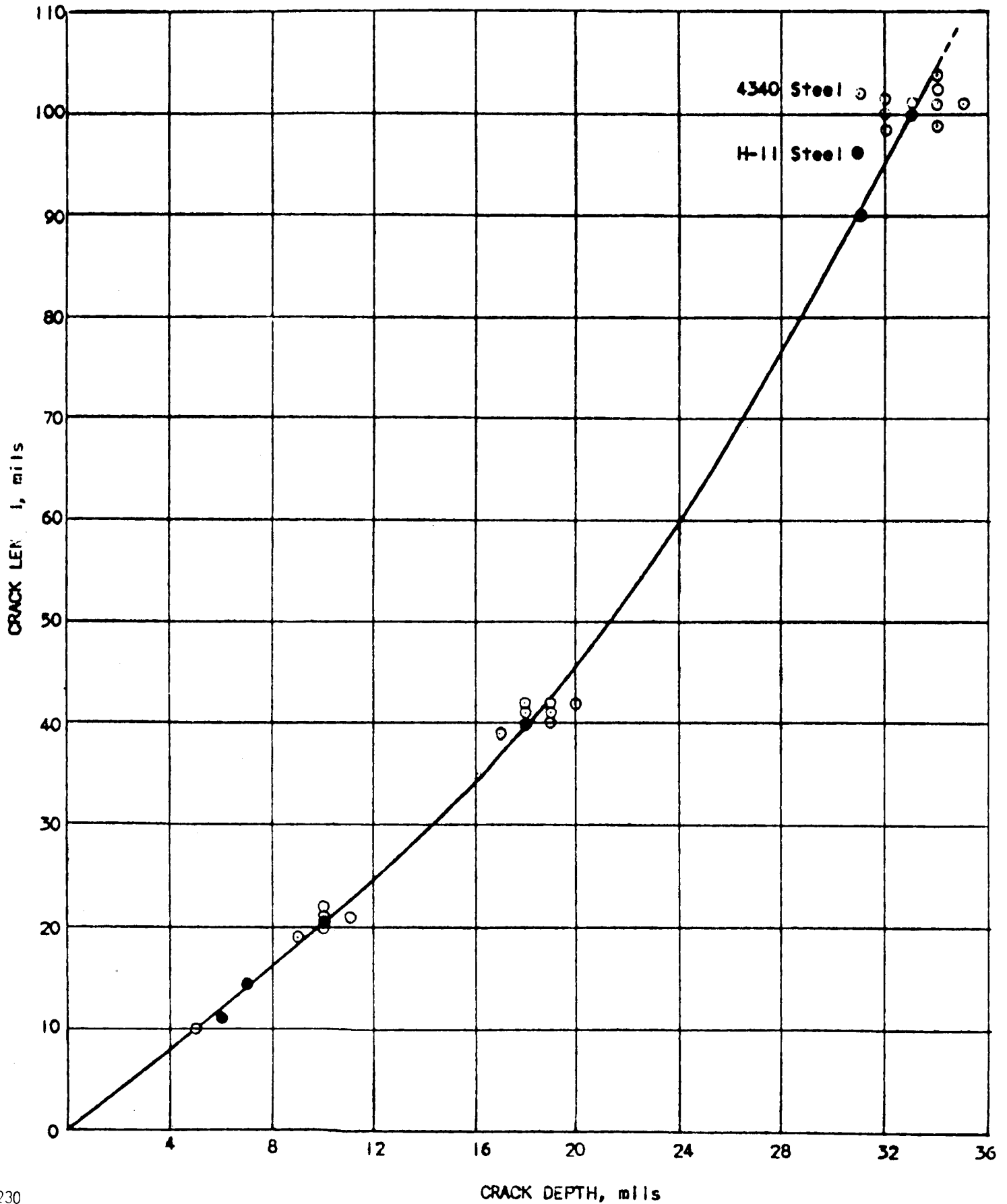
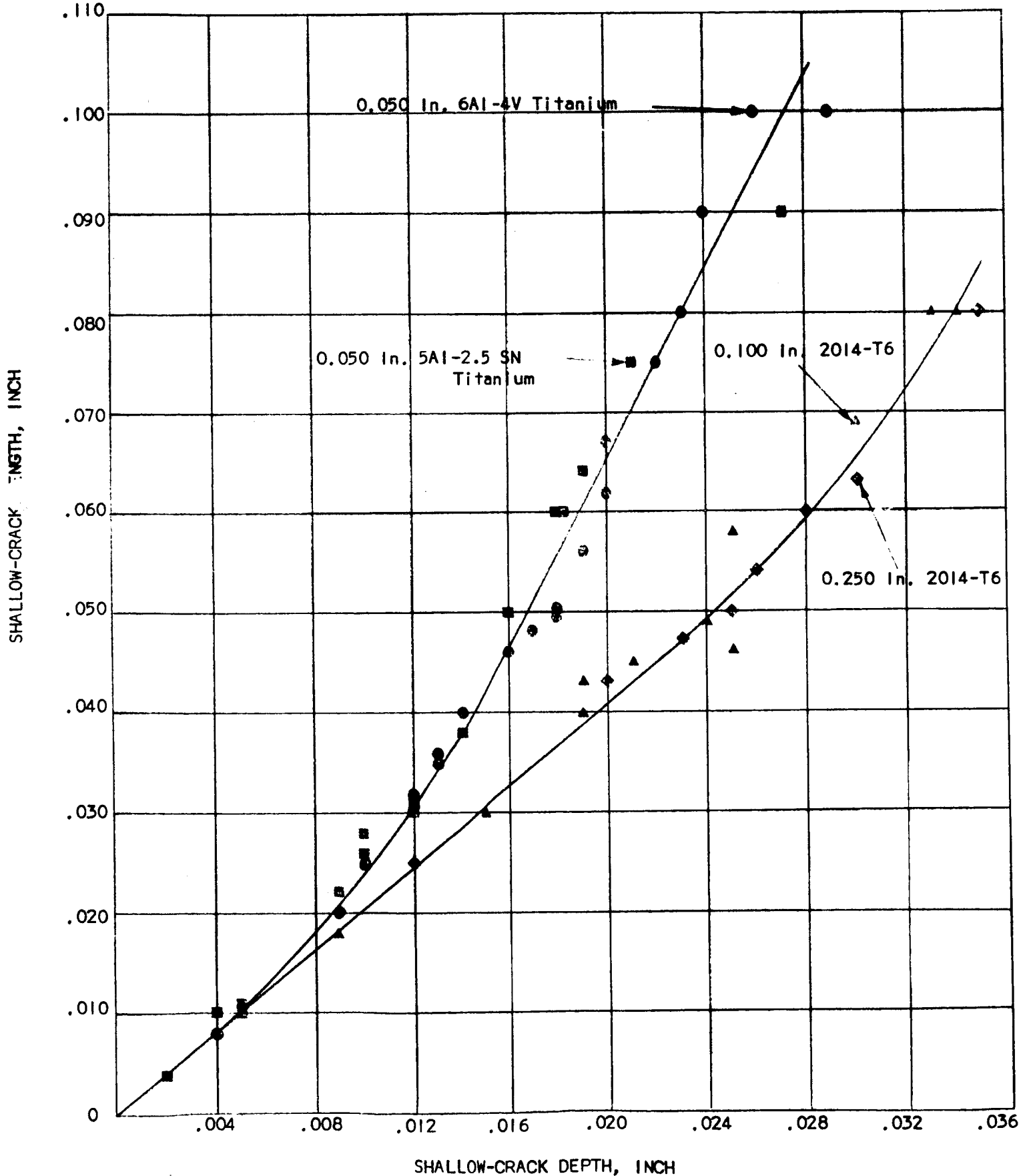


FIGURE 9

RELATION BETWEEN CRACK LENGTH AND CRACK DEPTH OF SHALLOW-CRACKS IN
0.050 IN. 6AL-4V TITANIUM, 0.050 IN. 5AL-2.5 SN TITANIUM, 0.100 IN.
AND 0.250 IN. 2014-T6 ALUMINUM.



APPENDIX IV
PLATE UNIAXIAL TENSILE DATA

APPENDIX IV - PLATE TENSILE DATA SUMMARY

UNIAXIAL TENSILE DATA - HEAT 1 PLATE

SPEC. NO.	AGING TEMP., °F	TIME AT TEMP. HRS.	0.2% YIELD STRESS, (KSI)	ULTIMATE STRESS, (KSI)	% ELONG. (2-IN. GAGE)
2-4	875	3	247.3	252.5	10.0
2-8	875	3	244.8	250.8	11.0
2-10	875	3	247.8	253.7	10.0
2-22	875	8	NA	263.9	8.0
2-23	875	15	NA	268.3	9.0
2-6	900	3	257.7	264.2	8.5
2-7	900	3	259.1	264.4	8.5
2-8	900	3	260.7	265.2	9.0
2-16	900	8	NA	266.6	9.0
2-24	900	8	NA	265.7	8.0
2-25	900	8	NA	264.0	9.5
2-26	900	15	NA	269.1	9.0
2-5	925	3	263.5	267.2	9.0
2-12	925	3	265.7	269.2	9.0
2-13	925	3	259.7	267.7	10.0
2-28	925	8	NA	266.5	7.5
2-29	925	15	NA	266.5	9.0
2-30	950	3	NA	269.0	8.0
2-17	950	8	NA	261.6	10.0
2-31	950	8	NA	263.5	8.5
2-32	1000	1	NA	255.0	9.0
2-18	1000	3	NA	252.4	9.5
2-33	1000	3	NA	255.0	10.0
2-19	1000	8	NA	242.9	12.0

NOTES:

1. All results obtained with .505-in. diameter specimens
2. Not available
3. All specimens longitudinal

APPENDIX IV (Cont'd.)

TENSILE DATA ON HEATS A AND B PLATE
TO CHECK SPECIFICATION CONFORMANCE

SPEC. No.	SPECIMEN ORIENTATION	0.2% YIELD STRESS, (KSI)	ULTIMATE STRESS, (KSI)	% ELONG. (2 in. Gage	% RED. IN AREA
-----------	-------------------------	-----------------------------------	------------------------------	-------------------------------	-------------------

HEAT A PLATE TENSILE DATA

AP 31	L	253.0	259.0	11.0	45.5
AP 32	L	252.0	258.5	11.0	44.9
AP 33	L	253.6	258.8	11.0	44.0
AP 34	T	255.0	260.8	8.0	32.5
AP 35	T	253.0	260.0	10.0	36.6
AP 36	T	254.0	260.3	9.0	38.8

HEAT B PLATE TENSILE DATA

P-31	L	254.5	264.0	9.0	41.9
P-32	L	257.0	265.0	11.0	41.3
P-33	L	253.5	263.0	8.0	38.5
P-34	T	265.5	270.0	8.0	33.4
P-35	T	264.0	267.5	8.0	33.4
P-36	T	259.0	269.0	7.0	34.4

NOTES:

1. L = Longitudinal

T = Transverse

2. All results obtained with 0.505-in. diameter specimens

3. Aged at 900°F for 3 hours

APPENDIX IV (Cont'd.) - PLATE TENSILE DATA SUMMARY

UNIAXIAL TENSILE DATA - HEATS-A AND B PLATE AGED AT 950°F

HEAT-A PLATE						
SPEC. NO.	TIME AT TEMPERATURE (HOURS)	SPECIMEN ORIENTATION	0.2% YIELD STRESS (KSI)	ULTIMATE STRESS (KSI)	% ELONG. (IN 2")	% RED. IN AREA
AP217	1	L	247.8	255.5	10.0	42.2
AP218	1	L	248.3	254.7	10.0	49.6
AP241	1	T	247.6	254.5	9.0	39.0
AP242	1	T	247.0	254.6	8.0	39.0
AP219	3	L	251.7	260.1	11.0	48.1
AP220	3	L	250.6	260.4	10.0	44.2
AP243	3	T	254.2	261.3	10.0	38.7
AP244	3	T	254.7	261.6	7.0	36.6
AP221	6	L	250.6	256.3	10.0	39.2
AP222	6	L	247.8	256.3	11.5	44.7
AP245	6	T	251.7	259.8	10.0	35.7
AP246	6	T	252.7	259.6	10.0	35.7
AP223	12	L	239.9	247.6	12.0	37.4
AP224	12	L	240.7	248.1	13.0	50.9
AP247	12	T	243.5	252.4	10.5	39.1
AP248	12	T	241.9	251.2	10.5	41.1

HEAT-B PLATE						
P29	1	L	252.6	263.4	10.0	43.9
P210	1	L	254.1	260.2	8.0	42.6
P233	1	T	255.6	268.5	7.0	35.5
P234	1	T	258.8	269.8	6.0	31.5
P211	3*	L	266.9	274.8	8.0	47.9
P212	3*	L	264.9	274.1	8.0	45.8
P235	3*	T	274.2	284.9	6.5	30.9
P236	3*	T	273.0	284.5	6.0	33.2
P213	6	L	274.3	282.6	8.0	46.4
P214	6	L	270.5	279.8	7.5	42.1
P237	6	T	278.5	289.9	5.0	33.9
P238	6	T	275.7	285.9	4.5	29.9
P215	12	L	277.2	285.9	6.0	44.4
P216	12	L	275.7	283.6	8.0	46.3
P239	12	T	265.0	275.5	6.0	33.3
P240	12	T	263.3	277.7	6.5	40.2

NOTES:

1. L = Longitudinal; T = Transverse
2. All results obtained with 0.505" diameter specimens
3. *3 Hour specimens inadvertently aged at 915°F

APPENDIX IV (Cont'd.) - PLATE TENSILE DATA SUMMARY

UNIAXIAL TENSILE DATA - HEATS-A AND B PLATE AGED AT 900°F

HEAT-A PLATE

SPEC. NO.	TIME AT TEMPERATURE (HOURS)	SPECIMEN ORIENTATION	0.2% YIELD STRESS (KSI)	ULTIMATE STRESS (KSI)	% ELONG. (IN 2") GAGE	% RED. IN AREA
AP29	1	L	243.2	249.9	10.0	45.2
AP210	1	L	240.0	249.9	10.0	45.5
AP233	1	T	239.2	249.9	8.0	34.0
AP234	1	T	242.3	250.6	9.0	36.6
AP211	3	L	255.2	261.6	10.5	42.2
AP212	3	L	255.0	261.6	8.0	37.6
AP235	3	T	252.2	262.9	8.0	32.7
AP236	3	T	256.0	261.8	7.0	32.0
AP213	6	L	260.3	265.7	9.0	39.1
AP214	6	L	259.8	265.4	10.0	42.8
AP237	6	T	260.8	267.4	8.0	34.4
AP238	6	T	259.1	267.0	8.0	35.3
AP215	12	L	261.8	268.2	10.0	43.5
AP216	12	L	259.8	266.4	9.0	39.0
AP239	12	T	260.9	268.5	6.5	34.4
AP240	12	T	261.9	268.4	7.0	37.0

HEAT-B PLATE

P217	1	L	261.8	269.5	11.0	49.4
P218	1	L	264.4	268.7	9.0	43.6
P241	1	T	252.6	266.2	9.0	41.5
P242	1	T	254.1	266.4	9.5	42.1
P219	3	L	271.3	279.0	10.0	45.4
P220	3	L	266.8	276.6	9.5	46.4
P243	3	T	253.6	266.2	8.5	41.8
P244	3	T	255.6	266.9	8.5	40.8
P221	6	L	265.9	276.7	10.5	45.7
P222	6	L	265.5	275.5	9.0	44.6
P245	6	T	251.6	264.2	8.5	39.7
P246	6	T	252.6	265.0	9.0	41.2
P223	12	L	256.2	266.9	11.5	45.7
P224	12	L	258.5	268.8	11.0	46.6
P247	12	T	238.2	251.3	10.5	42.4
P248	12	T	238.7	253.6	8.5	38.6

NOTES:

1. L = Longitudinal; T = Transverse

2. All results obtained with 0.505" diameter specimens.

APPENDIX IV (Cont'd.) - PLATE TENSILE DATA SUMMARY

UNIAXIAL TENSILE DATA - HEATS-A AND B PLATE AS-RECEIVED AND AGED AT 875°F

HEAT-A PLATE

SPEC. NO.	TIME AT TEMPERATURE (HOURS)	SPECIMEN ORIENTATION	0.2% YIELD STRESS (KSI)	ULTIMATE STRESS (KSI)	% ELONG. (IN 2" GAGE)	% RED. IN AREA
AP21	1	L	240.4	248.8	10.5	47.4
AP22	1	L	238.6	246.5	11.0	48.2
AP225	1	T	236.8	245.5	10.0	39.6
AP226	1	T	234.8	240.0	9.5	40.1
AP23	3	L	250.1	260.9	11.0	44.3
AP24	3	L	254.2	259.9	12.0	51.1
AP227	3	T	248.6	258.3	9.5	40.7
AP228	3	T	250.4	259.8	8.0	36.6
AP25	6	L	254.7	263.4	9.0	43.5
AP26	6	L	259.1	265.7	10.0	39.5
AP229	6	T	249.4	264.7	7.0	35.7
AP230	6	T	255.3	265.3	6.5	36.7
AP27	12	L	265.4	271.5	8.0	37.6
AP28	12	L	264.5	272.5	8.0	37.7
AP231	12	T	264.9	272.0	8.0	32.8
AP232	12	T	261.9	270.7	8.0	29.8

HEAT-B PLATE

PXT	as Rec'd.	T	113.9	163.2	13.0	63.3
PXL	as Rec'd.	L	113.9	160.5	13.5	63.0
P21	1	L	245.9	257.2	8.5	42.4
P22	1	L	242.0	254.9	9.5	41.4
P225	1	T	247.2	259.0	8.0	38.4
P226	1	T	244.9	258.7	8.0	38.4
P23	3	L	257.7	269.2	7.5	39.4
P24	3	L	257.2	268.2	8.0	39.3
P227	3	T	261.5	276.8	5.0	28.5
P228	3	T	263.1	274.7	7.5	29.4
P25	6	L	268.5	277.7	6.0	38.9
P26	6	L	267.2	277.7	5.5	37.4
P229	6	T	273.4	283.9	5.5	25.2
P230	6	T	275.3	285.3	5.0	26.5
P27	12	L	283.1	290.9	7.0	37.2
P28	12	L	278.8	287.5	5.0	35.3
P231	12	T	279.5	294.4	5.5	24.7
P232	12	T	286.3	295.4	5.0	29.6

NOTES:

1. L = Longitudinal; T = Transverse
2. All results obtained with 0.505" diameter specimens

APPENDIX V

PLATE FRACTURE TOUGHNESS DATA 48-IN. AND 24-IN. PTC COUPONS

APPENDIX V
PLANE STRAIN FRACTURE TOUGHNESS DATA
48" x 4" x 3/4" SPECIMENS

HEAT-1 PLATE

SPEC. NO.	AGING TIME 900°F (HRS.)	CRACK LENGTH (IN.)	CRACK DEPTH (IN.)	GROSS FRACTURE STRENGTH (KSI)	NET FRACTURE STRENGTH (KSI)	KIC (KSI √IN.)	0.2% OFFSET YIELD (KSI)
I-13	3	Control		265.8	---	---	260.0
I-11	3	0.125	0.062	264.8	265.8	---	---
I-18	3	0.240	0.110	260.3	262.1	116.8	---
I-9	3	0.300	0.120	247.2	249.7	123.3	---
I-8	3	0.380	0.150	206.6	209.8	114.0	----
I-2	3	0.435	0.165	198.5	202.6	116.6	----
I-12	3	0.490	0.180	183.1	187.7	113.2	----
I-7	3	0.560	0.190	168.1	173.3	109.6	----
I-10	3	0.606	0.205	155.2	160.9	104.9	----
I-17	3	0.730	0.240	147.9	155.9	109.0	----
I-14	3	1.000	0.290	119.4	131.2	100.2	----
I-15	12	Control		273.0	----	----	268.0
I-6	12	0.102	0.059	273.3	273.7	----	----
I-16	12	0.165	0.079	271.5	272.4	101.1	----
I-4	12	0.363	0.153	191.2	194.0	102.8	----
I-3	12	0.655	0.199	139.1	144.6	95.7	----
I-5	12	0.849	0.235	122.9	130.5	94.0	----
I-1	12	0.883	0.285	113.0	121.6	90.5	----

NOTES:

1. All specimens are longitudinal
2. Blank in Kic column indicates non-applicable value
3. Gross fracture stress = failing load divided by gross area
4. Net fracture stress = failing load divided by gross area minus crack area

APPENDIX V (Cont'd)

PLANE STRAIN FRACTURE TOUGHNESS DATA

24" x 3" x 3/4" SPECIMENS

HEAT-A PLATE

SPEC. NO.	ORIENTATION AND AGING TIME AT 900°F (HRS)	CRACK LENGTH (IN.)	CRACK DEPTH (IN.)	GROSS FRACTURE STRESS, (KSI)	NET- FRACTURE STRESS, (KSI)	K _{IC} (KSI $\sqrt{\text{IN.}}$)	APPLICABLE 0.2% OFFSET YIELD (KSI)
AP4-1	L-3	0.224	0.104	263.3	265.4	----	254.8
AP4-2	L-3	0.296	0.131	251.5	254.9	125.3	254.8
AP4-3	L-3	0.383	0.173	200.1	204.8	111.2	254.8
AP4-4	T-3	0.246	0.111	243.8	246.1	110.3	254.8
AP4-5	T-3	0.306	0.130	225.1	228.6	112.9	254.8
AP4-6	T-3	0.377	0.152	180.8	184.6	98.7	254.8

NOTES:

1. L = Longitudinal; T = Transverse
2. Specimens aged 3 Hours at 900°F.
3. Blank in K_{IC} column indicates non applicable value
4. Gross fracture stress = failing load divided by uncracked gage area
5. Net-Fracture stress = failing load divided by uncracked gage area minus area of crack.

APPENDIX V (Cont'd.)

PLANE STRAIN FRACTURE TOUGHNESS DATA

24" x 3" x 3/4" SPECIMENS

HEAT B PLATE

SPEC. NO.	ORIENTA-TION	AGING TEMP. AND TIME °F, HRS)	CRACK LENGTH (IN.)	CRACK DEPTH (IN.)	GROSS FRACTURE STRESS (KSI)	NET FRACTURE STRESS (KSI)	K _{IC} (KSI √IN.)	APPLICABLE 0.2% YIELD STRESS (KSI)
P117	L	875 - 12	0.423	0.157	165.0	169.2	93.9	
P121	L	875 - 12	0.110	0.048	291.5	293.1	----	
P114	L	875 - 12	0.212	0.087	230.7	232.3	95.6	
P124	L	875 - 12	0.300	0.113	198.3	201.0	96.1	
P115	L	875 - 12	0.256	0.106	219.4	221.9	99.6	
P120	L	875 - 12	0.149	0.065	283.0	283.9	----	
P116	L	875 - 12	Control	----	290.2	----	----	274.5
P44	T	875 - 12	0.212	0.085	212.2	231.6	87.3	
P17	T	875 - 12	0.106	0.050	291.8	292.3	----	
P14	T	875 - 12	0.290	0.113	176.2	178.3	83.7	
P113	T	875 - 12	0.145	0.064	261.7	262.5	90.9	
P112	T	875 - 12	0.368	0.135	173.9	177.0	92.4	
P18	T	875 - 12	0.231	0.091	200.8	202.3	85.8	
P46	T	875 - 12	Control	----	294.6	----	----	272.5
P119	L	900 - 3	0.109	0.051	280.3	280.8	84.7	
P122	L	900 - 3	0.336	0.136	207.4	210.9	107.3	
P125	L	900 - 3	0.300	0.121	203.2	205.8	99.2	
P41	L	900 - 3	0.254	0.107	229.2	231.4	104.0	
P42	L	900 - 3	0.491	0.176	154.5	159.4	94.2	
P126	L	900 - 3	Control	----	282.0	----	----	280.3
P13	T	900 - 3	0.110	0.050	285.4	286.0	86.8	
P15	T	900 - 3	0.241	0.100	205.8	207.6	90.2	
P16	T	900 - 3	0.299	0.118	185.3	187.6	89.7	
P19	T	900 - 3	0.383	0.140	169.8	173.1	92.1	
P110	T	900 - 3	0.494	0.170	143.6	148.0	87.3	
31W1	T	900*- 3	0.150	0.070	272.7	273.6	96.4	
31W4	T	900*- 3	0.202	0.085	267.9	268.6	109.3	
P11	T	900 - 3	Control	----	288.7	----	----	282.5
P43	L	900 - 12	0.109	0.051	292.4	292.9	89.0	
P51	L	900 - 12	0.250	0.104	196.2	198.0	87.5	
P118	L	900 - 12	0.302	0.117	185.4	187.7	90.1	
P52	L	900 - 12	0.378	0.141	173.6	177.0	93.9	
P53	L	900 - 12	0.493	0.171	150.3	155.0	91.5	
P123	L	900 - 12	Control	----	284.3	----	----	277.6
P111	T	900 - 12	0.113	0.050	289.9	290.4	89.3	
P55	T	900 - 12	0.239	0.098	192.1	193.7	83.4	
P12	T	900 - 12	0.290	0.114	173.2	175.3	82.2	
31W2	T	900 - 12	0.379	0.127	174.7	177.8	93.3	
31W3	T	900 - 12	0.491	0.172	159.7	164.8	97.3	
31W6	T	900*- 12	Multiple Surface Cracks		211.0	----	----	
31W7	T	900*- 12	Multiple Surface Cracks		221.0	----	----	
P45	T	900 - 12	Control	----	294.8	----	----	288.6

NOTES:

1. L = Longitudinal; T = Transverse
2. Gross Fracture Stress = Failing Load divided by gross area
3. Net Fracture Stress = Failing Load divided by gross area minus crack area
4. * Aged at 910°F
5. Blank in K_{IC} column indicates non applicable value

APPENDIX VI

PLATE FRACTURE TOUGHNESS DATA 3-IN PTC COUPONS

APPENDIX VI

PLANE STRAIN FRACTURE TOUGHNESS DATA

8" x 11/16" x 5/16" SPECIMENS

HEAT-B PLATE

SPEC. NO.	ORIENTATION AND AGING TIME AT 900°F (HRS)	CRACK LENGTH (IN.)	CRACK DEPTH (IN.)	GROSS FRACTURE STRESS (KSI)	NET FRACTURE STRESS (KSI)	GROSS K_{IC} (KSI $\sqrt{IN.}$)	NET K_{IC} (KSI $\sqrt{IN.}$)	APPLICABLE 0.2% YIELD STRENGTH (KSI)
P61	L-3	0.122	0.058	253.5	265.5	82.4	84.9	265.9
P62	L-3	0.207	0.086	210.7	226.1	86.0	92.8	265.9
P63	L-3	0.285	0.105	163.3	184.9	76.5	87.2	265.9
P64	L-3	0.354	0.125	129.9	157.3	66.9	81.6	265.9
P65	L-3	0.443	0.150	107.8	146.2	61.5	84.2	265.9
P66	L-3	0.450	0.151	106.0	145.0	60.9	84.0	265.9
P67	L-12	0.120	0.055	256.6	263.0	80.9	83.1	276.4
P68	L-12	0.207	0.090	170.1	182.9	68.6	74.0	276.4
P69	L-12	0.295	0.107	142.4	162.7	67.3	77.3	276.4
P610	L-12	0.351	0.119	117.4	140.7	59.7	71.9	276.4
P611	L-12	0.454	0.148	94.9	129.6	54.4	74.7	276.4
P612	L-12	0.457	0.146	102.3	139.5	58.7	80.9	276.4
P613	T-3	0.120	0.055	247.2	253.4	77.7	79.8	273.6
P614	T-3	0.215	0.083	190.1	204.1	78.1	84.2	273.6
P615	T-3	0.430	0.130	93.9	121.0	51.7	67.0	273.6
P616	T-3	0.347	0.117	122.4	145.8	61.9	74.2	273.6
P617	T-3	0.458	0.142	101.6	137.5	58.1	79.2	273.6
P618	T-3	0.248	0.101	150.7	169.8	69.9	79.1	273.6
P619	T-12	0.121	0.053	231.6	237.4	72.9	74.9	264.1
P620	T-12	0.210	0.083	172.7	185.1	70.0	75.3	264.1
P621	T-12	0.270	0.103	141.1	158.3	64.2	72.3	264.1
P622	T-12	0.355	0.121	107.5	129.5	54.9	66.5	264.1
P623	T-12	0.445	0.140	97.3	130.7	54.9	74.3	264.1
P624	T-12	0.446	0.143	92.0	123.4	52.2	70.3	264.1
P6P1	SL-3	0.185	0.076	246.6	259.3	96.0	101.6	269.2
P6P2	SL-3	Control		273.5	----	----	----	269.2
P6P3	SL-3	0.134	0.054	273.7	280.5	91.6	94.3	269.2
P6P4	SL-3	*	*	273.7	NA	NA	----	269.2
P6P5	SL-3	0.325	0.119	159.8	185.6	79.5	93.0	269.2
P6P6	SL-3	0.463	0.147	126.0	167.1	72.7	97.3	269.2

NOTES:

1. All results obtained with 5/16" x 11/16" x 8" slab specimens
2. L = Longitudinal; T = Transverse; S = surface type specimen
3. Gross Fracture Stress = Failing load divided by gross area
4. Net Fracture Stress = Failing load divided by gross area minus crack area
5. 3 Hours specimens inadvertently aged at 915°F
6. * Failed away from crack

APPENDIX VII

WELDMENT TENSILE DATA W9 WELDS

APPENDIX VII - WELDMENT TENSILE DATA, SUMMARY

TYPE W9 WELDS IN HEAT-B PLATE

SPEC. NO.	CONDITION OF PLATE PRIOR TO WELDING	ORIENTATION	AGING TEMP., (°F)	AGING TIME (HRS)	0.2% YIELD STRENGTH (KSI)	ULTIMATE STRENGTH (KSI)	% ELONG (1" or 2" GAGE)	% RED IN AREA	REMARKS
2IAA1	As Rec'd.	L-AWM	875	1.5	223.5	240.6	8.0	22.3	
2IBB1	As Rec'd.	L-AWM	875	3.0	231.0	247.3	6.0	16.8	
2ICC1	As Rec'd.	L-AWM	875	6.0	250.7	256.3	1.0	2.5	G
2IDD1	As Rec'd.	L-AWM	875	12.0	255.1	268.0	1.0	4.1	G
2IGG1	Aged	L-AWM	875	1.5	217.6	234.5	8.5	29.6	H
2IHH1	Aged	L-AWM	875	3.0	224.4	239.7	6.0	22.8	H
2IJJ1	Aged	L-AWM	875	6.0	254.5	263.3	1.0	3.1	G
2IKK1	Aged	L-AWM	875	12.0	260.8	276.2	2.0	3.2	G
2IAA2	As Rec'd.	T	875	1.5	222.8	243.0	6.0	23.8	B,C
2IBB2	As Rec'd.	T	875	3.0	236.1	246.4	BOGM	37.3	B,C
2ICC2	As Rec'd.	T	875	6.0	235.3	250.3	4.5	30.0	B,C
2IDD2	As Rec'd.	T	875	12.0	251.7	256.1	2.0	39.3	B,C
2IGG2	Aged	T	875	1.5	223.9	242.0	1.0	3.2	A,F
2IHH2	Aged	T	875	3.0	232.4	247.2	7.0	47.0	B,C
2IJJ2	Aged	T	875	6.0	248.2	259.4	6.5	37.0	B,C
2IGG6	Aged	T	875	12.0	242.0	251.3	BOGM	26.2	B,C
2IAA3	As Rec'd.	L-AWM	900	1.5	232.4	247.7	1.0	5.5	G,H
2IBB3	As Rec'd.	L-AWM	900	3.0	240.8	258.7	4.5	18.3	G,H
2ICC3	As Rec'd.	L-AWM	900	6.0	257.4	257.4	1.0	6.3	G
2IDD3	As Rec'd.	L-AWM	900	12.0	NA	249.3	BOGM	1.6	H
2IGG3	Aged	L-AWM	900	1.5	225.7	241.1	6.0	24.6	
2IHH3	Aged	L-AWM	900	3.0	240.1	249.3	1.0	1.6	G
2IJJ3	Aged	L-AWM	900	6.0	261.7	274.1	3.0	6.3	G
2IKK3	Aged	L-AWM	900	12.0	261.8	275.6	1.0	3.3	G
2IAA4	As Rec'd.	T	900	1.5	224.2	242.5	4.5	27.7	B
2IBB4	As Rec'd.	T	900	3.0	235.0	244.9	BOGM	34.7	B,C
2ICC4	As Rec'd.	T	900	6.0	235.2	246.7	4.5	32.8	B
2IDD4	As Rec'd.	T	900	12.0	236.4	246.4	4.5	27.1	B,H
2IGG4	Aged	T	900	1.5	226.4	242.8	5.0	31.9	B,H
2IHH4	Aged	T	900	3.0	229.0	244.6	4.0	40.8	B
2IJJ4	Aged	T	900	6.0	246.2	225.1	6.0	41.4	B
2IJJ6	Aged	T	900	12.0	NA	213.3	0.5	3.2	A,K
2IAA5	As Rec'd.	L-AWM	950	1.5	268.7	274.7	4.0	6.3	G
2IBB5	As Rec'd.	L-AWM	950	3.0	268.1	282.4	2.0	9.7	G
2ICC5	As Rec'd.	L-AWM	950	6.0	NA	265.6	1.0	3.1	G
2IDD5	As Rec'd.	L-AWM	950	12.0	265.3	276.0	1.0	0.8	G
2IGG5	Aged	L-AWM	950	1.5	253.9	268.6	4.0	14.1	H
2IHH5	Aged	L-AWM	950	3.0	262.2	273.5	1.0	2.3	G
2IJJ5	Aged	L-AWM	950	6.0	254.6	273.5	3.0	10.9	G
2IKK5	Aged	L-AWM	950	12.0	266.5	269.8	1.0	3.3	G
2IAA6	As Rec'd.	T	950	1.5	232.3	249.2	3.0	26.5	B
2IBB6	As Rec'd.	T	950	3.0	NA	221.1	0	1.9	A,E
2ICC6	As Rec'd.	T	950	6.0	238.5	245.7	3.0	13.2	B,K
2IDD6	As Rec'd.	T	950	12.0	221.6	233.8	5.5	38.8	B
2IKK2	Aged.	T	950	1.5	NA	230.0	3.0	24.3	B,K
2IHH6	Aged	T	950	3.0	244.3	253.1	3.5	38.1	B
2IKK4	Aged	T	950	6.0	239.5	247.4	3.0	13.1	B
2IKK6	Aged	T	950	12.0	NA	182.3	0	0.4	A,G
7B2	As Rec'd.	T	As Welded		131.0	152.7	2.0	14.0	A
7B1	As Rec'd.	T	As Welded		132.0	150.1	2.0	13.6	A
4A31	As Rec'd.	L-AWM	As Welded		141.8	151.9	6.0	52.1	

NOTES:

1. L-AWM - Longitudinal all-weldmetal specimen; 0.250-in. diam., 1-in. gage.
2. T - Transverse across-the-joint specimen; 0.505-in. diam., 2-in. gage.
3. See Table XIII for definition of Remark codes.
4. BOGM - Broke outside gage mark
5. NA - not available
6. Plates aged prior to welding were aged at 900°F for 3 hours.

APPENDIX VIII

WELDMENT TENSILE DATA W7 AND W8 WELDS

APPENDIX VIII - WELDMENT TENSILE DATA SUMMARY

TYPE-W7 WELDS IN HEAT-TREAT

SPEC. NO.	AGING TEMP., (°F)	AGING TIME (HOURS)	ORIENTATION AND TYPE	0.2% YIELD STRENGTH (KSI)	ULTIMATE STRENGTH (KSI)	% ELONG (1" OR 2" GAGE)	% RED IN AREA	REMARKS
7A2	875	1.5	L-AWM	215.2	237.4	9.0	32.7	
7A6	875	3.0	L-AWM	220.9	238.7	8.5	38.1	
7A7	875	6.0	L-AWM	236.4	253.5	7.5	26.1	
7C10	875	12.0	L-AWM	249.5	264.7	6.5	32.7	
7A3	900	1.5	L-AWM	225.1	239.3	9.0	36.0	
7A5	900	3.0	L-AWM	230.5	247.8	8.5	37.7	
7A9	900	6.0	L-AWM	242.4	260.1	5.5	25.3	
7C11	900	12.0	L-AWM	251.5	266.7	3.0	11.7	
4A32	900	12.0	L-AWM	266.4	272.3	7.0	29.0	
7A1	950	1.5	L-AWM	236.6	254.5	8.5	37.6	
7A4	950	3.0	L-AWM	249.5	265.4	7.0	30.7	
7A8	950	6.0	L-AWM	251.5	267.2	5.0	19.0	
7C12	950	12.0	L-AWM	252.6	269.4	6.0	30.1	
7A15	900	3.0	T	246.7	256.4	2.0	10.1	D
7A19	900	6.0	T	254.4	268.4	4.0	16.0	D
7A23	900	12.0	T	259.2	271.8	4.0	25.4	B
7A13	950	3.0	T	256.0	266.0	4.5	26.8	B
7A17	950	6.0	T	252.1	263.6	3.5	35.2	B
7A21	950	12.0	T	249.5	260.5	4.5	28.5	B

NOTES:

1. L-AWM - Longitudinal all weldmetal specimen (0.250-in. diam.); 1-in. gage.
2. T = Transverse across-the-joint specimen (0.505-in diam.); 2-in. gage
3. For definition of remark codes see Table XIII.

APPENDIX VIII (Cont'd.), WELDMENT TENSILE DATA SUMMARY

TYPE - W8 WELDS IN HEAT-B PLATE

SPEC. NO.	CONDITION OF PLATE PRIOR TO WELDING	AGING TEMP. (°F)	AGING TIME (HRS)	ORIENTATION AND TYPE	0.2% YIELD STRENGTH (KSI)	ULTIMATE STRENGTH (KSI)	% ELONG. (1" or 2" GAGE)	% RED IN AREA	REMARKS
211A1	As Rec'd.	875	1.0	L-AWM	206.0	224.0	6.0	26.5	
211B1	As Rec'd.	875	2.5	L-AWM	220.0	236.0	4.0	10.1	
211C1A	As Rec'd.	875	5.5	L-AWM	248.0	260.0	3.0	12.4	
211C1B	As Rec'd.	875	5.5	L-AWM	241.0	256.0	7.0	31.1	
211D1	As Rec'd.	875	11.5	L-AWM	262.0	274.0	4.0	20.3	
211G1	Aged	875	1.0	L-AWM	190.0	212.0	7.0	25.9	
211H1	Aged	875	2.5	L-AWM	200.0	230.0	4.0	27.2	
211J1	Aged	875	5.5	L-AWM	248.0	260.0	7.0	29.2	
211K1	Aged	875	11.5	L-AWM	252.0	266.0	5.0	17.9	
211A2	As Rec'd.	875	1.0	T	203.0	225.0	8.0	33.3	B
211B2	As Rec'd.	875	2.5	T	206.0	221.0	7.0	36.6	B
211C2	As Rec'd.	875	5.5	T	219.0	237.0	5.0	28.2	B
211D2	As Rec'd.	875	11.5	T	224.0	243.0	5.0	28.8	B
211G2	Aged	875	1.0	T	208.0	220.0	7.0	36.3	A
211H2	Aged	875	2.5	T	216.0	227.0	8.0	38.5	B
211J2	Aged	875	5.5	T	234.0	243.5	4.0	20.6	C
211K2	Aged	875	11.5	T	236.0	244.5	3.0	16.3	C
211A3	As Rec'd.	900	1.0	L-AWM	234.0	248.0	8.0	37.0	
211B3A	As Rec'd.	900	2.5	L-AWM	261.0	265.0	4.0	7.9	
211B3B	As Rec'd.	900	2.5	L-AWM	234.0	222.0	5.0	20.2	
211C3	As Rec'd.	900	5.5	L-AWM	254.0	266.0	6.0	35.8	
211D3	As Rec'd.	900	11.5	L-AWM	255.0	276.0	5.0	18.5	
211G3	Aged	900	1.0	L-AWM	230.0	238.0	7.0	34.5	
211H3	Aged	900	2.5	L-AWM	230.0	246.0	7.0	33.9	
211J3	Aged	900	5.5	L-AWM	252.0	264.0	5.0	31.3	
211K3	Aged	900	11.5	L-AWM	264.0	274.0	5.0	27.9	
211A4A	As Rec'd.	900	1.0	T	220.0	235.0	5.0	27.0	B
211A4B	As Rec'd.	900	1.0	T	218.0	237.0	5.0	25.0	B
211B4	As Rec'd.	900	2.5	T	207.0	222.0	5.0	20.2	B
211C4	As Rec'd.	900	5.5	T	222.5	241.0	4.0	22.3	B
211D4	As Rec'd.	900	11.5	T	227.0	242.0	5.0	28.2	B
211G4	Aged	900	1.0	T	225.0	236.0	10.0	40.7	C
211H4	Aged	900	2.5	T	222.0	234.0	6.0	31.5	B
211J4	Aged	900	5.5	T	234.0	245.5	4.0	23.7	B
211K4	Aged	900	11.5	T	236.0	243.5	3.0	14.1	C
211A5	As Rec'd.	950	1.0	L-AWM	252.0	267.0	6.0	31.0	
211B5	As Rec'd.	950	2.5	L-AWM	232.0	256.0	5.0	26.6	
211C5	As Rec'd.	950	5.5	L-AWM	262.0	276.0	4.0	23.6	
211D5	As Rec'd.	950	11.5	L-AWM	250.0	262.0	3.0	16.7	
211G5	Aged	950	1.0	L-AWM	230.0	248.0	7.0	36.4	
211H5	Aged	950	2.5	L-AWM	250.0	262.0	3.0	13.6	
211J5	Aged	950	5.5	L-AWM	252.0	270.0	5.0	14.5	
211K5	Aged	950	11.5	L-AWM	244.0	264.0	5.0	17.5	
211A6	As Rec'd.	950	1.0	T	225.0	237.0	4.0	18.4	C
211B6	As Rec'd.	950	2.5	T	219.0	236.0	4.0	17.8	B
211C6	As Rec'd.	950	5.5	T	217.0	234.0	6.0	30.0	D
211D6	As Rec'd.	950	11.5	T	215.0	230.5	7.0	37.9	D
211G6	Aged	950	1.0	T	233.0	243.0	5.0	22.1	C
211H6	Aged	950	2.5	T	223.0	236.0	5.0	23.4	C
211J6	Aged	950	5.5	T	222.0	234.5	5.0	28.5	D
211K6	Aged	950	11.5	T	217.5	228.0	2.0	11.5	C

NOTES:

1. L-AWM - Longitudinal all weldmetal specimen; 0.250-in. diam, 1-in. gage.
2. T - transverse across-the-joint specimen; 0.505-in. diam, 2-in. gage.
3. See Table XIII for definition of Remark codes
4. Plates aged prior to welding were aged at 900°F for 3 hours.

APPENDIX IX

WELDMETAL FRACTURE TOUGHNESS DATA

APPENDIX IX - DATA SUMMARY HEAT 1 PLATE WELDS - FRACTURE TOUGHNESS

Spec. No.	Aging Time (Hours)	Aging Temp. (°F)	Crack Length (Inches)	Crack Depth (Inches)	Gross Fracture Stress (KSI)	Net Fracture Stress (KSI)	Gross K_{Ic} (KSI in)	Net K_{Ic} (KSI/in)	Applicable 0.2% Yield Stress (KSI)	Weld Type
24" x 3" x 3/4" Welds										
1A-1	3.0	900	0.041	0.019	266.3	266.4	NA	NA	238.0	W2
1A-2	3.0	900	Control		246.0	246.0	NA	NA		W2
1A-3	3.0	900	0.265	0.118	107.7	108.8	42.5	NA		W2
1A-4	3.0	900	0.220	0.105	112.3	113.1	46.5	NA		W2
1A-5	3.0	900	0.147	0.065	147.3	147.7	50.1	NA		W2
1A-6	3.0	900	0.064	0.035	250.0	250.1	NA	NA		W2
8" x 1/2" x 1/8"										
1A2-2	3.0	900	0.081	0.035	233.8	242.6	60.8	63.4	237.0	
(1A6-2)	3.0	900	0.050*	---	256.7	---	NA	NA		W2
(1A2-3)	3.0	900	0.050*	---	252.6	---	NA	NA		W2
1A6-3	3.0	900	0.085	0.035	229.1	238.1	NA	NA		W2
1A2-4	3.0	900	0.134	0.050	177.3	193.8	57.6	63.4	237.0	W2
(1A6-4)	3.0	900	0.134	0.045	209.3	228.3	67.9	74.8	237.0	W2
1A2-10	3.0	900	0.219	0.063	165.9	205.5	66.2	83.7	237.0	W2
(1A6-10)	3.0	900	0.214	0.063	124.0	153.2	48.3	60.3	237.0	W2
1A2-1	3.0	900	0.135	0.049	184.1	202.7				W2
(1A2-3)	3.0	900	0.137	0.053	170.0	187.8				W2
(1A2-4)	3.0	900	0.217	0.063	110.7	138.2				W2
5-3-B	3.0	900	Control		241.7	---	NA	NA		W3
5-3-H	3.0	900	0.030*	---	243.5	---	NA	NA		W3
5-3-D	3.0	900	0.030*	---	243.4	---	NA	NA		W3
5-3-E	3.0	900	0.104	0.060	199.4	217.6				W3
5-3-F	3.0	900	0.123	0.048	211.9	229.1				W3
5-3-G	3.0	900	0.147	0.057	205.2	229.7				W3
5-16-3	3.0	900	0.122	0.045	226.0	244.4				W4
5-16-4	3.0	900	0.095	0.037	240.3	252.2				W4
5-16-5	3.0	900	0.104	0.046	238.7	254.8				W4
5-16-6	3.0	900	0.115	0.046	224.1	241.3				W4
5-16-7	3.0	900	0.152	0.055	176.2	199.1				W4
5-80	12.0	900	Control		250.8	---	NA	NA		W1
5-80-A	12.0	900	0.180	0.057	149.6	172.3				W1
5-80-B	12.0	900	0.187	0.059	141.9	165.1				W1
1A2-5	12.0	900	Control		269.8	---	NA	NA		W2
1A6-5	12.0	900	Control		247.3	---	NA	NA		W2
1A2-6	12.0	900	0.050*	---	247.1	---	NA	NA		W2
(1A6-6)	12.0	900	0.050*	---	268.7	---	NA	NA		W2
(1A2-7)	12.0	900	0.080	0.032	207.0	213.0				W2
1A6-7	12.0	900	0.070	0.032	238.2	244.9				W2
1A2-8	12.0	900	0.132	0.045	168.8	183.1				W2
(1A6-8)	12.0	900	0.139	0.045	131.5	143.8				W2
(1A2-9)	12.0	900	0.214	0.059	108.7	132.4				W2
1A6-9	12.0	900	0.190	0.060	113.8	134.7				W2
(1A6-11)	12.0	900	0.202	0.059	110.5	131.7				W2
5-1-1	12.0	900	Control		237.2	---	NA	NA		W6
5-1-2	12.0	900	0.030	0.015	239.1	240.5				W6
5-1-3	12.0	900	0.080	0.036	204.5	212.3				W6
5-1-4	12.0	900	0.230	0.070	105.3	134.4				W6
5-1-5	12.0	900	0.125	0.046	161.5	174.6				W6
5-1-6	12.0	900	0.203	0.062	119.6	143.9				W6

NOTES:

- Specimen numbers in parenthesis indicate a resolution heat treat (1500°F 1 hr.) before aging.
- * Did not fail at crack.
- NA not applicable
- Blank in K_{Ic} columns indicate that K_{Ic} was not determined.
- See Table XI for definition of weld type.
- Gross fracture stress = failing load divided by gross area.
- Net fracture stress = failing load divided by gross area minus crack area.

APPENDIX IX (Cont'd.), EFFECT OF AGING TIME AND TEMPERATURE ON FRACTURE TOUGHNESS

PROPERTIES OF TYPE W7 AND W8 WELDMETAL - TRANSVERSE THICKNESS TYPE

8" x 11/16" x 5/16"

SPEC. NO.	AGING TIME (HOURS)	AGING TEMP. (°F)	CRACK LENGTH (INCHES)	CRACK DEPTH (INCHES)	GROSS FRACTURE STRESS (KSI)	NET FRACTURE STRESS (KSI)	GROSS KIC (KSI $\sqrt{\text{IN}}$)	NET KIC (KSI $\sqrt{\text{IN}}$)	APPLICABLE 0.2% YIELD STRENGTH (KSI)	WELD TYPE
214D1	1.5	875	0.050*	---	239.1	---	---	---	204.0	W8
214E1	1.5	875	0.137	0.065	196.4	202.9	66.2	68.7	204.0	W8
214F1	1.5	875	0.252	0.095	152.8	167.6	67.9	75.5	204.0	W8
4J9	1.5	875	0.194	0.083	153.5	163.0	60.4	64.4	204.0	W7
2A9	1.5	875	0.142	0.064	178.5	184.5	60.8	63.0	204.0	W7
4F3	1.5	875	0.050*	---	239.1	---	---	---	204.0	W7
214H1	3.0	875	0.062	0.029	240.5	242.1	---	---	214.0	W8
214J1	3.0	875	0.122	0.053	198.3	203.2	62.9	64.7	214.0	W8
214D2	3.0	875	0.247	0.091	142.6	155.5	61.7	68.7	214.0	W8
4J1	3.0	875	0.065	0.031	253.2	255.0	---	---	214.0	W7
2A1	3.0	875	0.119	0.053	201.0	205.6	63.1	64.7	214.0	W7
4H1	3.0	875	0.295	0.110	113.2	128.1	53.5	60.9	214.0	W7
214F2	6.0	875	0.050*	---	250.2	---	---	---	242.0	W8
214G2	6.0	875	0.134	0.063	151.6	156.6	49.4	51.1	242.0	W8
214H2	6.0	875	0.289	0.114	102.7	117.4	48.1	54.8	242.0	W8
4J2	6.0	875	0.108	0.049	190.9	194.6	56.5	57.7	242.0	W7
2A2	6.0	875	0.175	0.076	146.3	153.7	54.3	57.2	242.0	W7
4H2	6.0	875	0.050*	---	257.4	---	---	---	242.0	W7
214D3	12.0	875	0.050*	---	256.2	---	---	---	255.0	W8
214E3	12.0	875	0.124	0.051	185.4	189.8	58.3	60.1	255.0	W8
214F3	12.0	875	0.188	0.078	128.2	135.6	49.0	52.0	255.0	W8
4J11	12.0	875	0.106	0.048	205.4	209.2	60.6	61.8	255.0	W7
2A11	12.0	875	0.111	0.048	198.7	202.6	59.8	61.1	255.0	W7
4F5	12.0	875	0.280	0.101	111.6	124.2	51.1	57.0	255.0	W7
214H3	1.5	900	0.058	0.026	239.5	240.9	---	---	230.0	W8
214J3	1.5	900	0.159	0.064	185.2	193.1	66.0	69.0	230.0	W8
214D4	1.5	900	0.289	0.100	120.7	135.0	55.8	62.7	230.0	W8
4J3	1.5	900	0.106	0.054	196.0	200.1	59.5	60.9	230.0	W7
2A3	1.5	900	0.204	0.082	190.0	202.2	76.8	82.0	230.0	W7
4H3	1.5	900	0.050*	---	244.8	---	---	---	230.0	W7
214F4	3.0	900	0.050*	---	251.5	---	---	---	232.0	W8
214G4	3.0	900	0.115	0.044	192.1	195.8	58.0	59.2	232.0	W8
214H4	3.0	900	0.224	0.088	136.6	147.1	56.7	61.2	232.0	W8
4J4	3.0	900	0.052*	---	256.5	---	---	---	232.0	W7
2A4	3.0	900	0.119	0.055	203.1	208.0	63.1	64.8	232.0	W7
4H4	3.0	900	0.220	0.079	161.0	171.6	66.0	70.6	232.0	W7
214D5	6.0	900	0.050*	---	251.3	---	---	---	249.0	W8
214E5	6.0	900	0.120	0.057	178.4	182.9	55.2	56.7	249.0	W8
214F5	6.0	900	0.248	0.098	121.7	133.5	53.0	58.6	249.0	W8
4J12	6.0	900	0.110	0.048	227.6	232.0	68.4	69.9	249.0	W7
2A12	6.0	900	0.210	0.080	139.5	148.5	55.9	59.6	249.0	W7
4F6	6.0	900	0.053*	---	259.2	---	---	---	249.0	W7
214H5	12.0	900	0.050*	---	253.4	---	---	---	259.0	W8
214J5	12.0	900	0.115	0.050	178.2	182.1	53.8	55.1	259.0	W8
214D6	12.0	900	0.207	0.080	136.3	145.6	54.2	58.3	259.0	W8
4J5	12.0	900	0.050*	---	262.8	---	---	---	259.0	W7
2A5	12.0	900	0.118	0.047	179.5	183.2	54.9	55.9	259.0	W7
4H5	12.0	900	0.230	0.079	120.4	128.8	49.5	53.1	259.0	W7
214F6	1.5	950	0.050*	---	247.1	---	---	---	240.0	W8
214G6	1.5	950	0.132	0.056	182.7	187.7	59.3	61.0	240.0	W8
214H6	1.5	950	0.262	0.097	123.2	136.3	54.8	60.8	240.0	W8
4J6	1.5	950	0.107	0.046	216.5	220.4	64.0	65.2	240.0	W7
2A6	1.5	950	0.215	0.077	139.8	148.7	56.3	60.0	240.0	W7
4H6	1.5	950	0.052*	---	251.8	---	---	---	240.0	W7
214D7	3.0	950	0.050*	---	248.9	---	---	---	244.0	W8
214E7	3.0	950	0.112	0.049	199.1	203.2	59.8	61.1	244.0	W8
214F7	3.0	950	0.200	0.082	127.3	135.4	50.1	53.4	244.0	W8
4J10	3.0	950	0.050*	---	259.1	---	---	---	244.0	W7
2A10	3.0	950	0.111	0.048	215.2	219.4	64.0	66.0	244.0	W7
4F4	3.0	950	0.295	0.105	104.4	117.5	48.7	52.1	244.0	W7

APPENDIX IV (Cont'd.), EFFECT OF AGING TIME AND TEMPERATURE ON FRACTURE TOUGHNESS

PROPERTIES OF TYPE W7 AND W8 WELDMETAL - TRANSVERSE THICKNESS TYPE

8" x 11/16" x 5/16" (Cont'd.)

SPEC. NO.	AGING TIME (HOURS)	AGING TEMP. (°F)	CRACK LENGTH (INCHES)	CRACK DEPTH (INCHES)	GROSS FRACTURE STRESS (KSI)	NET FRACTURE STRESS (KSI)	GROSS KIC (KSI $\sqrt{\text{IN}}$)	NET KIC (KSI $\sqrt{\text{IN}}$)	APPLICABLE		WELD TYPE
									0.2% YIELD STRENGTH (KSI)		
214H7	6.0	950	0.050*	---	247.9	---	---	---	255.0		W8
214J7	6.0	950	0.124	0.050	220.8	226.0	70.1	71.9	255.0		W8
214D8	6.0	950	0.251	0.091	130.5	142.5	56.7	62.1	255.0		W8
4J7	6.0	950	0.194	0.074	131.5	138.6	50.5	50.5	255.0		W7
2A7	6.0	950	0.108	0.045	217.3	221.2	64.4	65.7	255.0		W7
4F1	6.0	950	0.050*	---	254.8	---	---	---	255.0		W7
214F8	12.0	950	0.050*	---	241.8	---	---	---	249.0		W8
214G8	12.0	950	0.115	0.050	194.3	198.5	59.1	60.5	249.0		W8
214H8	12.0	950	0.199	0.081	126.9	134.8	49.7	53.0	249.0		W8
4J8	12.0	950	0.050*	---	254.9	---	---	---	249.0		W7
2A8	12.0	950	0.113	0.048	179.1	182.7	53.7	54.8	249.0		W7
4F2	12.0	950	0.286	0.103	110.9	124.1	51.2	57.4	249.0		W7

NOTES:

1. * Did not fail at crack
2. Dash indicates non-applicable value
3. See Table for definition of weld types.
4. Gross fracture stress = Failing load divided by gross area.
5. Net fracture stress = Failing load divided by gross area minus crack area.

APPENDIX IX, (Cont'd.), WELDMETAL FRACTURE TOUGHNESS DATA - TYPES W7 AND W8 WELDS - LONGITUDINAL

ALL WELDMETAL 8"x 5/16" x 11/16" SPECIMENS AGED AT 900°F FOR 3 HOURS

SPEC. NO.	WELD TYPE	CRACK LENGTH (IN.)	CRACK DEPTH (IN.)	GROSS		NET		GROSS KIC (KSI \sqrt{IN})	NET KIC (KSI \sqrt{IN})	APPLICABLE 0.2% YIELD STRESS (KSI)
				FRACTURE STRESS (KSI)	FRACTURE STRESS (KSI)	FRACTURE STRESS (KSI)	FRACTURE STRESS (KSI)			
213D1	W8	0.090	0.040	206.4	212.4	212.4	212.4	61.3	62.8	230.5
213E1	W8	0.044	0.019	253.9	255.6	255.6	255.6	49.3	49.7	230.5
213G1	W8	0.151	0.054	179.9	192.8	192.8	192.8	61.8	66.6	230.5
213H1	W8	0.202	0.066	138.7	156.0	156.0	156.0	53.5	60.5	230.5
213J1	W8	0.305	0.079	109.8	138.7	138.7	138.7	48.9	62.0	230.5
2A31	W7	0.215	0.074	136.8	152.4	152.4	152.4	55.1	61.5	230.5
4E31	W7	0.150	0.059	168.3	178.1	178.1	178.1	57.9	61.5	230.5
4F31	W7	0.094	0.043	229.6	235.3	235.3	235.3	64.5	66.2	230.5
4G31	W7	0.044	0.023	253.5	255.0	255.0	255.0	51.5	51.9	230.5
4J31	W7	0.321	0.091	106.7	132.0	132.0	132.0	49.8	62.2	230.5

NOTES:

1. Gross fracture stress = Ultimate load divided by gross area
2. Net fracture stress = Ultimate load divided by gross area minus crack area.

HEAT-AFFECTED ZONE FRACTURE TOUGHNESS DATA

APPENDIX X (Cont'd.), HEAT-AFFECTED ZONE FRACTURE TOUGHNESS DATA - TYPE W7 WELDS - TRANSVERSE

THICKNESS TYPE 8" x 11/16" x 5/16" PTC SPECIMENS AGED AT 900°F FOR 3 HOURS

SPEC. NO.	PLATE CONDITION PRIOR TO WELDING	CRACK LENGTH (IN.)	CRACK DEPTH (IN.)	GROSS		NET FRACTURE STRESS (KSI)	GROSS K _{IC} (KSI V _{IN})		NET K _{IC} (KSI V _{IN})		APPLICABLE 0.2% YIELD (KSI)
				FRACTURE STRESS (KSI)	FRACTURE STRESS (KSI)						
4A1	Aged	0.254	0.099	188.0	207.5	88.4	97.8	246.6			
4A3	Aged	0.112	0.052	249.6	254.9	NA	---	246.6			
4A5	Aged	0.050*	---	262.5	262.5	---	---	246.6			
4A7	Aged	0.195	0.083	202.6	215.1	80.5	85.8	246.6			
4F7	As Rec'd.	0.055	0.024	252.8	254.0	NA	---	246.6			
4F8	As Rec'd.	0.256	0.103	174.3	192.5	66.8	86.8	246.6			
4F9	As Rec'd.	0.105	0.050	248.2	253.0	NA	---	246.6			
4F10	As Rec'd.	0.175**	0.094	145.3	154.4	NA	---	246.6			

NOTES:

1. * Failed away from installed notch.
2. ** Failed away from installed notch. The crack dimensions invalidate K_{IC}.
3. The plane of the partial thickness crack was oriented perpendicular to the plate rolling direction.
4. Plate aged prior to welding was aged at 900°F for 3 hours.